



THÈSE

Pour obtenir le grade de

DOCTEUR DE L'UNIVERSITÉ GRENOBLE ALPES

Spécialité : Sciences de la Terre et de l'Univers et de l'Environnement

Arrêté ministériel : 25 mai 2016

Présentée par

Truong An NGUYEN

Thèse dirigée par **Julien NÉMERY**, Maitre de Conférence,
Université Grenoble Alpes
et codirigée par **Nicolas GRATIOT**, Chargé de recherche IRD,
Université Grenoble Alpes
et **Thanh-Son DAO**, Hochiminh City University of Technology
préparée au sein du **Laboratoire Institut des Géosciences de l'Environnement**
dans l'**École Doctorale Sciences de la Terre de l'Environnement et des Planètes**

Modélisation biogéochimique des nutriments dans un estuaire tropical urbanisé et scénario de gestion de l'eutrophisation

Modeling of nutrient dynamics in an urbanized tropical estuary and application to eutrophication risk management

Thèse soutenue publiquement le **20 décembre 2021**, devant le jury composé de :

Monsieur Julien NÉMERY

MAITRE DE CONFÉRENCE, Grenoble-INP/Université Grenoble Alpes,
Directeur de thèse

Madame Marie-Paule BONNET

DIRECTEUR DE RECHERCHE, IRD, Rapporteure

Madame Sandra ARNDT

PROFESSEUR ASSOCIÉ, Université Libre de Bruxelles, Rapporteure

Madame Florentina MOATAR

DIRECTEUR DE RECHERCHE, INRAE, Examinatrice

Madame Josette GARNIER

DIRECTEUR DE RECHERCHE, CNRS, Présidente

Monsieur Nicolas GRATIOT

DIRECTEUR DE RECHERCHE, IRD, Co-directeur de thèse

Monsieur Thanh-Son DAO

PROFESSEUR ASSOCIÉ, Hochiminh City University of Technology,
Co-directeur de thèse

en présence de

Monsieur Georges VACHAUD

DIRECTEUR DE RECHERCHE ÉMÉRITE, CNRS, Invité

For my little family and my parents.

Acknowledgements

I was and still in a rush to finish my thesis, but I believe I need to calm down and write the first sentences of my thesis that I should have started three years ago. I feel so happy when I remember the good memories that helped me to finish this thesis. I sincerely thank my supervisors, who gave me the autonomy in this thesis and trust me completely. Julien Némery, you are the true supervisor that I always want to be. I really thank you for your availability and concern, not only for this thesis but for everything. Nicolas Gratiot, I thank you for your trust, for your help from the very first day I started working at CARE. Thanh-Son Dao, a true teacher and scientist who has been most respected since I was a student in Vietnam. You have given me lessons in meticulousness in doing science. Your spirit of doing true science is always a source of motivation for me. Thank you for your support during the sampling missions for Saigon River, and during the COVID lockdown.

I would like to thank my friends at CARE for supporting me on my sampling trips. Le Thi Minh Tam, Tran Quoc Viet, I will never forget the days working with you. The parties after the sampling missions were so memorable. I thank Emilie Strady for your help and support since 2015 and until now. Perhaps you were one of the first teachers who helped me get into science. I would like to express my sincere thanks to Nguyen Phuoc Dan. You are the person who is always ready to help me, the difficulties in collecting data for the model are solved by you. I would like to thank the leadership of CARE for facilitating me in sampling and analysis.

The first days of my PhD were the most unforgettable days for me because of the help of so many people for my thesis. I am really lucky to work with METIS team, Paris. You have helped me open up a research path that is right for me. Josette Garnier, you have been my mentor for more than three years. I always hope one day I will become a good scientist like you. I thank Vincent Thieu, you are probably the most attentive co-author of what I wrote in my first article. Goulven Laruelle, I really appreciate your guidance on the C-GEM model during the early days of my PhD. I thank Georges Vachaud (IGE) very much for your overwhelming support. You have spent a lot of time discussing and helping me with many ideas for my thesis. I would also like to thank you for your wishes in every Tet holiday.

A warm thank you to my colleagues at IGE. Sincere thanks to IGE for giving me a professional but warm working environment. Thank you to all of you who have been in room 139. Nico Hachgenei, thank you for your sincerity and listening. You are the one who has helped me learn so many new skills over the past three years. Perhaps you are the foreigner that I meet the most. Romane Caracciolo, thank you for your interest and questions about the Saigon River. Thank Tuyet Nguyen for many advices and discussion. Thanks to Carméline and Valérie for helping me deal with administrative procedures in France. Marc Descloitres, I am

very pleased with the discussions with you about teaching methods. Many thanks go to Sylvain Campillo (Isterre) for your help in sample analysis.

I would like to thank my friends in France who always help me and my little family. Thank you to Edmond and Vincent (Coup De Pouce) for your efforts in improving my French. Thank you to Marie-Pierre Viallet's family for always supporting my family during the past three years. You will always be one of my family members. I would like to thank Mr. Ngoc and Ms. Van for your warmly support for us.

I cannot imagine how I would have completed this thesis without the unconditional support of my wife (ma Vy). You have left so much things in Vietnam to let me pursue my scientific career. I am always grateful for your sacrifices for me and for our petit Vinh. Thank you son for being a source of inspiration for me to get everything done. After all, family is still the most important thing. Finally, I would like to thank my parents who have always been proud of their children.

Nguyen Truong An
Grenoble, 21 October 2021

Abstract

Urbanized tropical estuaries in emerging countries are experiencing an imbalance between urbanization and water quality management practices. The lack of monitoring and modeling programs has not allowed understanding the dynamics of nutrients. This thesis aims to study nutrient dynamics in a tropical estuary under the influence of a megacity. Three specific objectives are (i) assessing the biogeochemical functioning of an urbanized tropical estuary (Saigon River Estuary, Vietnam) receiving wastewaters of Ho Chi Minh Megacity (HCMC); (ii) quantifying the role of controlling factors (e.g., nutrient loads, reaction rates, hydrological conditions) in the eutrophication development; (iii) assessing eutrophication risk under the scenarios of rapid urbanization and increased wastewater treatment capacity.

The Carbon-Generic Estuarine Model (C-GEM), a one-dimensional, reaction-transport model, was applied after calibration with the limited datasets existing in developing countries. The biogeochemical functioning was evaluated by analyzing monitoring data (physiochemical, phytoplankton structure and abundance, and greenhouse gases) and completed by the modeling approach. The C-GEM was calibrated and validated for Saigon River Estuary at steady-state in the dry season to evaluate the intensity of biogeochemical reactions. Dynamics of nutrients, phytoplankton, eutrophication were assessed by the transient version of C-GEM for 2017-2018. Statistical methods (e.g., Principal component analysis, Redundancy analysis and Hierarchical Partitioning) were applied to evaluate the contribution of environmental parameters to the responses of phytoplankton, eutrophication, greenhouse gases emissions. Finally, scenarios oriented towards megacity development were evaluated using C-GEM to assess the eutrophication risk.

The results of this thesis are presented in four parts, respectively. The first part identifies the impact of domestic wastewater of the megacity on the temporal-spatial variations of nutrients, phytoplankton, eutrophication and greenhouse gases. There was no statistically significant difference in nutrient pollutant concentrations between the dry season and rainy season. However, the phytoplankton abundance in the dry season is about 100 times higher than that in the rainy season. High concentrations of organic carbon and nutrients (nitrogen and phosphorus) have resulted in oxygen depletion and abundant phytoplankton formation in the urban area of the estuary. The second part explains the biogeochemical functioning of urbanized tropical estuaries with the support of C-GEM model (steady-state version). The key biogeochemical processes (i.e., nitrification, denitrification, primary production) are quantified. This estuary effectively removes nitrogen thanks to the strong nitrification and denitrification processes. The third part studies the seasonal variation of nutrients and phytoplankton under the strong fluctuations of hydrological conditions of tropical estuaries. Residence time is one of the most important controlling factors affecting phytoplankton biomass. Finally, the

eutrophication risk assessment results based on megacity development show that an increase in the number of WWTPs still does not guarantee good water quality conditions of the estuary.

Applying the C-GEM model with minimal data source highlights biogeochemical processes and hydrological factors in nutrients and eutrophication dynamics in urbanized tropical estuaries. Thus, this study provides effective support for better management of eutrophication risks for developing countries.

Keywords: biogeochemical model; megacity; phytoplankton; Vietnam; tropical estuaries.

Résumé

Les estuaires tropicaux urbanisés des pays émergents connaissent un déséquilibre entre l'urbanisation et les pratiques de gestion de la qualité de l'eau. Le manque de programmes de suivi et de modélisation n'a pas permis de comprendre la dynamique des nutriments. Cette thèse vise à étudier la dynamique des nutriments dans un estuaire tropical sous l'influence d'une mégapole. Trois objectifs spécifiques sont (i) l'évaluation du fonctionnement biogéochimique d'un estuaire tropical urbanisé (estuaire de la rivière Saigon, Vietnam) recevant les eaux usées de la mégapole Ho Chi Minh (HCMC) ; (ii) la quantification du rôle des facteurs de contrôle (par exemple, les charges en nutriments, les taux de réaction, les conditions hydrologiques) dans le développement de l'eutrophisation ; (iii) l'évaluation du risque d'eutrophisation dans le cadre de scénarios d'urbanisation rapide et d'augmentation de la capacité de traitement des eaux usées.

Le Carbon-Generic Estuarine Model (C-GEM), un modèle de transport réactif unidimensionnel, a été appliqué après calibration avec les ensembles de données limités existant dans les pays en développement. Le fonctionnement biogéochimique a été évalué en analysant les données de surveillance (physiochimie, structure et abondance du phytoplancton, et gaz à effet de serre) et complété par l'approche de modélisation. Le C-GEM a été calibré et validé pour l'estuaire de la rivière Saigon en régime permanent pendant la saison sèche afin d'évaluer l'intensité des réactions biogéochimiques. Les dynamiques des nutriments, du phytoplancton, de l'eutrophisation ont été évaluées par la version transitoire du C-GEM pour 2017-2018. Des méthodes statistiques (par exemple, l'analyse en composantes principales, l'analyse de redondance et le partitionnement hiérarchique) ont été appliquées pour évaluer la contribution des paramètres environnementaux aux réponses du phytoplancton, de l'eutrophisation, des émissions de gaz à effet de serre. Enfin, des scénarios orientés vers le développement des mégapoles ont été évalués à l'aide de C-GEM pour évaluer le risque d'eutrophisation.

Les résultats de cette thèse sont présentés respectivement en quatre parties. La première partie identifie l'impact des eaux usées domestiques de la mégapole sur les variations spatio-temporelles des nutriments, du phytoplancton, de l'eutrophisation et des gaz à effet de serre. Il n'y avait pas de différence statistiquement significative dans les concentrations de polluants nutritifs entre la saison sèche et la saison des pluies. Cependant, l'abondance du phytoplancton pendant la saison sèche est environ 100 fois supérieure à celle de la saison des pluies. Les concentrations élevées de carbone organique et de nutriments (azote et phosphore) ont entraîné un appauvrissement en oxygène et la formation d'un phytoplancton abondant dans la zone urbaine de l'estuaire. La deuxième partie explique le fonctionnement biogéochimique des estuaires tropicaux urbanisés à l'aide du modèle C-GEM (version en régime permanent). Les processus biogéochimiques clés (i.e.,

la nitrification, la dénitrification, la production primaire) sont quantifiés. Cet estuaire élimine efficacement l'azote grâce aux forts processus de nitrification et de dénitrification. La troisième partie étudie la variation saisonnière des nutriments et du phytoplancton sous les fortes fluctuations des conditions hydrologiques des estuaires tropicaux. Le temps de résidence est l'un des plus importants facteurs de contrôle de la biomasse phytoplanctonique. Enfin, les résultats de l'évaluation du risque d'eutrophisation basée sur le développement des mégapoles montrent qu'une augmentation du nombre de STEP ne garantit toujours pas de bonnes conditions de qualité de l'eau de l'estuaire.

L'application du modèle C-GEM avec une source de données minimale met en évidence les processus biogéochimiques et les facteurs hydrologiques dans la dynamique des nutriments et de l'eutrophisation dans les estuaires tropicaux urbanisés. Ainsi, cette étude fournit un support efficace pour une meilleure gestion des risques d'eutrophisation pour les pays en développement.

Mots-clés: modélisation biogéochimique; mégapole; phytoplancton; Vietnam; estuaires tropicaux.

Contents

List of Figures	xiii
List of Tables	xxi
List of Abbreviations	xxiii
Introduction	2
Motivation	2
Knowledge gaps	3
Research objectives	3
Thesis outline	4
1 Background and state of the art	6
1.1 Hydrodynamics and biogeochemistry in estuaries	7
1.1.1 Introduction to estuaries	7
1.1.2 Hydrodynamics processes	7
1.1.3 Biogeochemical processes	11
1.2 State-of-art of water quality in tropical urbanized estuaries	19
1.2.1 Megacities in estuaries and coastal areas	19
1.2.2 Insights of biogeochemical processes in tropical urbanized estuaries	21
1.2.3 Difficulties of water quality management in developing countries	30
1.3 Water quality modeling approach in estuaries	35
1.3.1 Fundamental to water quality modeling	35
1.3.2 Application of reaction-transport model in estuaries	38
1.4 Conclusion of Chapter 1	41
2 Materials and methodology	42
2.1 Study site	43
2.1.1 Saigon River Estuary	43
2.1.2 Ho Chi Minh megacity (Southern Vietnam)	47
2.1.3 Water quality conditions in the Saigon River Estuary	51
2.2 Methods for water quality evaluation	54
2.2.1 Monitoring and sampling strategy	55
2.2.2 Measurement and analytical methods	58

Contents

2.2.3	Eutrophication status and GHGs calculation	59
2.2.4	Multivariate statistical analysis methods	63
2.3	Water quality modeling	65
2.3.1	Overview of C-GEM model	65
2.3.2	Data requirement	70
2.3.3	Model description and setup protocol	72
2.3.4	Model evaluation	78
2.4	Conclusion of Chapter 2	79
3	Eutrophication and greenhouse gases in an urbanized tropical estuary	80
	Introduction	82
3.1	Part 1: Spatio-temporal of environmental parameters	82
3.1.1	Physico-chemical parameters	82
3.1.2	Dissolved oxygen, nutrients and organic carbon	83
3.1.3	Eutrophication status	85
3.2	Part 2: Phytoplankton dynamics	87
3.2.1	Spatio-seasonal variations	87
3.2.2	Structure and density of phytoplankton	88
3.2.3	Drivers of eutrophication	91
3.3	Part 3: Interaction of eutrophication and GHGs	97
3.3.1	Longitudinal profiles	97
3.3.2	Greenhouse gases	97
3.3.3	Nitrogen and carbon cycling	104
3.3.4	Relationship of urban discharge, eutrophication and GHGs .	108
3.4	Conclusion of Chapter 3	113
4	Biogeochemical functioning of an urbanized tropical estuary: Implementing the generic C-GEM (reactive transport) model	115
4.1	Introduction	116
4.2	Materials and methods	119
4.2.1	Study area	119
4.2.2	Data collection	120
4.2.3	Model implementation	122
4.3	Results and discussion	130
4.3.1	Model simulations	130
4.3.2	Tidal effects on pollutant clouds	133
4.3.3	Processes and flux budgets	135
4.4	Conclusion	143

Contents

5 Modeling the seasonal nutrient dynamics and phytoplankton development in the Saigon River tropical estuary	144
5.1 Introduction	145
5.1.1 Risk of phytoplankton blooms at urbanized tropical estuaries	145
5.1.2 The complex interaction between phytoplankton and controlling factors	146
5.1.3 Estuarine biogeochemical modeling in emerging countries	147
5.1.4 Objectives	149
5.2 Materials and methods	149
5.2.1 Study area	149
5.2.2 Saigon River Estuary	149
5.2.3 Ho Chi Minh Megacity	150
5.2.4 Data collection	151
5.2.5 Model implementation	153
5.3 Results and discussion	160
5.3.1 Evaluation of model performance	160
5.3.2 Spatio-temporal evolution of nutrients and phytoplankton biomass	166
5.3.3 Seasonal evolution of primary production and nutrients cycling	169
5.3.4 Driving factors of phytoplankton evolution	171
5.4 Conclusion	173
5.5 Conclusion of Chapter 5	174
6 Eutrophication assessment in an urbanized estuary based on past, present and future nutrient loadings: A modeling approach	175
6.1 Introduction	176
6.1.1 Risk of eutrophication in coastal megacities	176
6.1.2 Ho Chi Minh Megacity, Vietnam	177
6.1.3 Tools for eutrophication management	178
6.2 Materials and methods	179
6.2.1 Study area	179
6.2.2 Urban canals and WWTPs	181
6.2.3 Nutrient loadings from urban canals	181
6.2.4 Description of scenarios	184
6.2.5 Model validation	186
6.3 Results and discussion	188
6.3.1 Responses of the tropical estuary to nutrient loadings	188
6.3.2 Role of WWTPs in eutrophication management	192
6.4 Conclusion	193
6.5 Conclusion of Chapter 6	194

Contents

Conclusion and perspectives	195
Conclusion	195
Limitation	196
Future research directions	197
Bibliography	198

List of Figures

1.1	Interaction of pollutants, biogeochemical processes and tidal effects in estuarine systems (adapted from de Souza Machado, Anderson Abel et al., 2016)	8
1.2	Illustration of tidal variation	9
1.3	Longitudinal profile of salinity in a) stratified estuary, b) partially mixed estuary, and c) well-mixed estuary (H. H. G. Savenije, 2012)	11
1.4	Carbon cycling in the aquatic system (adapted from Bianchi, 2007)	14
1.5	Nitrogen cycling in aquatic systems (adapted from Bange et al., 2017 and Pinto et al., 2021)	15
1.6	Phosphorus processes in aquatic. DOP is dissolved organic phosphorus, POP is particulate organic phosphorus, PIP is particulate inorganic phosphorus (adapted from Vilmin et al., 2015)	16
1.7	The world population of largest cities in 2015 and estimated in 2050 (Bange et al., 2017)	19
1.8	Dissolved inorganic nitrogen exported by rivers to the ocean in 2000 and predicted 2050 (Lee et al., 2016)	20
1.9	Conceptual model of nutrient retention (or so-called buffer zone/filtering zone) by estuaries. The main sources of pollution include (1) agriculture, livestock runoff, (2) urban runoff, (3) domestic, industrial wastewater. Mechanisms of nutrient retention and removal in estuaries include (1) nutrients (C, N, P) cycling (transformation), (2) adsorption-desorption and sediment exchange, (3) burial (sedimentation), (4) nutrient consumption by primary production (e.g., algal bloom) (adapted from Paerl et al., 2006).	22
1.10	Changes in physicochemical parameters and the relative dominance of plants and biodiversity depend on the degree of eutrophication in an aquatic environment (Le Moal et al., 2019)	25
1.11	Conceptual model of eutrophication and consequences (adapted from Whitall et al., 2007)	26
1.12	The contribution of major aquatic systems to global CO_2 emission (Bauer et al., 2013)	28
1.13	Conceptual model of net ecosystem production (gross primary production - respiration) and CH_4 , CO_2 emissions in the aquatic system (Grasset et al., 2020)	29
1.14	(a) Relationships between CH_4 flux and chlorophyll-a in the water column and (b) predicted CH_4 emission in eutrophication scenarios in lakes (Beaulieu et al., 2019)	30

List of Figures

1.15 Example of variations of salinity, temperature, turbidity, DO and water level in two days 20-21/07/2006 at Gironde estuary (Etcheber et al., 2011). The grey line is the tide fluctuation, and the red one is the parameter fluctuation.	32
1.16 Comparison of survey results at three monitoring stations (black dots) and longitudinal profiles along a salinity gradient (de Jonge et al., 2006)	32
1.17 Environmental Quality Status in Seine River (from 1970 to 2013) (Romero et al., 2016)	34
1.18 Illustration of pollutant transport by advection and dispersion/diffusion. C(t) is the concentration of variables as a function of time (t) and distance (x)	36
1.19 Simplified biogeochemical processes in the aquatic system (ellipse, rectangle, red line, green line, dot line represent the processes, the elements/pollutants, consumption, production and settling/deposition, respectively), DIC and CH_2O are dissolved inorganic and organic carbon (adapted from Regnier et al., 2013)	39
2.1 Overview of three biggest river estuarine systems in Vietnam and topography of Saigon River Basin, Southern Vietnam (topography data is from MERIT DEM, 2018)	44
2.2 Average monthly precipitation and sunshine duration from 2005-2016 in Saigon River (Data source from HCMC Statistical Year Books from 2010 to 2016)	45
2.3 Average of wind speed at 10 m (ms^{-1}) and the yearly average of normal irradiation ($kWhm^{-2} yr^{-1}$) in Saigon River Basin in 2007-2018 (Data source: Global Wind Atlas and Global Solar Atlas, 2018).	46
2.4 (a) Saigon River and tributaries, (b) urban canals, (c) Can Gio Mangrove (Bathymetry data is from Southern Vietnam Institute of Water Resources Research (SIWRR) in 2008 and 2016, only available for Saigon and Dongnai River)	47
2.5 Variation of water level at estuary mouth of Saigon River in 2018 and in 1-5 May 2018 (Data source: Vung Tau Station, UHSLC Data)	48
2.6 Average residual monthly discharge in Saigon and Dongnai River from 2013-2016 (adapted from T. T. N. Nguyen et al., 2019)	49
2.7 Land use and population densities in Saigon River Basin (Data source: Land use from JAXA, 2017, Population densities from General Statistics Office of Vietnam, 2019)	49
2.8 Population in HCMC from 1979 to 2020, predicted to 2050, and WWTP capacity.	51
2.9 Mean total suspended sediment (TSS), dissolved oxygen (DO), NH_4^+ , and PO_4^{3-} concentrations in 2012 - 2016 period: (a) along the Saigon River during the wet and dry seasons and (b) in urban canals of HCMC (adapted from T. T. Nguyen et al., 2020)	52

List of Figures

2.10 Molar ratios of Si:N and Si:P in Saigon River 2015-2017 (adapted from T. T. N. Nguyen et al., 2019)	52
2.11 Nhieu Loc Canal in 2012 (Source: Tuoitre News, 2012) and fish death in Nhieu Loc Canal in 2015 (Source: Vnexpress News, 2015)	54
2.12 Evolution of DO in Saigon River (urban section) from 2003 to 2021 (Data source: data of 2003-2015 period is from the center of monitoring Vietnam, data of 2016-2021 period is from CARE, see section 2.2 for detailed description of CEM and CARE monitoring programs)	54
2.13 Location of water quality survey by Vietnamese center environmental monitoring (CEM) in urban canals and along the Saigon River Estuary	55
2.14 Sampling sites of bi-weekly monitoring and longitudinal profile in the Saigon River Estuary	56
2.15 Sampling in Saigon River in 2019.	57
2.16 Measurement of nutrients in CARE lab.	58
2.17 Interpretation of respiration process by comparing excess dissolved inorganic carbon (EDIC) vs. AOU. The data sources are from 1641 measurements in 24 estuarine environments worldwide. Processes: The solid line indicates aerobic respiration; the dotted line indicates nitrification. (1) More rapid equilibration of O ₂ ; (2) allochthonous inputs of CO ₂ (riverine and lateral); and (3) Anoxic production of CO ₂ (from Borges and Abril, 2011)	63
2.18 Illustration of dendrogram (tree-like diagram) representing the results of HCA. A cluster share similarity between branch points (from Buttigieg and Ramette, 2014)	64
2.19 Description and interpretation for (a) PCA biplot and (b) RDA triplot. In RDA, the blue points explain for the objects (e.g., sampling site), the green arrows explain for responses (e.g., GHGs concentrations, phytoplankton densities), the red arrows explain for the predictors/explanatory variables (e.g., DO, TSS, TOC concentrations). The green points (optional) are nominal variables. (c) Interpretation: the relationship between variables explained by the red arrows. For instance, arrows 1 and 2 are almost perpendicular, cosines (a)=0, thus not correlate. Similarly, arrows 2 and 4 have a negative relationship because cosines (180) = -1. Same interpretation applies for both PCA and RDA, but the difference between PCA and RDA is that there is no separation between explanatory variables and responses in PCA (interpretation is adapted from Buttigieg and Ramette, 2014)	65
2.20 The state variables (rectangle) and processes (ellipse) in the biogeochemical module of C-GEM applied in the Saigon River Estuary. Red and black lines represent the consumption and production processes (adapted from Volta et al., 2014)	69

List of Figures

2.21	Model domain and sampling sites	73
2.22	Depth and Width of Saigon River Estuary	74
2.23	Comparison between observed (black marks) and simulated (black lines) profiles for average tidal amplitude and salinity along the Saigon River Estuary. The vertical gray lines correspond to tributaries or canals. Standard deviations (the gray area) of simulation come from hourly fluctuations over tidal cycles	76
3.1	Sampling sites of bi-weekly monitoring and longitudinal profiles . .	83
3.2	Temporal variations of (a) temperature, (b) pH, (c) TSS and (d) salinity at three sampling stations from July 2015 to December 2020. PC, BD and BK are Phu Cuong station at upstream, Bach Dang station at urban section and Binh Khanh station at downstream of Saigon River Estuary	84
3.3	Temporal variations of (a) DO, (b) NH_4^+ , (c) NO_3^- , (d) PO_4^{3-} , (e) DSi and (f) TOC at three sampling stations from July 2015 to December 2020.	85
3.4	Evolution of Chl-a and trophic index in the Saigon River from 2015 to 2020, at (a) Phu Cuong station and (b) Bach Dang station. Trophic index indicates several states of eutrophication, including ultraoligotrophic (0-2), oligotrophic (2-4), mesotrophic (4-6), eutrophic (6-8), and hypertrophic (8-10) states, respectively.	86
3.5	Evolution of Chl-a and trophic index in the Saigon River from 2015 to 2020, at (a) Hoa An station and (b) Binh Khanh station	87
3.6	Spatial cluster analysis of phytoplankton abundance for longitudinal profile monitoring in dry and rainy season. Red, green and blue colors describe the upstream, urban area and downstream section of Saigon River, respectively.	88
3.7	Densities of dominant phytoplankton species and Chl-a concentrations in longitudinal profile monitoring in (a) dry season, April 2017 and in (b) rainy season, October 2017. Legend: Total is total phytoplankton abundance.	89
3.8	Temporal phytoplankton densities at the sites (left panels) and the relationship between total phytoplankton density and Chl-a (right panels) at each sampling site. Legend: Total is total phytoplankton abundance, Others is the other dominant species.	91
3.9	PCA of 20 environmental variables (physicochemical parameters, Chl-a, metals) in (a) dry season and (b) rainy seasons in the Saigon River. Upstream, urban area and downstream are SG01, SG10, and SG18, respectively. The environmental variables with longer length are the controlling parameters. Note that the axes of PCA for rainy season were rotated for easier comparison.	92

List of Figures

- | | |
|--|-----|
| 3.10 RDA on the relationships between environmental variables (as driving factors) and phytoplankton abundances in (a) dry and (b) rainy season in the Saigon River. Lptcy <i>L. danicus</i> , Prdnm <i>Peridinium</i> sp, Alcsr <i>A. granulata</i> , Mcrcy - <i>Microcystis</i> spp, Eunot - <i>Eunotia</i> sp, Rphdp <i>R. raciborskii</i> , Trchl <i>T. volvocina</i> , Cyclt - <i>Cyclotella</i> cf. <i>meneghiniana</i> , Psdnbs - <i>Pseudanabaena</i> sp. | 93 |
| 3.11 Water quality variables and GHG concentrations in the Saigon River Estuary 2019-2020. The lines and color bands represent the mean values and maximum/minimum values of each parameter. The histogram represents water samples collected in the four urban canals of HCMC. Orange and blue colors indicate the samples collected during the dry and rainy seasons, respectively. | 98 |
| 3.12 Spatial and seasonal concentrations (in $\mu\text{g L}^{-1}$), water-air fluxes of GHGs (in $\text{g m}^{-2} \text{d}^{-1}$ or $\text{mg m}^{-2} \text{d}^{-1}$) and eutrophication index (TRIX) in dry and rainy season in the Saigon River Estuary. The water-air fluxes were calculated for each section (i) upstream, (ii) urban area of HCMC and (iii) downstream of HCMC. It is noticed that the maps were built by using the Inverse Distance Weighting Interpolation (QGIS 3.18.1, 19-Mar-2021) between 27 sampling sites over the 141 km of the Saigon River. No data were acquired in the upper 55 km of the Saigon river, from Dau Tieng Reservoir to UP01 (the river is then underlined with white background). | 99 |
| 3.13 Relationship between N_2O excess ($\text{N}_2\text{O}_{\text{xs}}$) and apparent oxygen utilization ($\text{AOU}=\text{DO}_{\text{air}}-\text{DO}_{\text{water}}$, i.e., difference between measured DO in water and its equilibrium saturation concentration) in (a) dry and (b) rainy season 2019 – 2020 in the Saigon River. Upstream (UP01-UP04, SG01-SG03); Urban (SG04-SG15); Downstream (SG16-SG23). The linear correlations of $\text{AOU}-\text{N}_2\text{O}_{\text{xs}}$ indicate nitrification as the main contributor to N_2O production. Correlation breaks indicate the impact of denitrification on N_2O production. | 105 |
| 3.14 Relationship between CO_2 excess ($\text{CO}_{2\text{xs}}$) and apparent oxygen utilization (AOU) in dry and rainy seasons in the Saigon River. The linear correlations of $\text{AOU}-\text{CO}_{2\text{xs}}$ indicate respiration as a major cause for CO_2 supersaturation. The allochthonous inputs of CO_2 can be either from rivers or lateral inputs. | 107 |
| 3.15 Relationship between CH_4 excess ($\text{CH}_{4\text{xs}}$) and apparent oxygen utilization (AOU) in dry and rainy seasons in the Saigon River. The negative correlations of $\text{AOU}-\text{CH}_{4\text{xs}}$ indicate methane oxidation (CH_4 consumption/methanotrophy). | 108 |
| 3.16 RDA and hierarchical partitioning analysis between explanatory variables (physio-chemical parameters, eutrophication) and responses (GHGs) in the Saigon River in (a) dry and (b) rainy season. The cosines of angles between vectors approximate their relationship (e.g., the approaching angles of 0° and 180° indicate positive and negative relationships). The vector with a longer length indicates a higher impact on the variation of the dataset. | 110 |

List of Figures

4.1	Model domain of Saigon River Estuary and monitoring stations	119
4.2	Depth and Width of Saigon River Estuary	123
4.3	Comparison between observed (red marks) and simulated (red lines) profiles for average tidal amplitude and salinity along the Saigon River Estuary. The vertical gray lines correspond to tributaries or canals. Standard deviations (grey area) of simulation come from hourly fluctuations over tidal cycles.	127
4.4	The state variables (rectangle) and processes (ellipse) in the biogeochemical module of C-GEM applied in the Saigon River Estuary. Red and green lines represent the consumption and production processes	128
4.5	Comparison of observed and simulated results of water quality along the Saigon River Estuary over a tidal cycle. The vertical lines are tributaries or canals. Lateral input are described by vertical lines. The black dotted lines are the maximum permissible limit for domestic use, aquatic life based on Vietnamese regulation on surface water quality QCVN 08:2015/BTNMT.	132
4.6	The tidal effect on the transport of the low DO concentration cloud along Saigon River Estuary. (a) DO concentration along Saigon River Estuary, (b) water particle displacement from km 108 during two tidal cycles. The displacement is calculated by multiplying velocity ($m s^{-1}$) and each hour (3600s). This displacement is only considered by the velocity (advection) of the water particle.	134
4.7	Intensity of biogeochemical processes and erosion/deposition rates affecting the concentrations of (a) DO, (b) TOC, (c) NH_4^+ , (d) NO_3^- , (e) PO_4^{3-} , (f) Phytoplankton, (g) TSS and (h) DSi. For example, Oxygen exchange, Net primary production and nitrification are affecting DO concentrations. The dashed lines are the net biogeochemical reactions.	137
4.8	Fluxes and reaction fluxes of (a) DO, (b) TOC, (c) NH_4^+ in urban and downstream sections of Saigon River Estuary in dry season 2014 - 2017. Process rates are in tons	141
5.1	The model domain of C-GEM, water quality stations in the Saigon River Estuary. Monthly discharge of Saigon River (at km 130) and Dongnai River are average data from 2014 - 2017. CARE and CEM are two monitoring and research centers, described in section 2.2 . . .	150
5.2	Biogeochemical processes in C-GEM applied for Saigon River Estuary.	154
5.3	Longitudinal depth profiles along Saigon River Estuary in 2019 - 2020.	159

List of Figures

5.4	The observed and simulated tidal range, salinity in the Saigon River from 2017 to 2018. Three dotted lines in the left panels are locations of three stations at km 86, 130 and 156. The grey line indicates Dongnai River. The tidal range observation data are calculated based on hourly water level data from the Vietnamese Center of Water Management and Climate Change (WACC). The residence time is calculated by dividing the simulated volume by the flow of each section.	163
5.5	Comparison of simulated and observed water quality along Saigon River. The model performance is calculated based on average values in the dry and rainy season 2017–2018.	165
5.6	The daily evolution of suspended sediment, dissolved oxygen, nutrients, organic carbon and phytoplankton biomass in three stations along Saigon River Estuary from 2017 to 2018. Blue points are observed data of bi-weekly monitoring.	168
5.7	Spatio-temporal evolution of nutrient limitation and the main biogeochemical processes in dry and rainy seasons 2017-2018 along Saigon River Estuary.	170
5.8	Schematic representation of the contribution of driving factors to phytoplankton bloom in the Saigon River Estuary in the dry and rainy season. The top panels are calculated based on the normalized factors in upstream, urban and downstream in 12 months. The independent effects on phytoplankton in lower panels are calculated based on the hierarchical partitioning method, calculated for each section.	172
6.1	Map of Saigon River Estuary, monitoring stations and HCMC population density in 2019.	180
6.2	Population in HCMC from 1979 to 2020, predicted to 2050, and WWTP capacity. Population data from 1979 to 2019 is from GSO Vietnam; prediction population is based on UN World Urbanization Prospects with a growth rate of 2.7% in 2020 and 1.3% in 2050. Total domestic wastewater discharge is calculated based on water consumption per capita	182
6.3	The nutrients concentration along canal axis based on parabola best-fit equation. The concentration is a function of distance, with the initial concentration at pollutant sources is. The blue points with standard deviation are observed data of 5 sampling sites in Ben Nghe canal in 2014-2017.	182
6.4	The NH_4^+ , PO_4^{3-} concentrations and fluxes at the outlet of canals. The nutrient concentrations are calculated based on the nutrient emission per capita and then applied the parabola best-fit equation to get the concentration at the outlet of the canals.	184

List of Figures

6.5 Comparison of observed and simulated water quality variables along Saigon River Estuary.	188
6.6 Simulated results of water quality variable along Saigon River Estuary in three scenarios. According to Vietnamese regulation on surface water quality, the background colors (red, orange, green, blue) are the concentration ranges for water quality assessment (QCVN 08:2015/BTNMT. The trophic status is classified according to the recommendation of Dodds and Welch (2000).	190

List of Tables

1.1	Major tidal constituents and periods (from Ji 2017)	10
1.2	The sequence of terminal electron acceptors utilized (by oxidation reactions) for organic matter decomposition under varying O ₂ concentrations in estuaries (Likens, 2010)	12
1.3	Difference of N and P in aquatic systems	17
1.4	The differences between temperate and tropical estuaries	24
1.5	Simplified governing equations of hydrodynamics model in estuaries	37
1.6	Processes controlling concentrations of nutrients in aquatic systems	38
1.7	Comparison of some well-known biogeochemical model applications in estuaries. The order of models indicates the simplicity to the complexity of the model	40
2.1	Data collection for model implementation and validation (see Figure 2.21 for the locations of the hydrological and water quality sampling stations)	70
2.2	Physical parameters to build the estuarine geometry and hydrodynamic module in the Saigon River Estuary	75
2.3	Determination of sediment parameters and adjustment of biological parameters for the application of the C-GEM model in the Saigon River Estuary	77
2.4	Boundary conditions used for the steady-state simulation of water quality variables in the Saigon River Estuary 2014-2017	78
2.5	Equations, ranges, and optimal values for assessing model performance	79
3.1	Dominant species of phytoplankton based on the spatial and temporal monitoring in the Saigon River	90
3.2	Comparison of mean GHGs concentrations and fluxes (CO ₂ equivalent) in estuaries under different environmental conditions (Tropical, Temperate, Mediterranean) and human pressures.	103
4.1	Data collection for model implementation and validation (see Figure 2.21 for the locations of the hydrological and water quality sampling stations)	121
4.2	Physical parameters to build the estuarine geometry and hydrodynamic module in the Saigon River Estuary	124
4.3	Determination of sediment parameters and adjustment of biological parameters for application of the C-GEM model in the Saigon River Estuary	125

List of Tables

4.4	Boundary conditions used for the steady-state simulation of water quality variables in the Saigon River Estuary 2014-2017	129
4.5	Equations, ranges, and optimal values for assessing model performance	130
4.6	Model performance statistics in the Saigon River Estuary during an average dry season for the 2014-2017 period	131
5.1	Biochemical reactions and formulations of the processes applied in C-GEM for Saigon River	157
5.2	Evaluation criteria for model performance	160
5.3	The performance of the simulated temporal variation by C-GEM in the Saigon River in dry, rainy seasons	161
6.1	Four scenarios for C-GEM application in Saigon River Estuary . . .	186

List of Abbreviations

<i>AOU</i>	Apparent Oxygen Utilization.
<i>BOD</i> ₅	The 5 day biochemical oxygen demand.
<i>CH</i> ₄	Methane.
<i>CH</i> ₄ <i>xs</i>	Methane excess.
<i>Chl-a</i>	Chlorophyll-a.
<i>CO</i> ₂	Carbon dioxide.
<i>CO</i> ₂ <i>xs</i>	Carbon dioxide excess.
<i>COD</i>	Chemical oxygen demand.
<i>DIC</i>	Dissolved inorganic carbon.
<i>DIN</i>	Dissolved inorganic nitrogen.
<i>DIP</i>	Dissolved inorganic phosphorus.
<i>DO</i>	Dissolved oxygen.
<i>DOC</i>	Dissolved organic carbon.
<i>DOP</i>	Dissolved organic phosphorus.
<i>DSi</i>	Dissolved silica.
<i>eDIC</i>	Excess dissolved inorganic carbon.
<i>GHGs</i>	Greenhouse gases.
<i>GPP</i>	Gross primary production.
<i>H</i> ₂ <i>S</i>	Hydrogen sulfide.
<i>HCA</i>	Hierarchical cluster analysis.
<i>HP</i>	Hierarchical partitioning.
<i>Kps</i>	Half-saturation constant.
<i>LPOC</i>	Labile particulate organic carbon.
<i>N</i> ₂ <i>O</i>	Nitrous oxide.
<i>N</i> ₂ <i>Oxs</i>	Nitrous oxide excess.
<i>NH</i> ₃	Ammonia.
<i>NH</i> ₄ ⁺	Ammonium.
<i>NO</i> ₂ ⁻	Nitrite.
<i>NO</i> ₃ ⁻	Nitrate.
<i>NPP</i>	Net Primary Production.

List of Abbreviations

<i>OC</i>	Organic carbon.
<i>Pac</i>	Maximal P sorption capacity.
<i>pbias</i>	Bias percentage.
<i>PCA</i>	Principal component analysis.
<i>PH</i> ₃	Phosphine.
<i>PIP</i>	Particulate inorganic phosphorus.
<i>PO</i> ₄ ³⁻	Excess dissolved inorganic carbon.
<i>POC</i>	Particulate organic carbon.
<i>POP</i>	Particulate organic phosphorus.
<i>R</i> ²	Coefficient of determination.
<i>RDA</i>	Redundancy analysis.
<i>RMSE</i>	Root mean square error.
<i>RPOC</i>	Refractory particulate organic carbon.
<i>RTMs</i>	Reactive-transport models.
<i>Si(OH)</i> ₄	Orthosilicic acid.
<i>SO</i> ₄ ²⁻	Sulfate.
<i>TN</i>	Total nitrogen.
<i>TOC</i>	Total Organic Carbon.
<i>TP</i>	Total phosphorus.
<i>TRIX</i>	Trophic index.
<i>TSS</i>	Total suspended sediment.
<i>BD</i>	Bach Dang station.
<i>BK</i>	Binh Khanh station.
<i>CARE</i>	Centre Asiatique de Recherche sur l'Eau.
<i>CEM</i>	Vietnamese Center of Monitoring.
<i>C-GEM</i>	The Carbon-Generic Estuarine Model.
<i>DONRE</i>	Department of Natural Resources and Environment.
<i>GSO</i>	General Statistics Office of Vietnam.
<i>HA</i>	Hoa An station.
<i>HCMC</i>	Ho Chi Minh City.
<i>NOAA</i>	National Oceanic and Atmospheric Administration.
<i>PC</i>	Phu Cuong station.
<i>SIWRR</i>	Southern Institute of Water Resources Research.
<i>WWTPs</i>	Wastewater treatment plants.
<i>WACC</i>	Center of Water Management and Climate Change.

List of Abbreviations

```
# this line ensures that tinytex doesn't try to update LaTeX
→ packages on every single knit
options(tinytex.tlmgr_update = FALSE)
```

Introduction

Motivation

Estuaries represent only a small proportion of the world's surface waters, but they are among the most productive ecosystems in nature. Rivers drain into estuaries, bringing in nutrients from continental uplands. However, coastal areas and estuaries and lower stretches of urbanized rivers are also the frequent sinks and sources of nutrient pollution, which likely cause eutrophication in estuaries (Lanoux et al., 2013; Paerl, 2006). These phenomena threaten water resources safety, especially for megacities in developing countries, where the balance between urbanization and environmental management is commonly a difficult trade-off. Besides, estuaries are known to be emitters of greenhouse gases (GHGs), which vary according to their hydrological and biogeochemical characteristics (Abril et al., 2005; Borges & Abril, 2011; Daniel et al., 2013; Marescaux et al., 2018). In this context, reactive transport models can provide valuable insight to better understand the complex biogeochemical dynamics of such estuaries and help predict the potential response of mass water bodies to anthropic perturbations. Under the pressure of multiple pollution sources (e.g., domestic wastewater, industrial inputs), the main factors controlling water quality in estuaries are biological and physical processes; in particular: (1) biogeochemical processes such as nitrification, denitrification, remineralization, primary production in water columns (J. Hu & Li, 2009; Vanderborgh et al., 2007; Volta, Laruelle, Arndt, & Regnier, 2016); (2) dilution process between riverine and marine waters (Etcheber et al., 2011; Lajaunie-Salla et al., 2019; Lanoux et al., 2013); (3) the interaction with sediment through adsorption/desorption process (Aissa-Grouz et al., 2018; Vilmin et al., 2015). In addition, eutrophication can significantly affect GHGs emissions in estuaries (Li et al., 2021), such as reducing CO_2 emissions by intense photosynthesis, while CH_4 emissions have been observed to increase exponentially with eutrophication status (DelSontro et al., 2019).

Studies on the anthropogenic impacts on water quality in estuaries by biogeochemical models are mainly available in temperate estuaries of industrialized countries (Gawade et al., 2017; Regnier et al., 2013). The Carbon-Generic Estuarine Model (C-GEM) is a generic one-dimensional, reactive-transport model that takes advantage of the relationship between estuarine geometry and hydrodynamics to minimize data requirements (Volta et al., 2014). Steady-state simulations of C-GEM have provided accurate descriptions of estuarine hydrodynamics and biogeochemical transformations in several temperate estuaries (G. Laruelle et al., 2017;

Introduction

G. G. Laruelle et al., 2019; Volta, Laruelle, & Regnier, 2016; Volta et al., 2014). Although several studies have been carried out in tropical estuaries through monitoring and experiments (e.g., Miguel, Lucas Lavo António Jimo (2018); Vipindas et al. (2018); J. Wu et al. (2013)), estuarine biogeochemical modeling applications are still missing in many countries of Southeast Asia, India, Africa, South and Central Americas (Regnier et al., 2013; Volta, Laruelle, Arndt, & Regnier, 2016). There is now a need to improve the parameterization of C-GEM to strengthen the robustness of simulations in tropical estuarine contexts. This is particularly important for water resource management in urbanized tropical estuaries such as in Saigon River Estuary, Vietnam (T. T. N. Nguyen et al., 2019), which is closely related to the social and economic development in Southern Vietnam. The most notable difference between temperate and tropical systems is the rate of biological processes. The higher temperature of tropical estuaries often increases the biological uptake, excretion of nutrients and microbial activity (e.g., nitrification and denitrification) (B. Eyre & Balls, 1999; Tappin, 2002). In most tropical estuaries, two distinct flow rates and retention time are found during the dry and rainy seasons (Dong et al., 2011), whereas higher flow rates occur in winter in temperate estuaries. Therefore, the factors controlling the intensity of biogeochemical processes will differ between the temperate and tropical systems.

Knowledge gaps

Based on this context and the literature review, the main knowledge gaps for understanding the water quality processes and eutrophication management in tropical urbanized estuaries are:

1. Incompleted information on impacts of human activities on the water quality, including nutrients, phytoplankton dynamics, and GHGs in urbanized tropical estuaries
2. Lacking information on the interaction between biogeochemical processes and hydrological regimes, and their impacts on eutrophication in tropical estuaries
3. Difficulties for policy makers to establish a robust strategy in emerging countries.

Research objectives

This PhD research aims to address the three above-mentioned knowledge gaps. The overall research objective is to better understand nutrient dynamics and eutrophication management comprehensively in tropical urbanized estuaries. Saigon River

Introduction

Estuary (Vietnam) was selected to conduct this study. Main thesis works include water sampling, analysis of physical-chemical parameters, nutrients, phytoplankton, GHGs and hydrodynamic and biogeochemical modeling. Four sub-objectives are formulated to achieve the thesis's objective.

1. Assessing nutrients, eutrophication and GHGs dynamics in Saigon River Estuary, based on a pluriannual monitoring approach.
2. Understanding the seasonal variation of nutrients and eutrophication in tropical estuaries
3. Modeling the biogeochemical functioning of urbanized estuaries with a reactive-transport model (C-GEM)
4. Helping for the establishment of a strategy of adaptation/mitigation to eutrophication risk in urbanized estuaries based on historical and projected nutrient loadings

Thesis outline

Chapter 1 presents the risks of water pollution, eutrophication, and increased greenhouse gases emissions from urbanized tropical estuaries in the context of emerging countries. The biogeochemical cycles (carbon, nitrogen, phosphorus, silica, phytoplankton) and the effects of the hydrological regime of estuaries are described. Current knowledge on the role of these processes in tropical estuaries is compared with temperate estuaries. Finally, several biogeochemical estuarine models are compared to identify the suitable model and to simulate the biogeochemical functioning of tropical estuaries under limited data availability.

Chapter 2 presents the characteristics of the study site, Saigon River Estuary and the influence of Ho Chi Minh megacity. The methods of sampling, analysis, and data processing are presented in detail. Then, the biogeochemical model C-GEM is presented with a focus on application for tropical estuaries.

Chapter 3 describes the spatio-temporal variation of nutrients, phytoplankton, eutrophication, and greenhouse gases in this urbanized tropical estuary. Control factors such as biogeochemical processes, hydrological regimes are analyzed, based on some statistical methods. Finally, the processes that are most likely to affect water quality evolution in this estuary are identified to cross-validate water quality modeling applications.

Chapter 4 presents the application of the C-GEM model at steady-state for Saigon River Estuary to quantify biogeochemical functioning. The model uses the average data for 2014-2017 to describe the average hydrodynamics and biogeochemical processes for the dry season period.

Introduction

Chapter 5 presents the application of the C-GEM model with a transient version, allowing the description of the seasonal evolution of phytoplankton and eutrophication. The model allows identifying the driving factors for the spatial-temporal variation of phytoplankton.

Chapter 6 presents solutions to manage eutrophication by evaluating the development-oriented scenarios of a megacity. Scenarios including the development of new WWTPs, population growth and climate change to 2050 are assessed.

1

Background and state of the art

Contents

1.1	Hydrodynamics and biogeochemistry in estuaries	7
1.1.1	Introduction to estuaries	7
1.1.2	Hydrodynamics processes	7
1.1.3	Biogeochemical processes	11
1.2	State-of-art of water quality in tropical urbanized es- tuaries	19
1.2.1	Megacities in estuaries and coastal areas	19
1.2.2	Insights of biogeochemical processes in tropical urban- ized estuaries	21
1.2.3	Difficulties of water quality management in developing countries	30
1.3	Water quality modeling approach in estuaries	35
1.3.1	Fundamental to water quality modeling	35
1.3.2	Application of reaction-transport model in estuaries . .	38
1.4	Conclusion of Chapter 1	41

This chapter presents a literature review of estuaries regarding water quality, focusing on tropical estuaries and the impacts of urban/wastewaters policies. In addition, knowledge gaps are shown in understanding the factors (such as hydrological regimes, biogeochemical processes) controlling water quality in tropical and temperate estuaries. In general, the growth of megacities is putting increasing pressure on the water quality of estuaries and coastal areas, a trend that is exacerbated in developing countries. Eutrophication and greenhouse gas emissions in tropical estuaries are expected to increase in the future. However, difficulties in monitoring and applying biogeochemical models in estuaries have made it difficult to promote effective management policies. Current knowledge shows that the dynamics of nutrients and phytoplankton are complex under the

1. Background and state of the art

influence of interactions of carbon (C), nitrogen (N), phosphorus (P) cycles and hydrological regimes (inflow discharge, residence time). Appropriate monitoring programs (location and frequency of sampling) are required to apprehend spatial and temporal variations in water quality in estuaries. The application of reaction-transport models can allow understanding the mechanisms of these processes. Data requirements are still the main challenge to applying these models in developing countries. However, if there are no models capable of accurately describing the evolution of phytoplankton and the purification capacity of estuaries, solutions to reduce pollutants such as the construction of wastewater treatment plants will not be effective. Therefore, developing a suitable model for urbanized tropical estuaries is extremely important to urbanization and ongoing climate changes

1.1 Hydrodynamics and biogeochemistry in estuaries

1.1.1 Introduction to estuaries

Estuaries are transitional areas between rivers and seas, transporting nutrients from rivers to seas. Estuaries have both river and sea characteristics, making them an area with rich and diverse ecosystems, providing resources and playing an important role in human development. That is why most densely populated areas are situated in coastal areas near estuaries (Vitousek et al., 1997). In addition, estuaries are also considered as a buffer zone capable of holding and removing human-induced pollutants (H. H. G. Savenije, 2012).

Estuaries are different from rivers and lakes hydrodynamically, chemically, and biologically. Compared to rivers and lakes, the unique characteristics of estuaries include the following (1) tides are a major driving force, (2) salinity and its variations usually play a significant role in hydrodynamics and water quality processes, (3) two-directional net flows (Figure 1.1). For pollutant transport aspect, flushing of pollutants is driven primarily by advection in rivers, while in estuaries, both advection and dispersion (mixing and turbulent diffusion) affect the transport of pollutants (Martin et al., 1998).

1.1.2 Hydrodynamics processes

Knowledge of the physical phenomena that determine the tidal flow, tidal mixing, and salt intrusion are drivers of water quality and are especially important for modeling and management (H. H. G. Savenije, 2012). The primary factors controlling estuarine hydrodynamic processes are (1) tides, (2) freshwater inflows, and

1. Background and state of the art

(3) geometry of the estuary (Regnier et al., 1998; Regnier et al., 2013; H. H. G. Savenije, 2012).

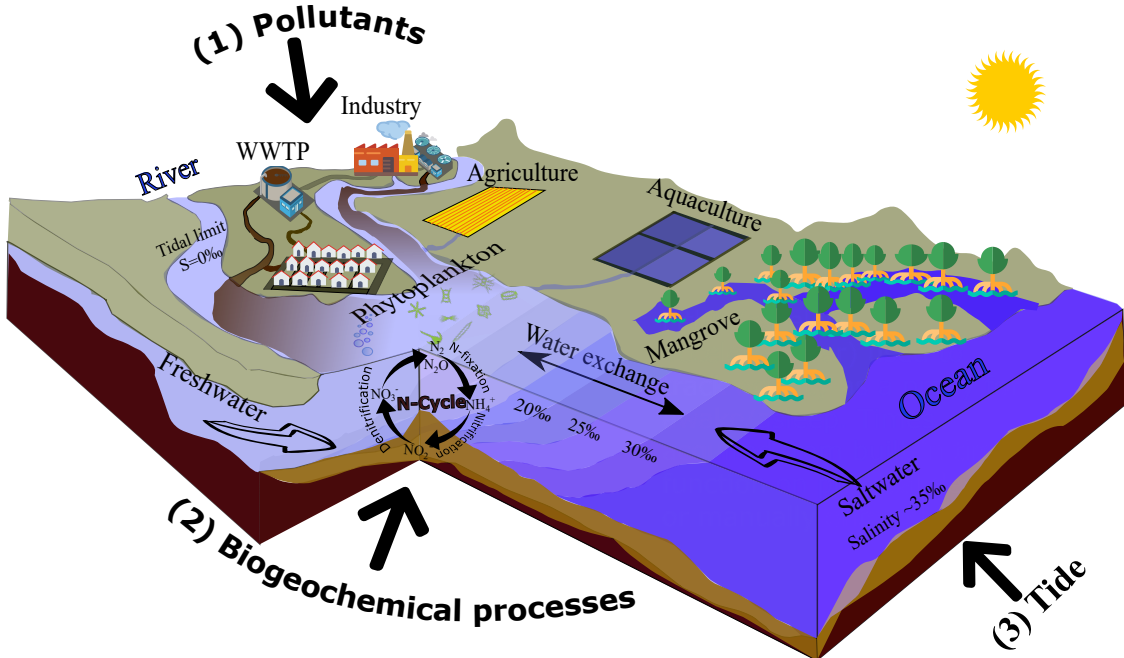


Figure 1.1: Interaction of pollutants, biogeochemical processes and tidal effects in estuarine systems (adapted from de Souza Machado, Anderson Abel et al., 2016)

Relationship of estuarine geometry and hydrodynamics

Studying the relationship between geometry and hydrodynamics is significant in reducing data requirements for hydrodynamics models in estuaries (Regnier et al., 2013; H. H. G. Savenije, 2012; H. H. G. Savenije, 2001). According to H. H. Savenije (2005), the geometries of alluvial estuaries often have common characteristics. Estuarine width and estuarine cross-sectional area typically decrease exponentially with distance from the mouth. Therefore, the geometry of estuaries can be expressed through a function of convergence lengths. Estuaries with funnel-like shapes (diminishing in width from estuary mouth to upstream) have short convergence lengths and small inflow, while prismatic estuaries have long convergence lengths and higher inflow (H. H. G. Savenije, 2012). Estuaries with funnel-shape also exhibit tidal dominance over inflow discharge; in other words, these estuaries often observe the saline intrusion (Jiang et al., 2020). H. H. Savenije (2005) suggested that the salt intrusion length at these estuaries is typically about two-thirds of the total estuarine length. For example, funnel-shaped estuaries, such as Scheldt (in Belgium), Delaware (in the USA), and Saigon (in Vietnam), are marine-dominated estuaries with short convergent lengths and long saline intrusion. Besides, features such as short convergence length, long salt intrusion length, funnel-shape estuaries often have long residence time, about 60–90 days in the Scheldt,

1. Background and state of the art

80 days in the Delaware estuary (Regnier et al., 2013; H. H. G. Savenije, 2012). In contrast, prismatic systems with long convergence lengths have shorter residence time and higher flushing capacity (H. H. G. Savenije, 2012).

Tidal processes

The tide is generated by interactions in the planetary ocean topography with Earth, Sun and Moon gravitational forces (principally). It acts as a periodic function consisting of multiple frequency components. The dominant periods are in the order of 12.3 (semi-diurnal) and 24 (diurnal) hours (H. H. G. Savenije, 2012). Tidal excursion, tidal amplitude and tidal periods are factors controlling the variation of water quality in estuaries.

Understanding and describing tidal oscillations in estuaries are extremely important in water quality modeling because (1) tides are a major factor controlling the flushing time of many estuaries, (2) tidal currents are largely responsible for turbulence and mixing in estuaries, and (3) tidal currents can generate residual flow that affects the long-term transport of pollutants (Hugo Fischer, 1979; Ji, 2017; O’Kane & Regnier, 2003; Regnier et al., 1997)

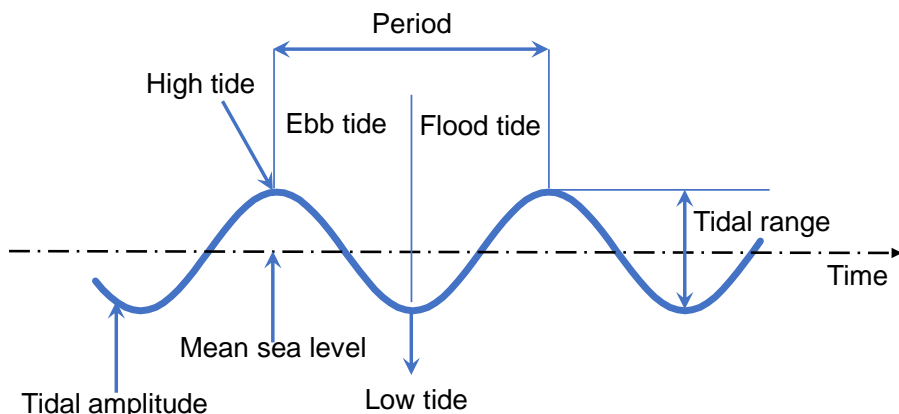


Figure 1.2: Illustration of tidal variation

Figure 1.2 illustrates the tidal variation and shows the important definitions related to tides.

Tides can be described as the sum of tidal constituents. Each constituent is a harmonic oscillation and has its amplitude, period, and phase, which can be extracted from measured tidal data using the harmonic analysis. The first five constituents, M_2 , S_2 , O_1 , K_1 , and N_2 (Table 1.1), are generally the most important tidal constituents (Ji, 2017; Martin et al., 1998; H. H. G. Savenije, 2012). For most systems, there will be two high and two low tides on the tidal curve per tidal day (or lunar day, about 24.84 h). Tides that occur twice during a tidal day are called semi-diurnal tides. Some areas, such as estuaries in the Gulf of Mexico, have only one high and one low tide per day, or daily tides. In most estuaries connected

1. Background and state of the art

to the Pacific Ocean, the magnitudes may be quite different, resulting in what is known as *mixed tides* (Martin et al., 1998).

Table 1.1: Major tidal constituents and periods (from Ji 2017)

Tidal symbol	Generating force	Period (h)
M2	Moon	12.421
S2	Sun	12.000
O1	Moon	25.819
K1	Moon, sun	23.935
N2	Moon	12.659
P1	Sun	24.067
K2	Moon, sun	11.967

Another important definition related to tidal effects on pollutant transport is the tidal excursion. The tidal excursion is the distance that a particle travels from low to high water, or vice versa (H. H. G. Savenije, 2012). This parameter is useful for describing the movement of pollutants in estuaries within tidal cycles. Freshwater inflows impose a net seaward movement on water particles over a tidal cycle. Hence, the ebb-tidal excursion should be slightly larger than the flood tidal excursion. For a typical maximum tidal velocity of 1 m s^{-1} and an M_2 period of 12.42 h, the tidal excursion is 14.2 km (Ji, 2017). Major factors that influence the propagation and amplitude of tides include bottom friction, water depth and shoreline, and Coriolis force (H. H. G. Savenije, 2012).

Salinity intrusion

The transport of pollutants and salinity intrusion at alluvial estuaries contribute to the estuarine shape and inflow discharge (H. H. G. Savenije, 2012). Salinity ranges from 0 to 33 ppt in estuaries and 35 ppt in the open oceans (Ji, 2017; H. H. G. Savenije, 2012). Figure 1.3 shows the influence of freshwater inflow on salinity intrusion in tidal estuaries. The well-mixed estuary occurs during low flow, resulting in a deeper salt intrusion (H. H. G. Savenije, 2012). In tropical estuaries, seasonal fluctuations in freshwater inflow often cause saltwater intrusion markedly different between the two seasons. In the dry season with low freshwater inflow, saline intrusion can often reach inland (Figure 1.3c), whereas in the rainy season, there is almost no effect of salinity (Figure 1.3a).

Flushing time and freshwater inflow

Besides the impact of freshwater inflow on salinity intrusion, inflow also directly affects the flushing time (also so-called residence time) of estuaries (Delhez et al., 2014; Martin et al., 1998; Regnier et al., 1998; Viero & Defina, 2016). The flushing

1. Background and state of the art

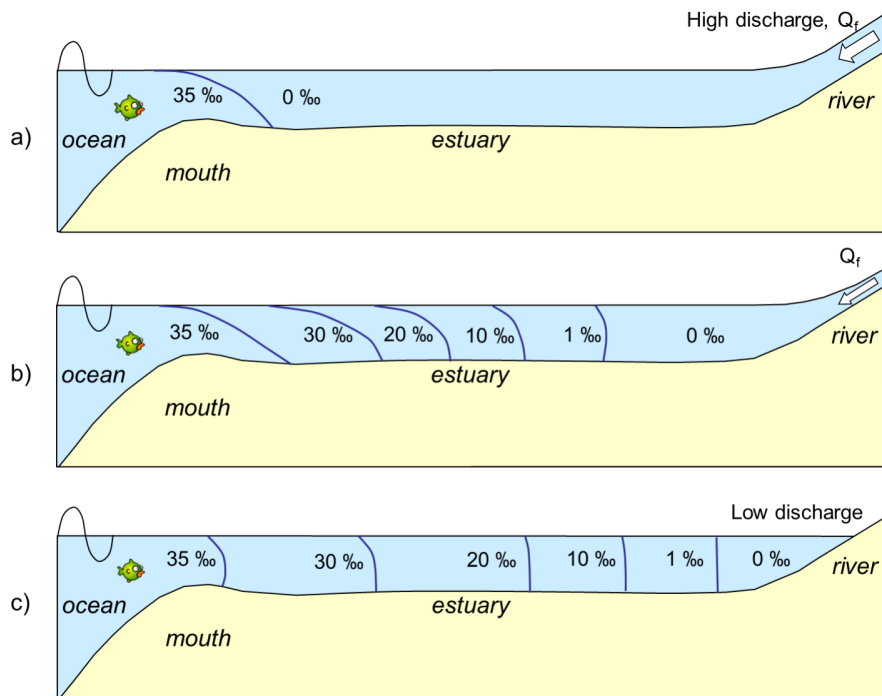


Figure 1.3: Longitudinal profile of salinity in a) stratified estuary, b) partially mixed estuary, and c) well-mixed estuary (H. H. G. Savenije, 2012)

time of estuaries represents the average time required to remove a fluid particle of freshwater or a conservative tracer from an upstream location (freshwater inflow) in an estuary to the sea. The flushing time is thus often used in the analysis of pollutant transport in estuaries (Ji, 2017). The flushing time in the estuary can be estimated from the volume of the estuary divided by the freshwater flow rate. Large freshwater inflow and strong tides lead to short flushing time (Martin et al., 1998).

Flushing time can affect the hydrodynamics, sediment distribution, and water quality processes such as eutrophication. An estuary with a very short flushing time is unlikely to have algal blooms because algae may not have enough time to grow before flushing out of the system (Lancelot & Muylaert, 2011). In addition, a waterbody with flushing shorter than the doubling time of algal cells inhibits the formation of algal blooms (Ji, 2017). Therefore, the flushing time is useful to evaluate the exchange rates of biogeochemical processes in estuarine systems such as nutrient fluxes, chlorophyll-*a* concentrations, primary production (Bianchi, 2007).

1.1.3 Biogeochemical processes

Major processes affecting nutrients concentrations in estuaries include (1) algal uptake and release, (2) hydrolysis converting particulate organic nutrients into dissolved organic forms, (3) mineralization and decomposition of dissolved organic nutrients, (4) chemical transformations of nutrients, (5) sediment sorption and

1. Background and state of the art

desorption, (6) settling of particulate matters, (7) nutrient fluxes from the sediment bed, and (8) external nutrient loadings (Ji, 2017). Figure 1.1 shows an overview of biogeochemical processes in estuaries under the influence of point discharges and tidal effects, especially on nutrients and phytoplankton parameters. The detailed processes related to oxygen, carbon, nitrogen, phosphorus, silica and phytoplankton will be detailed hereafter.

Oxygen dynamics

Dissolved oxygen (DO) is the most important parameter of water quality and is used to measure the available oxygen for biochemical activity in water. DO is depleted by oxidation of organic carbon, nitrification, and respiration and is replenished by surface exchange and photosynthesis (Bianchi, 2007). In polluted waters, bacterial oxygen consumption can rapidly outpace oxygen replenishment from the atmosphere and plant photosynthesis (Vanderborgh et al., 2007). The order of substances consumed in the water column of the estuaries depends on the oxygen conditions in the water. Table 1.2 presents the order of transformation in anoxic and oxic conditions.

Condition	Acceptor	Equation	Process	Products
Oxic	O ₂	$138O_2 + (CH_2O)_{106}(NH_3)_{16}(H_3PO_4) \rightarrow 106CO_2 + 16HNO_3 + H_3PO_4 + 122H_2O$	Aerobic respiration	CO ₂ H ₂ O
Hypoxic	NO ₃	$94.4HNO_3 + (CH_2O)_{106}(NH_3)_{16}(H_3PO_4) \rightarrow 106CO_2 + 55.2N_2 + H_3PO_4 + 177.2H_2O$	Denitrification	N ₂
Hypoxic	Mn (IV)	$236MnO_2 + (CH_2O)_{106}(NH_3)_{16}(H_3PO_4) + 472H^+ \rightarrow 106CO_2 + 8N_2 + 236Mn^{2+} + H_3PO_4 + 336H_2O$	Mn reduction	Mn (II)
Hypoxic	Fe (III)	$53SO_4^{2-} + (CH_2O)_{106}(NH_3)_{16}(H_3PO_4) \rightarrow 106CO_2 + 53S^{2-} + 16NH_3 + H_3PO_4 + 106H_2O$	Fe reduction	Fe (II)
Anoxic	SO ₄ ²⁻	$53SO_4^{2-} + (CH_2O)_{106}(NH_3)_{16}(H_3PO_4) \rightarrow 106CO_2 + 53S^{2-} + 16NH_3 + H_3PO_4 + 106H_2O$	Sulphate reduction	H ₂ S
Anoxic	-	$(CH_2O)_{106}(NH_3)_{16}(H_3PO_4) \rightarrow 53CO_2 + 53CH_4 + 16NH_3 + H_3PO_4$	Methanogenesis	CH ₄

Table 1.2: The sequence of terminal electron acceptors utilized (by oxidation reactions) for organic matter decomposition under varying O₂ concentrations in estuaries (Likens, 2010)

—

In the aquatic environment, the microbes use the electron acceptors in a progressive sequence, beginning with the most effective oxidizing agents such as O₂ and moving to weaker oxidizing agents as the stronger oxidizing agents are exhausted (Likens, 2010). In general, oxygen is firstly depleted, then oxidized manganese (Mn), and nitrate (NO₃⁻) will be converted to reduced manganese Mn(II) and N₂ gas. If respiration continues, which requires labile organic matter, oxidized iron Fe(III) may be converted to reduced iron Fe(II). Finally, methane is eventually

1. Background and state of the art

produced from organic matter, which microbes use in highly reduced environments as an electron acceptor (Likens, 2010).

Carbon dynamics

Like oxygen, organic carbon is an important element for the water quality of aquatic systems, which are considered a source of nutrients for aquatic organisms and can contaminate water at high concentrations (Bianchi, 2007). In water quality modeling studies, organic carbon can be divided into fast rate (labile) and slower rate (refractory) organic carbon. Labile particulate organic carbon (LPOC) has a decomposition time scale of days to weeks. Refractory particulate organic carbon (RPOC) has a decomposition time scale of months to seasons after settling and compacting into the sediment bed (Ji, 2017).

Sources of organic carbon

Unlike oxygen, whose origin is mainly from photosynthesis and exchange with the atmosphere, organic carbon comes from allochthonous and autochthonous sources. Specifically, organic carbon can come from organisms such as algae in estuaries and external sources such as wastewater, soils runoff, and groundwater input (Bianchi, 2007). In estuarine systems with strong human impact, the predominant organic carbon source often has high RPOC and low LPOC ratios (Bianchi, 2007; Ji, 2017). Sediments may also represent an important source to the water column of shallow estuarine systems (Bianchi, 2007).

In some estuaries, the Total Organic Carbon (TOC) is generally positively correlated with phytoplankton biomass, which indicates phytoplankton's dominance in organic carbon sources (Bianchi, 2007). However, many estuarine systems do not show positive correlations with phytoplankton biomass because of allochthonous inputs from soils, groundwater. The riverine sources are highly refractory in these estuaries, with only minor input from algal sources (Bianchi, 2007).

Carbon cycle in estuaries

The organic carbon cycle is closely related to nutrient cycles, including photosynthesis, respiration, and decomposition (Bianchi, 2007). The processes of carbon also depend on the oxygen condition in the water (Table 1.2). Figure 1.4 depicts the carbon cycle in aquatic systems, including major processes such as primary production, aerobic decomposition, and anaerobic decomposition. Under oxic conditions, bacteria decompose organic material to obtain energy for growth, break it down into simpler organic substances, and eventually convert it into inorganic substances. When insufficient oxygen is available, the resulting anaerobic decomposition is performed by completely different microorganisms (Ji, 2017). This process can produce hydrogen sulfide (H_2S), ammonia (NH_3), and methane (CH_4). The sequence transformation of OC under oxic and anoxic conditions is presented in Table 1.2.

1. Background and state of the art

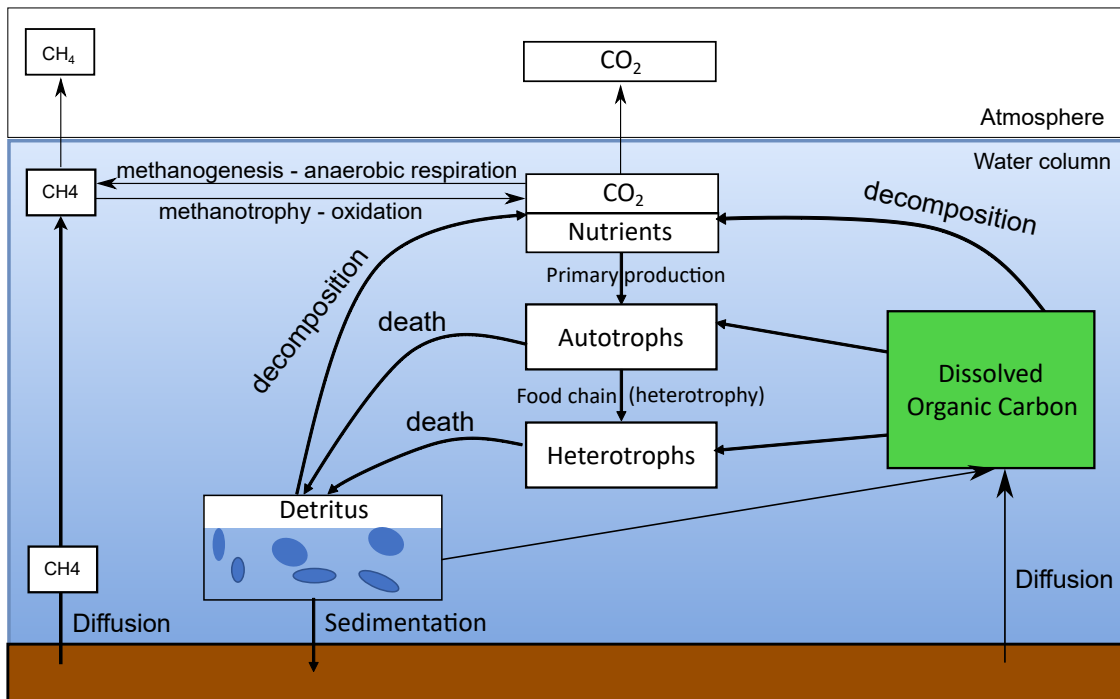


Figure 1.4: Carbon cycling in the aquatic system (adapted from Bianchi, 2007)

Nitrogen dynamics

Together with hydrogen, carbon, and oxygen, nitrogen is an essential element for living biomass. Nitrogen can thus limit rates of primary production in the aquatic system. The primary forms of reactive nitrogen which algae and bacteria can assimilate are nitrate, nitrite, ammonium (Likens, 2010). In estuarine systems, dominant inputs of N are linked to freshwater inputs from rivers (Nixon, 1995). Besides, groundwater discharge of N to estuaries has also been important (Bianchi, 2007).

Nitrogen cycles in estuaries

There are five main processes affecting N concentrations: nitrogen fixation, mineralization, nitrification, denitrification, algal uptake, anammox (Figure 1.5)

- Nitrogen fixation: Some blue-green algae can directly fix N_2 from the atmosphere. This process is usually insignificant in modeling studies.
- Mineralization: Organic nitrogen can be converted to NH_4^+ via mineralization.
- Nitrification: Under aerobic conditions, ammonia is oxidized to nitrite and nitrate via nitrification.
- Denitrification: Under anaerobic conditions, nitrate is reduced to gas forms as N_2 , N_2O and then released out of the water system.

1. Background and state of the art

- Algal uptake: Algae consume NH_4^+ and NO_3^- for growth via the photosynthetic process. Algae take up both NH_4^+ and $\text{NO}_2^- + \text{NO}_3^-$. While NH_4^+ is the preferred form of N for algal growth, algae will utilize $\text{NO}_2^- + \text{NO}_3^-$ for growth as the NH_4^+ concentration becomes depleted.
- Anammox: Some bacteria are capable of converting NO_3^- and NH_4^+ directly into gaseous forms. This process is less known in water quality models because of the frailty of anammox microorganisms in aquatic systems.

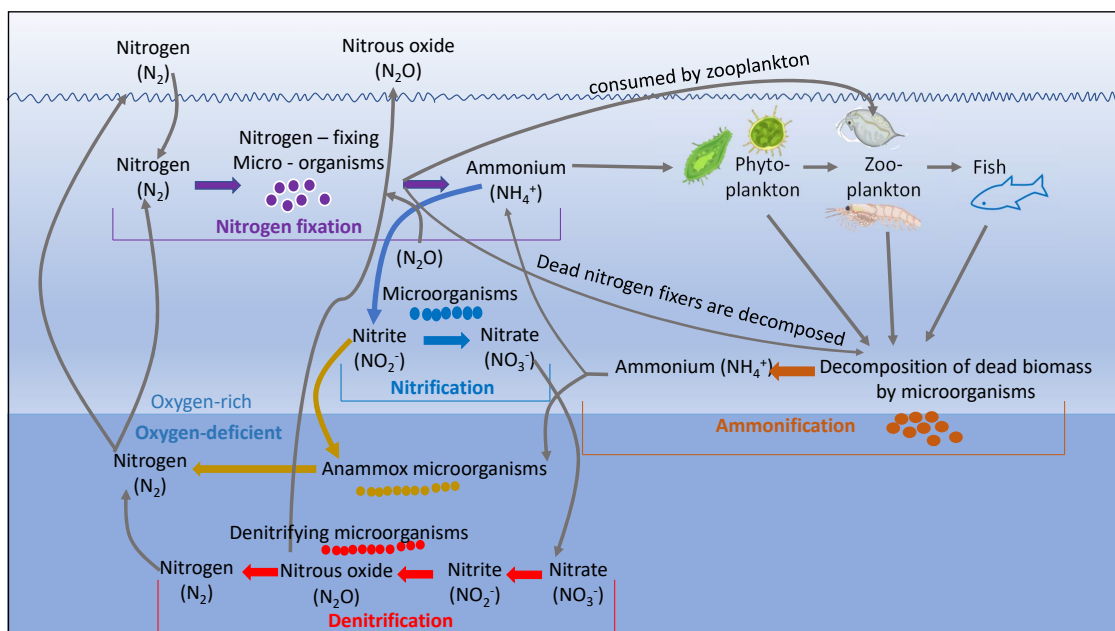


Figure 1.5: Nitrogen cycling in aquatic systems (adapted from Bange et al., 2017 and Pinto et al., 2021)

Phosphorus dynamics

Phosphorus (P) is an important element in aquatic ecosystems because it limits primary production (Bianchi, 2007). P is usually divided into the following categories:

- *Orthophosphate* frequently used to represent soluble reactive phosphorus (SRP). Orthophosphate constitutes the majority of phosphates. Many studies have focused on the *soluble reactive P* (SRP) (Bianchi, 2007).
- *Organic phosphate* is often found in plant tissue, waste solids, or other organic material. After decomposition, they can be converted to orthophosphate.

1. Background and state of the art

Unlike N, phosphorus does not have a gaseous phase. P has low solubility and is strongly adsorbed onto suspended solids that settle out of the water column.

Source of P

The pollution source of P often comes from human activities such as agricultural practices, domestic wastewater and animal production (Likens, 2010). Unlike N, inputs of atmospheric P sources are generally considered insignificant to coastal systems (Bianchi, 2007).

P cycles in estuaries

The P cycle operates similarly to the N cycle in many aspects, except the sorption process. Algae and plants take up dissolved phosphate (largely PO_4^{3-}), incorporate it into the food chain, and eventually return it to the water as organic P (Vilmin et al., 2015). Particulate phosphate sorbs to sediments and settle to the sediment bed (Aissa-Grouz et al., 2018; Vilmin et al., 2015). The fate and transport processes of phosphate are thus strongly influenced by the suspended sediment and sediment processes (Figure 1.6). It includes (1) inflow and outflow, (2) settling of the particulate P in the water column, (3); sorption and desorption in both the water column and the bed, (4); exchange between the water column and the bed via deposition/resuspension and diffusion, (5); losses by burial, and (6) algal uptake and metabolism.

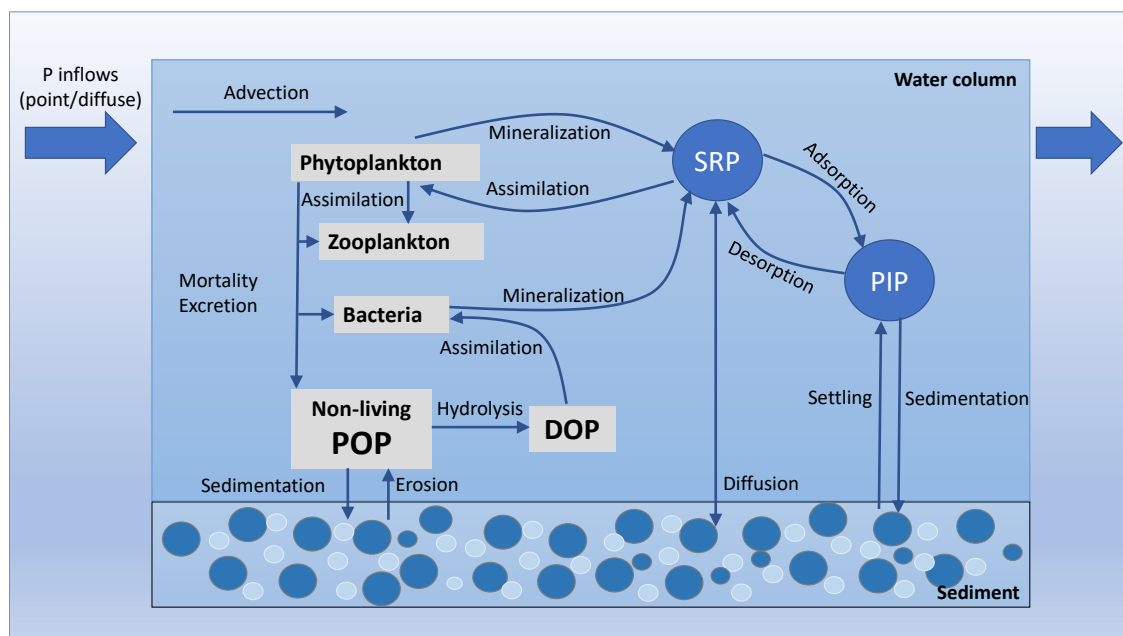


Figure 1.6: Phosphorus processes in aquatic. DOP is dissolved organic phosphorus, POP is particulate organic phosphorus, PIP is particulate inorganic phosphorus (adapted from Vilmin et al., 2015)

Difference between N and P

1. Background and state of the art

There are important differences between the two elements, including fixation, oxygen consumption, denitrification, settling process, and toxicity (Ji, 2017). These differences are reported in Table 1.3.

Table 1.3: Difference of N and P in aquatic systems

Process	N	P
Fixation	N can be fixed from N_2 gas by some bacteria. N is not as often limiting phytoplankton growth in estuaries.	P is not gaseous. There is a very small proportion of phosphine (PH_3 , a volatile P compound). Therefore, P has no atmospheric deposition contribution.
Oxygen consumption	N metabolisms normally use oxygen such as nitrification	P metabolisms do not use oxygen.
Denitrification	N can be removed from aquatic systems by denitrification, which converts NO_3^- to N_2O and N_2 .	No P exists in the gaseous form, so there is no real process of P removal from water
Settling and burial	N can adsorb to suspended sediments, but this process is not strong. Absorbed N easily returns to the water column before the suspended sediment settles to the bottom.	P has a strong ability to adsorb to suspended sediment and settle to the riverbed. This process (burial) can remove P from the water column.
Toxicity	NH_3 with high concentration can be toxic for fishes	P is nontoxic in an aquatic system

Silica dynamics

Silicon is an element required for the growth of some phytoplankton species. In water, silicates can convert to orthosilicic acid, $\text{Si}(\text{OH})_4$, the form that can be directly consumed by diatoms (Ji, 2017). Silica in waterbodies largely originates from the weathering and erosion of rocks on lands, and its concentrations in freshwater systems are usually between 0.7 and 7 mg L^{-1} (Horn and Goldman, 1994). Silica sources from human activities are usually minor, which is around 10% of the annual river load of DSi (Likens, 2010). The decrease of DSi is mainly due to diatom consumption, some studies have seen this phenomenon, but some activities such as dams can also reduce the DSi concentration.

As discussed above, the silica cycle is not as complex as C, N and P but is mainly concerned with the growth of diatoms, a phytoplankton group that uptake silica for development, forming an outer shell known as a frustule. After a diatom dies, DSi is released again to the water column and other nutrients through remineralization (Ji, 2017). Diatoms take up N, Si and P in a molar ratio of about 16:16:1 (N:P:Si). When dissolved silica (DSi) is depleted, the growth of diatoms is reduced, eventually leading to DSi concentrations limiting their growth. For instance, Chesapeake Bay exhibited strong Si limitation, with the ratio of available nutrients (Si:P) in the range of 100–300. The diatoms will then be replaced by other algae, such as green algae or cyanobacteria, that do not require DSi (Likens, 2010). In some urbanized estuaries, DSi limitation of diatoms has become more frequent because of increasing N and P inputs. Therefore, the increase in harmful algal blooms in estuaries over the past few decades may partly be due to lower Si availability (Likens, 2010).

1. Background and state of the art

Phytoplankton

Phytoplankton is an autotrophic organism and a key part of ocean and fresh-water ecosystems. Pierella Karlusich et al. (2020) reported that phytoplankton contributes to half of the global photosynthetic activity and can produce for 50% of dissolved oxygen in ocean.

Redfield ratio

Redfield ratio is commonly used to infer resource limitation in phytoplankton growth, which simply states that organisms will become limited by the resource in the lowest supply relative to their needs. Based on this ratio, Stumm and Morgan (1996) further modified the stoichiometry of the chemical reaction of photosynthesis (primary production) and oxidation (degradation) of organic matter by the following equation:



The ratio of nitrogen to phosphorus in phytoplankton biomass is usually in the range of 16:1 by moles (the ‘Redfield ratio’). If the N:P ratio is lower than 16:1, then N becomes the limiting factor for phytoplankton. However, most aquatic systems have P as a limiting factor (Bianchi, 2007; Likens, 2010). This can be explained by the treatment efficiency of P higher than N by the wastewater treatment plants. In addition, P is often easily adsorbed onto the sediment and buried in the riverbed.

Factors controlling phytoplankton growth

Seasonal changes in phytoplankton abundance and composition are primarily controlled by changes in riverine inputs, nutrients, tidal variability, algal respiration, light availability and consumption by grazers (Bianchi, 2007). In estuaries, the phytoplankton dynamics are controlled by salinity gradient, light availability, and water residence time (Lancelot & Muylaert, 2011). The most important factors controlling phytoplankton growth are the nutrients’ source and the ratio of these nutrient components (C, N, P) in the water. Processes that lead to a change in the concentration and ratio of nutrients will change the density of phytoplankton. Of particular importance for phosphorus is the adsorption to sediment particles in case of P limitation (Likens, 2010). Algae consume nutrients in a fixed stoichiometric ratio, and this ratio is relatively constant. When the limiting nutrient is depleted, the algal concentrations stop increasing, and the eutrophication process is retarded or even reversed. CO₂ is often not the limiting nutrient because of its dominance in nature. Silica receives little emphasis in water quality management because its abundant supply from natural sources is difficult to control.

1. Background and state of the art

1.2 State-of-art of water quality in tropical urbanized estuaries

1.2.1 Megacities in estuaries and coastal areas

Distribution of megacities in the 21st century

Estuaries are amongst the most populated areas of the world. About 60% of the world's population lives along estuaries and the coast. There are 22 in 32 largest cities in the world located beside estuaries (GRID-Arendal and UNEP, 2016). According to Hoornweg and Pope (2017), the rate of population growth and the formation of megacities by 2050 will be dominated by countries in Asia in tropical regions (Figure 1.7). This indicates that the pressures of population growth and urbanization for tropical estuaries will intensify in the future.

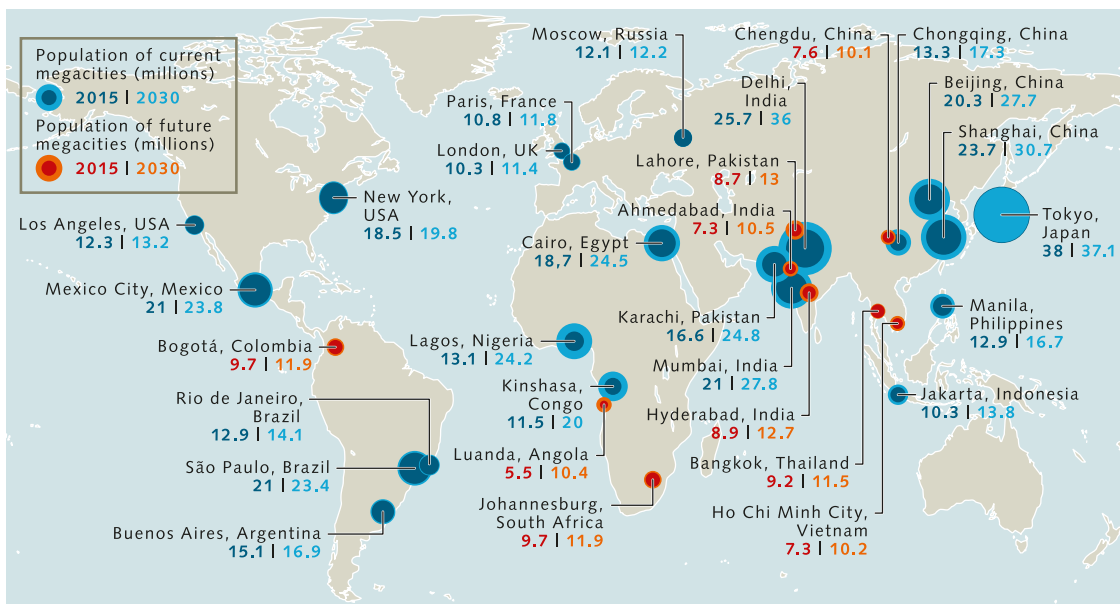


Figure 1.7: The world population of largest cities in 2015 and estimated in 2050 (Bange et al., 2017)

Water quality in estuaries of emerging countries

Since the last century, many studies have warned about the impact of urbanization on nutrient pollution in estuaries and coastal areas, especially in temperate countries in the US and Europe (Bianchi, 2007). The rapid urbanization of many emerging countries in the tropics, mainly in Asia and Africa, require some more research on these regions in this century. Comparing the nutrients export between 2000 and 2050, projections in several regions show that the total amount of nitrogen exported by rivers to the sea in South Asia will be many times higher than in

1. Background and state of the art

other regions (Figure 1.8). The rapid development of agriculture, industry, and urbanization of emerging countries significantly increase the nutrient loadings into the estuaries and, ultimately, the ocean.

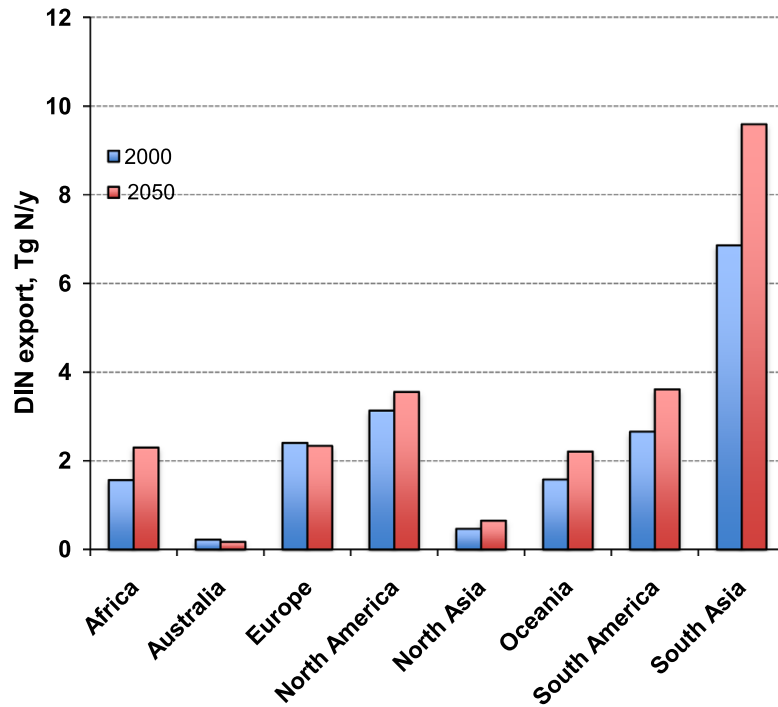


Figure 1.8: Dissolved inorganic nitrogen exported by rivers to the ocean in 2000 and predicted 2050 (Lee et al., 2016)

The imbalance between wastewater treatment efficiency and total wastewater emissions in developing countries in this century is similar to emissions in developed countries in temperate regions in the last century. In general, the studies in these areas showed a correlation between population and pollution emissions. Based on synthesis of Bianchi (2007), some notable reports are as follows. Survey results at the Skidaway River estuary (USA) from 1986 to 1996 showed a linear correlation between population growth and dissolved nutrients entering this estuary. During the 1990s, southeastern Queensland, Australia, was one of the most rapidly urbanizing regions globally, also observed this correlation. An increase in nutrients from industrial, agricultural, and municipal wastewater has contaminated estuarine waters, although estuaries are generally considered highly self-cleaning due to biogeochemical processes and seawater dilution. The eutrophication phenomenon was observed in many estuaries in temperate countries in the last century (Billen et al., 2011; Howarth et al., 2011).

Several studies have indicated the influence of megacities on tropical estuaries in developing countries. For instance, the impact of Ho Chi Minh Megacity (Vietnam) on the water quality in the Saigon River was reported (T. T. N. Nguyen et al., 2019). Other studies in tropical estuaries are the impact of Mumbai City (India) to

1. Background and state of the art

Mumbai coast (Sawant et al., 2007), Rio de Janeiro City (Brazil) to Guanabara Bay (de Carvalho Aguiar et al., 2011), Shenzhen City (China) to Shenzhen Bay (Zhou et al., 2020), Bangkok to Gulf of Thailand (Buranapratheprat et al., 2021), and Abidjan (Africa) to Ivory Coast (Dröge & Kroese, 2007). In developed countries, nutrient pollution is being controlled thanks to wastewater treatment systems and urbanization control. In many urbanized estuaries in developing countries, nutrient pollution is still not controlled, leading to an increase in eutrophication. For instance, phytoplankton biomass concentrations in Jakarta Bay (Indonesia) increased continuously from 2001 to 2013 (Damar et al., 2019).

1.2.2 Insights of biogeochemical processes in tropical urbanized estuaries

Eutrophication is one of the well-known topics when assessing anthropogenic impacts on estuaries and coastal waters. While eutrophication in temperate estuaries is usually limited by nitrogen concentration (Howarth et al., 2011), phosphorus limitation is more prevalent in tropical estuaries (Likens, 2010). Differences in climatic conditions such as temperature and light intensity between tropical and temperate estuaries can lead to differences in nutrient dynamics. This section provides a literature review on the biogeochemical processes in tropical estuaries under the influence of urbanization.

The nutrients retention

Estuaries can act as a buffer zone for pollutants originating from upstream rivers. A large part of the solutes and particles transported by the rivers can be retained and/or removed by estuaries before reaching the sea (Romero et al., 2019). Retention may include the assimilation of pollutants through the microorganism activities, phytoplankton consumption (Romero et al., 2019; Trinh et al., 2012) or by transformation; for example, NH_4^+ is removed by nitrification, or organic carbon is oxidized to CO_2 by aerobic degradation process. Similarly, the denitrification of NO_3^- to N_2 is also considered a natural decontamination mechanism of the estuaries (Garnier et al., 2009). Besides the biochemical processes, there are also physical processes such as adsorption of P into suspended sediments and the burial of pollutants into bed sediments (Aissa-Grouz et al., 2018; Vilmin et al., 2015). The retention and removal of nutrient pollutants including C, N, and P are mostly accounted for the processes described in Figure 1.9, including (1) nutrients (C, N, P) cycling, (2) adsorption-desorption and exchange at sediment interface, (3) burial (sedimentation), and (4) nutrient consumption by primary production (e.g., algal bloom).

1. Background and state of the art

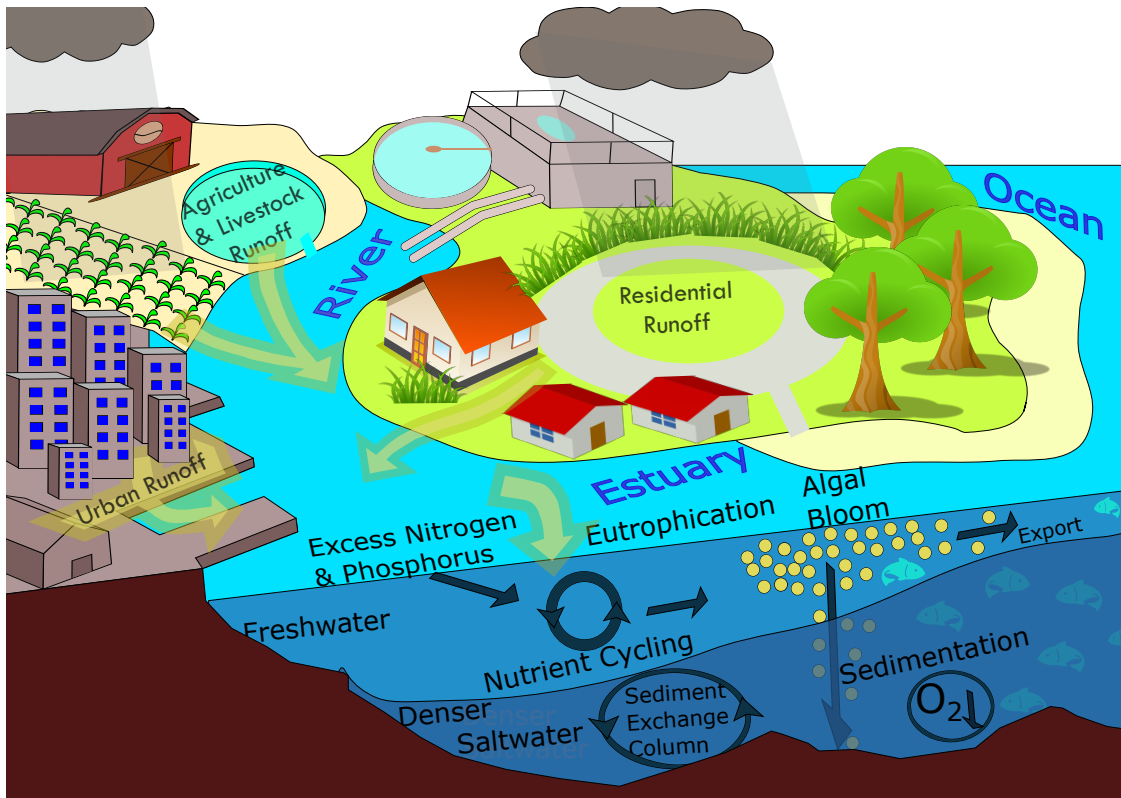


Figure 1.9: Conceptual model of nutrient retention (or so-called buffer zone/filtering zone) by estuaries. The main sources of pollution include (1) agriculture, livestock runoff, (2) urban runoff, (3) domestic, industrial wastewater. Mechanisms of nutrient retention and removal in estuaries include (1) nutrients (C, N, P) cycling (transformation), (2) adsorption-desorption and sediment exchange, (3) burial (sedimentation), (4) nutrient consumption by primary production (e.g., algal bloom) (adapted from Paerl et al., 2006).

According to Yu et al. (2019), the key factors controlling nutrient concentrations by removal, transformation or retention are still poorly understood in tropical-subtropical estuaries because of the lack of experiments and modeling application. However, the retention capacity of estuaries is likely to depend on the hydrological characteristics, particularly the flushing capacity, more than the climatic conditions in a short-term observation (B. D. Eyre, 2000; Garnier et al., 2013; Romero et al., 2019). River-dominated estuaries (with large freshwater inflow) typically have a strong flushing capacity (short retention time) with a lower estuarine retention capacity than estuaries with a long retention time. Le et al. (2010) found that in tropical systems, there are higher phosphate retention and lower silica retention than the temperate systems, while nitrogen retention was quite similar in these systems. However, the quality of pollutant sources in these two systems is often different, leading to a change in the main mechanisms of nutrient retention between them.

1. Background and state of the art

Factors	Temperate estuaries	Tropical estuaries
Climate ^(a)	<ul style="list-style-type: none"> • Season: 4 seasons • Light: Variable • Temperature: Variable 	<ul style="list-style-type: none"> • Two seasons: dry and rainy season • Light: Higher and relative constant • Temperature: Higher and relative constant
Hydrology ^(a)	<ul style="list-style-type: none"> • Discharge: More stable • Flushing capacity: More stable • Less mangrove system in temperate estuaries 	<ul style="list-style-type: none"> • Discharge: Large seasonal variation • Flushing capacity: High variation • The strong impact of mangroves in downstream
Nutrient loads ^(a)	<ul style="list-style-type: none"> • Stable or decrease in recent years 	<ul style="list-style-type: none"> • Increase by urbanization
Variables in water column ^(a)	<ul style="list-style-type: none"> • Silica: Can be limiting for production • Turbidity: more stable 	<ul style="list-style-type: none"> • Silica: Less likely to limit primary production • Turbidity: high seasonal variation
Variables in bottom sediments ^(a)	<ul style="list-style-type: none"> • High organic carbon content 	<ul style="list-style-type: none"> • Higher organic carbon and carbonate • High concentration of PO_4^{3-}
Seawater ^(a)	<ul style="list-style-type: none"> • Variable concentrations because of seasonal biological activities 	<ul style="list-style-type: none"> • Seawater concentrations are more stable due to constant input of insolation (light, temperature) than temperate
Phytoplankton ^(a)	<ul style="list-style-type: none"> • Easier shift to non-silicious phytoplankton • Reaction rates are lower ^(a, b) • There is a limitation of production in the cold period ^(b) • Nitrification is no longer a major factor because of the decrease of NH_4^+ ^(d) 	<ul style="list-style-type: none"> • The dominant phytoplankton group is diatom • Reaction rates: Higher biological uptake and excretion ^(a) • No temperature limitation for production ^(b) • Dominated by OM oxidation, nitrification, deposition ^(f, g, h)
Biogeochemical process		
Nutrient export to coastal zone, ocean	<ul style="list-style-type: none"> • Low nutrient retention rate. 75% of nutrients can be exported to the ocean. Less seasonal variation ^(c) • Less than 10% of nutrients were retained/buried in sediment ^(b) 	<ul style="list-style-type: none"> • Similarly, retention of nutrients is low in the rainy season but much higher in the dry season, thus less nutrient export ^(f) • Higher phosphate retention (higher sorption), but small nitrogen burial (around 2.5%) in sediment ^(b)
Assimilation capacity	<ul style="list-style-type: none"> • Net removal of N and Si, but a source of P because of P desorption ^(c) • 30–65% N can be removed by physical, biological processes in estuaries ^(d) 	<ul style="list-style-type: none"> • Act as a sink for OC, NH_4^+, PO_4^{3-} but a source for NO_3^- ^(g) • Higher N removal because of higher denitrification rate ^(b) • E.g., 50%, 37% and 11% C, N, P of external sources were removed by Pearl River in 1999 ^(g)
Climate change ^(b)	<ul style="list-style-type: none"> • Four seasons may become dry and wet seasons 	<ul style="list-style-type: none"> • Greater contrasting seasonal behavior
a: Eyre et al., 1999 b: Tappin 2002	c: Romero et al., 2019 d: Nixon et al. 1996	e: McKee et al., 1999 f: Le et al., 2010, Trinh et al., 2010 g: Hu et al., 2009, h: Yu et al. 2019

Table 1.4 details the differences between tropical and temperate estuaries in terms of nutrient retention and removal in estuaries before discharge into the sea. In addition, the differences in hydrological conditions, climate, and dominant bio-

1. Background and state of the art

Table 1.4: The differences between temperate and tropical estuaries

geochemical processes of these two regional estuaries are compared. Hydrologically, temperate estuaries generally have a more stable upstream discharge than tropical estuaries. This reduces the variation in the flushing capacity of temperate estuaries between seasons compared with the distinct seasonal variation of tropical estuaries (B. Eyre & Balls, 1999). In other words, in contrast to relatively constant retention capacity in temperate estuaries, the tropical estuaries often have very low retention in the rainy season to high retention in the dry season (McKee et al., 2000). In terms of biogeochemical processes, nitrification is likely one of the most important transformation processes in the water column in urban tropical estuaries because of very high ammonium input from domestic wastewater (Yu et al., 2019). In contrast, ammonium inputs of in temperate estuaries have largely dropped thanks to improved wastewater treatments, so that nitrification processes are no longer a major factor (Romero et al., 2019).

Eutrophication processes

Residence time and flushing capacity are factors that strongly influence retention capacity in estuaries. Estuaries with long residence time (weeks to months) have higher retention and removal capacity than estuaries with short residence time. However, long-term exposure to high nutrient pollutants may lead to algal blooms (Romero et al., 2019).

Definition of eutrophication

Eutrophication is defined as a natural process of increasing the organic material production over time. However, the research and definition of eutrophication mainly focus on “anthropogenic eutrophication” that is, the process of eutrophication under the human influence (Le Moal et al., 2019). Anthropogenic eutrophication is defined as a syndrome of an aquatic ecosystem associated with the overproduction of organic material induced by anthropogenic inputs of phosphorus and nitrogen (Le Moal et al., 2019). In general, an increase in nutrient inputs causes an increase in phytoplankton biomass and a decrease in light penetration in the water column, producing an undesirable disturbance to the balance of organisms in the water (Durand et al., 2011). Figure 1.10 depicts the interpretation of an increase in eutrophication under increasing water nutrients, leading to an increase in phytoplankton in the water, beginning with diatoms then macrophytes. When the number growth of diatoms is maximum, the oxygen in the water is depleted, and the formation of harmful phytoplankton species such as cyanobacteria replaces diatoms, and biodiversity in the water also decreases.

A literature review of eutrophication

1. Background and state of the art

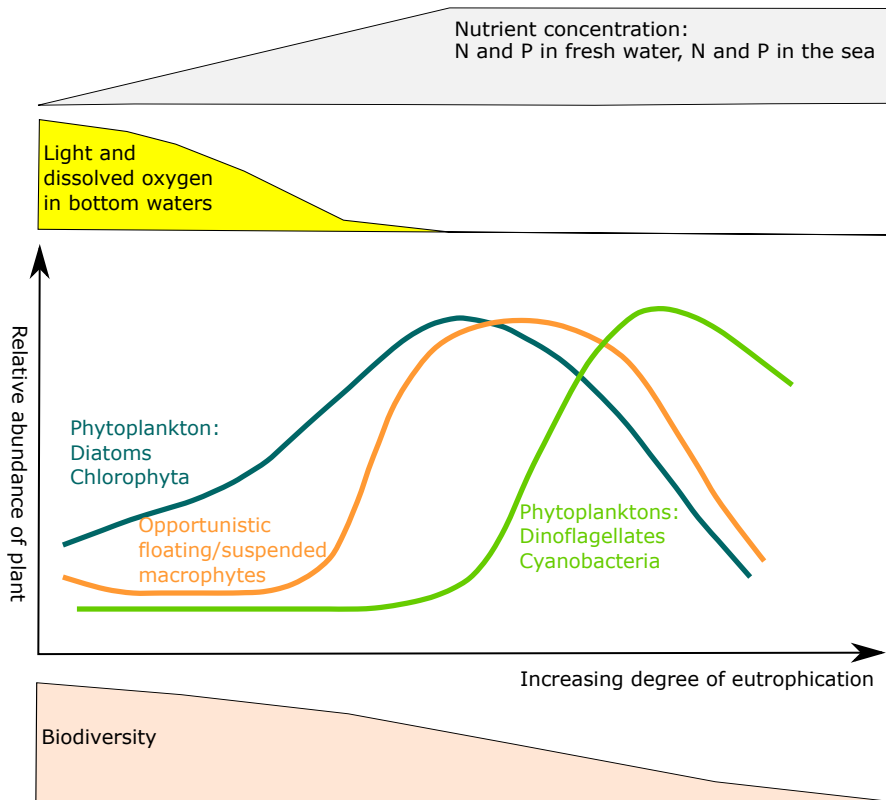


Figure 1.10: Changes in physicochemical parameters and the relative dominance of plants and biodiversity depend on the degree of eutrophication in an aquatic environment (Le Moal et al., 2019)

Studies on eutrophication have been numerous since the 1970s but focused solely on explaining the causes and consequences of eutrophication for lakes. Eutrophication in estuaries and coastal areas has been studied extensively since the 1990s (Cloern, 2001). These days, eutrophication studies in rivers, estuaries and coastal areas are viewed as a “new wine” in an “old bottle” (Le Moal et al., 2019). Research on eutrophication is considered the new wine because nutrient pollution (as the main cause of eutrophication) has changed from excess phosphorus to excess nitrogen. Meanwhile, consequences of eutrophication such as algal bloom, anoxia from the 1970s in the lakes are still present in rivers, estuaries and coastal areas today (Le Moal et al., 2019).

Eutrophication processes and consequences

The conceptual model of eutrophication and consequences is shown in Figure 1.11. The mechanism and consequences of eutrophication in different aquatic systems share the same general mechanism of eutrophication development (Whitall et al., 2007). The intensity of eutrophication depends on environmental factors, residence times, high temperatures, and sufficient light utilization (Le Moal et al., 2019). The little difference between the current conceptual model of eutrophication for estuaries and other aquatic systems is the change in rates of ecosystem

1. Background and state of the art

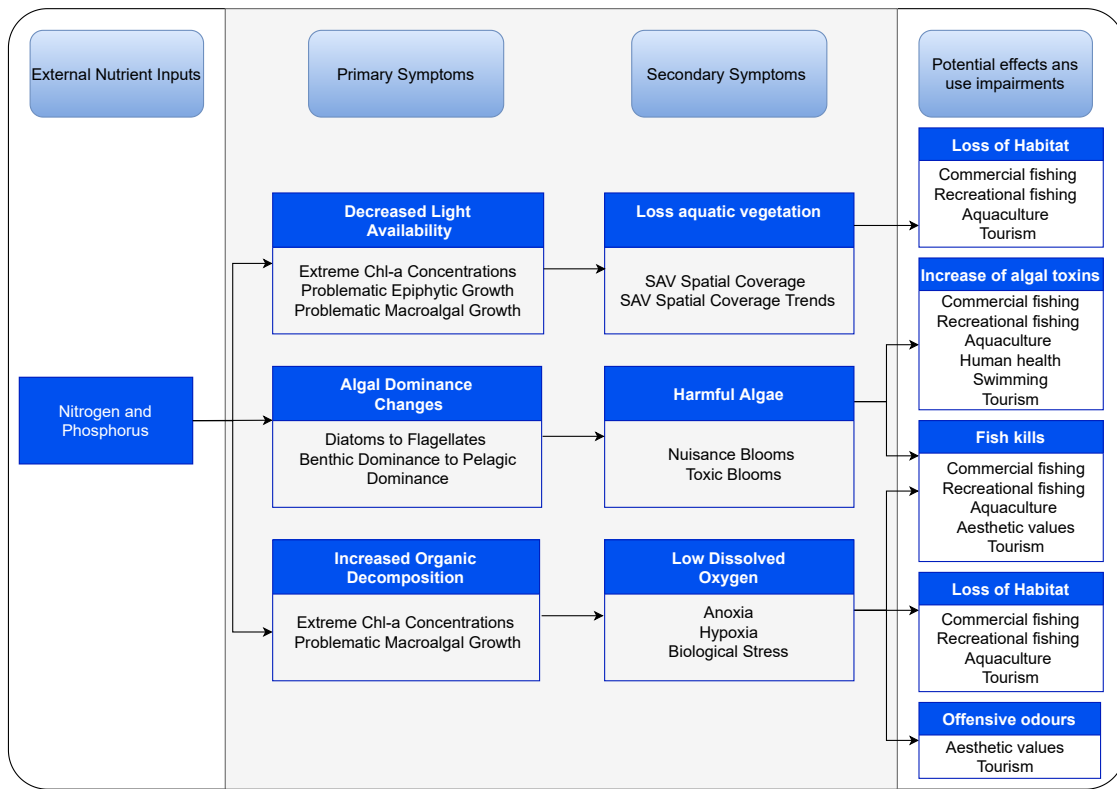


Figure 1.11: Conceptual model of eutrophication and consequences (adapted from Whitall et al., 2007)

metabolism (Whitall et al., 2007). The most notable effects of eutrophication are algal proliferation, or blooms, leading to large biomass production. Then these large biomasses are degraded, resulting in oxygen depletion in the aquatic environment. The hypoxia or anoxia condition can change all the communities' structure and function (plants, zooplankton, benthic fauna, fish). There is also the formation of toxic gases such as H₂S, or greenhouse gases (CO₂, CH₄) (Le Moal et al., 2019).

Eutrophication not only harms aquatic organisms but also directly affects the economy and human health. For example, the formation of toxic phytoplankton such as cyanobacteria has affected drinking water sources of approximately 400,000 residents in Ohio (USA) in 2014 (D. R. Smith et al., 2015). In coastal waters, eutrophication has indicated one billion dollars losses per year to the fisheries economy of European countries (Wurtsbaugh et al., 2019). Many North American and European countries effectively reduced eutrophication and many eutrophication-related problems for freshwater rivers, lakes, and coastal oceans (Wurtsbaugh et al., 2019). Although there are no statistics on the impact of eutrophication in developing countries, particularly in Asia, these reports in developed countries suggest that human health and economic losses in developing countries may be stronger because of the increasing severity of eutrophication in recent years.

1. Background and state of the art

Greenhouse gases

In addition to studies warning about the risk of eutrophication in estuaries, there has been more and more research on greenhouse gas emissions (GHGs) in recent years (Borges et al., 2018; Daniel et al., 2013; Marescaux et al., 2018). Estuaries offer ideal conditions for GHGs production since they receive large amount of organic carbon and nitrogen (Daniel et al., 2013).

Although estuaries occupy a small portion of the global ocean area (about 0.2–0.3%), their CO₂ emissions are a disproportionately large flux (about 0.25 Pg C yr⁻¹) compared to the CO₂ exchanges between the open ocean and atmosphere (Bauer et al. (2013), Figure 1.12). Similarly, Bange (2006) estimated that N₂O accounted for about 33% of the oceanic greenhouse gases emission. In the study of Global Methane Budget 2000–2017, Saunois et al. (2020) estimated that around 50% of CH₄ emissions from the coastal and open sea were attributed to estuaries (3–3.5 Tg CH₄ yr⁻¹). While CO₂ makes the largest contribution in terms of concentration to global warming, methane (CH₄) and nitrous oxide (N₂O) are important trace gases in the atmosphere. CH₄ and N₂O absorb infrared radiation respectively 300 and 25 times more effectively, than CO₂ (Burgos et al., 2015). Therefore, the impact of these two gases on global warming is many times greater than that of CO₂. The increase in eutrophication at the estuaries poses a risk of increasing their concentrations. However, the uncertainty of estuarine GHGs emission flux is high due to limited spatial and temporal coverage during field observations (Bauer et al., 2013).

In contrast to developed countries where GHGs in estuaries are expected to decrease because of nutrient and organic carbon reduction (Murray et al., 2015), such emissions would likely increase in developing countries, especially in tropical and sub-tropical regions (Cotovicz et al., 2016). Indeed, most developing countries are located in the tropical region and have high population densities but limited environmental management practices (e.g., sewage treatment facilities). Uncertainties of GHGs estimation might be high in developing countries in Southeast Asia due to the lack of GHGs monitoring (David et al., 2018). The knowledge on how GHGs emissions are affected by water pollutants in a fast-growing urban area is still limited (Fernandez et al., 2020; Li et al., 2021; I. Park & Song, 2018). Several studies clearly showed the increase of N₂O emission because of increased nitrogen loadings to estuarine environments, stimulating microbial processes (Bange, 2006; Garnier et al., 2009). The existing research indicates that the most important factors controlling N₂O emission are dissolved inorganic nitrogen (DIN) and oxygen levels. Bräse et al. (2017) found that the main process responsible for N₂O production in Elbe Estuary (Germany) was denitrification in the 1990s, but it has been changed into nitrification since 2008. The positive relationship between N₂O and NH₄⁺ in several studies in tropical estuaries (e.g., Mandovi estuary, India; Yangtze River, China) suggested that nitrification is the main process for N₂O production

1. Background and state of the art

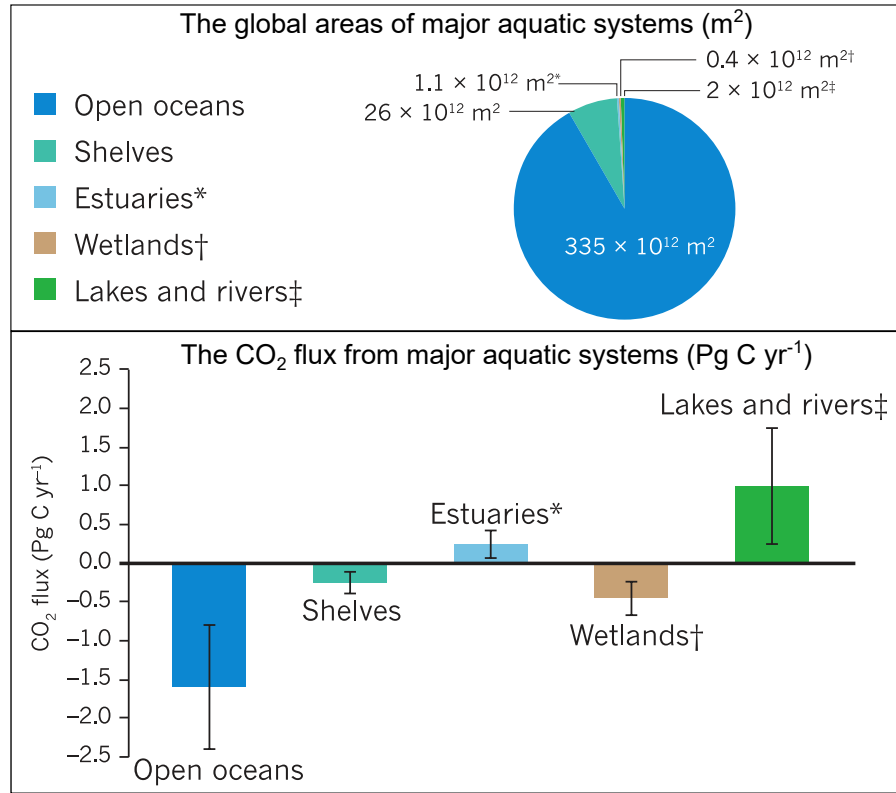


Figure 1.12: The contribution of major aquatic systems to global CO_2 emission (Bauer et al., 2013)

(Manjrekar et al., 2020; G. L. Zhang et al., 2010). However, the contribution rate of nitrification or denitrification to N_2O production is still unclear, e.g., in tropical systems (Beaulieu et al., 2019; Daniel et al., 2013).

GHGs vs. eutrophication

The GHGs formation in urbanized estuaries is also influenced by the same source, which is wastewater from megacities. Eutrophication can significantly affect GHGs emissions (Li et al., 2021), such as reducing CO_2 emissions by intense photosynthesis, while CH_4 emissions have been observed to rise exponentially with eutrophication indicators (i.e., chlorophyll a) (DelSontro et al., 2019). CO_2 concentrations depend on photosynthesis and aerobic/anaerobic respiration of organic matter (Davidson et al., 2015; Silvennoinen et al., 2008). Higher CH_4 emissions can be expected from tropical and subtropical regions than temperate ones because of higher pollutant inputs and stronger biological activities (Huertas et al., 2019). Autochthonous primary production arising with a high amount of untreated domestic wastewater can create easily biodegradable organic matters. More CH_4 is thus produced due to oxygen consumption and anaerobic decomposition of organic matter from urban effluents (Garnier et al., 2013; Huttunen et al., 2003). Grasset

1. Background and state of the art

et al. (2020) proposed a conceptual model describing non-linear relations between trophic status and GHGs emission in aquatic systems (Figure 1.13). This pattern is established based on the observed data at 20 freshwater mesocosms. As trophic status increased from mesotrophic to hypereutrophic, there was a nearly linear increase in CH₄ while CO₂ decreased gradually. However, the CO₂ equivalent (total CH₄ and CO₂ in terms of global warming potential) is elevated at hypereutrophic (Grasset et al., 2020).

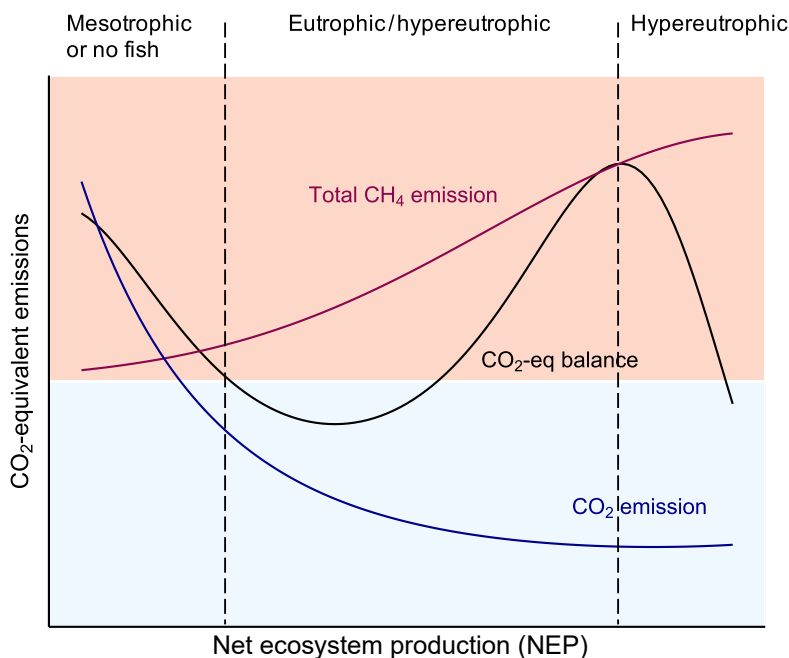


Figure 1.13: Conceptual model of net ecosystem production (gross primary production - respiration) and CH₄, CO₂ emissions in the aquatic system (Grasset et al., 2020)

Benassi et al. (2021) and Fernandez et al. (2020) found that GHGs concentrations were highest in hypereutrophic regions or during large phytoplankton blooms, i.e., higher trophic state resulting in higher GHGs emissions. In lakes, CH₄ emission can be doubled under hypereutrophic conditions, especially in tropical regions with a 2°C increase (Sepulveda-Jauregui et al., 2018). Beaulieu et al. (2019) also concluded that an increase in eutrophication by triple nutrient concentrations in the next century might lead to a double concentration of CH₄ (Figure 1.14). (L. Zhang et al., 2021) reported that the increase in CH₄ emissions would be even faster than the increase in nutrients at a subtropical region if phosphorus is the limiting factor of eutrophication.

Studies on the impact of urbanization on tropical estuaries are still limited. However, these studies also have similar findings with other studies in developed countries on the impact of eutrophication on GHGs emissions (e.g., Cotovicz et al. (2021); W. Zhang et al. (2021); X. Wang et al. (2018); Noriega et al. (2013); Skerratt et al. (2013); Benassi et al. (2021)). Most urbanized tropical estuaries

1. Background and state of the art

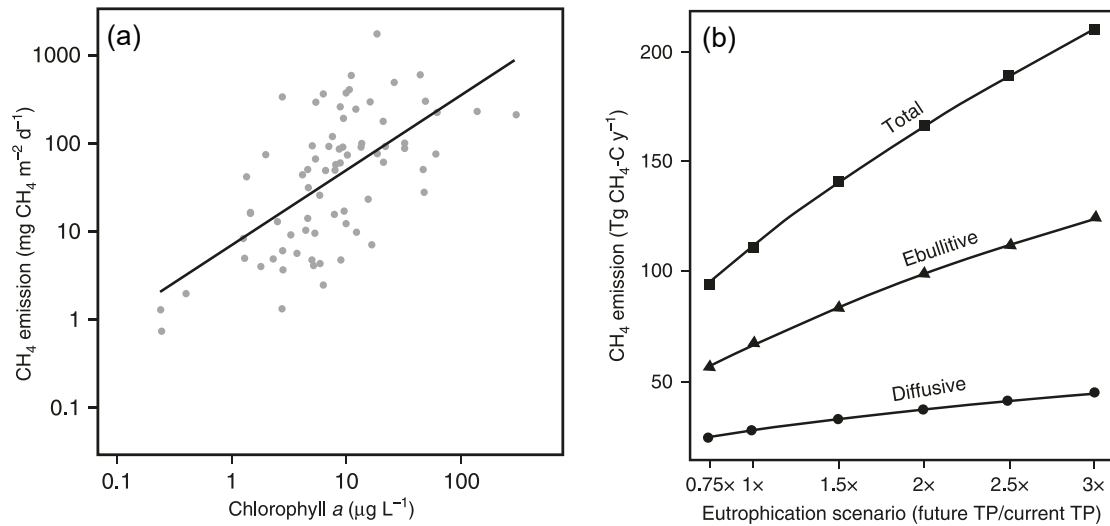


Figure 1.14: (a) Relationships between CH_4 flux and chlorophyll-a in the water column and (b) predicted CH_4 emission in eutrophication scenarios in lakes (Beaulieu et al., 2019)

show that CO_2 , CH_4 , and N_2O are linearly correlated with increased eutrophication (e.g., Cotovicz et al. (2016); Cotovicz et al. (2021)). In addition, studies in urbanized tropical estuaries mainly focused on one or two GHGs, and only surveyed a short period without season effects and a short area (focus mainly urban area). This leads to interpretations of the interaction of eutrophication and GHGs that are not fully described. For example, the reduction of CO_2 towards the sea may be due to either dilution, consumption of phytoplankton (Noriega et al., 2013), and CO_2 to CH_4 conversion. Besides, the change of N_2O concentration under the variation of NH_4^+ and NO_3^- also affects other GHGs. Therefore, a complete investigation including physiochemical parameters, nutrients, organic carbon and GHGs is needed to understand the processes leading to changes in eutrophication and GHGs in estuaries.

1.2.3 Difficulties of water quality management in developing countries

Managing estuaries means managing human activities, which involves complex socio-economic and political issues (Atkins et al., 2011). As a result, the management of estuaries and the coastal area has a long track record of a few successes and many failures or under achievements (Wolanski & Elliott, 2014). According to Wolanski and Elliott (2014), the essence of anthropogenic problems comes from three sources: (1) materials that are put into the estuaries, (2) materials taken out from the estuaries, and (3) wider problems such as climate change. The failure to control “materials that are put into the estuaries” is due to a lack of balance between wastewater volume and wastewater treatment capacity. The failure to

1. Background and state of the art

quantify the “materials taken out from the estuaries” is due to the lack of intensive monitoring and biogeochemical model application that allows the calculation of retention capacity and transformation of nutrients.

Difficulties for the implementation of water quality and hydrological monitoring in estuaries

While these failures have been and are being remedied in developed countries, they are increasingly common in emerging countries with megacities. Ultimately, addressing these issues requires understanding the nutrient dynamics at these urbanized estuaries through appropriate monitoring programs and modeling applications. However, understanding the nature of estuaries through observation is a long-term mission and a high cost because of the complex fluctuations of tidal estuaries. There is thus currently no universal method for designing water quality monitoring programs that guarantee both spatial and temporal scales for all estuaries (Hartnett et al., 2011). Building appropriate water quality monitoring programs that represent estuaries is difficult because of complex pollutant transport patterns at tidal estuaries. Two important factors to consider for monitoring programs at estuaries are (1) appropriateness of time series and (2) appropriateness of sampling station density (de Jonge et al., 2006). High-frequency monitoring is essential to address current and future water-quality issues/evaluations in estuarine systems (Etcheber et al., 2011).

The characteristic feature of estuaries and tidal rivers is the influence of the tides, which usually have two high tides and two low tides, i.e., twice landward and twice seaward flow per day. This has resulted in water quality having a strong fluctuation depending on the hydrological regime. As shown in Figure 1.15, the survey results of indicators such as salinity, DO, and turbidity fluctuated in intensity and differed between indicators within only 48 hours of the survey. Therefore, high resolution of hydrologic regimes monitoring is essential to understand the variability of water quality in estuaries (Etcheber et al., 2011).

Identifying monitoring locations is important because of large fluctuations of concentrations with tide, season and weather conditions (Hartnett et al., 2011). This explained freshwater river was increasingly monitored, while estuaries were not, although they received high loads of pollutants (de Jonge et al., 2006). As shown in Figure 1.16, with only three routine monitoring stations along the salinity gradient, the results always show the effect of mixing between fresh and seawater, i.e., the phosphate concentration only decreases towards the sea. However, longitudinal profiles with more points allowed observing more complex oscillation trends, especially in the region with salinity concentrations from 10 to 20 (Figure 1.16).

1. Background and state of the art

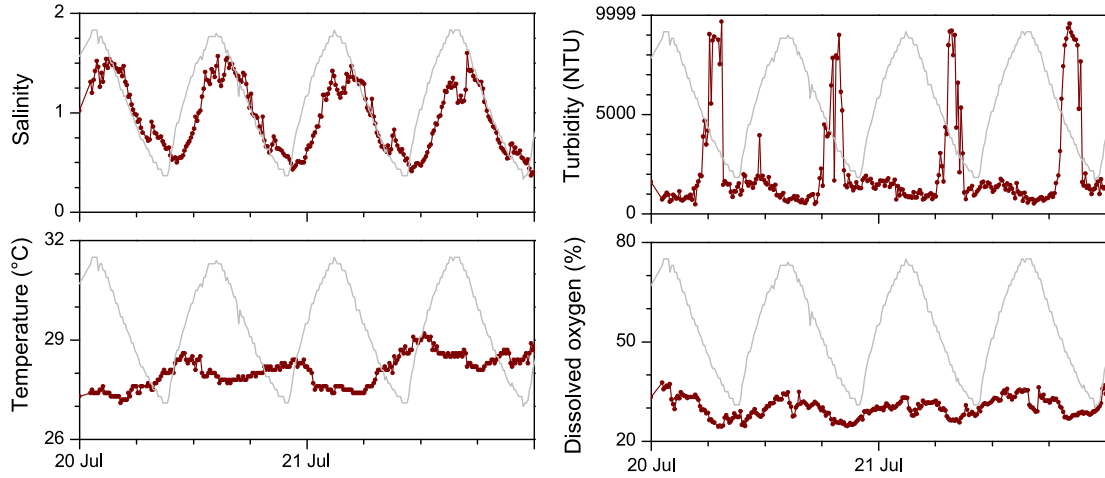


Figure 1.15: Example of variations of salinity, temperature, turbidity, DO and water level in two days 20-21/07/2006 at Gironde estuary (Etcheber et al., 2011). The grey line is the tide fluctuation, and the red one is the parameter fluctuation.

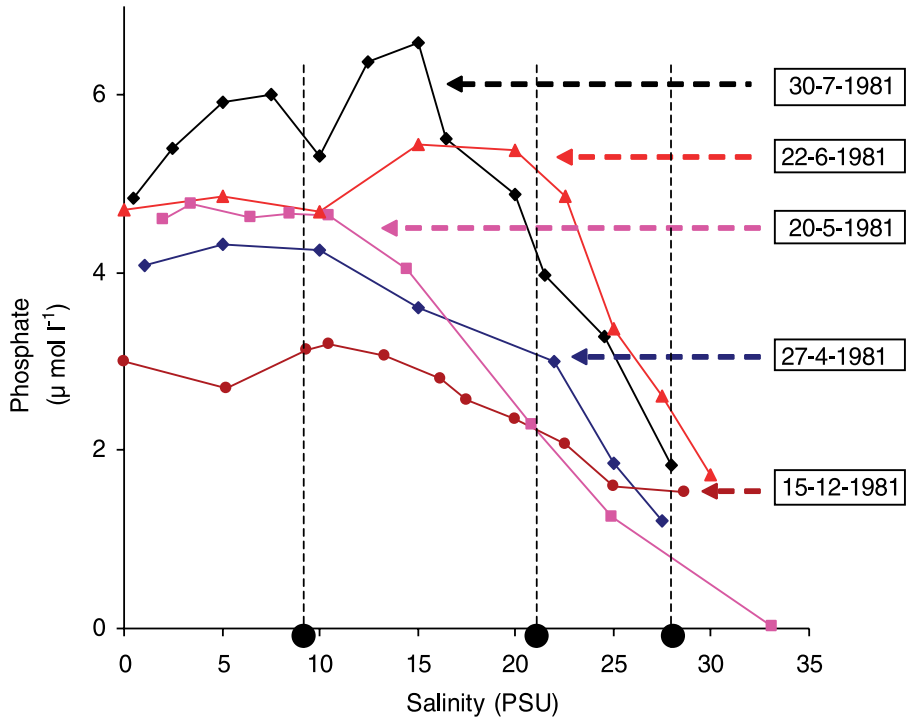


Figure 1.16: Comparison of survey results at three monitoring stations (black dots) and longitudinal profiles along a salinity gradient (de Jonge et al., 2006)

Difficulties for the implementation of water quality modeling tools

In developing countries, the difficulty in applying water quality modeling to estuaries mainly stems from the required data. As discussed above, emerging countries with inadequate monitoring programs have led to insufficient information to implement estuarine models. Missing data also leads to the inaccurately described biogeochemical processes and pollutant transport of estuaries. The quantity and

1. Background and state of the art

quality of the data determine the confidence that can be placed on the model application. Uncertainties in external driving forces, such as winds and inflow rates, propagate uncertainties in model results. If the data used for model setup and calibration is not reliable, the results would not be reliable, no matter how well the model was applied to previous studies.

Lack of modelers can be widespread in developing countries. However, the lack of connection between the modeler and the monitoring center is more critical. Failure to apply well documented (e.g., MIKE, a commercial model) can stem from the modeler's failure to understand the sampling conditions, data uncertainty. Although calibration and validation are based on observed data, no field data should be considered perfectly accurate. Therefore, the difficulty in applying the model in developing countries is from the lack of modelers who can understand internal processes and observation.

In addition, failures in model application leading to wrong decisions in water quality management of estuaries can also be attributed to model selection. Because of the lack of data, it is preferable to use simple models over more complex ones. In particular, simple models often ignore the retention and transformation characteristics over time (e.g., seasonal) of estuaries, which does not detect eutrophication growth or algal blooms over time (Arndt et al., 2009, 2011). Therefore, understanding and using models that accurately describe hydrodynamics and biogeochemical processes are necessary to quantify nutrient dynamics in estuaries and improve management efficiency.

Lessons in eutrophication management in industrial countries

Successful lessons in the management or recovery of estuaries have been observed in many developed countries, where the solution has been used was the reduction of the amount of wastewater entering estuaries (Wolanski & Elliott, 2014).

The results of a 40-year survey at the Seine river and estuary (France) have shown the evolution and effectiveness of freshwater quality policies (Romero et al., 2016). Two decades ago, the Seine estuary used to have summer anoxic episodes, then the extension of WWTPs and agricultural policies has kept the estuary almost always in good condition since 2010 (Figure 1.17). Besides the construction of WWTPs, policies such as the ban of phosphates in household detergents have also reduced PO_4^{3-} concentrations significantly since the 1990s (Romero et al., 2016).

The effectiveness of management policies in improving water quality is demonstrated through the stages of development of WWTPs (Figure 1.17). However, the effectiveness of new WWTPs with a suitable capacity to the urbanized tropical estuaries in developing countries is still questionable because of the lack of long-term observation. Besides, Wolanski and Elliott (2014) argue that policies to reduce pollution do not always succeed because the consequences of eutrophication can

1. Background and state of the art

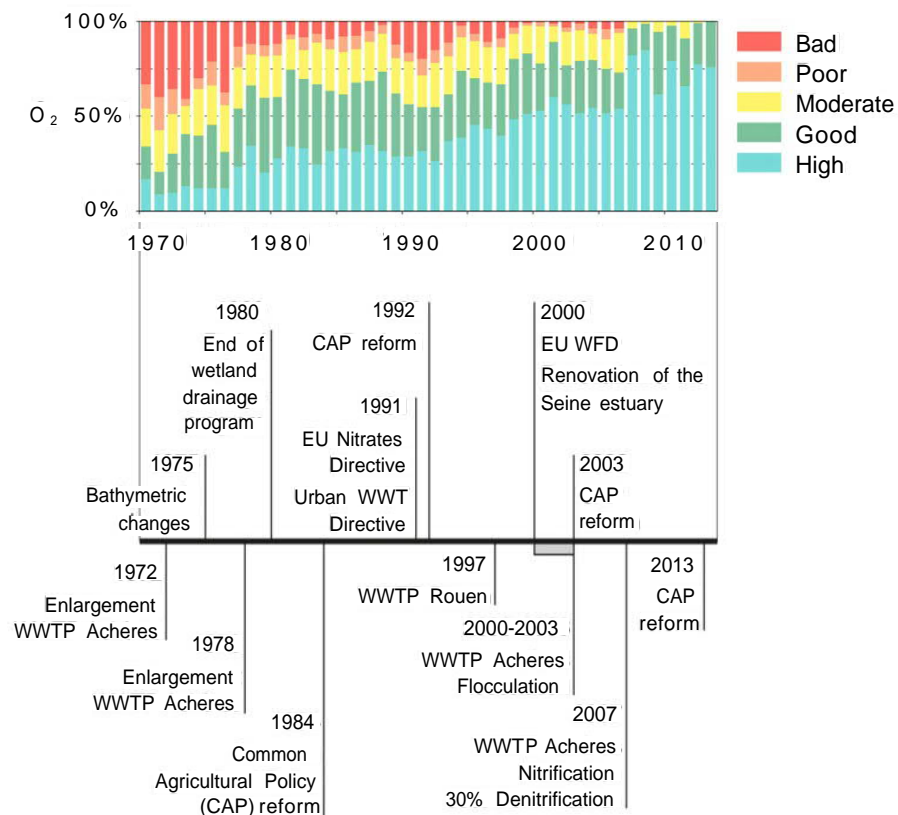


Figure 1.17: Environmental Quality Status in Seine River (from 1970 to 2013) (Romero et al., 2016)

linger when estuaries have lost their purification capacity. Schindler et al. (2008) concluded that eutrophication of lakes could not be controlled by reducing the nitrogen input because this action can increasingly favor nitrogen-fixing cyanobacteria; the lake thus remained highly eutrophic. Therefore, the determination of policies to reduce pollution should pay attention to the composition and proportion of nutrients (N, P, Si). The contribution of biogeochemical models for estuaries is critical (Wolanski & Elliott, 2014).

In rapidly urbanizing countries, questions about management policies align with megacities' strong impact to reduce eutrophication in estuaries. Improvements in water quality and control of eutrophication in estuaries are also seen in some of the highly urbanizing countries in Asia. Shenzhen Bay (China) is an example of the impact of urbanization on the water quality of estuaries and coastal areas in the 1990s. Similar to other developing countries, a large amount of WWTP cost constraints for N and P mitigation policies in wastewater would discourage governments of China. Therefore, monitoring programs and biogeochemical models were implemented to find other solutions in improving coastal regions adjacent to Shenzhen Bay, China. The monitoring results showed that phosphorus was the potential limiting nutrient for primary production in this area. Simulation results

1. Background and state of the art

also showed that improving the P treatment efficiency of WWTP will help reduce eutrophication. In addition, the removal efficiency of P was also higher than N; reducing phosphorus was thus performed first, followed by nitrogen years later. As a result, eutrophication has almost disappeared in this area since 2005 in this bay (Zhou et al., 2020). This experience of urban river restoration at this tropical bay shows that reductions in nutrient concentrations through WWTP are inevitable. The assistance of modeling in the accurate description of biogeochemical processes and eutrophication development is essential. This helps reduce the cost of building WWTPs that meet the region's demographic trends.

1.3 Water quality modeling approach in estuaries

1.3.1 Fundamental to water quality modeling

The variation of water quality is mainly governed by (i) the physical transport (e.g., velocity, advection, diffusion/dispersion, settling and burial) and (ii) the biogeochemical processes (e.g., the transformation of nutrients) (O'Kane & Regnier, 2003; Shanahan et al., 1998). A water quality model usually includes these components according to the following equation:

$$\frac{\partial(HC)}{\partial t} = - \underbrace{U \frac{\partial(HC)}{\partial x}}_{\text{Advection}} + \underbrace{\frac{\partial}{\partial x} \left(HD \frac{\partial C}{\partial x} \right)}_{\text{Dispersion}} + \underbrace{S}_{\text{Settle}} + \underbrace{R}_{\text{Transform}} + \underbrace{Q}_{\text{Load}}$$

where:

- C, t, x pollutant concentration, time, distance, respectively
- U, D, H advection velocity, dispersion coefficient, total water depth, respectively
- *Advection* accounts for the concentrations of pollutants follow the current movement as it flows downstream (see Figure 1.18)
- *Dispersion* accounts for the spreading pollutants by turbulent mixing and molecular diffusion from the location of high concentration to low concentration
- *Settle* accounts for the difference between the resuspended particles and the settling particles

1. Background and state of the art

- *Transform* accounts for the rate of the biogeochemical processes that happen in the water column (see Figure 1.19 for an example of simplified biogeochemical processes)
- *Load* accounts for the external sources such as runoff, wastewater treatment plant, lateral loads from tributaries

The hydrodynamic model provides the advection and dispersion components (Figure 1.18), including velocity and turbulent diffusion coefficients. Some hydrodynamic models also provide the information of settling velocity to calculate the amount of settling pollutant and burial. The biogeochemical module provides the transformation of pollutants, which describes the rate of substance variations due to biological and chemical processes, which is usually expressed by a Michaelis–Menten equation. Therefore, the estuarine models are usually called reaction–transport models to describe the substances' behavior according to hydrodynamics and biogeochemistry.

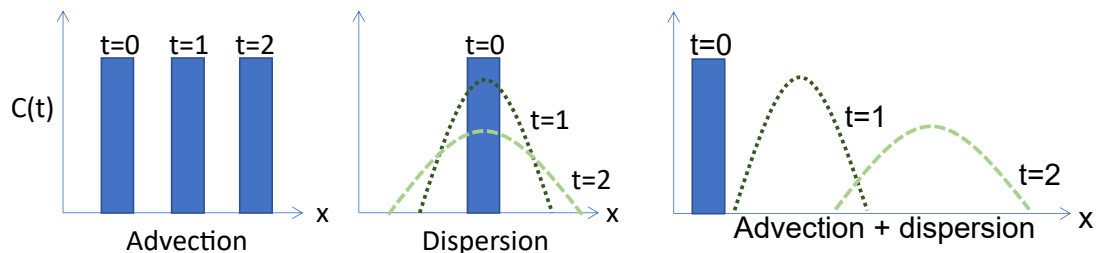


Figure 1.18: Illustration of pollutant transport by advection and dispersion/diffusion. $C(t)$ is the concentration of variables as a function of time (t) and distance (x)

Governing equations for hydrodynamics

To simulate water quality in estuaries, it is first necessary to determine the physical transport information of the substances. The hydrodynamics model is thus set up first. The required common equations are shown in Table 1.5. The tide effect equation is one of the main differences between the hydraulic model in the tidal estuaries and rivers.

In reality, these above equations need to be numerically solved with some approximations. The shallow water approximation is widely used in the studies of rivers, then the continuity and momentum equations can be further simplified (H. H. G. Savenije, 2012), for instance:

1. Background and state of the art

Table 1.5: Simplified governing equations of hydrodynamics model in estuaries

Equation.Type	Formula	Description
Continuity equation	$\frac{\partial \zeta}{\partial t} + \frac{\partial(Hu)}{\partial x} + \frac{\partial(Hv)}{\partial y} = 0$	Conservation of water mass where ζ is water surface elevation, H is total water depth, u and v are velocity components
Momentum equation (x-direction)	$\frac{\partial u}{\partial t} + u \frac{\partial u}{\partial x} + v \frac{\partial u}{\partial y} = -g \frac{\partial \zeta}{\partial x} - \frac{\tau_{bx}}{\rho H} + \frac{\tau_{sx}}{\rho H} + A_H \left(\frac{\partial^2 u}{\partial x^2} + \frac{\partial^2 u}{\partial y^2} \right)$	Conservation of momentum in x-direction where g is gravity acceleration, τ_{bx} is bottom stress, τ_{sx} is surface stress, ρ is water density, A_H is horizontal eddy viscosity
Momentum equation (y-direction)	$\frac{\partial v}{\partial t} + u \frac{\partial v}{\partial x} + v \frac{\partial v}{\partial y} = -g \frac{\partial \zeta}{\partial y} - \frac{\tau_{by}}{\rho H} + \frac{\tau_{sy}}{\rho H} + A_H \left(\frac{\partial^2 v}{\partial x^2} + \frac{\partial^2 v}{\partial y^2} \right)$	Conservation of momentum in y-direction with same parameters as x-direction equation
Tidal equation	$\zeta(x, t) = \sum_{i=1}^n A_i \cos(\omega_i t - k_i x + \phi_i)$	Tidal elevation where A_i is amplitude, ω_i is angular frequency, k_i is wave number, and ϕ_i is phase of tidal component i

$$\frac{\partial H}{\partial t} + \frac{\partial(Hu)}{\partial x} = Q$$

$$\frac{\partial(Hu)}{\partial t} = - \underbrace{\frac{\partial(Huu)}{\partial x}}_{\text{Advection}} - \underbrace{gH \frac{\partial \eta}{\partial x}}_{\text{Pressure}} - \underbrace{C_B |u| u}_{\text{Friction}} + \underbrace{\frac{\partial}{\partial x} (H A_H \frac{\partial u}{\partial x})}_{\text{Dispersion}} + \tau_x$$

where $H (= h + \xi)$ =total water depth, h =the equilibrium water depth, ξ =surface displacement level, u =water velocity in x-direction, $|u|$ =water speed, Q =water inflow/outflow from external sources, C_B =bottom drag coefficient, A_H =horizontal viscosity, τ_x =wind stress

Governing equations for water quality

The water quality model simultaneously uses the information in the hydraulic model (e.g., advection and dispersion) and combines it with the biogeochemical processes equations to obtain the variable concentrations over time and space. Besides biogeochemical reactions, the concentration of substances changes according to other processes such as sorption or exchange with the atmosphere. Although many processes lead to changes in the concentration of substances, a water quality model is always based on the conservation of mass equation principle. The total mass of an element such as C, N or P will remain the same; they only change the chemical formula under the influence of reactions in water, sediment, air. The main processes leading to the change in the concentration of variables are presented in Table 1.6.

1. Background and state of the art

Table 1.6: Processes controlling concentrations of nutrients in aquatic systems

Processes	Equation	Description
Hydrodynamic transport	$\frac{\partial C}{\partial t} + \frac{\partial(uC)}{\partial x} + \frac{\partial(vC)}{\partial y} + \frac{\partial(wC)}{\partial z} =$ $\frac{\partial}{\partial x} \left(K_x \frac{\partial C}{\partial x} \right) + \frac{\partial}{\partial y} \left(K_y \frac{\partial C}{\partial y} \right) + \frac{\partial}{\partial z} \left(K_z \frac{\partial C}{\partial z} \right)$ <p>where C = concentration of a water quality state variable, u, v, w = velocity components in the x, y, and z directions, respectively, K_x, K_y, K_z = turbulent diffusivities in the x, y, and z directions (Park 2005)</p>	For the 3D model, nutrients are advected, dispersed within the water column in x, y and z -direction and transported into the system following the flow. Please note that this equation only applies in the water column with external sources of pollutants.
Biogeochemical processes	$\frac{\partial C}{\partial t} = k \cdot C + R$ <p>where k = kinetic rate (1/time) and R = internal/external loadings (Park 1995). Kinetic rate (e.g., algal growth rate) can be illustrated by MichaelisMenten formulation</p> $k_c = k_{max} \frac{C}{K_M + C}$ <p>where k_c = reaction rate (1/time), k_{max} = maximum rate(1/time), C = nutrient concentration (mg/L), and K_M = concentration (mg/L) at half saturation k_{max}</p>	Biogeochemical reactions transform or remove nutrients by processes such as nitrification and denitrification. Kinetic equations can represent the essence of these processes. Each variable often has each kinetic equation related to its reaction (such as nitrification). The kinetic rate can be phytoplankton growth rate, bacteria, or other reactions (e.g., nitrification, organic carbon degradation).
Sediment-water exchange Adsorption and desorption	<p>Langmuir isotherm model is used to describe substrate P sorption onto sediments, suspended sediments</p> $\frac{PIP}{SS} = \frac{P_{ac} \times SRP}{SRP + K_{ps}}$ <p>Where P_{ac} = the maximal sorption capacity of P onto suspended solids (SS), and K_{ps} = the half-saturation constant, PIP = concentration of particulate inorganic phosphorus, SRP = concentration of soluble reactive phosphorus</p>	Some nutrients, such as P, have strong interaction between the particulate and the dissolved nutrients. Their concentrations are thus affected by the suspended sediments and bed sediments.
Water-air exchange	<p>Reaeration is a function of current velocity, wind speed and temperature, which affect saturated DO (Regnier et al., 1997)</p>	The reaeration process can add dissolved oxygen to the waterbody from the atmosphere

1.3.2 Application of reaction-transport model in estuaries

The applications of estuarine biogeochemical models

The water quality models for estuaries have existed for more than 50 years (e.g., Espey and GH Ward. (1972)), including simple 0-dimensional models (0D models) to complex 3-dimensional models (3D models). Models can be classified into three categories as follows:

- 1. The apparent zero end-member concentration model:** This was a one-dimensional estuarine model which provided the quantitative estimates of primary productivity, nutrient fluxes in the saline part of the estuary to the point of zero salinity. The limitation was to introduce large errors in estimating the long-term residual constituent flux towards the coastal zone because it ignored all processes taking place in the tidal river (Kaul & Froelich, 1984).
- 2. Box model:** Box models treat the estuary as a single, vertically and horizontally well-mixed box with steady residual hydrodynamic characteristics (Regnier et al., 2013). These models are still widely used to assess global estuarine

1. Background and state of the art

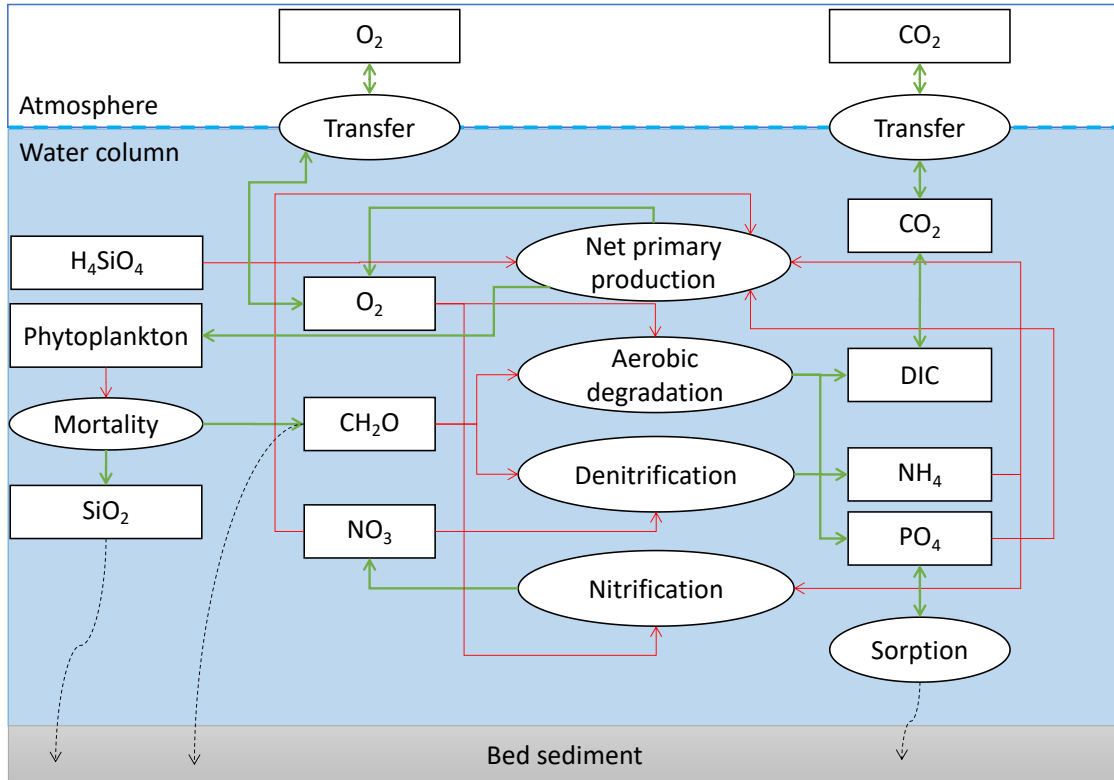


Figure 1.19: Simplified biogeochemical processes in the aquatic system (ellipse, rectangle, red line, green line, dot line represent the processes, the elements/pollutants, consumption, production and settling/deposition, respectively), DIC and CH_2O are dissolved inorganic and organic carbon (adapted from Regnier et al., 2013)

dynamics (Garnier et al., 2010; G. G. Laruelle et al., 2009). However, the results of flux calculation in the box models were usually inaccurate because they neglect the transient behavior of the flow and scalar fields (Arndt et al., 2009, 2011; Regnier et al., 2013).

3. **Reaction-transport models (RTMs):** RTMs describe the coupling of the transport and reaction in the estuaries. Thus, they can provide a mechanistic description of process interactions over a spectrum of scales. These models are particularly suitable for quantifying process rates and material fluxes at spatial and temporal scales that observations cannot achieve (Regnier et al., 2013). RTMs are the same approach with the overview of the nutrient dynamic model, which ensures to cover two main parts (i) hydraulics and (ii) biogeochemical processes.

From 1980 to 2013, most of the estuarine biogeochemical model applications were mainly in the temperature climate zone (Volta, Laruelle, Arndt, & Regnier, 2016). The recent studies of the estuarine biogeochemical model were reported for the estuaries in Western Europe, North America and few studies in Australia

1. Background and state of the art

and China. Some well-known models have been applied extensively for estuaries such as MIKE (Arndt et al., 2009, 2011), MOHID 3D (Fossati & Piedra-Cueva, 2013; Trancoso et al., 2005), HEM- 3D (Kyeong Park et al., 1995; K. Park et al., 2005), GEM 3D (Blauw et al., 2009; Mojica et al., 2015), ELCOM-CAEDYM 3D (Miguel, Lucas Lavo António Jimo, 2018; Robson & Hamilton, 2004), MOSES 1D (Hofmann et al., 2008; Soetaert & Herman, 1995), C-GEM (Volta et al., 2014; Volta, Laruelle, Arndt, & Regnier, 2016); CONTRASTE (Regnier & Steefel, 1999). There were very few studies about the nutrient dynamics models in the estuarine systems for tropical estuaries, such as Southeast Asian countries, even though the estuarine water quality in these countries is facing water pollution and eutrophication.

Strengths and weaknesses of simplified and complex models

Table 1.7: Comparison of some well-known biogeochemical model applications in estuaries. The order of models indicates the simplicity to the complexity of the model

Model	Requirement	Usage.scope	Applied.area
C-GEM 1D, daily - seasonal	Simplified hydro-geometrical characteristics, tidal period; biogeochemical reactions	Biogeochemical dynamics in estuaries. Reduces data requirements by using an idealized representation of the estuarine geometry.	Scheldt estuary (Volta et al., 2014, 2016)
CONTRASTE 1D, daily - seasonal	Bathymetrical maps, Hydrodynamic description in detail in upstream, tidal forcings. Biogeochemical reactions	The time series of nutrient transformations and fluxes along the estuarycoastal zone	Scheldt estuary (Regnier et al., 1997, 1999)
MOSES 1D, yearly	Biogeochemical, pelagic, reactive-transport model	Fate and turnover of nutrients entering the estuary; and fluxes in the estuary	Scheldt estuary (Hofmann et al., 2008)
HEM-3D daily - seasonal	Detail bathymetry. Hourly tide, daily discharge. Meteorological data. Water quality	Nutrient dynamics (21 state variables), algal groups, fecal coliform bacteria	Kwang-Yang Bay (Park et al., 1995, 2005)
ELCOM- CAEDYM 3D, daily - seasonal	Detail bathymetry, meteorological data, tidal elevation, Water quality	Nutrient dynamics, phytoplankton bloom, phytoplankton species	Mozambique coast (Miguel et al., 2018)
MOHID 3D, daily - yearly	Detail bathymetry, Hourly tide, daily discharge upstream, Atmosphere, Water quality, Algal species	Mainly Phytoplankton and macroalgae, zooplankton dynamics	Vouga Estuary (Trancoso et al., 2005)
MIKE 1-3D + water quality module	Detail bathymetry, hourly tide, daily discharge upstream and tributaries. Water quality	Depend on water quality module, for instance, nutrients dynamics and diatom development.	Scheldt estuary (Arndt et al., 2009, 2011)
Delft3D + GEM/water quality module	Detail bathymetry, hourly tide, daily discharge upstream and tributaries. Water quality	Describes the behavior of nutrients, organic matter, and primary producers in estuaries	Dutch coastal waters Blauw et al., 2008

Although water quality modeling for estuaries has greatly improved over time, the adoption of modern models has not always been consistent for many estuaries. In previous decades, mixing diagrams and steady-state box models were often used, but the disadvantage of these models was that they ignored the influence of tides (Arndt et al., 2009). As in the synthesis report of Espey and GH Ward. (1972) reaction-transport models allowed an accurate description of biogeochemical processes under the complex influence of many factors in estuaries such as tide, requiring time-costly computation. Today the computational limitation is not an important factor, but the lack of applications of reaction-transport models

1. Background and state of the art

still exists in many developing countries because of insufficient monitoring plans and access to relevant data series (Regnier et al., 2013). Therefore, selecting or developing appropriate models to apply on a regional or global scale is critical under the great influence of wastewater from emerging countries (Regnier et al., 2013; Volta et al., 2014).

The model selection is an important step for modeling application because no single model can apply for estuaries systems, even with a very advanced model. One model can be applied for the estuarine system if it can reach these criteria:

1. Whether the model outputs obtain the studied objectives?
2. Whether the hydrodynamic processes take into account the tidal regime?
3. Which data/parameters are in need for the model?
4. Which assumption and limitation of the model?

Table 1.7 compares the usage scope of some well-known estuarine biogeochemical models. According to the data requirement from simple to complex, the order of the models is C-GEM, CONTRASTE, ... MIKE, Delft3D. For the not-well monitoring estuarine systems in many tropical estuaries, the C-GEM, CONTRASTE or MOSES models are suitable if the ultimate study's objective is to qualify the impact of point sources, tide and biogeochemical processes. At the same time, HEM-3D, CAEDYM, MOHID are more suitable for the more complex requirements such as dynamics of phytoplankton groups and species. Although 1D reaction-transport models such as CONTRASTE can describe estuarine biogeochemical dynamics, the data requirement at the boundaries of estuarine systems still needs to ensure that high temporal variability is described. Therefore, reaction-transport models are often applied in intensively monitored estuaries such as Scheldt (Belgium/Netherlands) (Arndt et al., 2009).

1.4 Conclusion of Chapter 1

The chapter gives an overview of the important processes in modeling water quality for urbanized tropical estuaries. The difficulties and limitations of the current models are also presented. The next chapter presents methods of monitoring, data processing, and model selection.

2

Materials and methodology

Contents

2.1 Study site	43
2.1.1 Saigon River Estuary	43
2.1.2 Ho Chi Minh megacity (Southern Vietnam)	47
2.1.3 Water quality conditions in the Saigon River Estuary	51
2.2 Methods for water quality evaluation	54
2.2.1 Monitoring and sampling strategy	55
2.2.2 Measurement and analytical methods	58
2.2.3 Eutrophication status and GHGs calculation	59
2.2.4 Multivariate statistical analysis methods	63
2.3 Water quality modeling	65
2.3.1 Overview of C-GEM model	65
2.3.2 Data requirement	70
2.3.3 Model description and setup protocol	72
2.3.4 Model evaluation	78
2.4 Conclusion of Chapter 2	79

This chapter describes the research area and methods to study the biogeochemical functioning of an urbanized tropical estuary by monitoring, experiment, statistical analysis and modeling.

The area of study is Saigon River Estuary, located in the South of Vietnam, with the characteristics of tropical estuaries strongly impacted by urbanization (Ho Chi Minh megacity). The topographic, morphological and hydrological features of Saigon River Estuary are presented first. The urbanization of HCMC is then presented for the 1979 to 2020 period and trends for 2050. The pollution status of Saigon River Estuary is reported based on the previous studies. Finally, water management plans of this urbanized estuary (e.g., construction, upgrading of waste treatment system) are discussed to assess water pollution risks in the future.

2. Materials and methodology

In terms of research methods, this study was conducted in the period 2018-2021. In addition to available hydrological and water quality data from the national environmental monitoring center, we collected nutrients, carbon, phytoplankton, and greenhouse gases concentration data. Multivariate statistical methods were used to evaluate the correlation between explanatory variables (e.g., environmental, hydrological parameters) and responses (e.g., greenhouse gases, phytoplankton densities). Finally, a biogeochemical estuarine model for tropical estuaries is presented in detail, from the platform model to the setup protocol to allow the reader to replicate this research for another area.

2.1 Study site

Vietnam is a coastal country stretching over 3260 km from the north (subtropical climate) to the south (tropical climate). Nearly half of Vietnam's cities are adjacent to the sea and have a large population living there. The coastal areas of Vietnam have been affected by urbanization and climate change for many years. Vietnam's three largest river estuarine systems that play the most important role in Vietnam's economy are the Red River Delta, the Saigon - Dongnai river basin, and the Mekong River Delta (Figure 2.1). In the Mekong Delta, many studies have assessed the impacts of climate change, particularly sea level rise and subsidence affecting the country's agriculture. Mainly studies have also been carried out in the Red River Delta to assess agricultural activity and urbanization on water quality. The Saigon - Dongnai river basin is a special area, mainly affected by the region's rapid urbanization, especially the megacity of HCMC.

2.1.1 Saigon River Estuary

Location and topography

Location

The Saigon River Estuary is located in the south of Vietnam, part of the Saigon-Dongnai River basin. The Saigon River flows through Tay Ninh, Binh Duong, Dongnai, HCMC and Long An administrative provinces. The Saigon River Basin has a total area of 4717 km^2 and borders the following areas in turn:

- The North and the Northwest border Cambodia, a country with many-sided relations with Vietnam in terms of politics, economy and culture.
- The southeast direction borders the East Sea of Vietnam and provides marine resources, oil, gas, and international shipping.

2. Materials and methodology

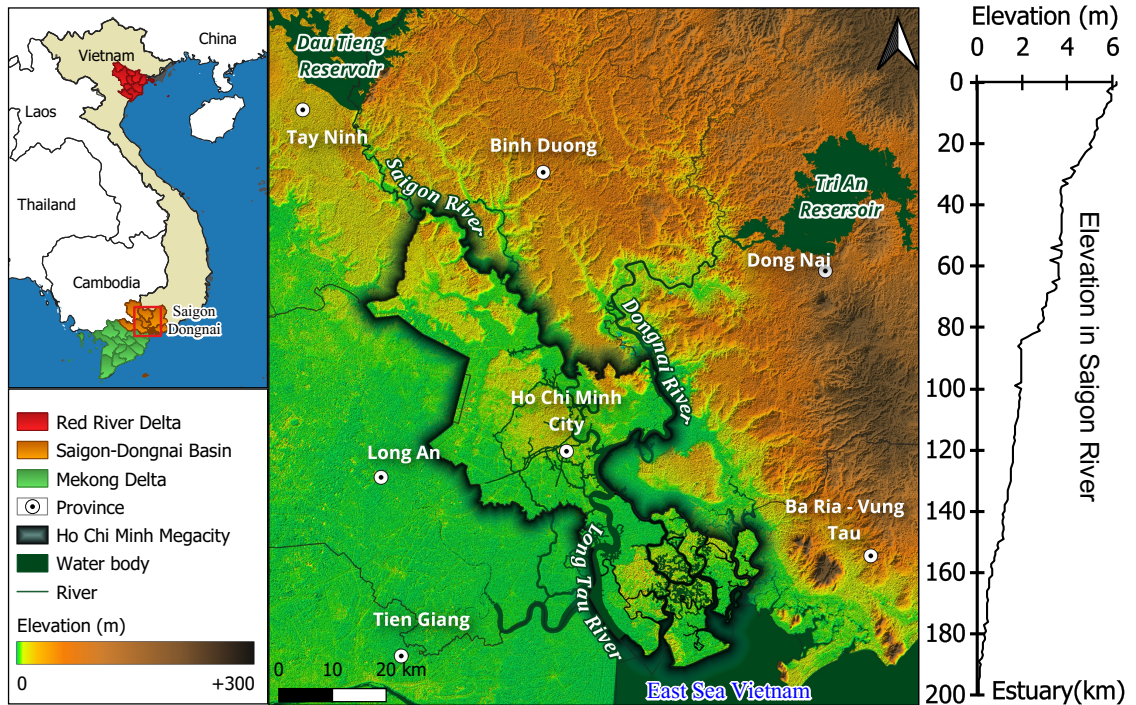


Figure 2.1: Overview of three biggest river estuarine systems in Vietnam and topography of Saigon River Basin, Southern Vietnam (topography data is from MERIT DEM, 2018)

- The southwest direction borders the Mekong River Delta, which mainly produces food, aquatic products and fruit trees. HCMC is about 170 km from the largest city of the Mekong Delta (Can Tho City).
- The North and the Northeast border with the highland area, which is mainly for crops.

Topography

The Saigon River originates from the Vietnam-Cambodia border area with terrain about 200 m high and is controlled at Dau Tieng Reservoir in the territory of Vietnam. Dau Tieng reservoir is one of the largest reservoirs in Vietnam, with a total water surface area of 270 km^2 , a volume of 1580 million m^3 . Dau Tieng Reservoir regulates floods and aims at mitigating saline intrusion downstream, storing fresh water and supplying irrigation water to Tay Ninh, Bin Duong, Bin Phuoc provinces and HCMC. From Dau Tieng Reservoir to the estuary mouth (about 200 km), the Saigon River has a small slope of about 1.3% (Figure 2.1). Elevation of more than 100 km from estuary mouth is less than 2 m; the areas surrounding this river are thus sensitive to saline intrusion and flooding, as a hydrological response of the watershed to rainfall and tide.

2. Materials and methodology

Climate and hydrology

Located in the tropics, the Saigon River Estuary experiences two distinct seasons: the rainy and dry seasons. The rainy season is from May to November (hot and humid climate, high temperature with lots of rain), and the dry season is from December to April of next year (dry climate, high temperature and little rain). This area has 160 to 270 hours of sunshine $month^{-1}$ (Figure 2.2), with an average temperature of $27^{\circ}C$, maximum up to $40^{\circ}C$, and minimum down to $13.8^{\circ}C$. Solar radiation intensity is of about $4.5 \text{ kWh } m^{-2} d^{-1}$ and of about 1100 kWh yr^{-1} (Figure 2.3). The average daytime temperature ranges mainly from 25 to $28^{\circ}C$. The average rainfall is 2000 mm yr^{-1} , of which 90% falls during the rainy season (about 159 rainy days yr^{-1} with about $200 - 500 \text{ mm month}^{-1}$) (HCMC Statistical Year Book, 2010 to 2016).

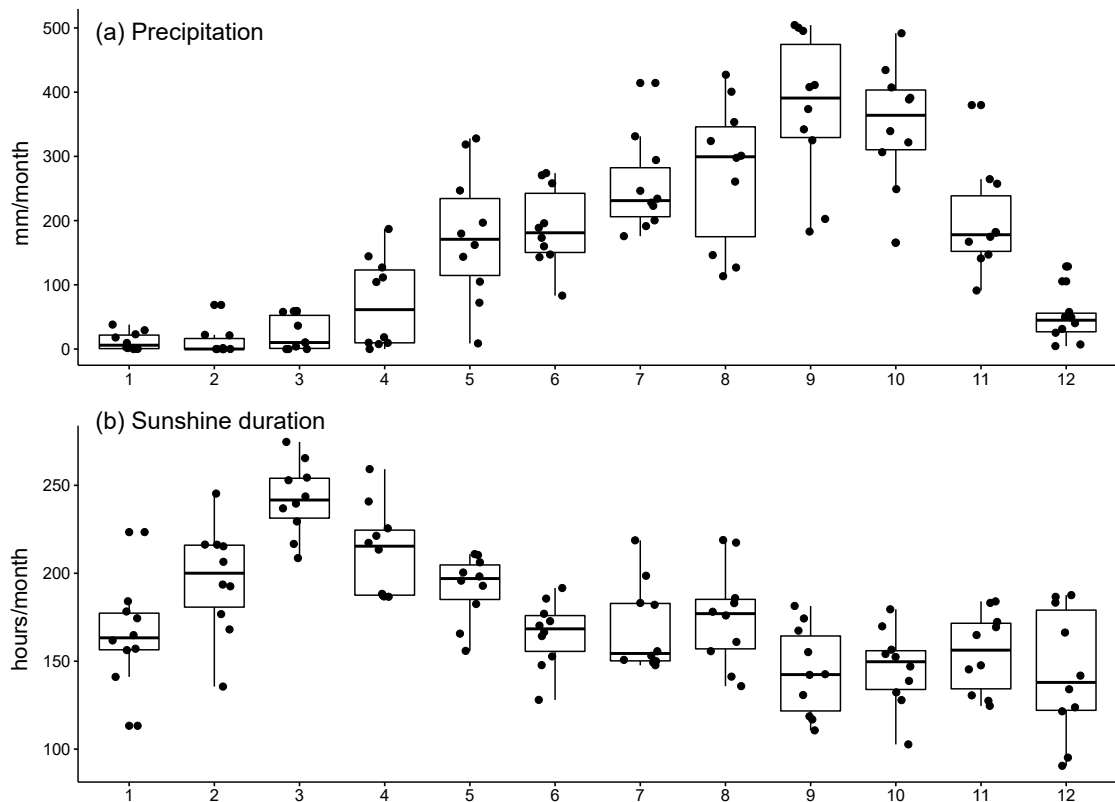


Figure 2.2: Average monthly precipitation and sunshine duration from 2005-2016 in Saigon River (Data source from HCMC Statistical Year Books from 2010 to 2016)

This area is affected by two main wind directions: The West - Southwest and North - Northeast monsoons. West - Southwest wind from the Indian Ocean, average speed 3.6 ms^{-1} , in the rainy season. Wind North - Northeast wind from the East Sea, average speed 2.4 ms^{-1} , in the dry season. There is also a trade wind in the south-southeast direction from March to May, averaging 3.7 ms^{-1} (HCMC Statistical Year Book 2010). The average wind speed at 10 m above the

2. Materials and methodology

surface of the Saigon River fluctuates around 2 ms^{-1} upstream and about 4 ms^{-1} near the estuary (Figure 2.3).

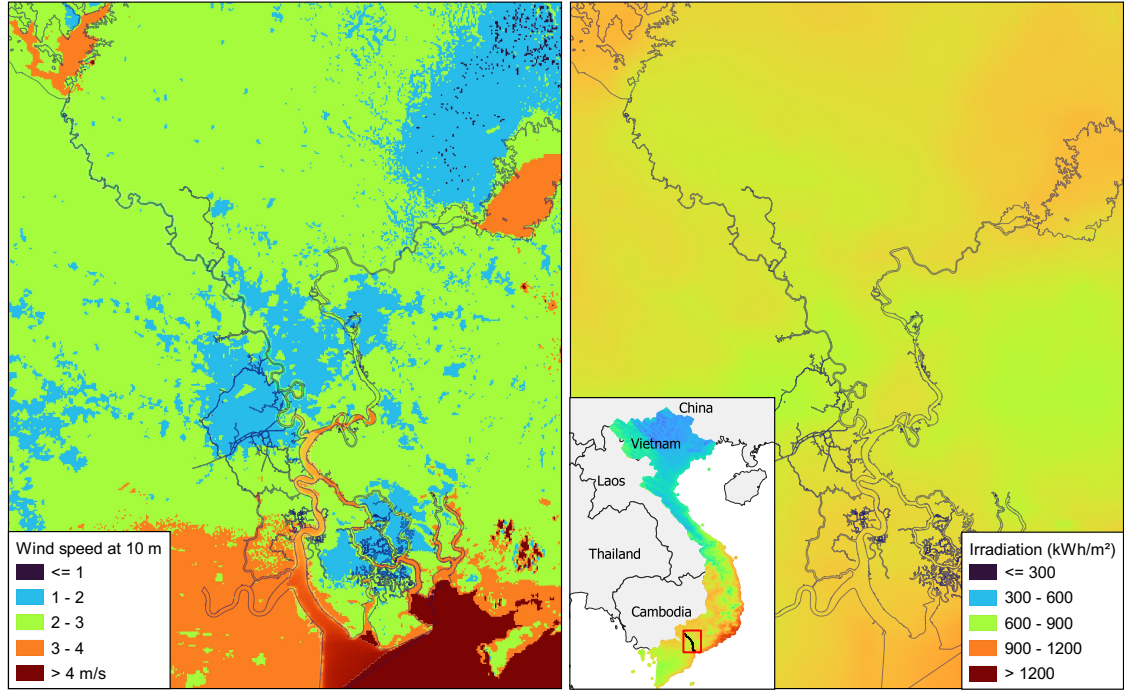


Figure 2.3: Average of wind speed at 10 m (ms^{-1}) and the yearly average of normal irradiation ($\text{kWhm}^{-2}\text{ yr}^{-1}$) in Saigon River Basin in 2007-2018 (Data source: Global Wind Atlas and Global Solar Atlas, 2018).

In terms of hydrology, the Saigon River and its estuary have a very diverse network of rivers and canals. The Saigon River is about 30 m in width upstream and about 225-370 m in HCMC. The average water depth is 18 m. From Dau Tieng Reservoir to the estuary mouth, 200 km downstream, the Saigon River ($18 \pm 14\text{ m}^3\text{s}^{-1}$) joins, in turn, several notable tributaries such as the Thi Tinh River ($20 \pm 11\text{ m}^3\text{s}^{-1}$) and the Dongnai River ($632 \pm 446\text{ m}^3\text{s}^{-1}$) (Figure 2.6), forming Long Tau River and flowing through Can Gio Mangrove and into the East Sea of Vietnam (Figure 2.4). In addition, the Saigon River is connected to an urban river (Vam Thuat River, $4\text{ m}^3\text{s}^{-1}$) and three urban canals of HCMC (combined discharge of $5.5\text{ m}^3\text{s}^{-1}$) before the confluence with Dongnai River (T. T. Nguyen et al., 2020). The semi-diurnal regime influences the Saigon River from the East Sea of Vietnam (Figure 2.5). The tidal amplitude ranges from 1.5 m during neap tide to about 4 m during a spring tide (Schwarzer et al., 2016).

Land use

Figure 2.7 presents the land use and population density of the Saigon River watershed. Land use in the watershed of the Saigon River significantly varies from North to South. Upstream HCMC (North of the city, Tay Ninh and Binh

2. Materials and methodology

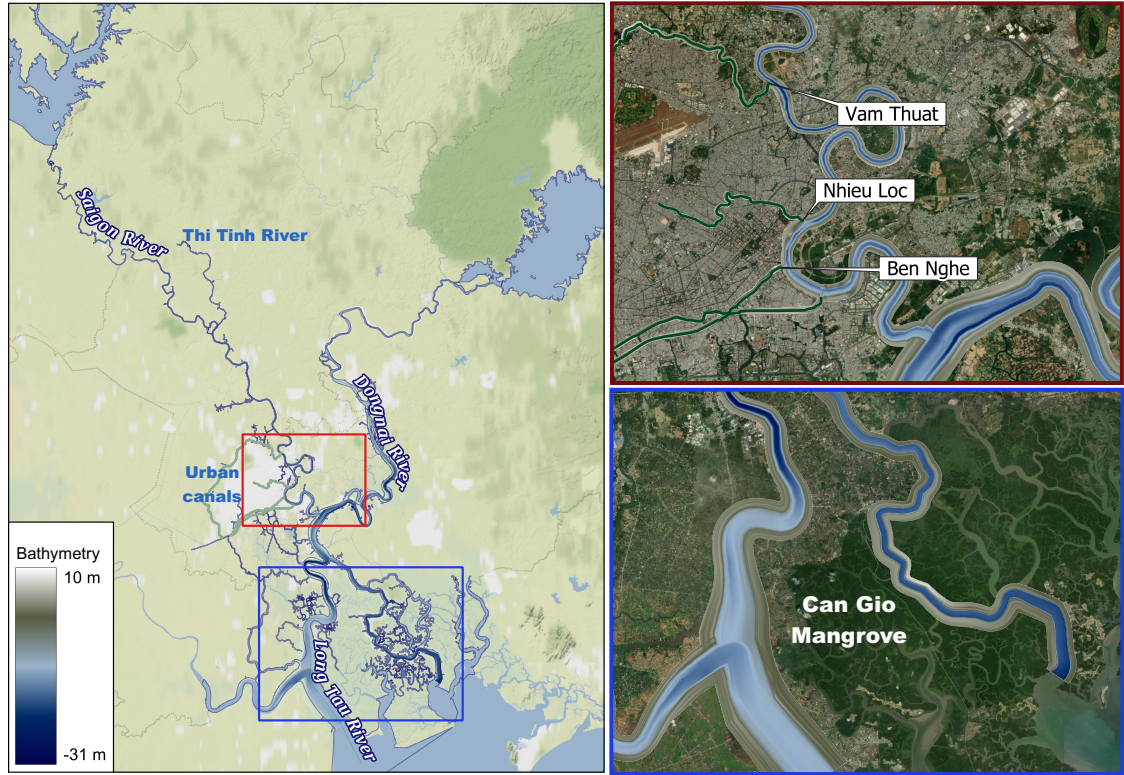


Figure 2.4: (a) Saigon River and tributaries, (b) urban canals, (c) Can Gio Mangrove (Bathymetry data is from Southern Vietnam Institute of Water Resources Research (SIWRR) in 2008 and 2016, only available for Saigon and Dongnai River)

Duong provinces), mainly agricultural activities (paddy rice and rubber tree farms). Urban settlements and industrial zones belonging to HCMC and part of Dongnai province are dominant. Downstream of the estuary, the Can Gio mangrove system is recognized as a biosphere reserve by UNESCO.

2.1.2 Ho Chi Minh megacity (Southern Vietnam)

Population

HCMC, formerly known as Saigon (before 1975), has the largest population and fastest growth rate in Vietnam. The Saigon River is mainly located in the territory of this city and directly receives wastewater from human activities through a system of canals, as shown in Figure 2.4. The population in 1929 was 123,890 people, of which 12,100 were French, and its population reached 498,000 people in 1943. In 1967 the city had grown threefold with a population of 1.5 million people. However, this population increase was mainly due to immigration (Nguyen Van Tien, 2021). Since 1979, HCMC's population has grown rapidly from more than 3 million to 9 million by 2020. The population distribution in HCMC is uneven. While some districts such as 4, 5, 10 and 11 have densities of over 40,000

2. Materials and methodology

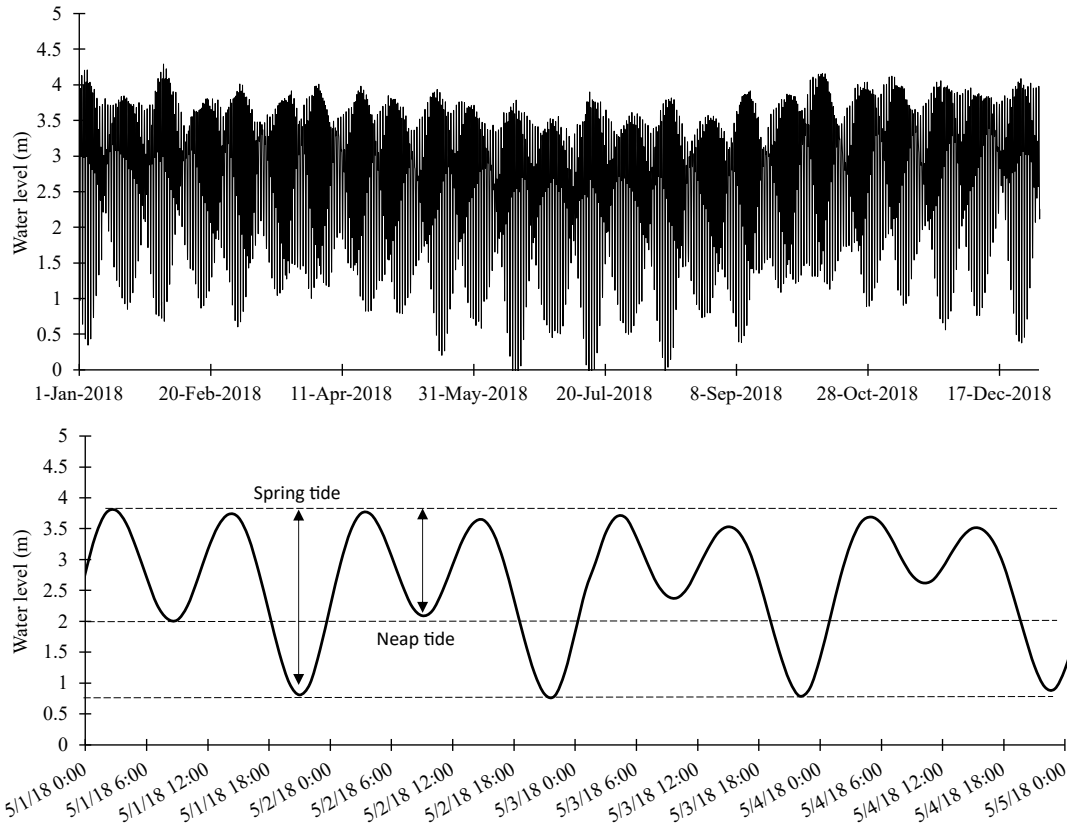


Figure 2.5: Variation of water level at estuary mouth of Saigon River in 2018 and in 1-5 May 2018 (Data source: Vung Tau Station, UHSLC Data)

inhabitants km^{-2} , the suburban district of Can Gio has a relatively low density of 100 persons km^{-2} (Figure 2.7). Regarding population growth, while the natural growth rate is about 1.07%, the mechanical growth rate is up to 2.5% (Source: General Statistics Office Of Vietnam - GSO, 2019). The population growth rate also varied each period, the period 1999-2009 was 3.5%, while the period 2009-2019 was lower with an increased rate of 2.3%. If based on the average population growth rate of 2.8%, the population of HCMC is estimated to be more than 20 million people by 2050 (T. T. Nguyen et al., 2020). However, according to UN World Urbanization Prospects 2018, the population growth rate in HCMC will decrease from 2.8% in 2019 to 1.3% in 2050. The population of HCMC is thus estimated at 16 million people in 2050. This estimate is appropriate because the HCMC government is increasingly taking measures to control immigration in the future (Source: Vietnam Ministry of Construction, 2020).

HCMC is the largest economic and trading center of Vietnam. The city occupies about 0.6% area but 10% population of Vietnam and accounts for more than 30% of the value of industrial production and 35% of foreign projects. The economy of HCMC is diversified from mining, fisheries, agriculture, processing industry, construction to tourism, finance. Regarding economic sectors, services

2. Materials and methodology

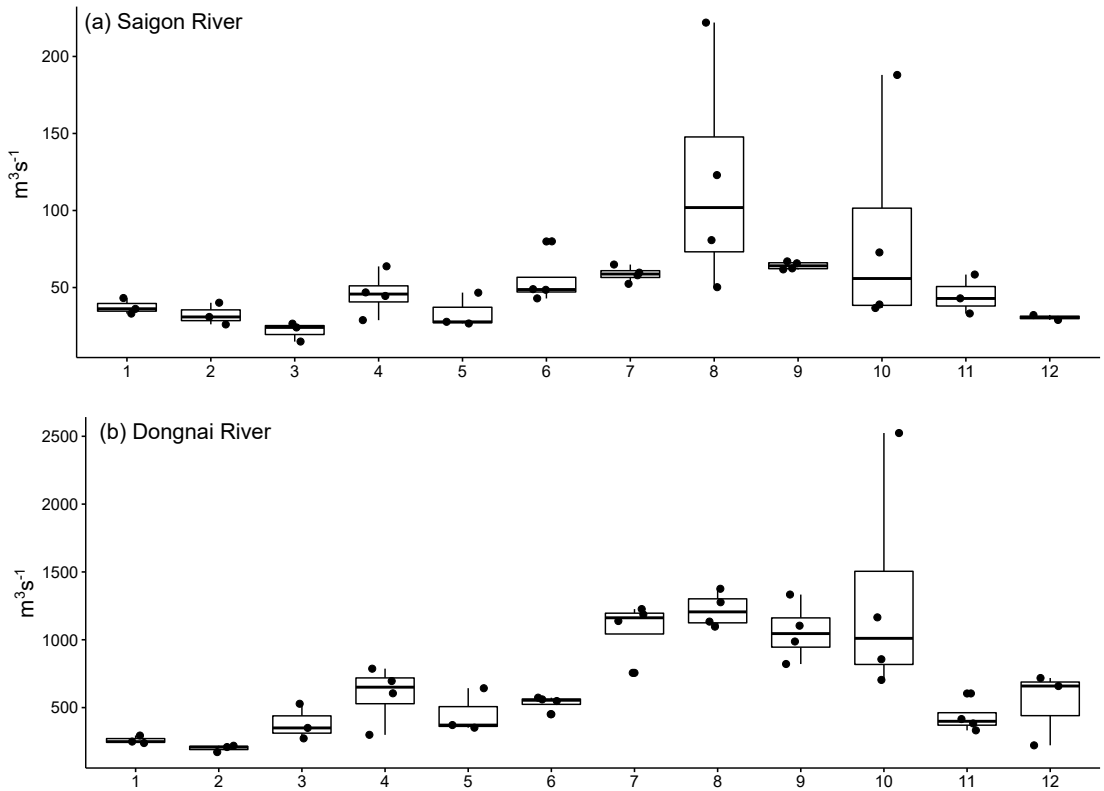


Figure 2.6: Average residual monthly discharge in Saigon and Dongnai River from 2013-2016 (adapted from T. T. N. Nguyen et al., 2019)

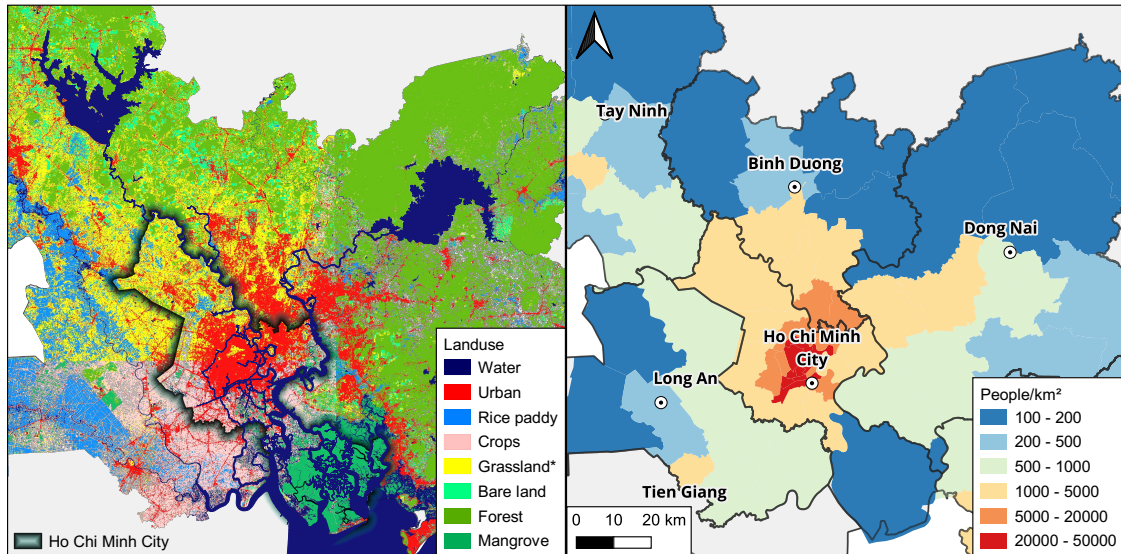


Figure 2.7: Land use and population densities in Saigon River Basin (Data source: Land use from JAXA, 2017, Population densities from General Statistics Office of Vietnam, 2019)

accounted for the highest proportion, about 50%. The industry and construction

2. Materials and methodology

accounted for 48%, while agriculture, forestry and fishery accounted for only 2% (HCMC statistics book, 2016). In 2020, HCMC had 24 export processing zones and industrial parks with about 62 km^2 . All industrial parks in HCMC have centralized wastewater treatment systems. Up to now, HCMC is the first city in the country to reach the target of 100% of industrial parks operating with centralized wastewater treatment systems of $63000\text{ m}^3\text{ d}^{-1}$ (www.hepza.gov.vn). Thus, if the WWTPs of these industrial parks are operated according to the design, wastewater from these industrial zones should not be a source of pollution for the Saigon River.

Sewerage and wastewater treatment capacities

The sewerage and sanitation system of HCMC was built in the 1870s during the French colonial period. Until now, domestic water and rainwater have been collected and transported together by the sewer system and by urban canals and creeks (Tran Ngoc et al., 2016).

The current WWTPs system in HCMC cannot deal with the total domestic wastewater volume of about 9 million people (about $2.5\text{ million m}^3\text{ d}^{-1}$). Before 2006, all domestic wastewater was discharged directly into canals and the Saigon River; treated wastewater is about 12% in 2021 (Figure 2.8). In response to the increase in domestic wastewater, the Vietnamese government called for the total construction of 12 WWTPs to treat about $3\text{ million m}^3\text{ d}^{-1}$ by 2040 (Vietnam Prime Ministerial Decision Jan. 2010, n24/Q-TTg). However, there are currently only three WWTPs in operation; one WWTP is under construction, while other WWTPs are still in the fundraising stage. The total estimated cost is over 2 billion USD for the remaining WWTPs. Therefore, we estimate that in 2025 HCMC could treat about $780,000\text{ m}^3\text{ d}^{-1}$, equivalent to 27% of the total wastewater volume of about 2.8 million people and $3\text{ million m}^3\text{ d}^{-1}$, equivalent to 54% of the wastewater of about 16 million people in by 2050 (Figure 2.8).

Canal network

In the urban area of HCMC, there are four main canals, with a total length of 76 km, including Nhieu Loc - Thi Nghe; Tan Hoa – Lo Gom; Tau Hu – Kenh Doi; Kenh Te - Ben Nghe; Tham Luong - Vam Thuat. This system plays an important role in draining water for the inner city of HCMC. However, this system currently receives domestic wastewater and stores it before discharging it into the Saigon River. Figure 2.4 depicts four canals that directly lead wastewater to the Saigon River, starting from the upstream Vam Thuat River, then Nhieu Loc, Ben Nghe, and Kenh Te canals.

2. Materials and methodology

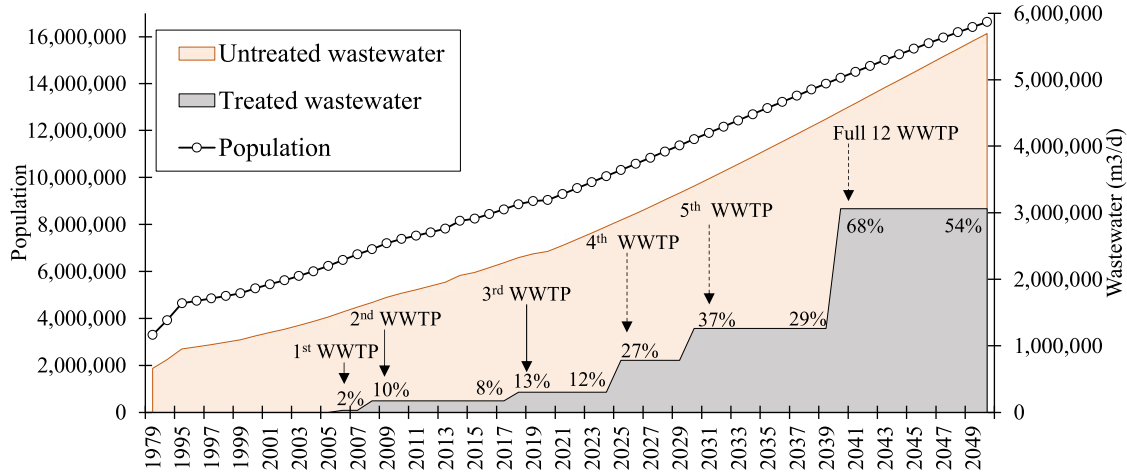


Figure 2.8: Population in HCMC from 1979 to 2020, predicted to 2050, and WWTP capacity.

2.1.3 Water quality conditions in the Saigon River Estuary

Spatial and seasonal variation of water quality

Several studies have assessed the overall status of water quality (specifically nutrients pollution) in the Saigon River Estuary and its canal system (T. T. N. Nguyen et al., 2019, 2020; Strady et al., 2017). T. T. N. Nguyen et al. (2019); T. T. Nguyen et al. (2020) show that nutrients and organic carbon concentration in the Saigon River increases significantly when receiving domestic wastewater from HCMC. The DO concentration also declines quickly when the Saigon River flows through this area (Figure 2.9a). Very high concentrations of PO_4^{3-} and NH_4^+ were found in urban canals (Figure 2.9b), with values 10 and 20 times higher than in the Saigon River. This cannot be denied the impact of domestic wastewater on the canal system without WWTPs. However, upstream to downstream of the canals also show that this system plays a role in pollutant retention. Part of the wastewater is diluted before being discharged from the system, while the pollutants deposited as sludge in the canal are regularly dredged (T. T. Nguyen et al., 2020). Figure 2.9 presents the water quality along the Saigon River in 2012-2016 (T. T. Nguyen et al., 2020).

Regarding the eutrophication status, T. T. N. Nguyen et al. (2019) found that the upstream and downstream of Saigon River are in a mesotrophic state, while the urban section was in a eutrophic state. In addition, 3-year monitoring also shown that P is the limiting factor for phytoplankton development based on the Redfield ratio (C:N:P:Si) (Figure 2.10). The N:P ratio in the Saigon River was about 70:1, much higher than 16:1. Therefore, the control of P concentration should be of concern for the authorities to control eutrophication in the Saigon River, especially in the rapidly urbanizing districts of HCMC (T. T. N. Nguyen et al., 2019).

2. Materials and methodology

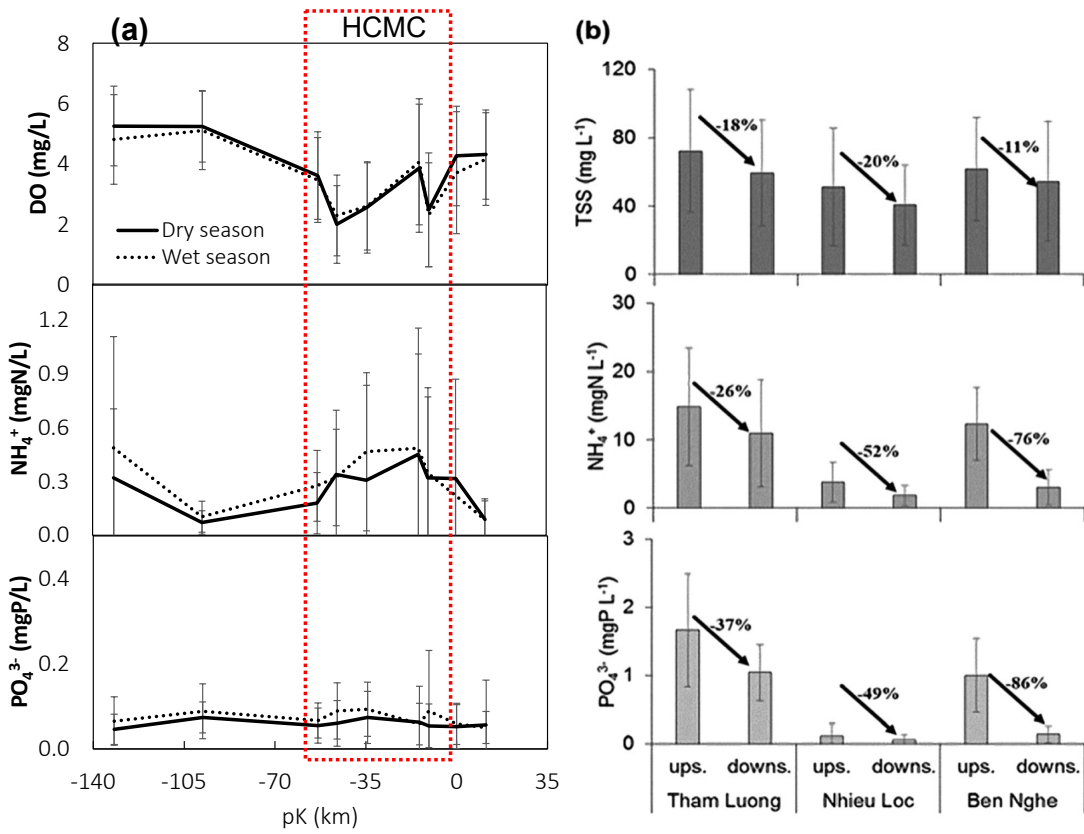


Figure 2.9: Mean total suspended sediment (TSS), dissolved oxygen (DO), NH_4^+ , and PO_4^{3-} concentrations in 2012 - 2016 period: (a) along the Saigon River during the wet and dry seasons and (b) in urban canals of HCMC (adapted from T. T. Nguyen et al., 2020)

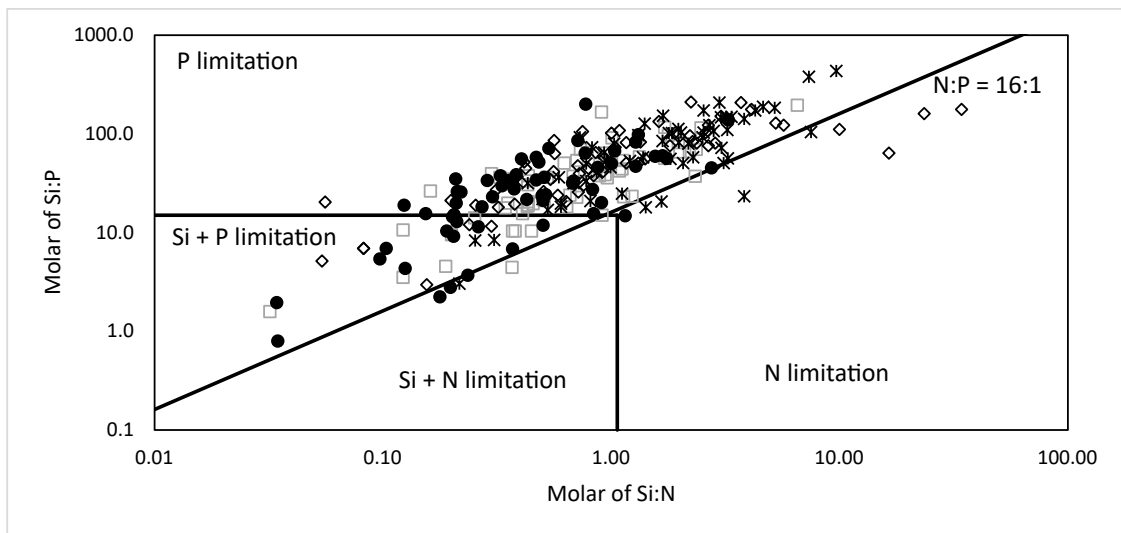


Figure 2.10: Molar ratios of Si:N and Si:P in Saigon River 2015-2017 (adapted from T. T. N. Nguyen et al., 2019)

2. Materials and methodology

Current water quality management tools

The water quality of the Saigon River is assessed to be directly affected by domestic wastewater from the HCMC megacity. Therefore, the HCMC government has had programs to monitor the water quality of the Saigon River since the 1990s. This program is completed with monitoring points from Dau Tieng Reservoir to the estuary and other sampling sites in the urban canals, with a monthly frequency since 2012.

By 2019, according to the Ministry of Natural Resources and Environment of Vietnam (Decision 154/QD-TCMT, February 15, 2019), the water quality of major rivers affected by tides in Vietnam must be simulated by two software QUAL2K and MIKE 11. The requirement to use this two software is to calculate the total maximum daily loads of rivers (Source: Ministry of Natural Resources and Environment of Vietnam - MONRE, 2019). The QUAL2K model is applied to the north of Vietnam because of its low tidal influence. The MIKE model is used to the south of Vietnam because of its ability to solve tidal problems (MONRE, 2019). Therefore, many Vietnamese scientists have applied the MIKE model to simulate hydraulic processes in the Saigon River. However, currently, there is only one study using the MIKE model to assess water quality in the Saigon River (H. D. Nguyen et al., 2019). The remaining studies mainly evaluate saline intrusion. In addition, the researches on water quality modeling in Vietnam are mostly used internally, rarely published internationally. To the author's knowledge, there has been no published assessment of biogeochemical processes and hydrological regimes on the changes in the Saigon River's water quality and the risk of eutrophication under the impact of urbanization.

The risk of water pollution in the future

During 20 years of monitoring the water quality of the Saigon River, the dissolved oxygen concentration in the 2000s was very low. In 2008, the water quality improved thanks to the operation of WWTPs (but only 10% of the total wastewater was treated). The water quality improvement is also supported by the activities of dredging canals in the inner city. However, almost all the canals suffered serious pollution levels during this period, and fish deaths were frequent (Figure 2.11). In recent years, DO concentration has tended to decrease gradually and often until anoxic conditions (Figure 2.12). Concentrations of pollutants in this river are still highly fluctuating but note that it is on a deteriorating trend.

Managing water quality in the Saigon River is to control the source of domestic wastewater before being discharged into the canal system and the Saigon River. However, the planification construction of 12 WWTPs is expected to cost more than 2 billion USD, while the construction of only one WWTP had lasted from 10 years before operation. Therefore, the step-by-step planning of construction

2. Materials and methodology



Figure 2.11: Nhieu Loc Canal in 2012 (Source: Tuoitre News, 2012) and fish death in Nhieu Loc Canal in 2015 (Source: Vnexpress News, 2015)

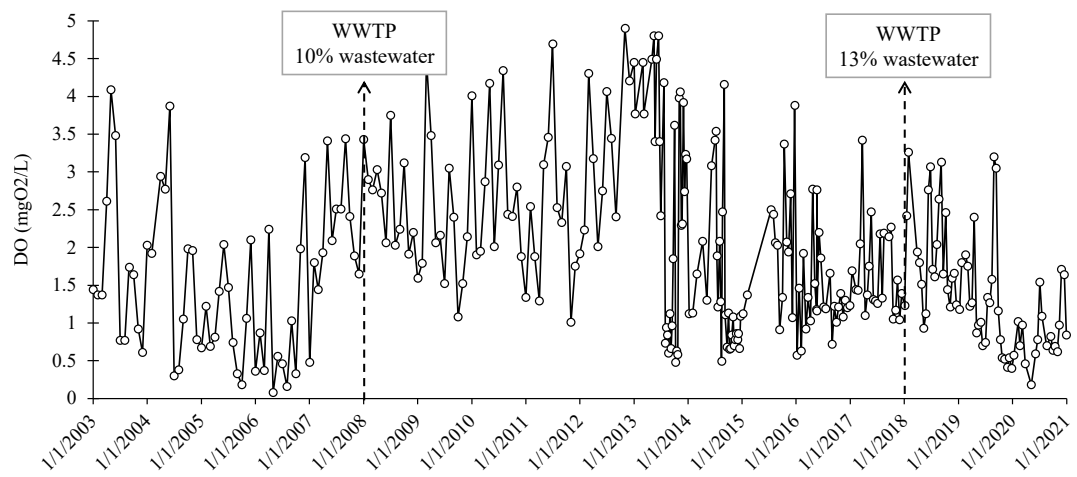


Figure 2.12: Evolution of DO in Saigon River (urban section) from 2003 to 2021 (Data source: data of 2003-2015 period is from the center of monitoring Vietnam, data of 2016-2021 period is from CARE, see section 2.2 for detailed description of CEM and CARE monitoring programs)

and selection of treatment technology will be extremely important to the financial viability of the region. Similar to the lessons on water pollution control from the Seine River (France) or Shenzhen Bay (China), solutions to reduce pollutants need to be based on research and support of biogeochemical models. This can optimize costs and improve the effectiveness of future pollution mitigation in the context of HCMC's rapid urbanization.

2.2 Methods for water quality evaluation

Following the monitoring effort undertaken at CARE laboratory (<http://carerescif.hcmut.edu.vn/>), this study extended the data collection for 2 years, 2019 – 2020. The available data used for this study are also described in detail below.

2. Materials and methodology

2.2.1 Monitoring and sampling strategy

Vietnamese water monitoring program

Vietnamese Center of Monitoring (CEM) of the Department of Natural Resources and Environment of HCMC (DONRE) has been responsible for monitoring water quality and hydrology in the Saigon River since the 2000s. After many modifications of the monitoring strategy, by 2012, this program was operating more stably. CEM surveyed 26 points along the Saigon River and its tributaries (approximately 300 km in total length) and 15 points in the urban canals (Figure 2.13 for sampling sites using in this study). The measured parameters include temperature, pH, TSS, salinity, turbidity, NH_4^+ , PO_4^{3-} , COD, BOD_5 , DO, metals (Pb, Cu, Cd, Hd, Mn), oil, coliforms and *E. coli*. Monitoring frequency is bi-weekly for locations along the river and monthly for sampling sites at urban canals.

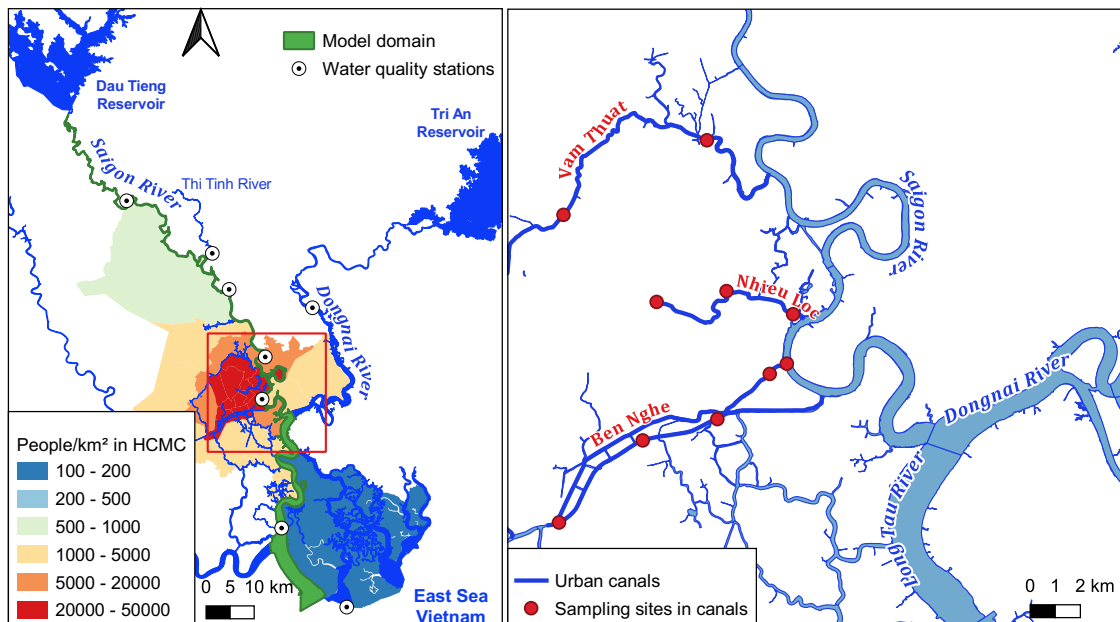


Figure 2.13: Location of water quality survey by Vietnamese center environmental monitoring (CEM) in urban canals and along the Saigon River Estuary.

In addition, CEM monitors water levels and discharge at several monitoring stations along the Saigon River. Each month, at these monitoring stations, some operators will observe the water level and hourly velocity for 48 hours continuously to calculate the daily inflow and outflow. CEM uses the velocity index method to calculate residual discharge. The flow calculation method of CEM is presented more in details in Camenen et al. (2021).

Bi-weekly monitoring

This bi-weekly monitoring program is conducted by Center Asiatique de Recherche sur l'Eau (CARE, Vietnam). This program has been implemented since 07/2015

2. Materials and methodology

and continues to survey the temporal evolution of water quality in three areas along the Saigon River and one area in the Dongnai River (Figure 2.14). Four sampling sites represent four areas of (i) an upstream station on the Saigon River (SG01) representative of the reference water status before HCMC, (ii) a station located in the urban area (SG10) representative of the impact of the megacity and (iii) a downstream station after the confluence of the Saigon and Dongnai Rivers (SG18) that aims at assessing the global impact of HCMC to the estuarine and coastal waters. Four sampling sites of CARE coincide with the sampling location of CEM. However, CARE analyzed additional indicators including POC, DOC, NO_3^- , TN, TP, Chl-a, phytoplankton density.

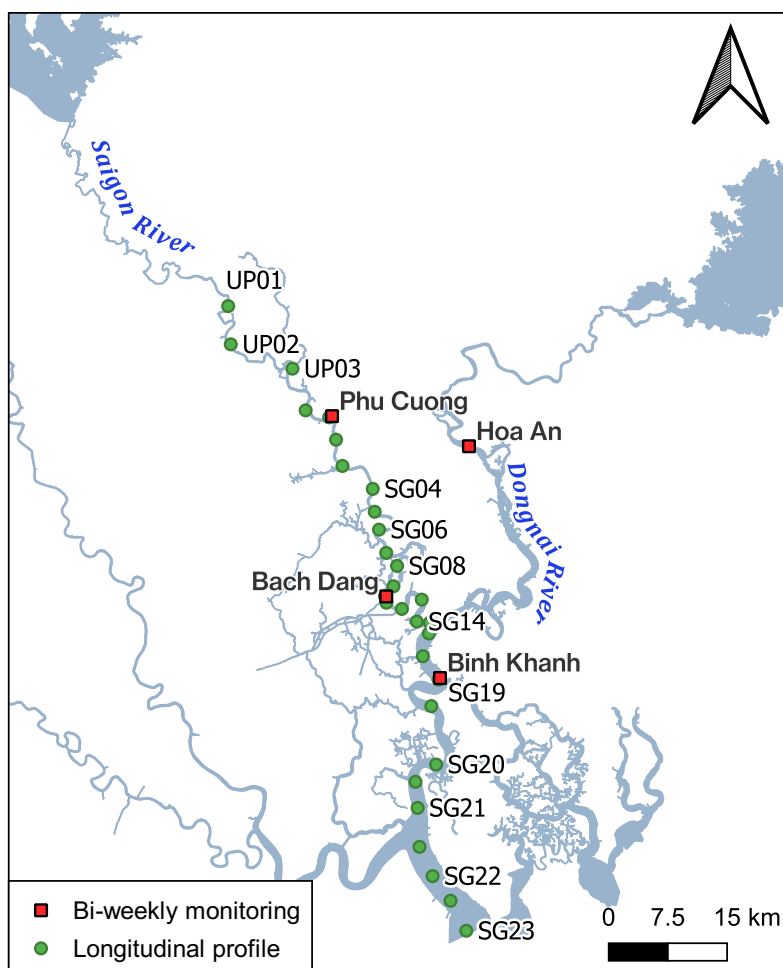


Figure 2.14: Sampling sites of bi-weekly monitoring and longitudinal profile in the Saigon River Estuary

At the survey site, water samples were taken about 30 cm below the water surface and stored in a 2.5 L polypropylene flask for phytoplankton analysis and a 5 L flask for nutrient analysis. The sample was taken during low tide when the Saigon River receives water from tributaries and urban canals. Samples were taken at the mid-river location by using boats or bridges. Physicochemical parameters of water

2. Materials and methodology

samples were measured immediately using the multi-parameter probe (WTW 3420), including temperature, pH, conductivity, salinity, dissolved oxygen concentration and percentage of oxygen saturation.

In addition to water quality monitoring, CARE measures the water level and calculates the discharge by a high-resolution (10-minute) probe for 2017 – 2019 in the upstream area of the Saigon River (Camenen et al., 2021). This data will be discussed in the C-GEM model application.

Longitudinal profile



Figure 2.15: Sampling in Saigon River in 2019.

Four sampling campaigns were conducted at 27 sampling sites covering 141 km of Saigon River and four sampling sites in urban canals of HCMC (close to SG07, SG09, SG11 and SG12) in dry (April 2019 and March 2020) and the rainy season (October 2019 and 2020) (Figure 2.14 and Figure 2.15). Each campaign was carried out on three consecutive days: 14 sampling sites (UP01 – SG 10) on the first day, four sampling sites in urban canals on the second day and 13 sampling sites (SG10 – SG23) on the third day. A GPS was used to mark each point's longitude and latitude values and calculate the distance (km) point to point. For each survey, discrete samples of surface water were collected for physicochemical parameters, total suspended sediment (TSS), nutrients (nitrate- NO_3^- , ammonium- NH_4^+ , phosphate- PO_4^{3-} , total N and total P), organic carbon (particulate organic carbon-POC, dissolved organic carbon- DOC), chlorophyll-a (Chl-a), alkalinity, GHGs (N_2O , CO_2 , CH_4) and phytoplankton identification

In the field, physicochemical parameters (temperature, pH, conductivity, salinity, dissolved oxygen, Chl-a and turbidity) were measured in situ at surface using WTW multiparameters probe and along the vertical profile using Hydrolab Multi-parameter probe. The water transparency was measured with a secchi disk. Five liters of surface water (0–30 cm below the surface) were filled in polypropylene

2. Materials and methodology

bottles for nutrients, organic carbon and Chl-a analysis. For phytoplankton, a 2-L polypropylene bottle for phytoplankton identification and counting was sampled and fixed *in situ* with Lugol solution (Smayda & Sournia, 1978). For GHGs sampling, 100 ml of surface water was carefully filled in borosilicate serum bottles avoiding air bubbles. Then, 50 μ L of mercuric chloride (2%) was added to stop biological activities before sealing by a rubber septum (Garnier et al., 2009) .

2.2.2 Measurement and analytical methods

Total suspended solid, nutrients and organic carbon

In the laboratory, samples were immediately filtered through a Whatman GF/F filter (porosity 0.7 μ m) at the Centre Asiatique de Recherche sur l'Eau (CARE, Ho Chi Minh University of Technology, Vietnam) (Figure 2.16) for analysis of dissolved parameters and TSS. Total alkalinity was analyzed using 40 ml of filtered water with pH electrode (WTW 3420) and HCl 0.1M as titrant.



Figure 2.16: Measurement of nutrients in CARE lab.

Dissolved nutrients (PO_4^{3-} , NO_3^- , NH_4^+ and, SiO_2 as DSi) were analyzed using standard colorimetric methods (American Public Health Association: APHA 1995). Unfiltered waters were used to measure Total N and Total P using the persulfate digestion process and standard colorimetric method (APHA 1995). A TOC analyzer apparatus (TOC-V Shimadzu, CARE laboratory, HCMC, Vietnam) was used to determine Dissolved Organic Carbon (DOC) in filtered water samples (Sugimura and Suzuki 1988). Particulate organic carbon (POC) was measured by

2. Materials and methodology

Cavity Ring-Down Spectrometer (Picarro, Inc.) coupled with a Combustion Module (CM-CRDS, ISTerre laboratory, Grenoble, France) based on López-Sandoval et al. (2019) and Guédron et al. (2021) for sample preparation and analytical methods. POC is expressed in % or in concentration mgCL^{-1} by multiplying POC% and TSS concentrations. TOC is then calculated as the sum of DOC and POC concentrations.

Chlorophyll-a and phytoplankton

Chlorophyll a was measured after filtration through a second GF/F filter using acetone (90%) extraction and spectrophotometry measurement (Aminot and Kérouel 2004).

For phytoplankton counting, one litter of water sample was settled at least 48 h in the laboratory (Smayda & Sournia, 1978). The supernatant (top water) was removed and the settling material, including phytoplankton, was transferred into a measuring beaker and concentrated to 10 – 30 mL depending on the amount of settling material. Phytoplankton was observed at 100 – 400 x magnification on a microscope (Optika 150) and identified to species or genus levels, based on morphology following the system of (Komárek & Anagnostidis, 1988, 1999, 2005) for cyanobacteria, Krammer (1991) for diatoms and other taxonomy books for green algae, golden algae, dinoflagellates and euglenoids. Phytoplankton was enumerated with a Sedgewick Rafter counting cell (volume of 1 mL; PYSER-SGI, England) with a total counted number from 400 individuals or more for each sample (Smayda & Sournia, 1978) to ensure that samples were statistically representative. An individual of phytoplankton is defined as a single cell, a trichome or a colony of phytoplankton as they commonly occur in nature.

Greenhouse gas: CO₂, CH₄, N₂O

GHGs (N₂O, CH₄, CO₂) concentrations were determined with a gas chromatograph apparatus in METIS laboratory, Paris, France (Clarus, Perkin Elmer) based on previously analytical methods (Garnier et al., 2009, 2013; Marescaux et al., 2018).

2.2.3 Eutrophication status and GHGs calculation

Eutrophication index

The eutrophication status in the estuarine and coastal areas can be assessed by the trophic index (TRIX). The TRIX index was previously applied in several countries, such as Mahanadi estuary, India (Srichandan et al., 2019), Foz de Almargem coastal lagoon, Portugal (Coelho et al., 2007). TRIX was calculated based on the linear relation of Chl-a (μgL^{-1}), dissolved inorganic nitrogen–DIN (mgL^{-1}),

2. Materials and methodology

dissolved inorganic phosphorus–DIP (mgPL^{-1}) and the absolute percentage of deviation from oxygen saturation values (aD%DO). The term k is the sum of the minimum logarithmic value of each variable (LogMin) and m is the scale factor (Vollenweider et al., 1998).

$$TRIX = \frac{\log_{10}(\text{Chla} \times aD\%DO \times DIN \times DIP) - k}{m}$$

Five trophic state categories were classified based on TRIX index (from 0 to 10) (Cabral & Fonseca, 2019): Ultra-oligotrophic ($0 < \text{TRIX} < 2$), Oligotrophic ($2 < \text{TRIX} < 4$), Mesotrophic ($4 < \text{TRIX} < 6$), Eutrophic ($6 < \text{TRIX} < 8$), Hypertrophic ($8 < \text{TRIX} < 10$).

GHG fluxes calculation

Water-to-air fluxes of N_2O , CO_2 and CH_4 were calculated using the GHGs concentrations for each sampled station. After, these fluxes per station were daily averaged considering the upstream, urban and downstream sections of Saigon River Estuary.

The water-air flux rates ($\text{mg m}^{-3} \text{ d}^{-1}$) were determined as:

$$F = k(C_w - C_a) = k(C_w - p_a \times k_h)$$

Where:

- C_w is the gas transfer velocity (cmh^{-1})
- C_a is the greenhouse gases concentration in surface water
- C_a is the concentration of greenhouse gases in equilibrium with the atmosphere
- P_a is the partial pressure above the surface water at equilibrium with the atmosphere. We used atmospheric values of 1.865, 0.32 and 410 μatm (or 0.189, 0.032 and 41.54 Pa) for CH_4 , N_2O and CO_2 , respectively, which correspond to global averages of atmospheric GHGs concentrations in 2019-2020, provided by the NOAA, Global Monitoring Laboratory (<https://gml.noaa.gov/ccgg/trends/global.html>, last accessed date April 15, 2021). The differences between the global and local atmospheric concentrations were assumed to be small compared to high GHGs concentrations in the surface water of the Saigon River (Jay, 2009).

k_h ($\text{mol m}^{-3} \text{ Pa}^{-1}$) is Henry's law constant corrected in a given temperature which was used to calculate concentrations of GHGs in equilibrium with the atmosphere.

2. Materials and methodology

$$k_h(T) = k_h^0 \times \exp \left[\frac{-\Delta_{\text{sol}}H}{R} \left(\frac{1}{T} - \frac{1}{T^0} \right) \right]$$

where k_h is Henry's law constant at the reference temperature $T_0 = 298.15$ K; $\Delta_{\text{sol}}H$ is the enthalpy of dissolution. The values of k_h^0 and T^0 are averaged empirical values (Sander 2015):

CO_2 : 3.4×10^{-4} ($\text{mol m}^{-3} \text{Pa}^{-1}$) and 2400 (K)

CH_4 : 1.4×10^{-5} ($\text{mol m}^{-3} \text{Pa}^{-1}$) and 1600 (K)

N_2O : 2.4×10^{-4} ($\text{mol m}^{-3} \text{Pa}^{-1}$) and 2600 (K)

The gas transfer velocity (k) was computed with the following equation:

$$k = k_{600} \times \sqrt{\frac{600}{Sc}}$$

Where:

k_{600} is the normalized gas transfer velocity to a Schmidt number of 600, cm h^{-1} .

Sc_c is the Schmidt number of a given gas at a given temperature in degree Celsius ($^\circ\text{C}$) as described in Wanninkhof (1992).

$$Sc_{\text{CO}_2}(t_w) = 1911.1 - 118.11 \times t_w + 3.4527 \times t_w^2 - 0.04132 \times t_w^3$$

$$Sc_{\text{CH}_4}(t_w) = 1897.8 - 114.28 \times t_w + 3.2902 \times t_w^2 - 0.039061 \times t_w^3$$

$$Sc_{\text{N}_2\text{O}}(t_w) = 2301.1 - 151.1 \times t_w + 4.7364 \times t_w^2 - 0.059431 \times t_w^3$$

The normalized gas transfer velocity was derived from an empirical equation for estuaries which was a function of wind speed, estuarine surface area and water current velocity (Abril et al., 2009).

$$k_{600} = 1.80e^{-0.0165v} + [1.23 + 1.00 \log(TSS)] \times [1 - 0.44 \text{TSS}/1000] \times U_{10}$$

Where:

v is the water current velocity, m s^{-1} (average values from modeling output of (A. T. Nguyen, Némery, et al., 2021)).

S is the estimated surface area of the estuary, km^2 (all areas with tidal influence, including Saigon River, Can Gio Mangrove, parts of Dongnai River and Vam Co River).

U_{10} is the estimated wind speed at 10 m height, m s^{-1} ($2.18 - 4.47 \text{ m s}^{-1}$, data from Global Wind Atlas, <https://globalwindatlas.info>, last accessed date April 15, 2021).

TSS is total suspended sediment in mg L^{-1} .

2. Materials and methodology

Interpretation of internal processes

The participation of nitrification and denitrification in N₂O production can be investigated by using the correlation of excess N₂O (N₂O_{xs}) and Apparent Oxygen Utilization (AOU) (Brase et al., 2017). A linear correlation of AOu and N₂O_{xs} indicates the dominance of nitrification in N₂O production (Brase et al., 2017; Nevison et al., 2003). It is noticed that when mixing is dominant, this linear correlation cannot be used as a proxy for nitrification because of the predominance of linear dilution. The dominance of N₂O is produced by the denitrification process when there is an effect on the linearity of N₂O_{xs}/AOU by increasing the relative amount of N₂O (Brase et al., 2017)

$$N_2O_{xs} = N_2O_{water} - N_2O_{air}$$

$$AOU = O_2_{air} - O_2_{water}$$

Where:

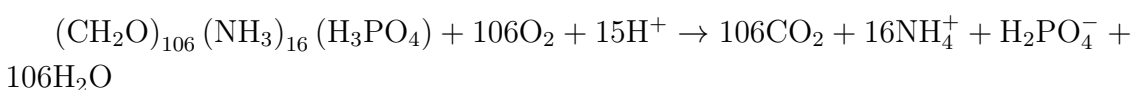
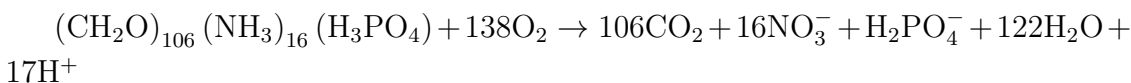
N₂O_{water} is N₂O concentration in the water (μgNL^{-1})

N₂O_{air} is the theoretical equilibrium concentration (μgCL^{-1})

O₂_{water} is the dissolved O₂ in water ($\text{mgO}_2\text{L}^{-1}$)

O₂_{air} is the theoretical equilibrium concentration of the water to atmospheric O₂ concentration ($\text{mgO}_2\text{L}^{-1}$)

Similar to the relationship of N₂O_{xs} and AOU, the relationship of excess CO₂ and AOU can indicate the dominance of respiration and photosynthesis in CO₂ consumption or production (Dinauer & Mucci, 2017). Figure 2.17 illustrates the interpretation of photosynthesis and respiration processes by comparing linear correlation between excess CO₂ and AOU. Figure 2.17 also presents other factors such as allochthonous inputs of CO₂ or anoxic production of CO₂ when the linear correlation between excess CO₂ and AOU is broken. Besides, based on the phytoplankton respiration equation (Redfield et al., 1963) of the degradation of organic carbon into CO₂, the ratio CO₂_{xs}/AOU (mol/mol, phytoplanktonic respiration quotient in aerobic) should be 0.77 (106/138) or 1.0 (106/106).



Besides, the negative relationship between CH₄ (CH₄_{xs} = CH₄_{water} - CH₄_{air}) and AOU can provide information on CH₄ oxidation in water (Bui & Thi Ngoc Oanh, 2018). However, their positive correlation cannot provide information about biological processes related to CH₄ because CH₄ production mainly occurs in sediment (Borges & Abril, 2011; Sierra et al., 2020).

2. Materials and methodology

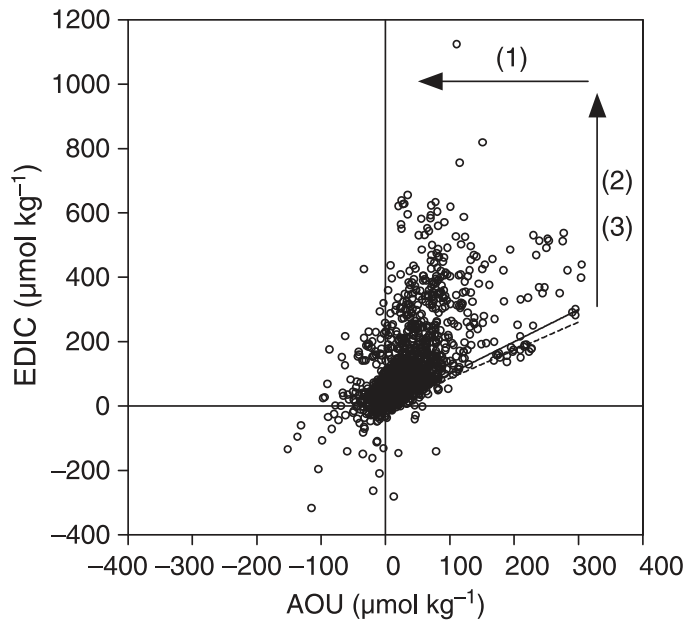


Figure 2.17: Interpretation of respiration process by comparing excess dissolved inorganic carbon (EDIC) vs. AOU. The data sources are from 1641 measurements in 24 estuarine environments worldwide. Processes: The solid line indicates aerobic respiration; the dotted line indicates nitrification. (1) More rapid equilibration of O₂; (2) allochthonous inputs of CO₂ (riverine and lateral); and (3) Anoxic production of CO₂ (from Borges and Abril, 2011)

2.2.4 Multivariate statistical analysis methods

Multivariate statistical analysis was applied to environmental parameters, phytoplankton, GHGs to identify spatiotemporal variation and the relationship between these parameters.

Spatial and temporal cluster analysis

Non-parametric tests were performed on bi-weekly monitoring dataset to identify spatial differences between sampling sites and seasonal differences between dry and rainy seasons in Saigon River by Kruskal-Wallis test with a significance level of $p<0.05$. Hierarchical cluster analysis (HCA) was performed based on Ward's method and Euclidean distance (as a parameter to measure the similarity) to combine the samples with a high similarity relationship into a cluster (Figure 2.18).

It should be noted that the HCA is a heuristic procedure and not a statistical test because choosing different clustering methods will lead to different results. Therefore, the choice of method should be consistent with the objectives of the study (Borcard et al., 2018). Clustering methods include Single-linkage, Complete-linkage, Average-linkage, and Ward's method. Ward's method was chosen for this study because of its ability to be effective in grouping of phytoplankton species of sampling sites along the Saigon River.

2. Materials and methodology

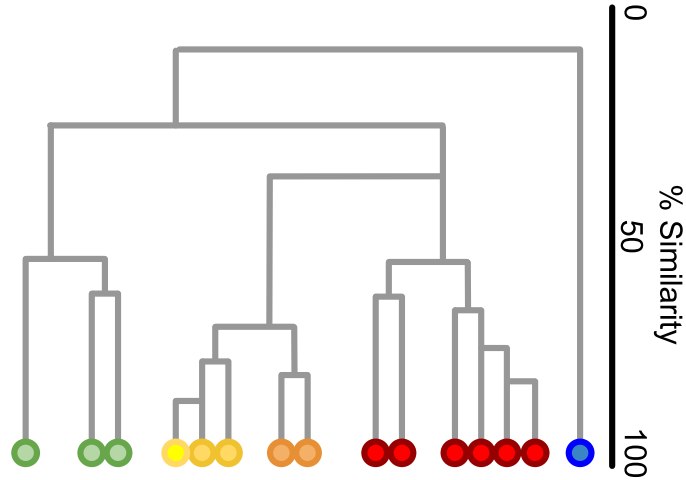


Figure 2.18: Illustration of dendrogram (tree-like diagram) representing the results of HCA. A cluster share similarity between branch points (from Buttigieg and Ramette, 2014)

Principal component analysis and redundancy analysis

Principal component analysis (PCA) was used to determine the patterns of environmental variables in dry and rainy seasons. PCA also detected the similarities of data samples between sampling sites. The redundancy analysis (RDA) was used to identify the main drivers of environmental variables on the phytoplankton community and on GHGs in the Saigon River. Figure 2.19 presents the interpretation of PCA and RDA results.

For analysis of phytoplankton dynamics: The redundancy analysis (RDA) was used to identify the main drivers of environmental variables on the phytoplankton community in Saigon River. Although we used phytoplankton abundances in the RDA, the use of phytoplankton biomass/biovolume would give a more ecologically sounding relation. Therefore, phytoplankton abundances are recommended when there is a correlation between phytoplankton abundances and chlorophyll-a as a proxy for phytoplankton biomass (e.g., Varol and Sen (2018); Hoang et al. (2018); Baek et al. (2020)). In the RDA, phytoplankton abundance data were transformed by hellinger transformation to reduce the influence of high proportion taxa.

Hierarchical partitioning

The hierarchical partitioning (HP) method was used to discriminate independent effects of environmental variables on the variation of research subjects (e.g., phytoplankton densities, GHGs). The HP method tested all possible models in a regression hierarchy to distinguish the variables having high independent correlations with the dependent variable. This method calculates the explained proportion of each predictor/explanatory variable into independent and joint contribution with all other variables (Nally, 1996). The HP method effectively separated the

2. Materials and methodology

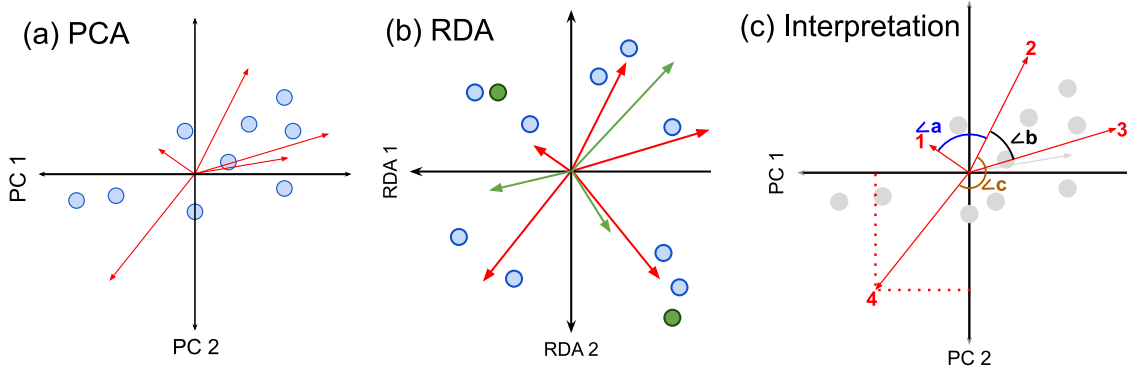


Figure 2.19: Description and interpretation for (a) PCA biplot and (b) RDA triplot. In RDA, the blue points explain for the objects (e.g., sampling site), the green arrows explain for responses (e.g., GHGs concentrations, phytoplankton densities), the red arrows explain for the predictors/explanatory variables (e.g., DO, TSS, TOC concentrations). The green points (optional) are nominal variables. (c) Interpretation: the relationship between variables explained by the red arrows. For instance, arrows 1 and 2 are almost perpendicular, cosines (a)=0, thus not correlate. Similarly, arrows 2 and 4 have a negative relationship because cosines (180°) = -1. Same interpretation applies for both PCA and RDA, but the difference between PCA and RDA is that there is no separation between explanatory variables and responses in PCA (interpretation is adapted from Buttigieg and Ramette, 2014)

independent effects of each environmental parameter which could not be done by separate regression methods (e.g., RDA) (Nally, 1996). Therefore, we use the HP method to estimate the contribution of a single environmental parameters and eutrophication index to the concentrations of GHGs in water column.

The multivariate statistical procedures were done by R software version 3.6.3 (2020-02-29) (R Development Core Team) with the help of FactoMineR (Lê et al., 2008) for PCA, vegan packages (Oksanen et al., 2019) for RDA and hier.part package (Walsh & Ralph, 2020) for HP.

2.3 Water quality modeling

2.3.1 Overview of C-GEM model

Carbon-Generic Estuary Model (C-GEM) is a one-dimensional, computationally efficient reaction-transport model that reduces data requirements using a generic, theoretical framework based on the direct relationship between estuarine geometry and hydrodynamics (Volta et al., 2014). The relationship between estuarine geometry and hydrodynamics is described in Literature Review, which discusses the effect of convergence length on hydrodynamics processes. The biogeochemical reaction network of C-GEM and its parameterization were built upon the study of more than 40 temperate estuaries (Volta, Laruelle, Arndt, & Regnier, 2016). Although

2. Materials and methodology

C-GEM requires minimal data input, C-GEM accurately describes estuarine hydrodynamics and biogeochemical processes (G. Laruelle et al., 2017; G. G. Laruelle et al., 2019; Volta, Laruelle, Arndt, & Regnier, 2016).

Model assumptions

The one-dimensional barotropic, cross-sectionally integrated mass and momentum conservation equations for a channel with arbitrary geometry derived from the following assumptions:

- Well-mixed estuaries
- Small aspect ratio (depth is much smaller than width)
- Buoyancy distribution is constant throughout the cross-section
- Coriolis and lateral pressure gradient terms are negligible
- Wind stress and precipitation or evaporation are negligible impacts

Therefore, the C-GEM model is not suitable to evaluate the benthic-pelagic exchanges. In other words, studies on shallow estuaries with intense element recycling within the sediments are not recommended using this model.

Model platform

Geometry:

C-GEM uses an idealized representation of the estuarine geometry, which can describe the estuarine width by an exponential equation along the estuary gradient.

$$\bar{B}(x) = B_0 \exp\left(-\frac{x}{b}\right)$$

Where x is the distance from estuarine mouth [m], B₀ is the width at estuarine mouth (x = 0) [m], b is the width convergence length [m]. Convergence length is an important parameter linking geometry and hydrodynamics at tidal estuaries. It will be used to calculate the diffusion coefficient of the pollutant transport equation. This is the parameter that reduces the data requirements for hydrodynamics modeling at tidal estuaries.

Hydrodynamics

Based on the above assumptions, the continuity and momentum conservation equations in the literature review become as below (Nihoul & F.C., 1976; Regnier et al., 1998; Regnier & Steefel, 1999).

$$r_s \frac{\partial A}{\partial t} + \frac{\partial Q}{\partial x} = 0$$

2. Materials and methodology

$$\frac{\partial U}{\partial t} + U \frac{\partial U}{\partial x} = -g \frac{\partial \xi}{\partial x} - g \frac{U |U|}{C_h^2 H}$$

where:

x, t are distance along the longitudinal axis [m] and time [s].

R_s is the dimensionless storage water ratio.

A is cross-sectional area=H.B [m^2].

H is instantaneous water depth [m]= the tidally averaged water depth h + the water elevation $\xi(x, t)$.

Q is the cross-sectional discharge [$m^3 s^{-1}$] = $A[m^2].U[ms^{-1}]$.

C_h is Chézy coecient [$m^{1/2}s^{-1}$].

The coupled partial dierential equations above are solved by specifying the elevation ξ at the estuarine mouth and the river discharge at the upstream limit of the model domain. rs, Ch need to be calibrated. $\xi(0, t)$ is represented by a sum of harmonics of the form (Regnier & Steefel, 1999) , then the water depth at estuary is calculated as below:

$$\xi(1, t) = \sum_{k=1}^N H_k f_k \cos [2\pi (\nu_k t + V_k + \mu_k - K_k)]$$

$$H(1, t) = \bar{h}_0 + \frac{1}{2} H_k \sin \frac{(2\pi t)}{T_k}$$

where:

H_k, f_k : the amplitude of the k th tidal constituent and the nodal corrections on the amplitude

T_k : frequency = $1/T_k$. Saigon River estuary is in semi-diurnal regime, dominated by m^2 constituent, thus the tidal period $Tk = 12.42h$ will apply in C-GEM

V_k, μ_k, K_k : astronomical argument , phase and phase lag of the equilibrium tide

$H(1, t), h_0$: The water depth at estuarine mouth and at estuarine mouth[m]

Transport and reaction module

The solute $C(x, t)$ in an estuary can be described by the one-dimensional, tidally resolved, advection-dispersion equation

$$\frac{\partial C_i}{\partial t} = -U \frac{\partial C_i}{\partial x} + \frac{1}{A} \frac{\partial}{\partial x} \left(AD \frac{\partial C_i}{\partial x} \right) + P_i$$

$$\frac{\partial D}{\partial x} = -K \frac{Q_r}{A}$$

$$D_0 = 26 \cdot (\bar{h}_0)^{0.5} \cdot (N \cdot g)^{0.5}$$

2. Materials and methodology

$$K = 4.38 \frac{h_0^{0.36}}{B_0^{0.21} b^{0.14}}$$

$$N = \frac{Q_b T}{P}$$

where:

C_i : concentration of the species i

Q , A : are provided in the hydrodynamic module

D : the dispersion coefficient calculated which mainly based on estuarine geometry (convergence length and ratio of freshwater/volume)

N : the dimensionless Canter Cremers estuary number defined as the ratio of the freshwater entering the estuary during a tidal cycle to the volume of salt water entering the estuary over a tidal cycle.

Q_b is the bankfull discharge [$m^3 s^{-1}$], T is the tidal period [s], P is the tidal prism [m^3]

Q_r : the freshwater discharge [$m^3 s^{-1}$]

K : the dimensionless Van der Burgh coefficient

B_0 : the width at the estuarine mouth [m]

b : the width convergence length [m]

P_i : sum of volumetric biogeochemical reactions and exchanges which affecting species i.

The biogeochemical module implemented in C-GEM allows assessing the concentrations of eight state variables, namely ammonium (NH_4^+), nitrate (NO_3^-), phosphate (PO_4^{3-}), total organic carbon (TOC), Silica (DSi), dissolved oxygen (DO), phytoplankton (diatoms and non-diatoms) and TSS. Seven biogeochemical processes are simulated in C-GEM (Figure 2.20), including oxygen exchange through the air-water interface, aerobic degradation (organic carbon mineralization), nitrification, denitrification, primary production, phytoplankton mortality and TSS erosion deposition (Volta, Laruelle, Arndt, & Regnier, 2016). Currently, the C-GEM model is only suitable for well-mixed estuaries where biogeochemical processes mainly occur in the water column. Benthic processes are considered not to affect the concentration of variables in the water column.

The primary production process corresponds to the growth of phytoplankton and oxygen production through the uptake of C, N, P, and Si in the water column under soluble form depending on environmental forcings, especially light penetration. The light availability in the water column is affected by Total Suspended Sediment (TSS), which is calculated by the model through the simulation of erosion deposition processes. Nitrification consumes DO in the water column, which potentially eliminates a high concentration of ammonium. Denitrification contributes

2. Materials and methodology

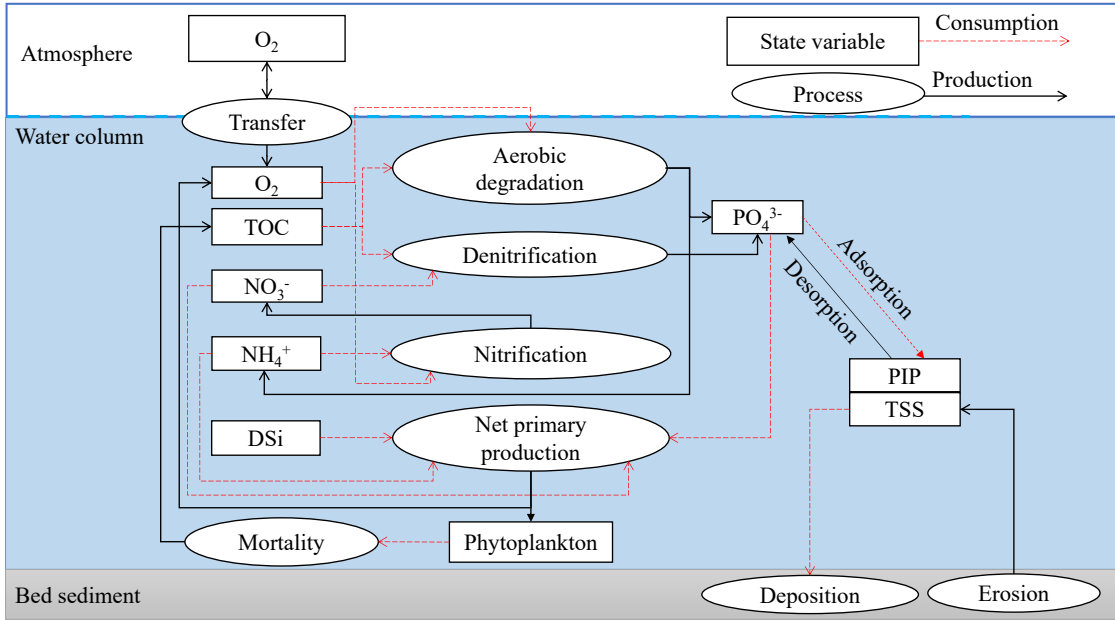


Figure 2.20: The state variables (rectangle) and processes (ellipse) in the biogeochemical module of C-GEM applied in the Saigon River Estuary. Red and black lines represent the consumption and production processes (adapted from Volta et al., 2014)

to anaerobic TOC consumption, PO_4^{3-} production and nitrogen elimination by converting NO_3^- into the inert N_2 gas that escapes from the water column into the atmosphere. Mineralization of organic matter (aerobic degradation) consumes TOC and O_2 while producing PO_4^{3-} and NH_4^+ . Phosphate release from bottom sediment might have a high impact on the phosphorus simulation at shallow estuaries (Vilmin et al., 2015). Note that the modular structure of C-GEM allows for a relatively simple implementation of new processes in its biogeochemical module and increasing the complexity of the N and P cycles could be the subject of future studies.

It should also be noted that the sediment processes (erosion deposition) in the C-GEM model do not directly affect the geomorphological processes of the riverbed. The setup of sediment transport in C-GEM is mainly aimed at assessing the influence of suspended sediments on light diffusion and phytoplankton growth in the water column. The equations for erosion and deposition processes were described by Volta et al. (2014).

Numerical solution

The non-linear partial differential equations were solved using a finite difference scheme on a regular grid, with a grid size $x = 2000\text{m}$ and a time step $t = 300\text{s}$.

- Transport and reaction terms are solved in sequences within a single time step using an operator-splitting approach (Regnier et al., 1997).

2. Materials and methodology

- The adective term is integrated using a third-order accurate total variation diminishing algorithm with ux limiters, ensuring monotonicity.
- The dispersive term is solved by a semi-implicit Crank–Nicholson algorithm.
- Erosion–deposition is numerically integrated using the Euler method.
- The primary production dynamics, which requires vertical resolution of the photic depth, is calculated according to the method described in Vanderborght et al. (2007).

2.3.2 Data requirement

The data required to implement the C-GEM model for Saigon River depends on spatio-temporal scales. A steady-state version of C-GEM is established to determine the dominant biogeochemical processes and the influence of average tidal-resolved conditions in the absence of high-resolution data. The data requirements for steady-state C-GEM are shown in Table 2.1.

The steady-state version does not allow the estimation of the evolution of seasonal variables and phytoplankton development, which also cannot be determined by conventional monitoring. Therefore, the C-GEM model is applied to Saigon River Estuary with a steady-state version first (Chapter 4) and then a transient version (Chapter 5) with more data availability.

Variable	Location	Frequency	Period
Water level, velocity, discharge	7 stations in mainstream 3 stations in tributaries	Monthly	2014 – 2017
T°, salinity, TSS, DO, NH ₄ ⁺ , PO ₄ ³⁻ , COD, BOD ₅	13 stations in mainstream 11 stations in canals 1 station estuary mouth	Monthly Bi-weekly Monthly	2014 – 2017 2014 – 2017 2008 – 2013
T°, salinity, TSS, DO, NH ₄ ⁺ , PO ₄ ³⁻ , TN, TP, NO ₃ ⁻ , TOC, DSi, chlorophyll a	3 stations at Saigon River 1 station at Dongnai River	Bi-weekly	2016 – 2017
Sunshine hours and wind speed	At HCMC	Monthly	2014 – 2017
Estuarine width and depth	83 cross-sections	One time	2008, 2016

Table 2.1: Data collection for model implementation and validation (see Figure 2.21 for the locations of the hydrological and water quality sampling stations)

2. Materials and methodology

Climate data

With a steady-state version, C-GEM needs 10 m wind speed and sunshine duration. Wind speed requires calculating oxygen exchange surface water and atmosphere. Sunshine duration is to calculate irradiation for the photosynthesis rate of phytoplankton. Climate condition data were obtained from the statistical office of HCMC (www.pso.hochiminhcity.gov.vn) with the monthly resolution.

With the transient version, C-GEM uses online-high resolution data from <http://www.lthe.fr/LTHE/IMG/LOGGERNET/IGE-MeteoCARE>, the CARE weather station, which provides 10 minutes wind speed and solar radiation. However, CARE station is far more than 10 km from Saigon River; wind speed data from Global Wind Atlas is thus used instead.

Geometry data

C-GEM 1D does not need detailed bathymetry data. The model only requires an average depth and width of each 2 km along 200 km of Saigon River. The width of the estuary is used to calculate the estuarine convergence length. Mean depth and width for 83 cross-sections along the 200 km long Saigon River Estuary were extracted from bathymetry surveys performed in 2008 and 2016, provided by the Southern Institute of Water Resources Research (SIWRR, Vietnam).

Hydrological data

With the steady-state version, C-GEM needs the average daily discharge at upstream of Saigon Estuary. In addition, the C-GEM requires tidal period and tidal range for a description of generic tidal variation from East Sea Vietnam. Indeed, the steady-state version acts as a quasi-hydrodynamic model with all input parameters constant, but the results are still representative for the fluctuations of the variables over a representative tidal cycle.

The discharge from urban canals of HCMC is calculated based on water usage per capita (T. T. Nguyen et al., [2020](#)). Discharge from tributaries, including Thi Tinh River, Dongnai River, is interpolated from monthly discharge to daily discharge, provided by CEM. However, to avoid misinterpretations from interpolation, the discharge values of the monitoring month will be equal to all days of that month. These errors mainly affect the simulation results downstream of the Saigon River, while the upstream and urban areas are only affected by upstream discharge. At the lower boundary, the water level at the estuary mouth is provided by hourly water level from the Vung Tau station, East Sea Vietnam (<https://uhslc.soest.hawaii.edu/data/>).

2. Materials and methodology

Water quality data

Water quality data were obtained from the Center of Environment Monitoring (CEM, Vietnam) and the Centre Asiatique de Recherche sur l’Eau (CARE, Vietnam). With the steady-state version, C-GEM mainly uses the average concentration provided by CEM. As shown above, CEM lacks data for NO_3^- , Si and Chl-a, CARE data complete lacking CEM data. With the transient version, C-GEM uses bi-weekly data of CEM and CARE from 2017 to 2020. Similar to hydrological data, the daily water quality of boundary conditions is interpreted from bi-weekly data. In addition, the results of 4 longitudinal profiles in April 2019, October 2019, March 2020, and October 2020 are also used to complement to model inputs.

2.3.3 Model description and setup protocol

The generic estuarine model C-GEM was applied in the Saigon River Estuary (200 km, Figure 2.21) to reproduce the nutrient dynamics over a generic tidal cycle representative of dry season conditions. The version of C-GEM used in this study was built upon the steady-state version described in Volta, Laruelle, Arndt, and Regnier (2016), with some parameter values adjusted for tropical monsoon conditions in the Saigon River Estuary. Based on a literature review, the updated values of the modified parameters (discussed below) fall within the ranges provided by Volta, Laruelle, Arndt, and Regnier (2016). The setup process is the same for the steady-state and transient versions; only the input data differs.

Idealized geometry

C-GEM was designed to account for the interdependency between geometry and hydrodynamics in tidal alluvial estuaries. The width convergence length, which controls the system’s shape, is thus a very sensitive parameter for hydrodynamics. Therefore, the value of the convergence length was carefully calibrated against observations (Figure 2.22). The impact of freshwater flow on this estuarine morphology was very different between the upstream (before Dongnai River confluence) and downstream sections (Gugliotta et al., 2020). The estuarine width ranges from 60 m from Dau Tieng Reservoir (km 0) to 350 m (km 140) and rapidly increases to 3690 m at the estuary mouth. This particular geometry justifies the use of a second convergence length to reproduce the entire width profile of the Saigon River Estuary. C-GEM geometry used a short convergence length from the estuary mouth (km 200) to the confluence of the Saigon and Dongnai rivers (km 142). From this confluence to the upstream section (km 142 – km 0), the width of the river only decreases slowly and gradually (with a longer convergence length). Such a strategy was previously used with C-GEM for applications to other estuaries (G. G. Laruelle et al., 2019; Volta, Laruelle, & Regnier, 2016). The depth of the Saigon River Estuary gradually increases from 2.5 m at the outlet of Dau Tieng

2. Materials and methodology

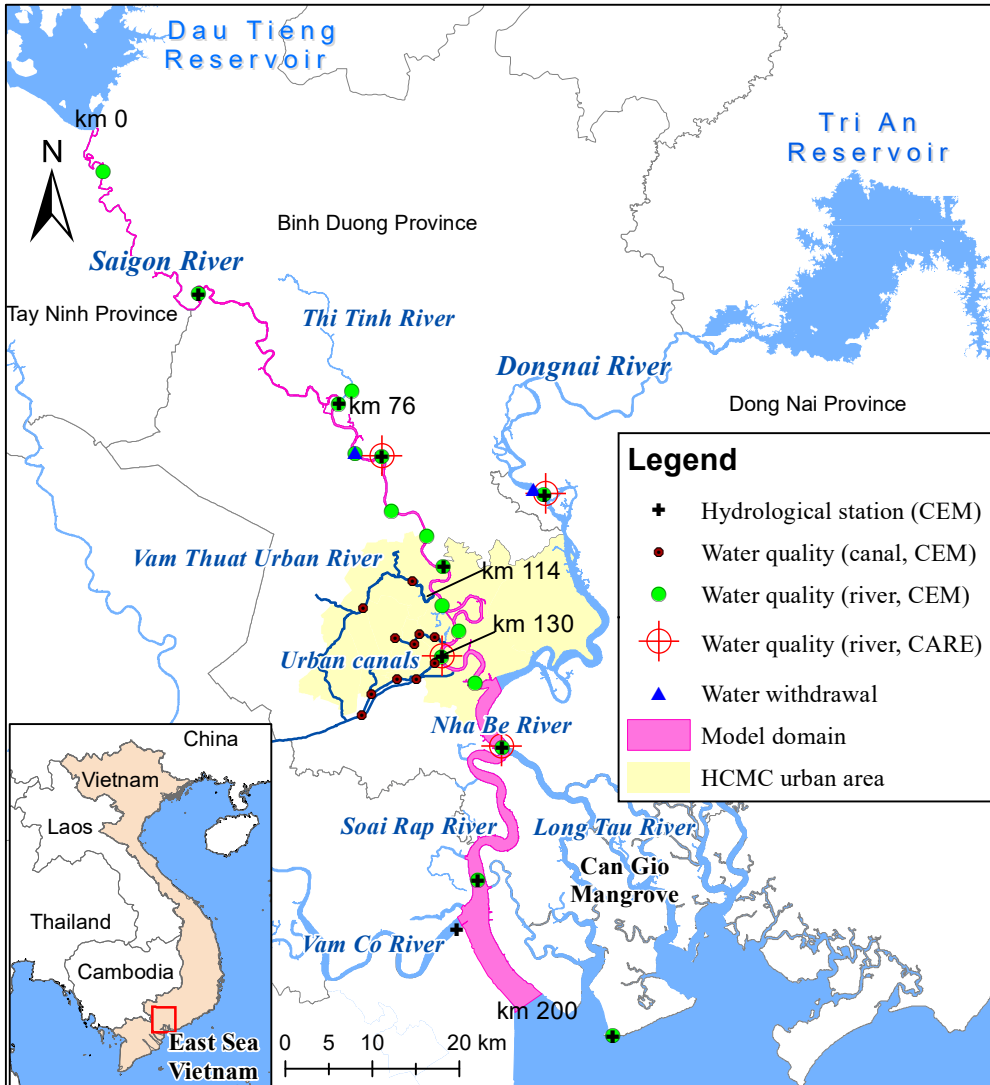


Figure 2.21: Model domain and sampling sites

reservoir to 19 m at km 60. The river's depth is then almost constant over the next 80 km (i.e., until the confluence with the Dongnai River); it then decreases gradually to 9.6 m at the estuary mouth. The idealized geometry in the model captured well the mean estuarine depth and width, which were extracted from 83 cross-sections of the bathymetry (Figure 2.22).

Hydrodynamics and transport module

The one-dimensional hydrodynamic module of C-GEM described the hydrodynamics of the 200 km long reach along Saigon River Estuary based on the continuity and cross-sectional integrated momentum equations. Water elevation at the estuary mouth and freshwater discharge at the upstream limit of the model domain was required to solve the hydrodynamics module. Parameters related to

2. Materials and methodology

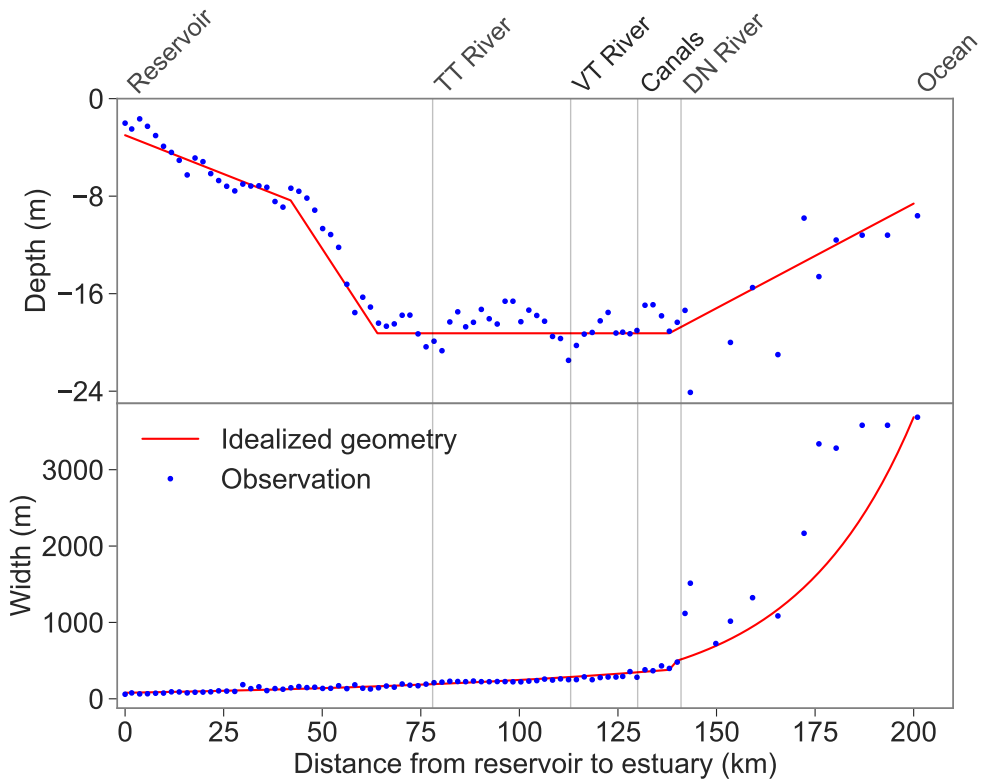


Figure 2.22: Depth and Width of Saigon River Estuary

the characteristics of the tidal amplitude and period are also required to calculate the water elevation at the estuary mouth to constrain the downstream boundary.

2. Materials and methodology

Description	Value	Unit
Width at the estuary mouth, at km 140 (Dongnai tributary) and estuarine upper limit	3690, 350, 60	m
Width convergence length at the estuary mouth, at km 140 (Dongnai tributary)	28000, 92500	m
Depth at the estuary mouth and upstream limit of the model domain	9.61, 2.49	m
The tidal amplitude at the estuary mouth	2.80	m
Tidal period	45720	s
Mean freshwater inflow (from the reservoir) in dry season 2014-2017	17.61	m^3s^{-1}
Lateral discharge from tributaries at Thi Tinh (TT River), Dongnai (DN River) in dry season 2014-2017	6.29, 392.9	m^3s^{-1}
Lateral discharge from the urban river (VT River) and three urban canals	4.3, 5.54	m^3s^{-1}
Chézy coefficient C_h (0 – 40 km), C_h (40 – 140 km), C_h (140 – 200 km)	15, 25, 60	$\text{m}^{1/2}\text{s}^{-1}$
Storage water ratio, r_s	1.0	-

Table 2.2 summarizes the parameters used to solve these hydrodynamics equations for the Saigon River Estuary. Chézy coefficient was the only parameter being fixed for the calibration of the hydrodynamic module, as it was not measured in the Saigon River Estuary. Chézy coefficient typically ranges from $40 - 60 \text{ m}^{1/2} \text{ s}^{-1}$ along alluvial estuaries (H. H. G. Savenije, 2001). The Chézy coefficient was calibrated based on comparing simulated tidal amplitude profiles and mean tidal observations at seven stations along Saigon River Estuary (Figure 2.23). Calibrated results shown that the Chézy coefficient applied Saigon Estuary ranged from 15 to $60 \text{ m}^{1/2} \text{ s}^{-1}$. The upper reaches of the Saigon River were much rougher than other alluvial estuaries. The sudden change of topography of upstream Saigon River Estuary compared to downstream probably explains this larger difference between Chézy coefficients in these two areas than the values reported by H. H. G. Savenije (2001).

After validating the hydrodynamics module, the transport module was implemented to reproduce the dynamics of dissolved variables (e.g., ammonium, dissolved oxygen) and total suspended sediment. The transport module was validated by comparing salinity simulation and observation during the dry season 2014 -

Table 2.2: Physical parameters to build the estuarine geometry and hydrodynamic module in the Saigon River Estuary

2. Materials and methodology

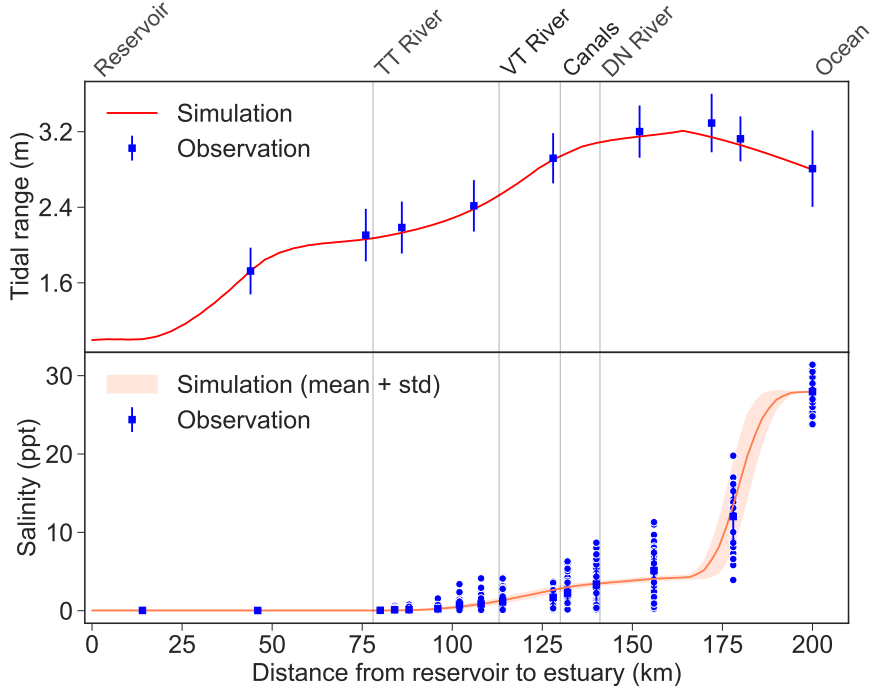


Figure 2.23: Comparison between observed (black marks) and simulated (black lines) profiles for average tidal amplitude and salinity along the Saigon River Estuary. The vertical gray lines correspond to tributaries or canals. Standard deviations (the gray area) of simulation come from hourly fluctuations over tidal cycles

2017. Salinity was used because it is not affected by biogeochemical processes. In addition, salinity distributions reflect the combined processes such as advection-dispersion and mixing processes along Saigon River Estuary. Salinity simulations for the 2014-2017 dry season in Saigon River are depicted in Figure 2.23. The fit of data and model has ensured the precise transport of solutes along the Saigon River over tidal cycles

Biogeochemistry and sediment module

In our simulations, seven of the eighteen biogeochemical parameters used by C-GEM were modified to suit the tropical conditions in the Saigon River Estuary (Table 2.3). These reaction rate constants (except aerobic degradation rate constant) are higher than the C-GEM applications for temperate estuaries. In particular, nitrification, denitrification rate constants are 2-12 times higher. However, these parameters were in the ranges reported by (Volta, Laruelle, Arndt, & Regnier, 2016). In addition, they are similar to findings of biogeochemical reactions in tropical estuaries reported by Miranda et al. (2008) or Vipindas et al. (2018). The eleven other biogeochemical parameters were similar, including phytoplankton maintenance rate constant ($4.11 \times 10^{-7} s^{-1}$), phytoplankton excretion constant (0.05), phytoplankton growth constant (0.29), Redfield ratio (C:Si:N:P = 106:15:16:1),

2. Materials and methodology

Michaelis – Menten constant terms for dissolved silica (1.07), phosphate (0.2), ammonium (228.9), nitrate (26.07), organic carbon (186.25), oxygen in aerobic degradation (31.0), oxygen in nitrification (51.25), dissolved nitrogen (1.13).

Modified parameters	Unit	This study	Reference range
Biological dynamics			
Maximum specific photosynthetic rate	s ⁻¹	5.58 x 10 ⁻⁵	0.107 – 18.2 x 10 ⁻⁵ (a)
Photosynthetic efficiency	m ² s (μmol photons s) ⁻¹	4.11 x 10 ⁻⁷	1.67 – 6.94 x 10 ⁻⁷ (a)
Phytoplankton mortality rate constant	s ⁻¹	37 x 10 ⁻⁸	23 – 350 x 10 ⁻⁸ (a)
Phytoplankton growth constant	-	0.3	0.1 – 0.5 ^(a)
Aerobic degradation rate constant	μmolC L ⁻¹ s ⁻¹	1.44 x 10 ⁻⁴	0.8 – 9.26 x 10 ⁻⁴ (a)
Denitrification rate constant	μmolC L ⁻¹ s ⁻¹	5.00 x 10 ⁻⁴	0.26 – 522 x 10 ⁻⁴ (a)
Nitrification rate constant	μmolN L ⁻¹ s ⁻¹	4.62 x 10 ⁻⁴	0.106 – 21.7 x 10 ⁻⁴ (a)
Particle dynamics			
Critical shear stress for erosion and deposition: km 0 – km 140; km 140 – estuary mouth	Newton m ⁻²	0.25; 0.6	0.17 – 0.6 ^(b)
Erosion coefficient: from km 0 – km 140; km 140 – estuary mouth	kgTSS m ⁻² s ⁻¹	6.0 x 10 ⁻⁶ 1.0 x 10 ⁻⁶	1.0 – 5.0 x 10 ⁻⁶ (b)
Settling velocity	m s ⁻¹	1.0 x 10 ⁻⁴	0.1 – 10 x 10 ⁻⁴ (b, c)

(a): Volta et al., (2016); (b): Letrung et al., (2016); (c): Le et al., (2020)

The TSS concentration has a direct impact on light extinction and then on phytoplankton development. The sediment parameters (critical shear stress and erosion coefficient) were thus determined before adjusting biological ones, though a calibration process only involved hydrological parameters and SPM concentration profiles. The boundary conditions of variables concentrations were the mean values of observations from 2014 – 2017 in the dry season (Table 2.4).

Table 2.3: Determination of sediment parameters and adjustment of biological parameters for the application of the C-GEM model in the Saigon River Estuary

2. Materials and methodology

Site	Unit	Upper	TT River	VT River	Canals	DN River	Lower*
Salinity	-	0.03	0.06	1.70	1.69	0.04	27.95
TSS	mgL ⁻¹	49.0	54.9	67.7	50.8	68.8	83.5
Chl-a**	µgL ⁻¹	4.02	4.02	149.71	104.28	7.61	1.62
DSi	mgL ⁻¹	0.80***	2.84***	1.14	1.06	2.48	0.50
NO ₃ ^{-**}	mgNL ⁻¹	0.40	0.50	0.71	0.45	0.39	0.70
NH ₄ ⁺	mgNL ⁻¹	0.23	0.29	3.36	2.06	0.10	0.01
PO ₄ ³⁻	mgPL ⁻¹	0.05	0.07	0.11	0.07	0.03	0.03
DO	mgL ⁻¹	5.02	4.20	1.66	2.32	4.16	5.34
TOC***	mgL ⁻¹	3.58	3.85	13.66	12.41	3.86	3.21

* Lower boundary used the mean concentrations from 2008 – 2013

** Mean concentrations 2016 – 2017

*** Unpublished data from snapshot measurements 2019-2020

**** TOC was calculated based on BOD₅. $TOC = 1.4 \times BOD_5 + 0.6 (R^2 = 0.67, n = 87)$

TT River is Thi Tinh River; VT River is Vam Thuat River; DN River is Dongnai River

2.3.4 Model evaluation

The model calibration and validation processes were quantitatively evaluated using statistical criteria (Table 2.5). The parameters used for the evaluation included the coefficient of determination (R^2), root mean square error (RMSE) and the bias percentage (pbias). The performance of the hydrodynamics module was assessed by comparing the mean values of simulated variables to observations at eight hydrological stations. The simulation of water quality variables was compared with the mean data at 14 water quality monitoring stations along the Saigon River Estuary.

Table 2.4: Boundary conditions used for the steady-state simulation of water quality variables in the Saigon River Estuary 2014-2017

2. Materials and methodology

Statistical indicator	Equation	Range	Optimal value
R ²	$\left[\frac{\sum_{i=1}^n (O_i - \bar{O})(S_i - \bar{S})}{\sqrt{\sum_{i=1}^n (O_i - \bar{O})^2} \sqrt{\sum_{i=1}^n (S_i - \bar{S})^2}} \right]^2$	0.0 to 1.0	1.0
RMSE	$\sqrt{\frac{1}{n} \sum_{i=1}^n (O_i - S_i)^2}$	0.0 to $+\infty$	0
pbias	$\frac{\sum_{i=1}^n O_i - S_i}{\sum_{i=1}^n O_i} \times 100$	$-\infty$ to $+\infty$	0

O : Observation; S : Simulation; n : number of samples

2.4 Conclusion of Chapter 2

This chapter has provided full information of study site, including the environmental, hydrological, and climatic conditions of the Saigon River Estuary, and the impact of a megacity on the water quality in this estuary. The methods of sampling, analysis, statistical analysis and modeling have been presented in detail. The following chapters will focus on presenting the results by applying the above methods.

Table 2.5: Equations, ranges, and optimal values for assessing model performance

3

Eutrophication and greenhouse gases in an urbanized tropical estuary

Contents

Introduction	82
3.1 Part 1: Spatio-temporal of environmental parameters	82
3.1.1 Physico-chemical parameters	82
3.1.2 Dissolved oxygen, nutrients and organic carbon	83
3.1.3 Eutrophication status	85
3.2 Part 2: Phytoplankton dynamics	87
3.2.1 Spatio-seasonal variations	87
3.2.2 Structure and density of phytoplankton	88
3.2.3 Drivers of eutrophication	91
3.3 Part 3: Interaction of eutrophication and GHGs	97
3.3.1 Longitudinal profiles	97
3.3.2 Greenhouse gases	97
3.3.3 Nitrogen and carbon cycling	104
3.3.4 Relationship of urban discharge, eutrophication and GHGs	108
3.4 Conclusion of Chapter 3	113

Urbanized tropical estuaries are known as hot spots of eutrophication and greenhouse gases (GHGs) in emerging countries. This chapter presents the nutrients, organic carbon, phytoplankton, and greenhouse gases concentrations in the Saigon River Estuary and compares them with other estuaries in different climates. Several internal processes (e.g., nitrification, denitrification, aerobic degradation of organic carbon) are interpreted to identify the main processes affecting water quality and GHGs emissions at urbanized estuaries.

There was a clear separation of nutrients, organic carbon, GHGs, phytoplankton abundance between the urban area and the remaining area of Saigon River

3. Eutrophication and greenhouse gases

because of polluted urban emissions of Ho Chi Minh Megacity (HCMC). The major phytoplankton were diatoms (e.g., *Cyclotella* cf. *meneghiniana*, *Leptocylindrus danicus*), cyanobacteria (e.g., *Microcystis* spp). The dominance of potentially toxic cyanobacteria in the Saigon River possess health risk to local residents, especially upon the increasing temperature context and nutrient loading into the river in the next decades. Phytoplankton densities in dry season were about 100 times higher than in the rainy season. Calculation of the eutrophication index shows that 30-50% of the Saigon River (based on river length) was in the eutrophic state and 10% was in the hypertrophic state, mainly in the urban section. While the concentrations of nutrients did not differ significantly between the dry and wet seasons, the concentrations of GHGs (N_2O , CH_4) and phytoplankton densities were markedly different.

High eutrophication and phytoplankton abundance may enhance carbon dioxide (CO_2) consumption by photosynthesis in the water column. However, the GHGs results at this urbanized estuary were always in supersaturation state. The average concentrations of CO_2 , CH_4 and N_2O at Saigon River in 2019-2020 were $3174 \pm 1725 \mu\text{gC-CO}_2 L^{-1}$, $5.9 \pm 16.8 \mu\text{gC-CH}_4 L^{-1}$ and $3.0 \pm 4.8 \mu\text{gN-N}_2\text{O} L^{-1}$, respectively. Their concentrations were 13 – 18 times, 52 – 332 times, and 9 – 37 times higher than the global mean concentrations of GHGs, respectively. The increase in eutrophication status along the dense urban area was linearly correlated with increased GHGs concentrations. Both nitrification and denitrification resulted in elevated N_2O concentrations in this urban area of the estuary. The high concentration of CO_2 was contributed by the high concentration of organic carbon and mineralization process. GHGs fluxes at Saigon River Estuary were comparable to other urbanized estuaries regardless of climatic condition. Control of eutrophication in urbanized estuaries through the implantation of efficient wastewater treatment facilities will effectively mitigate the global warming potential caused by estuarine emissions.

Chapter 3 uses the information presented in two articles:

Nguyen AT, Dao TS, Strady E, Nguyen TTN, Aimé J, Gratiot N, Némery J. (2021). Phytoplankton characterization in a tropical tidal river impacted by a megacity: the case of the Saigon River (Southern Vietnam). Environ Sci Pollut Res Int. <https://doi.org/10.1007/s11356-021-15850-x>

An Truong Nguyen, Julien Némery, Nicolas Gratiot, Thanh-Son Dao, Thi Minh Tam Le, Christine Baduel, Josette Garnier (*in press*). Does eutrophication enhance greenhouse gas emissions in urbanized tropical estuaries? Environmental Pollution journal. <https://doi.org/10.1016/j.envpol.2022.119105>

3. Eutrophication and greenhouse gases

Introduction

Saigon River Estuary is an urbanized tropical estuary in Southeast Asia. This river receives a large amount of untreated wastewater from Ho Chi Minh megacity (HCMC), resulting in high concentrations of nutrients, organic matter, chlorophyll-a, and oxygen deficiency in the water column. Several studies have revealed that this estuary was experiencing eutrophication in the urban area (T. T. N. Nguyen et al., 2019; Strady et al., 2017). Eutrophication can significantly affect GHGs emissions (DelSontro et al., 2019; Dinauer & Mucci, 2017; Li et al., 2021). This chapter presents the results of water quality monitoring (Figure 3.1 for sampling locations) in 5 years 2015 at Saigon River Estuary (Part 1), spatio-temporal variation of phytoplankton (Part 2) and interaction between GHGs and eutrophication (Part 3). Descriptions of the monitoring program, analysis methods, and data interpretation are detailed in Chapter 2. The contents presented below focus on results and discussion.

3.1 Part 1: Spatio-temporal of environmental parameters

3.1.1 Physico-chemical parameters

Figure 3.2 presents the monitoring data of physico-chemical parameters (temperature, pH, TSS and salinity). The water temperature at Saigon River ranges from about 28°C to 33°C, the highest temperature is usually in March and April of the dry seasons and the lowest at the end of the rainy season or the beginning of the dry season (December) (Figure 3.2a). While the temperature did not differ between the three monitoring stations, the pH concentration was significantly different between Phu Cuong station (PC) and Bach Dang station (BD), Binh Khanh station (BK) with lower pH concentration at PC. The lower pH at PC shows that this area is slightly acidic ($\text{pH} < 7$). There was no difference in pH between BD and BK stations with a range from 6 to 7.5 and no difference between rainy and dry seasons. The pH levels at PC, BD and BK are 6.5, 6.8 and 6.8, respectively.

TSS concentrations ranged from about 20 mgTSSL^{-1} to more than 300 mgTSSL^{-1} (Figure 3.2c). The evolution of TSS at all three stations is usually not seasonal, however in general TSS concentration at PC - upstream is the lowest. The mean TSS concentrations at PC, BD and BK were 32, 95 and 75 mgTSSL^{-1} , respectively.

3. Eutrophication and greenhouse gases

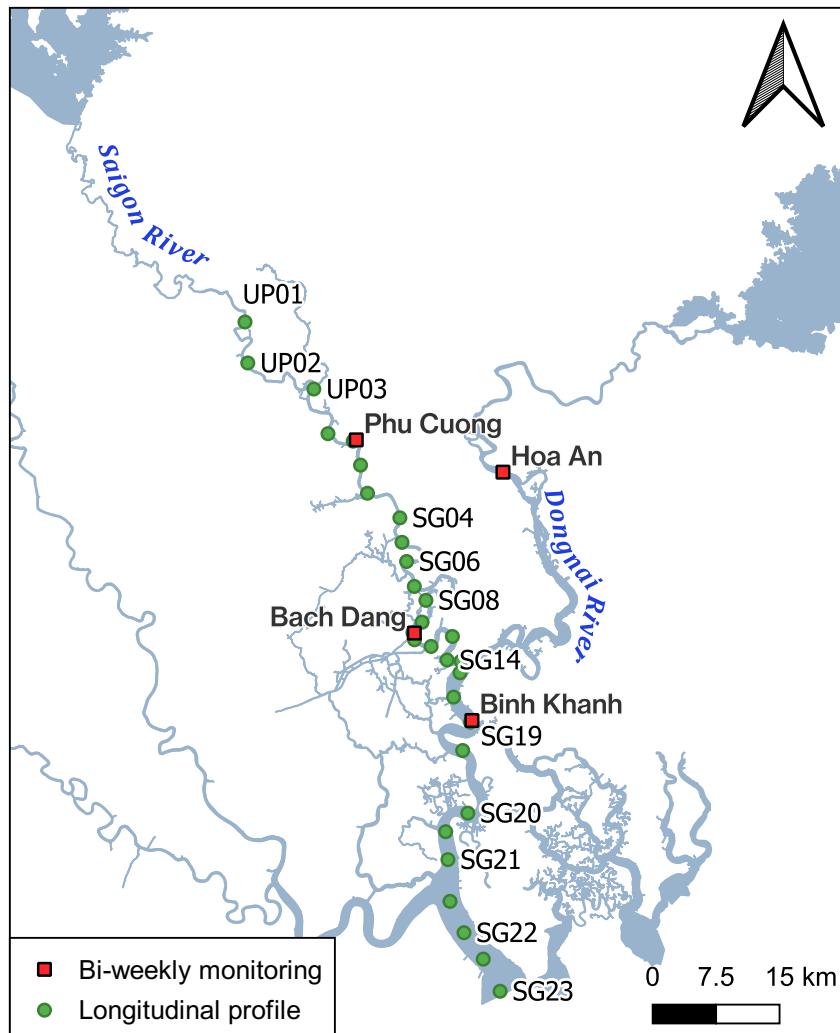


Figure 3.1: Sampling sites of bi-weekly monitoring and longitudinal profiles

3.1.2 Dissolved oxygen, nutrients and organic carbon

Monitoring data of DO, nutrients (NH_4^+ , NO_3^- , PO_4^{3-} , DSi), organic carbon at three monitoring stations in five years along the Saigon River are shown in Figure 3.3. The evolution of DO, nutrient and TOC concentrations at all three monitoring stations fluctuated strongly and did not have a seasonal trend. However, there was a clear difference in concentration between monitoring stations.

The lowest oxygen concentration was at the BD - urban section station, with an average value of $1.5 \pm 0.8 \text{ mgL}^{-1}$ (Figure 3.3a). DO concentrations can range from less than 1 mgL^{-1} to about 4 mgL^{-1} . DO concentrations at PC and BK were 2.1 ± 1.0 and $3.3 \pm 1.1 \text{ mgL}^{-1}$, respectively. While DO was not significantly different between PC and BK, NH_4^+ concentration depicted this distinct phenomenon. The NH_4^+ concentration at BK was only about $0.1 \pm 0.1 \text{ mgNL}^{-1}$, while the NH_4^+ concentrations at PC and BD were 0.5 ± 0.2 and $0.7 \pm 0.5 \text{ mgNL}^{-1}$,

3. Eutrophication and greenhouse gases

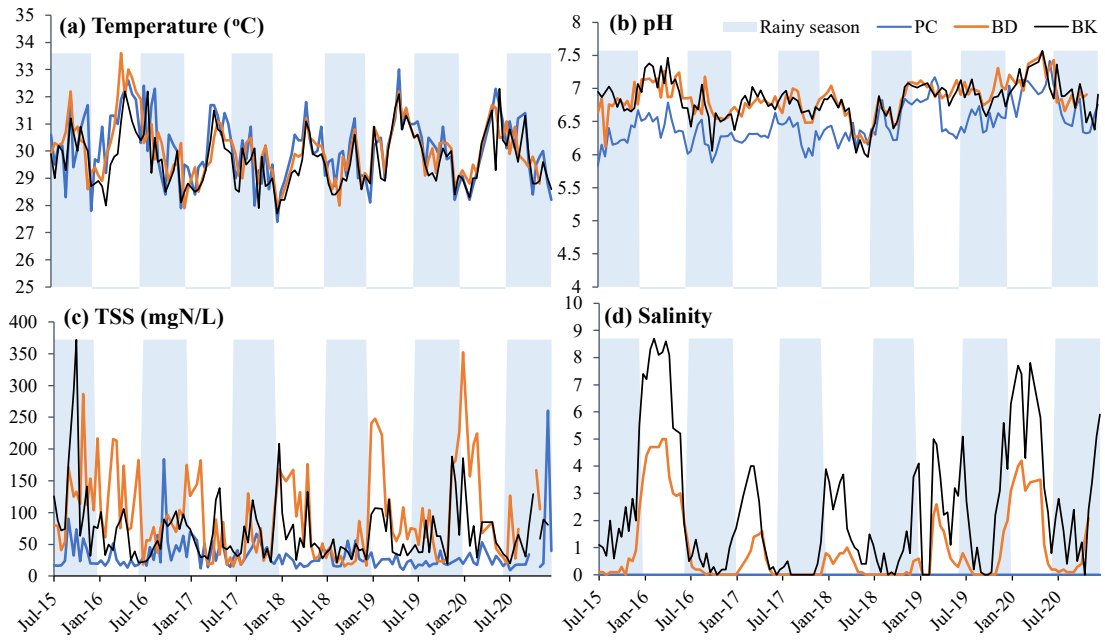


Figure 3.2: Temporal variations of (a) temperature, (b) pH, (c) TSS and (d) salinity at three sampling stations from July 2015 to December 2020. PC, BD and BK are Phu Cuong station at upstream, Bach Dang station at urban section and Binh Khanh station at downstream of Saigon River Estuary

respectively. During the 5 years of monitoring, the concentration of NH_4^+ at BD exceeded 2 mgNL^{-1} four times, the remaining time periods were lower than 1 mgNL^{-1} (Figure 3.3b).

While BK- downstream has the lowest concentration of NH_4^+ , the lowest concentration of NO_3^- was observed at PC - upstream, reaching about $0.2 \pm 0.2 \text{ mgNL}^{-1}$. The NO_3^- concentrations at BD and BK were quite similar at 0.7 ± 0.3 and $0.6 \pm 0.3 \text{ mgL}^{-1}$, respectively (Figure 3.3c). The concentration of PO_4^{3-} is a special pollutant in the Saigon River, its average concentration is only about 0.05 mgPL^{-1} with the concentration at BD being 0.07 ± 0.05 . The concentration of PO_4^{3-} at PC and BK is almost not different, reaching about $0.04 \pm 0.02 \text{ mgPL}^{-1}$. In the dry season of 2020, the concentration of PO_4^{3-} decreased markedly, almost not detected in the analysis, while the concentrations of PO_4^{3-} were highest in rainy season of 2019 and 2020, the, reaching about 0.17 mgP for three monitoring stations (Figure 3.3d).

DSi concentration in three years from 2017 to 2019 was very low, only 1 mgSiL^{-1} , however from the end of 2019 DSi concentration gradually increased from 1 to over 9 mgSiL^{-1} in 2020. In the rainy season of 2020, the concentration of DSi decreased rapidly which was similar to PO_4^{3-} . TOC monitoring results showed that TOC concentrations at PC, BD and BK were 4.8 ± 1.5 , 6.3 ± 2.6 and $3.9 \pm 2.0 \text{ mgCL}^{-1}$, respectively. TOC concentrations did not differ by seasons and did not tend to increase or decrease as strongly as found in DSi and PO_4^{3-} .

3. Eutrophication and greenhouse gases

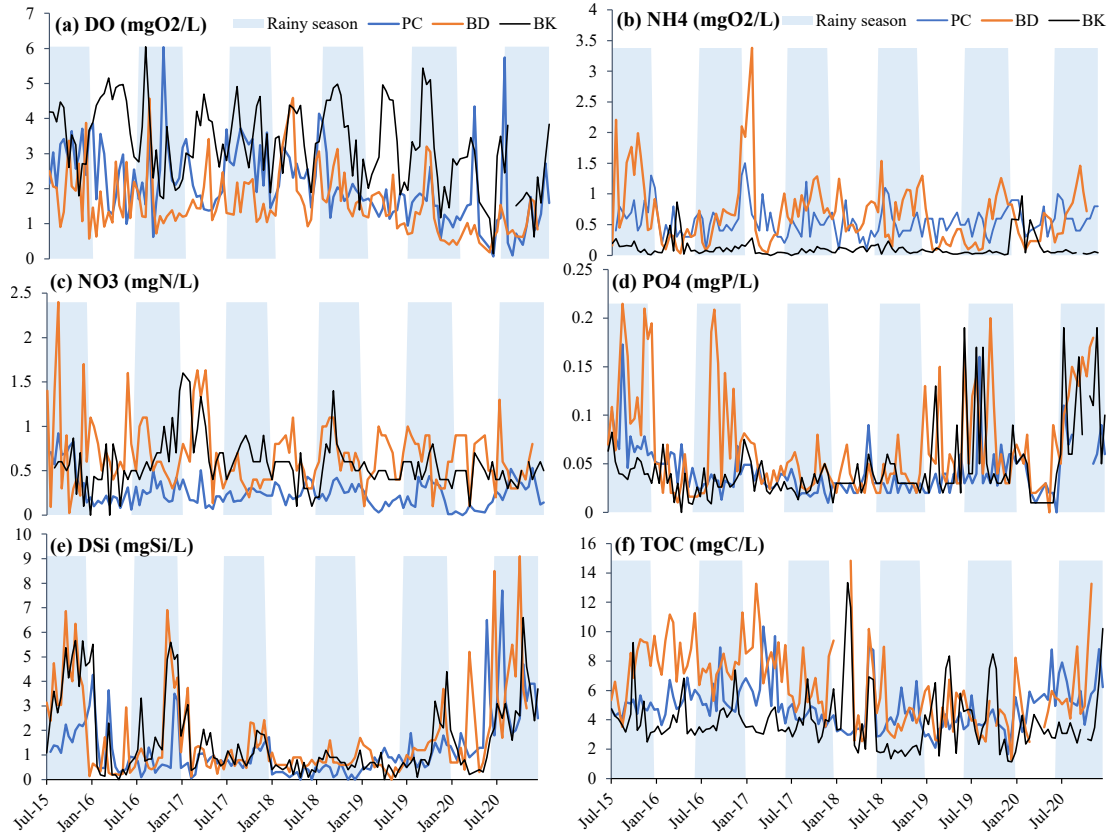


Figure 3.3: Temporal variations of (a) DO, (b) NH₄⁺, (c) NO₃⁻, (d) PO₄³⁻, (e) DSi and (f) TOC at three sampling stations from July 2015 to December 2020.

3.1.3 Eutrophication status

The Chl-a monitoring for about 5 years from 2015 to 2020 shows that differences between the two seasons, with higher Chl-a concentrations in the dry seasons (Figure 3.4 and Figure 3.5). Besides, Chl-a was the parameter with the most different results among the three stations along the Saigon River. The average Chl-a concentrations at PC, BD and BK were 3.3 ± 6.0 , 21.2 ± 26.4 and $1.0 \pm 1.0 \mu\text{gChl-aL}^{-1}$, respectively. Besides, a monitoring station at Dongnai River, a major tributary of Saigon River was also reported with a concentration of $3.7 \pm 3.9 \mu\text{gChl-aL}^{-1}$. Trophic status was also calculated based on the concentrations of Chl-a, DO, DIN ($\text{NH}_4^+ + \text{NO}_3^-$) and PO₄³⁻ to assess the risk of eutrophication in the Saigon River.

Figure 3.4 depicts Chl-a concentrations and trophic index at Phu Cuong (PC) and Bach Dang (BD). Chl-a concentration in PC only once in 5 years of survey exceeded $30 \mu\text{gChl-aL}^{-1}$ in the dry season 2019. Meanwhile, Chl-a concentration in BD in dry season was often higher than $30 \mu\text{gChl-aL}^{-1}$, peaked in the dry season of 2017 with a concentration of $150 \mu\text{gChl-aL}^{-1}$. According to the calculation of the trophic status at Saigon River, the PC station is mainly in the oligotrophic (2–4),

3. Eutrophication and greenhouse gases

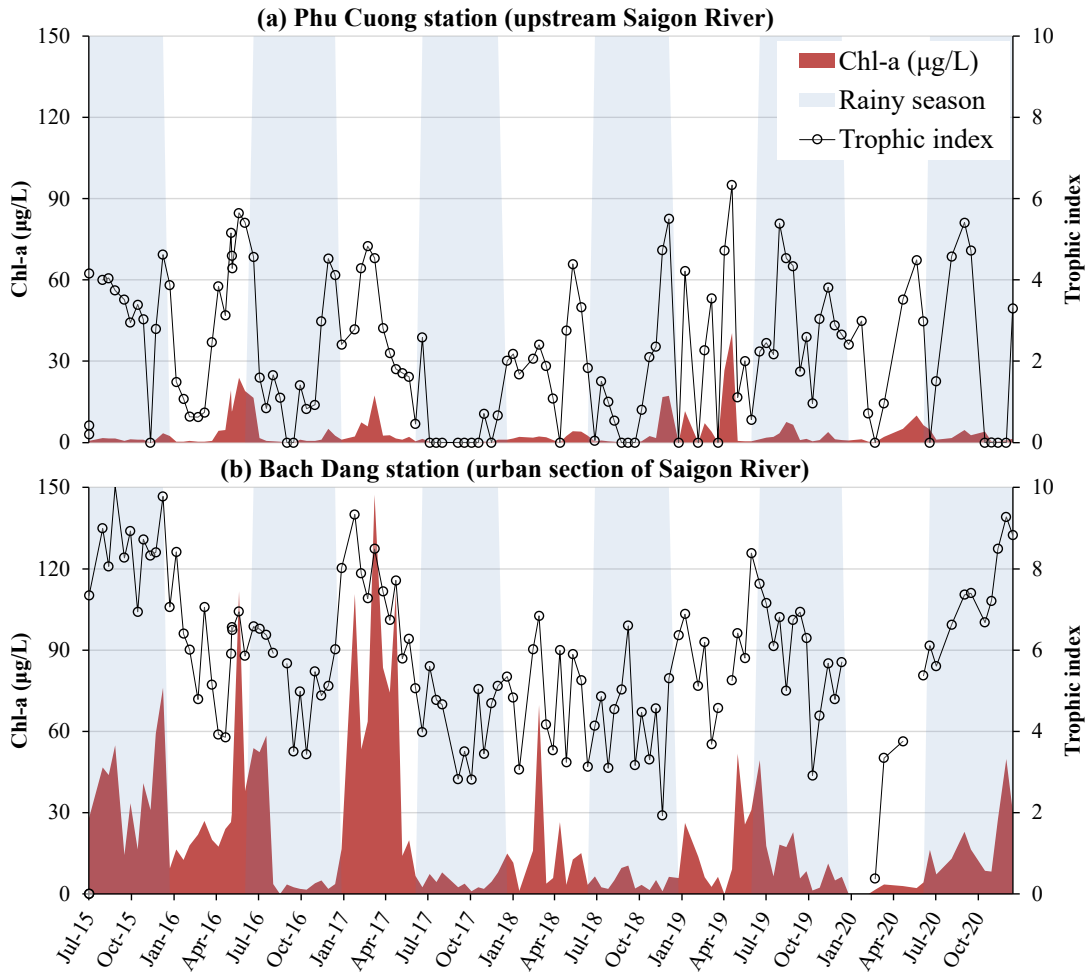


Figure 3.4: Evolution of Chl-a and trophic index in the Saigon River from 2015 to 2020, at (a) Phu Cuong station and (b) Bach Dang station. Trophic index indicates several states of eutrophication, including ultraoligotrophic (0–2), oligotrophic (2–4), mesotrophic (4–6), eutrophic (6–8), and hypertrophic (8–10) states, respectively.

mesotrophic (4–6) state in the dry season and sometimes ultraoligotrophic (0–2) in the rainy season (eg. 2017–2018 and 2020). At the BD station, hypertrophic status (8–10) was determined during the wet season of 2015, 2020 and summer 2017. The remaining time, urban sections of Saigon River were mainly mesotrophic (4–6) and eutrophic (6–8) stages.

Figure 3.5 depicts Chl-a concentration and trophic index at Binh Khanh (BK) and Hoa An (HA) station. Both of these stations have low Chl-a concentration, especially at HA – Dongnai River. Therefore, the trophic indexes of these two stations are often in the state of ultraoligotrophic (0–2), oligotrophic (2–4).

3. Eutrophication and greenhouse gases

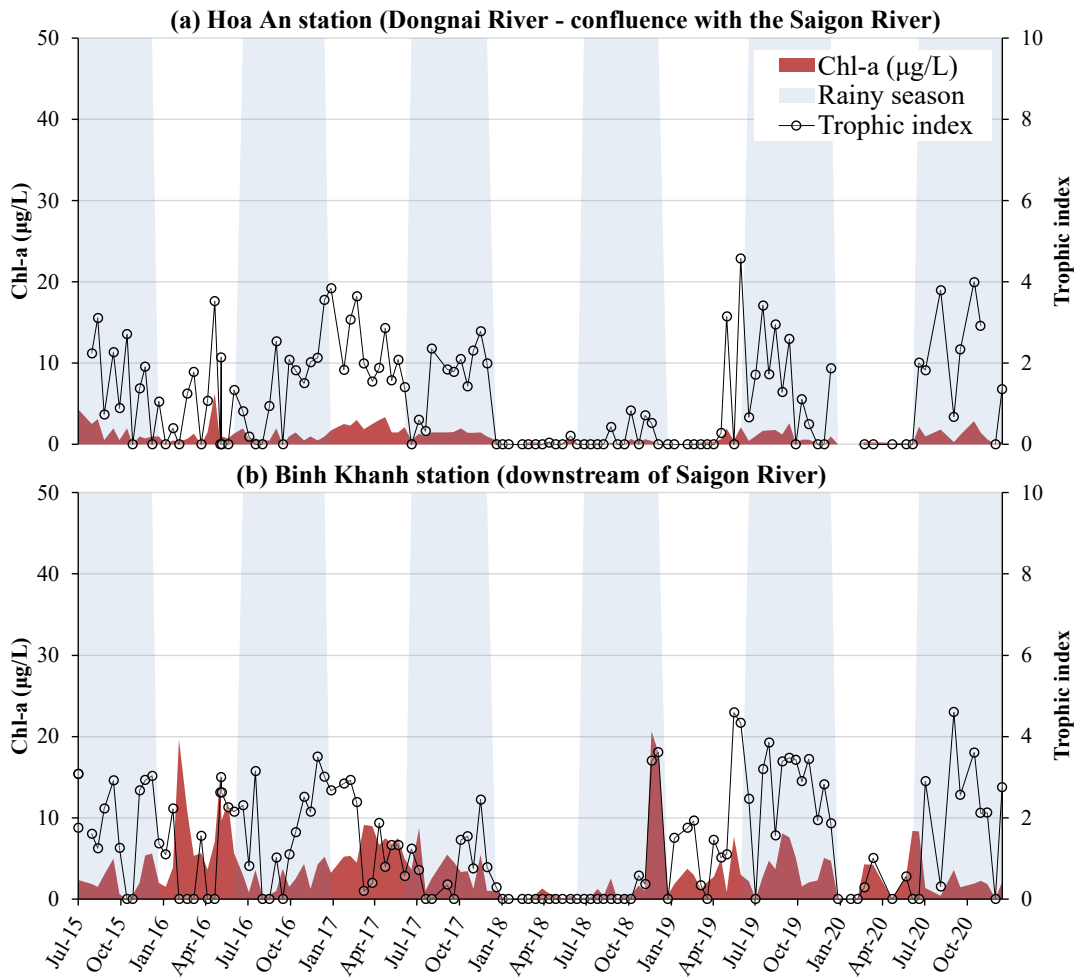


Figure 3.5: Evolution of Chl-a and trophic index in the Saigon River from 2015 to 2020, at (a) Hoa An station and (b) Binh Khanh station

3.2 Part 2: Phytoplankton dynamics

3.2.1 Spatio-seasonal variations

The HCA on phytoplankton densities during the dry season shown three major site groups in which phytoplankton community and densities were closely similar: SG01-SG04, SG05-SG12 and SG13-SG18 (Figure 3.6). It also illustrated a higher similarity of phytoplankton's characteristics between two groups SG01-SG04 and SG05-SG12, than downstream group (SG13-SG18). Three groups were identified during the rainy season: SG01-SG07, SG08-SG12 and SG13-SG18 (Figure 3.6). Unlike HCA for the dry season, the similarity in phytoplankton compositions in the rainy season at upstream SG01 stretched to SG07, which is located in the urban area of HCMC. The close similarity of phytoplankton's characteristics among the sites SG13-SG18 was comparable between the dry and the rainy seasons and had the

3. Eutrophication and greenhouse gases

most difference with the two groups in the upstream and urban areas. In general, HCA results show that phytoplankton composition and densities along the Saigon River varied along three sections of Saigon River (i) upstream, (ii) urban area and (iii) downstream of HCMC. The temporal variation of phytoplankton communities at these sections will be analyzed in turn based on bi-weekly monitoring over a year at three representative sites (SG01, SG10 and SG18).

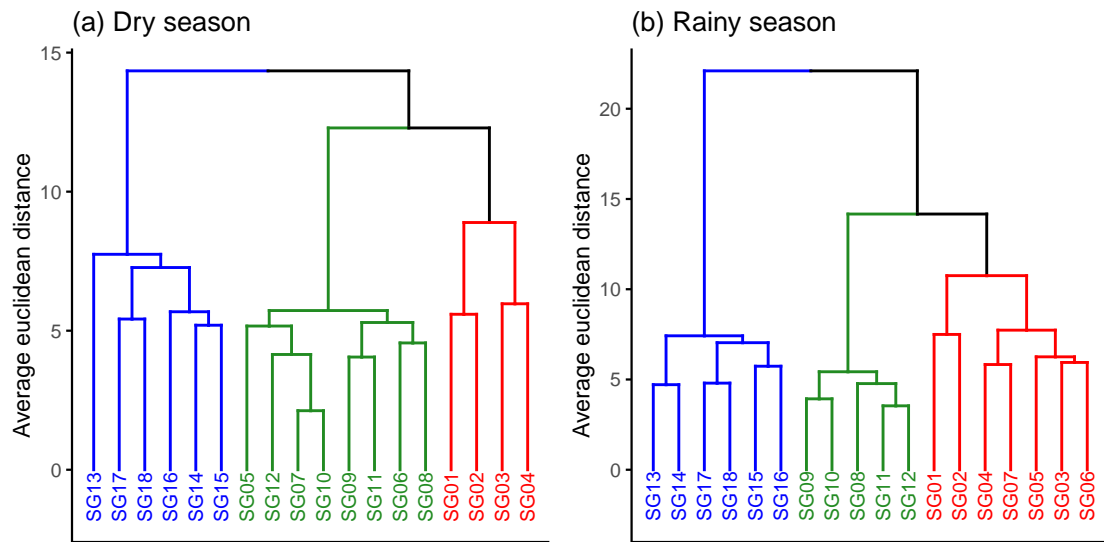


Figure 3.6: Spatial cluster analysis of phytoplankton abundance for longitudinal profile monitoring in dry and rainy season. Red, green and blue colors describe the upstream, urban area and downstream section of Saigon River, respectively.

3.2.2 Structure and density of phytoplankton

The dominant phytoplankton communities identified along the two longitudinal profiles are presented in Figure 3.7. It consisted in mainly species of diatoms (e.g., *Cyclotella cf. meneghiniana*, *Leptocylindrus danicus* Cleve 1889, *Synedra* sp, *Amphiprora* sp, *Aulacoseira granulata* (Ehrenberg) Simonsen 1979, *Nitzschia cf. palea*; *Navicula* sp), cyanobacteria (e.g., *Raphidiopsis raciborskii* (Woloszynska) Aguilera et al. 2018, *Microcystis* spp, *Pseudanabaena* sp, *Dolichospermum* sp, *Oscillatoria* sp), green algae (e.g, *Scenedesmus acuminatus* (Lagerheim) Chodat 1902), and euglenoids (e.g., *Euglena* sp, *Trachelomonas volvocina* (Ehrenberg) Ehrenberg 1834) (Table 3.1).

3. Eutrophication and greenhouse gases

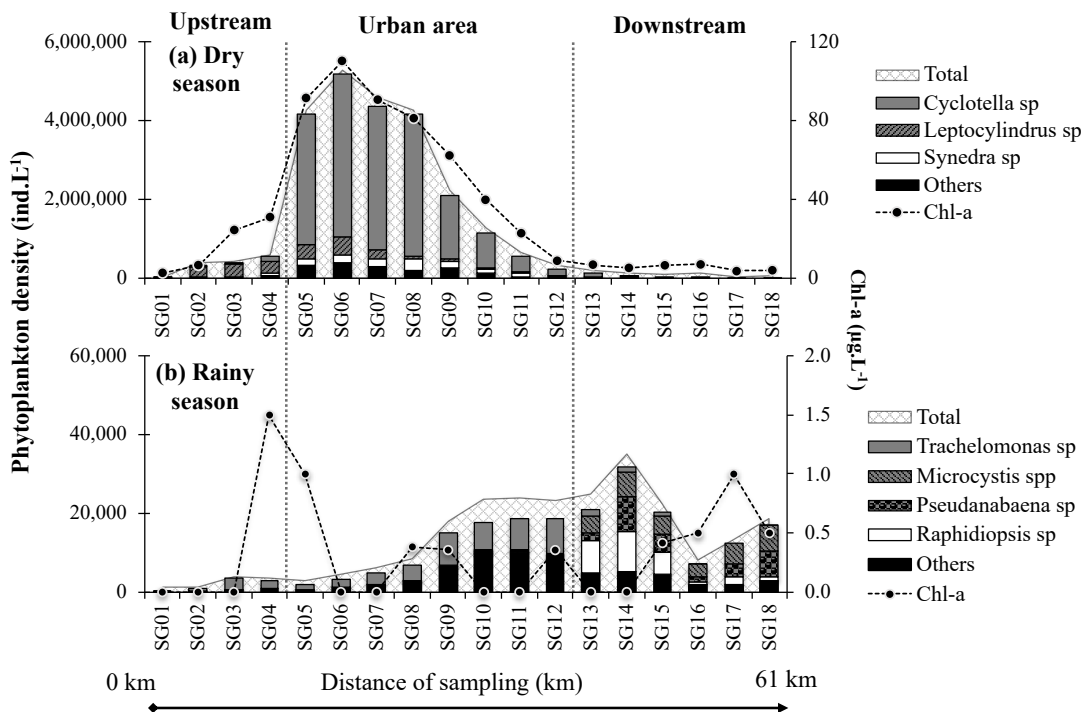


Figure 3.7: Densities of dominant phytoplankton species and Chl-a concentrations in longitudinal profile monitoring in (a) dry season, April 2017 and in (b) rainy season, October 2017. Legend: Total is total phytoplankton abundance.

Stations/ profiles of sampling	Dominant species (percentage composition, dominant index Y)	
	Dry season	Rainy season
Longitudinal profile (total distance 61 km)	<i>Cyclotella cf. meneghiniana</i> (72%, 0.72), <i>Leptocylindrus danicus</i> (9%, 0.09), <i>Synedra</i> sp (6%, 0.06), <i>Amphirora</i> sp (3%, 0.03), <i>Aulacoseira granulata</i> (3%, 0.03)	<i>Trachelomonas volvocina</i> (21%, 0.2), <i>Microcystis</i> spp* (13%, 0.06), <i>Pseudanabaena</i> sp (11%, 0.1), <i>Raphidiopsis raciborskii</i> (11%, 0.04), <i>Cyclotella cf. meneghiniana</i> (6%, 0.05), <i>Nitzschia cf. palea</i> (6%, 0.04), <i>Anabaena</i> sp (5%, 0.04), <i>Oscillatoria</i> sp (4%, 0.04), <i>Euglena</i> sp (4%, 0.04), <i>Scenedesmus acuminatus</i> (3%, 0.03), <i>Navicula</i> sp (2%, 0.02)
SG01 (0 km)	<i>Leptocylindrus danicus</i> (38%, 0.17), <i>Aulacoseira granulata</i> (45%, 0.12)	<i>Eunotia</i> sp (10%, 0.06), <i>Peridinium</i> sp (60%, 0.15)
SG10 (41 km)	<i>Cyclotella cf. meneghiniana</i> (70%, 0.70), <i>Leptocylindrus danicus</i> (30%, 0.27)	<i>Cyclotella cf. meneghiniana</i> (36%, 0.22), <i>Leptocylindrus danicus</i> (35%, 0.21), <i>Trachelomonas volvocina</i> (24%, 0.09),
SG18 (61 km)	<i>Cyclotella cf. meneghiniana</i> (68%, 0.49), <i>Microcystis</i> spp (13%, 0.06), <i>Leptocylindrus danicus</i> (13%, 0.08)	<i>Microcystis</i> spp (50%, 0.34), <i>Pseudanabaena</i> sp (17%, 0.05), <i>Raphidiopsis raciborskii</i> (16%, 0.05)

**Microcystis* spp. consisted of three species *Microcystis aeruginosa*, *Microcystis botrys* and *Microcystis wesenbergii*

3. Eutrophication and greenhouse gases

Table 3.1: Dominant species of phytoplankton based on the spatial and temporal monitoring in the Saigon River

The longitudinal profiles along the Saigon River revealed contrasted phytoplankton densities, varying from 48,200 to 5,296,000 individuals L^{-1} during the dry season (April 2017) and from 1,400 to 35,120 individuals L^{-1} during the rainy season (October 2017) (Figure 3.7). During the dry season, the phytoplankton densities shown a similar range of lower densities (< 0.5 million individuals L^{-1}) in upstream (SG01-SG04) and downstream (SG11-SG18), but they drastically increased up to around 5.0 million individuals L^{-1} from SG05 to SG10. In contrast, during the rainy season longitudinal profile, there was no sudden increase in phytoplankton densities, but they gradually increased from SG01 to SG14 and decreased in downstream of Saigon River (Figure 3.7b). Beside the significant difference in phytoplankton densities between dry and rainy seasons (lower than 100 times), the dominant species along the Saigon River also differed between the two distinct seasons. The dominant phytoplankton species in dry season longitudinal profile were *Leptocylindrus danicus* (SG01 to SG04, km 0 to km 13) and *Cyclotella cf. meneghiniana* (SG05 to SG18, km 17 to km 61) (Figure 3.7a, Table 3.1). The dominant species in rainy season longitudinal profile were *Trachelomonas volvocina* (SG01 to SG12, km 0 to km 45), *Raphidiopsis raciborskii* (SG13 to SG15, km 49 to km 53), and *Microcystis* spp., *Pseudanabaena* sp (SG13 to SG18).

The phytoplankton communities at the three sampling sites (SG01; SG10; SG18) are presented in Figure 3.8. The dominant phytoplankton species, genera and their densities varied among the sites and were globally characterized by: diatoms, (e.g. *A. granulata*, *Navicula* spp., *L. danicus*, *Cyclotella cf. meneghiniana*), cyanobacteria (e.g. *Microcystis* sp., *R. raciborskii*, *Pseudanabaena* sp.) green algae (e.g. *S. acuminatus*), euglenoids, (e.g. *T. volvocina*) and dinoflagellates (e.g. *Peridinium* sp.) (Figure 3.8). A high correlation between total phytoplankton density and chlorophyll-a at SG01 ($R^2 = 0.91$) and SG10 ($R^2 = 0.93$) was observed (Figure 3.8). The phytoplankton densities varied between sites with several orders of magnitude, from 400–327,500 individuals L^{-1} at SG01, 9,330–2,733,000 individuals L^{-1} at SG10, and 1,360–45,700 individuals L^{-1} at SG18 (Figure 3.8). At SG01, the densities were elevated in March and April 2017 (mainly *L. danicus* and *A. granulata*) and very low ($< 50,000$ individuals L^{-1}) the rest of the survey (Figure 3.8a). At SG10, phytoplankton densities were extremely high from January to May 2017 (70% *C. meneghiniana* and 30% *L. danicus*) and lower than 200,000 individuals L^{-1} the remaining months (Figure 3.8b). At SG18 – downstream of Saigon River, there was no significant difference in phytoplankton density between rainy and dry seasons ($p > 0.1$). Phytoplankton densities were the highest during two periods, from January to March 2017 (mainly *C. meneghiniana*) and from June

3. Eutrophication and greenhouse gases

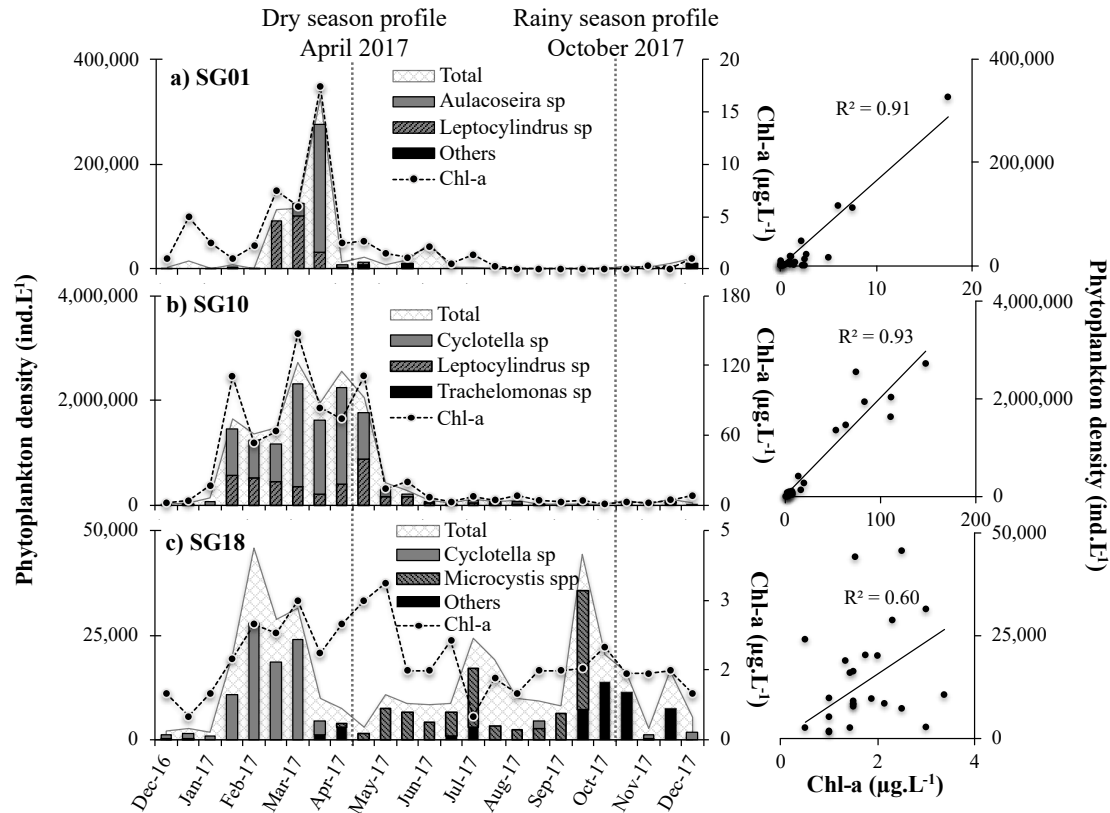


Figure 3.8: Temporal phytoplankton densities at the sites (left panels) and the relationship between total phytoplankton density and Chl-a (right panels) at each sampling site. Legend: Total is total phytoplankton abundance, Others is the other dominant species.

to November 2017 (mainly *Microcystis* spp), and lower than 10,000 individuals L⁻¹ the rest of the year (mainly *L. danicus*, *Pseudanabaena* sp and *R. raciborskii*).

3.2.3 Drivers of eutrophication

Impact of urban discharge on phytoplankton communities

Based on bi-weekly monitoring data at SG01, SG10 and SG18, the PCA was used to identify the various patterns of environmental parameters and similarities between upstream, urban area and downstream sections of the Saigon River. The PCA results could be used to identify the impact of urban discharge on the phytoplankton biomass, supported by the high correlation of Chl-a and phytoplankton abundances ($R^2 = 0.9$, Figure 3.8). Similar to the HCA results on phytoplankton abundances along the Saigon River, the PCA results on environmental parameters separate the three monitoring locations (SG01, SG10 and SG18) (Figure 3.9). The PCA results shown that the water quality in SG10 suffered from the most diverse environmental parameters (TSS, TOC, nutrients, Chl-a and dissolved metals), which were mainly related to pollution from the urban area of HCMC. During

3. Eutrophication and greenhouse gases

the dry season, the first principal component (PC1) mainly represented metal, pH and salinity variables mainly linked to SG18 (downstream section) (Figure 3.9). In PC2 of the dry season and PC1 of the rainy season, the most important variables were the nutrients, TOC, Chl-a, which are associated with SG10 (urban section of the Saigon River). This illustrated that the urban area was affected by urban discharges containing high pollutant concentrations from the connecting canals and creeks during both seasons.

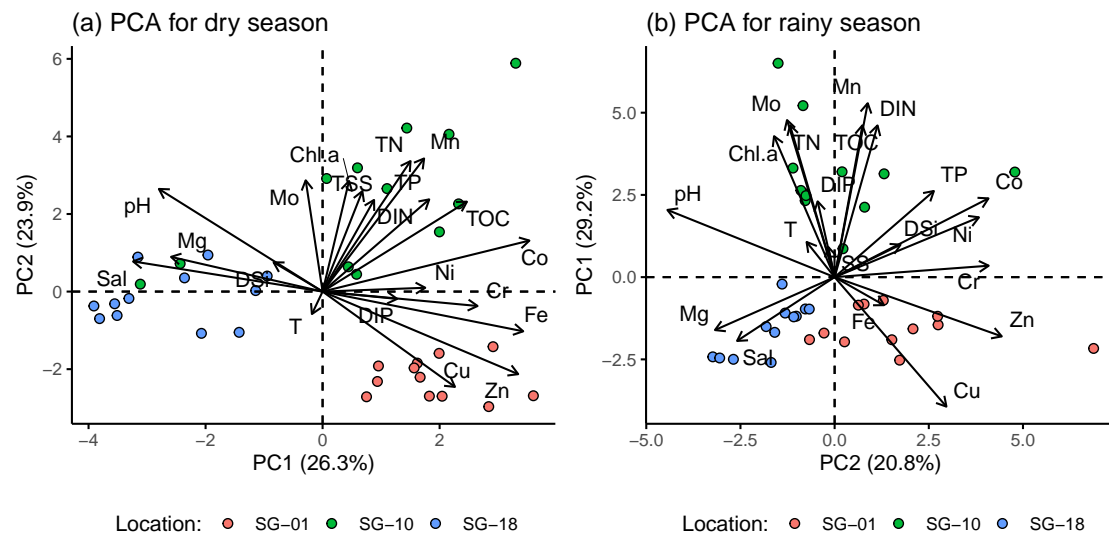


Figure 3.9: PCA of 20 environmental variables (physicochemical parameters, Chl-a, metals) in (a) dry season and (b) rainy seasons in the Saigon River. Upstream, urban area and downstream are SG01, SG10, and SG18, respectively. The environmental variables with longer length are the controlling parameters. Note that the axes of PCA for rainy season were rotated for easier comparison.

RDA method allowed to evaluate the influence of environmental variables on the phytoplankton composition and abundances (Cavalcanti et al., 2020; Varol & Sen, 2018). Based on RDA, 18 environmental parameters can explain 72% ($R^2_{adjusted} = 0.35$) and 68% ($R^2_{adjusted} = 0.31$) of variation of phytoplankton abundances during dry and rainy seasons, respectively. Only abundances of *L. danicus*, *Cyclotella* cf. *meneghiniana*, *Microcystis* spp, *Eunotia* sp had a clear relationship with environmental parameters while other dominant species (mainly in rainy season) such as *Peridinium* sp, *A. granulata*, *T. volvocina*, *R. raciborskii*, *Pseudanabaena* sp have not been explained by RDA. It is noticed that even though total phytoplankton abundance in the Saigon River was highly correlated with phytoplankton biomass (assessed by chlorophyll *a*), the use of phytoplankton abundances had some limitations in assessing ecological relationship because some phytoplankton species, with lower densities, did not have a high correlation with chlorophyll *a* such as *R. raciborskii*, *Peridinium* sp.

3. Eutrophication and greenhouse gases

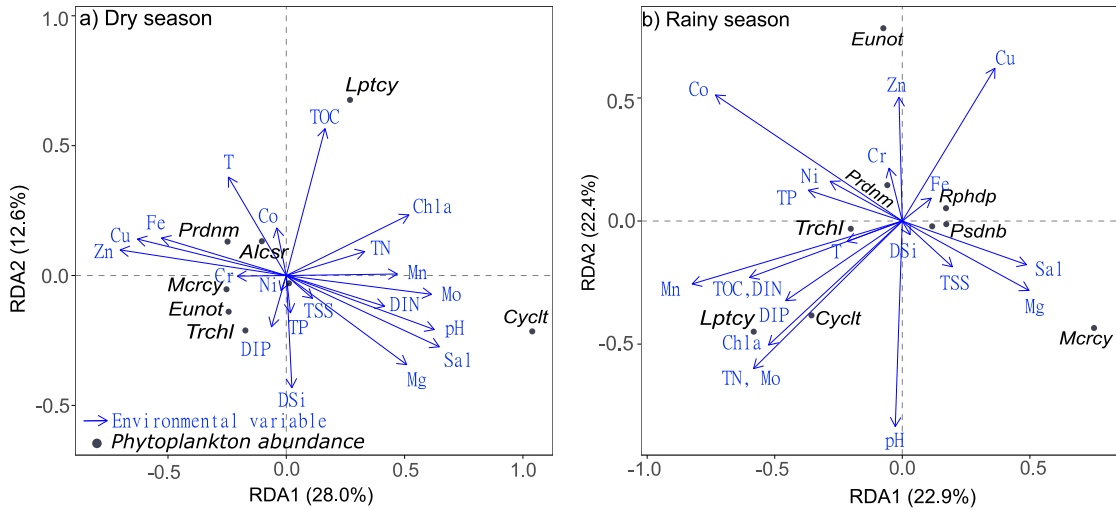


Figure 3.10: RDA on the relationships between environmental variables (as driving factors) and phytoplankton abundances in (a) dry and (b) rainy season in the Saigon River. Lptcy L. danicus, Prdn Peridinium sp, Alcsr A. granulata, Mcrcy - Microcystis spp, Eunot - Eunotia sp, Rphdp R. raciborskii, Trchl T. volvocina, Cyclt - Cyclotella cf. meneghiniana, Psdn - Pseudanabaena sp.

During the dry season, the abundance of *Cyclotella* cf. *meneghiniana* was related with pH, salinity, TN, DIN, Chl-a, Mn, Mg and Mo (Figure 3.10a). This indicates that the majority of *Cyclotella* cf. *meneghiniana* abundance contributed to the biomass of Chl-a measured at the urban area of the Saigon River. While Mn plays an important role in the photosynthesis, Mg is an essential element in algal cellular proliferation which reduces the loss of chlorophyll pigments (Bogorad, 1966). Therefore, the increase of Mn and Mg in the urban area could support the growth of phytoplankton in the Saigon River. However, according to the longitudinal profile during the dry season, there was no difference in Mn, Mg concentrations between at SG04 and SG05, while diatom abundance suddenly increased from about 500,000 to 4,000,000 ind L^{-1} . *Cyclotella* cf. *meneghiniana* became the highest densely phytoplankton, replacing *L. danicus* at SG05. Therefore, the metals (Mn and Mg) were not factors leading to the predominance of *Cyclotella* cf. *meneghiniana* in the Saigon River. Relationship between *Cyclotella* cf. *meneghiniana* and salinity clarified this phenomenon. The salinity intrusion of the Saigon River during the dry season was about 90-100 km from the estuary mouth (SG05-SG06), the salinity reached a maximum of about 0.5 during the dry season at SG05. Therefore, the salinity at SG04 was rarely greater than zero. This interesting finding shown that freshwater diatom *Cyclotella* cf. *meneghiniana* can also dominate in non-zero salinity areas (urban area and downstream section). The second dominant diatom in the Saigon River, *L. danicus* was not associated with nutrients but with TOC and inversely correlated with DSi and Mg. The silicate is a macronutrient for diatoms because it is the main component of the frustules of diatoms (Wetzel,

3. Eutrophication and greenhouse gases

2001). However, it is out of our expectation that there was no correlation between diatoms and DSi. The sufficient levels of silicate in the Saigon River ($> 0.5 \text{ mg L}^{-1}$) helps to explain the lack of this relationship (T. T. N. Nguyen et al., 2019). Besides that, the increase of Mg concentration from SG01 to SG18 (1224 to 14092 $\mu\text{g L}^{-1}$) has led *Cyclotella cf. meneghiniana* outgrown *L. danicus* which fell sharply at SG18. *Leptocylindrus danicus* and TOC were positively linked in this study because high phytoplankton abundance contributed to the TOC in surface water, as previously stated in H.-Q. Nguyen et al. (2020).

During the rainy season, RDA results generally show that diatom densities (*Cyclotella cf. meneghiniana*, *L. danicus*) were positively related to variance of TOC, nutrients (DIN, TN, DIP) and metals (Mn, Mo, Co). The positive relationship of phytoplankton divisions with nitrogen and phosphorus compounds in this study is supported by previous investigations (Liu et al., 2020; Varol & Sen, 2018). The abundance of *Eunotia* sp. during the rainy season was highly related with the Cu, Zn, Co concentrations but negatively related with pH. This species might be sensitive lower concentration of pH in SG01 where the pH was about 6.2 – 6.4. This was in contrast to *Cyclotella cf. meneghiniana* or *L. danicus* that dominated at SG10 (pH range 6.7 - 6.8). This result shows that the small difference in pH between upstream (SG01) and urban area (SG10) may result in the change of dominant species along the Saigon River.

Spatiotemporal effect on phytoplankton densities

In the longitudinal profiles along the Saigon River (SG01 - SG18) and during the bi-weekly monitoring (SG01, SG10 and SG18), we found significant difference of phytoplankton's characteristics between the urban area and the upstream and downstream parts of HCMC (Figure 3.7), suggesting influence of localized environmental factors. The phytoplankton abundance in the urban area were much higher than in upstream and downstream of Saigon River. The phytoplankton abundances at SG01 and SG18 (Figure 3.8a, c) were within the range of the phytoplankton abundances in the Vam Co River (an affluent of the downstream Saigon River) 920 – 383,600 individuals L^{-1} (Dao & Bui, 2016). During the dry season longitudinal profile, the diatom *L. danicus*, a brackish water species, was dominated at the first four sites, SG01-SG04, which could be related to the slight increase of salinity up to SG01 observed at these stations and could support the conditions for the occurrence and out competition of this diatom to other phytoplankton. The freshwater species (except *L. danicus* – a brackish diatom) dominated during the dry period in March and April 2017 at the site SG01, which is coherent with the freshwater characteristic (salinity ~ 0) nearly all year around at the site SG01. The abundance of phytoplankton at SG10 during the dry season was around 10 and 100 times higher than that at SG01 and SG18, respectively

3. Eutrophication and greenhouse gases

(Figure 3.8). These results were comparable with the phytoplankton abundance in the Tigris and Paraguay Rivers which have been also under effect of anthropogenic pressures (de Domitrovic, 2002; Varol & Sen, 2018). At SG10, the dominance of *Cyclotella* cf. *meneghiniana* and *L. danicus* could be driven by environmental parameters such as salinity, trace elements (e.g. Mo, Mn) and high concentrations of nutrients from urban discharge. Dao and Bui (2016) also observed the dominance of diatoms (*Cyclotella* spp and *Eunotia* spp) in the surface waters of Vam Co River (15 km from Saigon River Estuary mouth), which is in accordance with the dominance of diatoms species (e.g. *Navicula* sp., *A. granulata*, *Cyclotella* cf. *meneghiniana*, and *L. danicus*) in our study (Table 3.1).

Unlike upstream and urban area of HCMC, phytoplankton abundance was quite low in the downstream of HCMC (Figure 3.7) and dominated by both diatoms (*Cyclotella* cf. *meneghiniana*) and cyanobacteria (e.g. *Microcystis* spp, *Pseudanabaena* sp, *Raphidiopsis raciborskii*) (Table 3.1). The site SG16 is the meeting point of the Saigon and Dongnai Rivers, and the water discharge of the Dongnai River is around 12 times higher than the one of the Saigon River (T. T. N. Nguyen et al., 2019). The phytoplankton community and abundance would thus be much more influenced by the water from the Dongnai River than by water from the Saigon River at site SG18. Proliferation and bloom forming of cyanobacteria have been commonly observed in the Tri An Reservoir, upstream of the Dongnai River (Dao & Bui, 2016; H.-Q. Nguyen et al., 2020). We found that there was a high similarity of cyanobacteria groups (*Microcystis* spp) found in downstream HCMC and at Tri An Reservoir (Dao & Bui, 2016). Therefore, the commonly presence and dominance of cyanobacteria (Table 3.1) especially at SG18 (Figure 3.8c) could result of (i) the consequence of the diffusion of waters enriched with cyanobacteria, from Tri An Reservoir (H.-Q. Nguyen et al., 2020); and/or (ii) the saline intrusion and anthropogenic emission which enhanced the cyanobacterial development in the most active estuarine section (Paerl & Huisman, 2009) .

Beside the influence of localized environmental factors, seasonal effects lead to a significant change in phytoplankton communities in tropical estuaries (Bledsoe et al., 2004; Cavalcanti et al., 2020; van Chu et al., 2014) . The results of bi-weekly monitoring show that there was a clear difference in the abundance and phytoplankton species between the dry and rainy seasons in the Saigon River. In contrast to the rainy season, the residual water discharge in the Saigon River was very low ($30m^3 s^{-1}$) during the dry season (Camenen et al., 2021). The residence time of the water body in this urban section of Saigon River was estimated to be around two months (A. T. Nguyen, Némery, et al., 2021). High load of nutrients from HCMC and long residence time may strongly enhance the phytoplankton development during the dry season in the urban section of the Saigon River. Ferreira et al. (2005) found that higher phytoplankton biomass is more prevalent in estuaries with long residence time even without anthropogenic impact. However,

3. Eutrophication and greenhouse gases

during the rainy season, stronger water discharge from upstream of the Saigon River had shorten residence time of water body. This leads to a decrease of phytoplankton development before being flushed out of the estuary during the rainy season. The seasonal variation in phytoplankton abundance in the Saigon River has also been found in other tropical estuaries such as Bach Dang Estuary (Vietnam) (van Chu et al., 2014), Red River (Vietnam) (Duong, Hoang, et al., 2019) and Paciencia River Estuary (Brazil) (Cavalcanti et al., 2020). During the dry season, *L. danicus* and *A. granulata* were dominant in upstream of HCMC (SG01), while the freshwater algae *Peridinium* was dominant there in rainy season. At SG10, there was the dominance of another freshwater species (*T. volvocina*) beside the dominance of *Cyclotella* cf. *meneghiniana* and *L. danicus* (Figure 3.8). The appearance of freshwater algae could be due to the prevention of saline intrusion supported by the high discharge in the rainy season. This could also be related to the Saigon River morphometry, which is very deep at this location (> 12 m), and has a lower water current locally, freshwater algae from inland, and eutrophic canals and creeks connecting to the river.

During the rainy season longitudinal profile, the similarity of phytoplankton characteristics among the sites did not clearly separate as in dry season (Figure 3.7). This may be linked with the higher water discharge upstream of Saigon River during the rainy season, resulting in the influence of inland water down to the urban area. The supporting evidences for this hypothesis are that (i) there was not a significant increase of phytoplankton abundance along Saigon River (max of 35,120 ind L^{-1}), and (ii) typical inland algae (*T. volvocina*; Reynolds, 2006) dominated during the rainy season longitudinal profile. Besides, the dominance of the freshwater species of *T. volvocina* and *Pseudanabaena* sp. at the site urban section of Saigon River by the end of the rainy season (Oct, Nov 2017) is supported by the dominance of *T. volvocina* at 12 sites during the rainy season (Figure 3.7). The euglenoids *Trachelomonas* and dinoflagellates *Peridinium* are typical genera of nutrient enrich trophic lakes observed in the Saigon River.

Another noteworthy difference is the formation of cyanobacterial species during the rainy season. Bi-weekly monitoring and longitudinal profile during rainy season both detected cyanobacterium *Microcystis* spp and *R. raciborskii* in the downstream of the Saigon River. While *Microcystis* spp could have originated from Tri An Reservoir (Dao & Bui, 2016), Cyanobacterium *R. raciborskii* may be related to the high TSS concentrations in the downstream area during the rainy season. Some cyanobacterial species such as *R. raciborskii* and *Microcystis* spp. have air aerotopes in their cells, giving them a buoyant capacity to surfaceeater (Mhlanga et al., 2006). The cyanobacterium *R. raciborskii* has a filamentous form which helps to capture more light in turbid waters (Reynolds, 2006). Therefore, the species *R. raciborskii* could withstand the low radiation in water column in high TSS conditions and maintain their normal photosynthesis activities in topwater.

3. Eutrophication and greenhouse gases

3.3 Part 3: Interaction of eutrophication and GHGs

3.3.1 Longitudinal profiles

The spatial variations of water quality variables in the Saigon River in dry and rainy seasons are shown in Figure 3.11. Temporal variation of several water quality parameters was observed between the dry and rainy seasons. Spatial variation was also observed between upstream sites and downstream sites of HCMC. TSS and NO_3^- concentrations were not significantly different between seasons ($p > 0.05$). In the dry season, salinity, water temperature, pH, DO, Chl-a and alkalinity were higher ($p < 0.05$), while TOC, PO_4^{3-} , NH_4^+ were lower in comparison to the rainy season ($p < 0.05$). Besides, the difference in concentrations between seasons and water quality variables varied along the Saigon River. Salinity, TSS, pH and DO gradually increased from 0 to 23 ppt, 11 to 340 mgL^{-1} , 5.7 to 8.1 pH, 0.5 to $6.2 \text{ mgO}_2 \text{ L}^{-1}$, respectively.

In the urban section (SG03 to SG11), Chl-a increased from 0.1 to $26.2 \mu\text{gL}^{-1}$ in the dry season. NH_4^+ , PO_4^{3-} increased significantly in rainy season, $0.1 - 1.1 \text{ mgN L}^{-1}$ and $0.01 - 0.61 \text{ mgP L}^{-1}$, respectively. TOC had a slight increase while POC had a stronger increase in this area up to 15% and then decreased sharply to nearly 0% at the estuary mouth. NO_3^- fluctuated from $0.1 - 0.8 \text{ mgN L}^{-1}$ between sampling sites in both seasons. The total alkalinity in upstream of Saigon River to the urban influences was relatively low ($5 - 45 \text{ mgCaCO}_3 \text{ L}^{-1}$), with even lower values observed during the rainy season (Figure 3.11).

3.3.2 Greenhouse gases

GHG concentrations

The spatial distributions of the GHGs in dry and rainy seasons in the Saigon River are illustrated in Figure 3.12. In general, GHGs tended to increase gradually in the urban section and to decrease downstream. The concentrations of CO_2 were $404 - 5947 \mu\text{gC L}^{-1}$ (mean 2697 ± 1792) in the dry season and $739 - 5620 \mu\text{gC L}^{-1}$ (mean 3641 ± 1567) in the rainy season. The difference in CO_2 concentration between the two seasons was about 30%, with a higher CO_2 concentration in the rainy season. CH_4 concentrations were $0.6 - 3.6 \mu\text{gC L}^{-1}$ (mean 1.8 ± 1.1) and $0.9 - 117 \mu\text{gC L}^{-1}$ (mean 11.3 ± 22.7) respectively, meaning that the concentration of CH_4 in the dry season was about seven times lower than in the rainy season. N_2O concentrations ranged from 0.1 to $20.1 \mu\text{gN L}^{-1}$ (mean 4.6 ± 6.2) in dry season and from 0.0 to $2.9 \mu\text{gN L}^{-1}$ (mean 1.2 ± 0.9) in rainy season. The concentration of N_2O in the dry season was around four times higher than in the rainy season. These results clearly show that there were important seasonal differences in GHGs in the Saigon River. Compared to the global mean atmospheric concentration,

3. Eutrophication and greenhouse gases

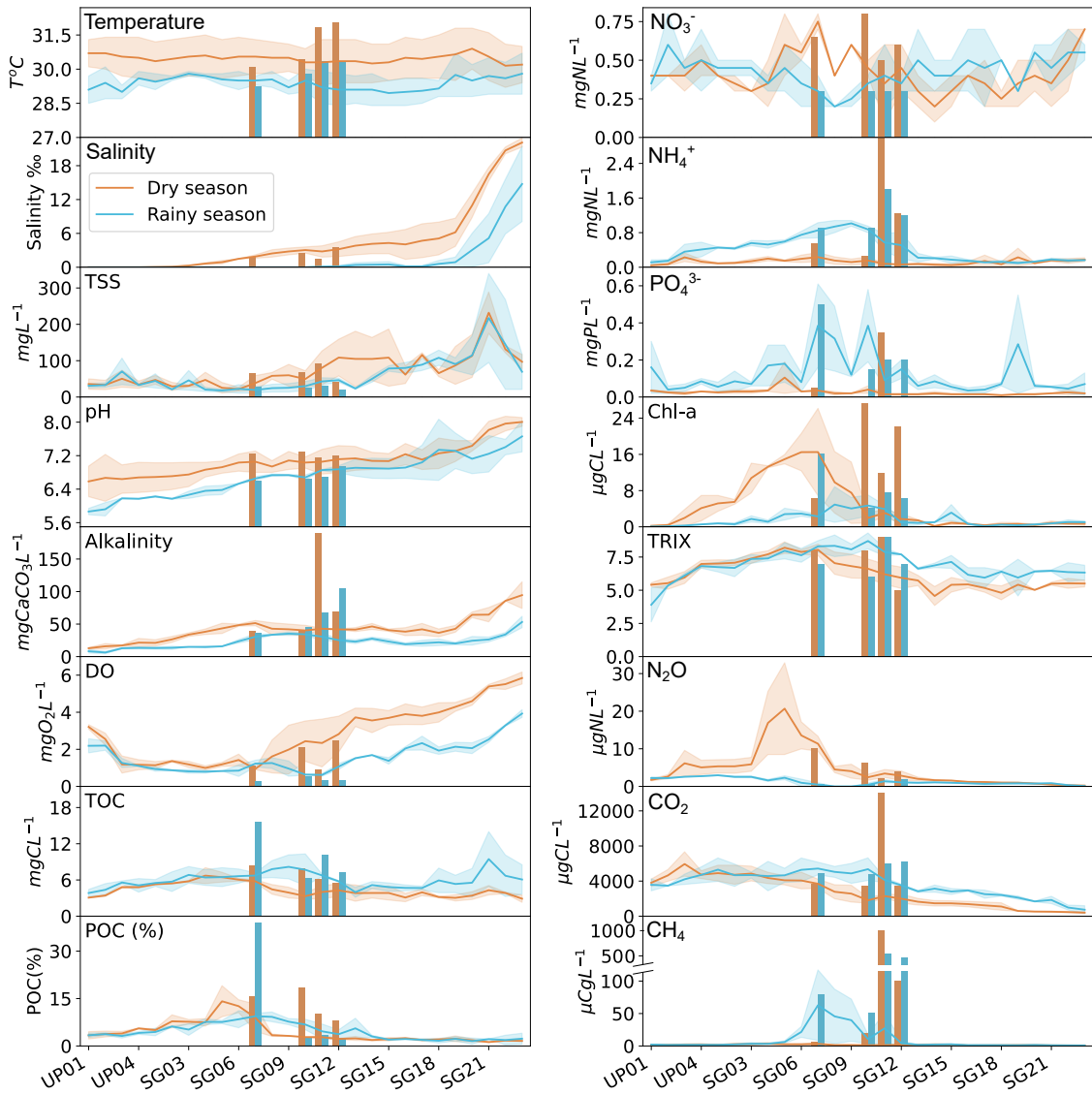


Figure 3.11: Water quality variables and GHG concentrations in the Saigon River Estuary 2019-2020. The lines and color bands represent the mean values and maximum/minimum values of each parameter. The histogram represents water samples collected in the four urban canals of HCMC. Orange and blue colors indicate the samples collected during the dry and rainy seasons, respectively.

the average saturation concentrations of CO_2 , CH_4 , N_2O in the dry and rainy seasons were 13, 52, 37 and 18, 332, 9 times higher, respectively. Calculations based on global warming potential, i.e., CO_2 , CH_4 , N_2O expressed in total CO_2 equivalents ($\text{CO}_2\text{-eq}$) in the Saigon River, led to concentrations of $14311 \mu\text{gCO}_2\text{-eqL}^{-1}$ in dry season and $14935 \mu\text{gCO}_2\text{eqL}^{-1}$ in the rainy season. Their respective contributions are 69.1%, 0.5%, 30.4% and 89.4%, 2.8%, 7.8%, respectively for the three gases (CO_2 , CH_4 , N_2O).

In urban canals of HCMC, the concentrations of GHGs (except N_2O) were much higher than in the Saigon River. The mean concentrations of CO_2 , CH_4 and N_2O

3. Eutrophication and greenhouse gases

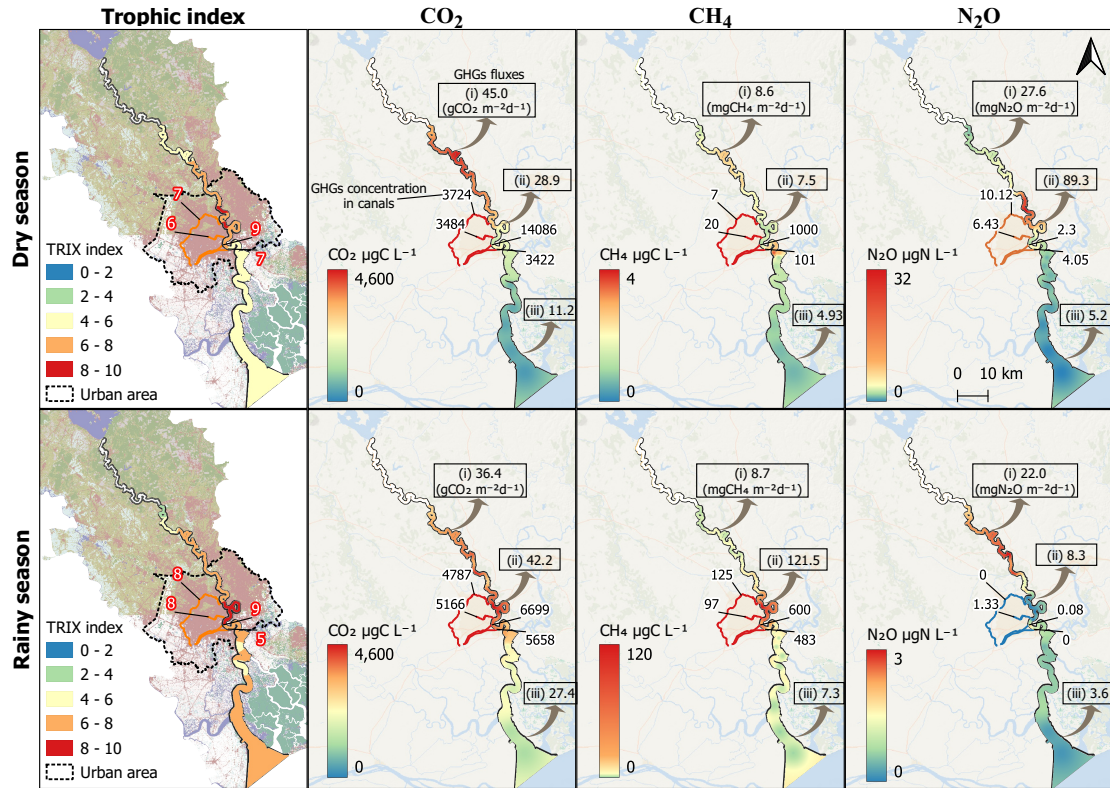


Figure 3.12: Spatial and seasonal concentrations (in $\mu\text{g L}^{-1}$), water-air fluxes of GHGs (in $\text{g m}^{-2} \text{d}^{-1}$ or $\text{mg m}^{-2} \text{d}^{-1}$) and eutrophication index (TRIX) in dry and rainy season in the Saigon River Estuary. The water-air fluxes were calculated for each section (i) upstream, (ii) urban area of HCMC and (iii) downstream of HCMC. It is noticed that the maps were built by using the Inverse Distance Weighting Interpolation (QGIS 3.18.1, 19-Mar-2021) between 27 sampling sites over the 141 km of the Saigon River. No data were acquired in the upper 55 km of the Saigon river, from Dau Tieng Reservoir to UP01 (the river is then underlined with white background).

were $5878 \pm 2739 \mu\text{gC L}^{-1}$, $304 \pm 298 \mu\text{gC L}^{-1}$ and $3.0 \pm 3.0 \mu\text{gN L}^{-1}$ respectively. During the monitoring campaign, we observed plenty of gas bubbles appearing on the water surface of urban canals (Photo S2 in Appendix). At Ben Nghe Canal (close to SG10), CH₄ concentrations were more than 600 and $1000 \mu\text{gC-CH}_4 \text{ L}^{-1}$ in dry and rainy seasons, respectively. On the opposite, the N₂O concentrations in this canal were $2.3 \mu\text{gN-N}_2\text{O L}^{-1}$ in dry season, and very low in rainy season (Figure 3.12). For other canals, the CO₂ concentrations were within the same range of CO₂ concentration in the Saigon River, while CH₄ concentrations were 2 – 25 times higher than those in the river.

GHGs fluxes

The high supersaturation values of GHGs suggest that this tropical estuary contributed significantly to GHGs emissions. With the normalized gas transfer

3. Eutrophication and greenhouse gases

velocity of $12.3 \text{ cm } h^{-1}$ ($10 - 18 \text{ cm } h^{-1}$), the mean density fluxes of CO_2 , CH_4 , N_2O in the Saigon River were 31870 ± 11224 , $26.5 \pm 42.5 \text{ mg C } m^{-2} d^{-1}$ and $26.0 \pm 29.6 \text{ mg N } m^{-2} d^{-1}$. Similar to the concentrations of GHGs (Figure 3.12), the distribution of GHGs fluxes varied between the upstream and downstream sections of the Saigon River and between the rainy and dry seasons. During the dry season, CO_2 fluxes were higher in the upstream (about $78000 \text{ mgC } m^{-2} d^{-1}$ at UP03 in 2020) and much lower in the estuary mouth (about $1700 \text{ mgC } m^{-2} d^{-1}$ at SG23). CH_4 flux decreases gradually from about $8 \text{ mgC } m^{-2} d^{-1}$ in the upstream and urban section to about $5 \text{ mgC } m^{-2} d^{-1}$ in the estuary mouth. N_2O flux was the highest at urban section SG05 (5km landward from an urban canal) with $341 \text{ mgN } m^{-2} d^{-1}$ and undersaturated at estuary mouth with $-1.5 \text{ mgN } m^{-2} d^{-1}$. CO_2 fluxes in the upstream section did not differ significantly between the two seasons, while the CO_2 flux in the urban section in the rainy season was about 1.5 times higher than in the dry season. The higher CO_2 flux tended to move further downstream in the rainy season, compared to the dry season. The CO_2 flux at the estuary mouth thus reached more than $18000 \text{ mgC } m^{-2} d^{-1}$, about 10 times higher than in the dry season. CH_4 fluxes reached the highest level in urban section with up to $466 \text{ mgC } m^{-2} d^{-1}$ in SG07, where urban wastewater is directly discharged. It is about 70 times higher than CH_4 fluxes values observed in upstream and downstream sections. In contrast to CH_4 , there was no increase of N_2O flux in the urban section in the rainy season but instead, a decrease (about ten times) compared to the dry season. The N_2O fluxes at upstream and downstream in rainy season were not significantly different from dry season.

Comparison with other estuarine systems

GHGs in the Saigon River Estuary were supersaturated, indicating that this tropical urbanized estuary is a source of CO_2 , CH_4 , and N_2O to the atmosphere during both seasons. We compared our present GHGs concentrations and associated fluxes between Saigon River with other subtropical and temperate systems experiencing different environmental conditions (Table 3.2). In addition, the emission fluxes of CH_4 and N_2O were converted to CO_2 equivalents to evaluate the total impact of GHGs on global warming potential. Overall, this comparison shows that the concentrations/fluxes of GHGs in the estuaries, heavily affected by emissions from urbanization, industry, and agriculture, were much higher than other areas, whatever the climatic region considered, revealing that anthropogenic activity is the main driver.

GHGs concentrations in the Saigon River were at the same level as in other urbanized estuaries such as Nanfei River, China, (W. Zhang et al., 2021), Zambezi River, Africa (Teodoru et al., 2015), Guadalete Estuary, Spain, (Burgos et al., 2015) and Seine River, France (Marescaux et al., 2018) (Table 3.2). Zambezi River had

3. Eutrophication and greenhouse gases

TOC concentration of about 5.8 mgCL^{-1} , close to the 5.2 mgCL^{-1} of the Saigon River. The CO_2 concentrations of the two systems in their urban areas were similar, but the CH_4 concentration in the Zambezi River was about two times higher while the N_2O concentration was about 10 times smaller than that of the Saigon River. Similarly, the Indian Adyar River, highly polluted because of untreated domestic wastewater in Chennai city, also shown high CH_4 and low N_2O concentrations (Rajkumar et al., 2008). The high CH_4 and low N_2O concentrations were also observed in the urban area of Saigon River in the rainy season (Figure 3.12). Based on CO_2 equivalents calculation, the reduction of N_2O will contribute more efficiently to the reduction in global warming potential than the reduction of CH_4 . Therefore, controlling the concentration of nutrients in wastewater and in the river can be thus considered in priority to improve the effectiveness of reducing global warming.

Concentrations of GHGs in non-urban estuaries can be about 10-100 times lower than in urbanized estuaries, especially for CO_2 and N_2O . The rivers, peat-dominated or mangrove-dominated regions (e.g., B. Hu et al. (2018); Müller et al. (2016); Reithmaier et al. (2020)) revealed low GHGs concentrations regardless of climatic region (tropical or temperate estuaries). This may suggest that despite the existence of higher rates of nitrification and aerobic/anaerobic respiration in tropical/subtropical estuaries than in temperate estuaries, linked to high temperature, these rates might be masked by polluted water from urban discharge. For example, Guadalete Estuary (Spain), an urban estuary in a south Mediterranean region and Po River (Italy) with continental temperate climate still had CO_2 , CH_4 and N_2O concentrations several times higher than the peat-dominated river of the tropical region in Malaysia. Moreover, the Po River (Italy) under the impact of nitrate pollution can lead to N_2O concentrations/fluxes much higher than the ones in urbanized tropical estuaries such as Saigon River (Vietnam), Adyar River (India).

River	Description	Climate	CO_2 μgCL^{-1}	FCO_2 gCO_2	CH_4 $\mu\text{gC L}^{-1}$	FCH_4^* gCO_2eq	N_2O $\mu\text{gN L}^{-1}$	FN_2O^{**} gCO_2eq	F_{total}^{***} gCO_2eq	Reference
Saigon River (Vietnam)	Dominated by urban, 10M inhabitants	Tropical	3174	35.56	5.89	0.64	3.03	8.79	45.0	This study
Adyar River, India	Dominated by urban, 8M inhabitants	Tropical	NA	NA	756	28.3	0.42	0.13	NA	Rajkumar et al. 2008
Zambezi River, Africa	Mainly mining, industrial and agricultural activities	Tropical	3600	12.4	11.2	1.36	0.33	NA	NA	Teodori et al. 2013
Saribas rivers, Malaysia	Non-urban, dominated by oil palm plantations	Tropical	NA	13.7	0.75	0.08	0.23	0.03	13.9	Müller et al. 2016
Nanfei River, China	Dominated by urban, 10M inhabitants	Subtropical	8052	39.6	66	3.14	5.7	2.24	45.0	Zhang et al. 2021
Shark River estuary, USA	Mangrove-dominated estuary	Subtropical	NA	4.048	NA	0.03	NA	0.03	4.1	Reithmayer et al. 2020
Guadalete Estuary, Spain	Receive discharge of urban effluents and agriculture crop	Mediterranean	NA	NA	5.7	0.22	3.84	1.22	NA	Burgos et al. 2015
Bay of Cádiz (SW Spain)	A tidal creek receiving waters of fish farm	Mediterranean	864	5.5	0.59	0.04	0.384	0.56	6.1	Ferrón et al. 2007
Lower Seine River, France	Heavily urbanized and industrialized	Temperate	2500	NA	2.75	NA	2.5	NA	NA	Marescaux et al. 2018
Duliujiang River, China	Natural river	Warm temperate	480	0.56	1.2	0.12	0.001	0.36	1.0	Hu et al. 2018
Po River, Italy	Nitrate pollution. Intensive farming, 16M inhabitants	Continental temperate	5483	22.7	2.54	0.28	4.69	22.35	45.3	Laini et al. 2011

* CH_4 flux in $\text{gCO}_2\text{eq/m}^2/\text{d} = \text{FCH}_4 \text{ gCH}_4 \text{ m}^{-2}\text{d}^{-1} \times 28$

** N_2O flux in $\text{gCO}_2\text{eq/m}^2/\text{d} = \text{FN}_2\text{O} \text{ gN}_2\text{O} \text{ m}^{-2}\text{d}^{-1} \times 298$

*** F_{total} is total CO_2 equivalent flux = $\text{FCO}_2 + \text{FCH}_4 + \text{FN}_2\text{O}$

NA is not available

Table 3.2: Comparison of mean GHGs concentrations and fluxes (CO₂ equivalent) in estuaries under different environmental conditions (Tropical, Temperate, Mediterranean) and human pressures.

10³

3. Eutrophication and greenhouse gases

3.3.3 Nitrogen and carbon cycling

The statistical methods (RDA, HP) allowed evaluating the relationship and contribution of eutrophication, physicochemical variables to the variations of GHGs in the Saigon River Estuary. We searched here to identify more precisely the processes involved in the production and consumption of GHGs to evaluate the behavior of GHGs in this urbanized tropical estuary.

Nitrification and denitrification

N_2O is predominantly released via microbial processes, such as nitrification and denitrification, occurring in the water column, sediments or in suspended particles (Bange, 2008). It is known that N_2O production from these processes is highly dependent on DO concentration (de Bie et al., 2002). In water column with the presence of O_2 , N_2O is mainly formed during the first step of nitrification, as a by-product of ammonium oxidation, from NH_4^+ to NO_2^- (Garnier et al., 2007), but also as nitrifier denitrification at low oxygenation (Wrage et al., 2001; Zhu et al., 2013). Besides, denitrification can play the main role in N_2O production under hypereutrophic condition and associated anoxia (Galantini et al., 2021). Manjrekar et al. (2020) found a positive relationship between N_2O and NH_4^+ in several tropical estuaries, which suggested that nitrification was the possible mechanism for N_2O production in these systems. in the Saigon River, we did not detect this correlation (Figure 3.8). In dry season, the N_2O production in the Saigon River can be due to nitrifier denitrification under low DO concentration condition (2mg L^{-1}). In rainy season, denitrification may account mostly for the N_2O production with lower DO concentration (1 mg L^{-1}) (Figure 3.11).

Several studies determined N_2O production by nitrification process based on a linear relationship between N_2O excess ($\text{N}_2\text{O}_{\text{xs}}$, i.e., N_2O supersaturation) and apparent oxygen utilization (AOU) (e.g., Nevison et al. (2003); Santoro et al. (2021); Brase et al. (2017)). We explored such a linear relationship in upstream and downstream of Saigon River in the dry season. These positive correlations are indicative of O_2 consumption linked to N_2O production. Therefore, most of N_2O production in upstream, downstream sections and some parts in the urban area of HCMC was mainly derived from nitrification/nitrifier denitrification processes, as shown by a modeling approach we applied in previous work (A. T. Nguyen, Némery, et al., 2021). We also observed a break of linearity with the highest N_2O supersaturation values at the highest AOU (i.e. low DO condition) in the urban stretch of Saigon River (SG04 – SG07 with $\text{N}_2\text{O}_{\text{xs}}$ of $4.5 – 35 \mu\text{g NL}^{-1}$, Figure 3.13a). The broken linear relationship of AOU and $\text{N}_2\text{O}_{\text{xs}}$ was mainly observed at highly urbanized estuaries, which provide the most intense N_2O production, supported by the denitrification process (Murray et al., 2015). Besides, N_2O emissions in the estuarine system are generally higher due to the propensity of nitrifying bacteria to

3. Eutrophication and greenhouse gases

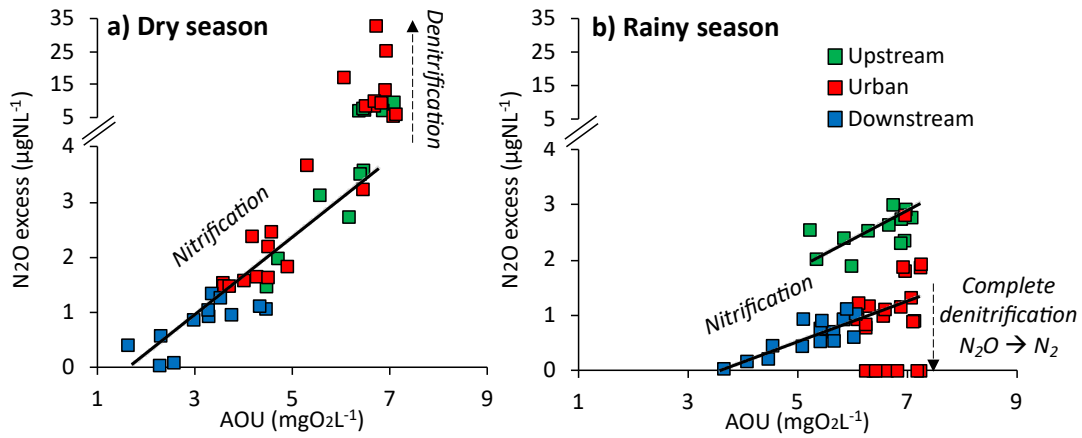


Figure 3.13: Relationship between N₂O excess (N₂O_{xs}) and apparent oxygen utilization (AOU=DO_{air} - DO_{water}, i.e., difference between measured DO in water and its equilibrium saturation concentration) in (a) dry and (b) rainy season 2019–2020 in the Saigon River. Upstream (UP01–UP04, SG01–SG03); Urban (SG04–SG15); Downstream (SG16–SG23). The linear correlations of AOU-N₂O_{xs} indicate nitrification as the main contributor to N₂O production. Correlation breaks indicate the impact of denitrification on N₂O production.

attach onto suspended particulates, supporting high activities due to their longer residence times than the water itself (Brion et al., 2000; Murray et al., 2015). There were some stations in urban areas aligned with the AOU-N₂O_{xs} slope in upstream and downstream stations. We hypothesized that the N₂O in these locations could be the result of nitrification/nitrifier denitrification (Figure 3.13a).

Besides nitrifier denitrification, the combined nitrification and denitrification under moderate oxygen conditions (1–2 mg L⁻¹) in the urban area of Saigon River might also explain the higher increase in N₂O than in the upstream and downstream areas. de Bie et al. (2002) and Murray et al. (2015) found that at intermediate O₂ saturation with high concentrations of NH₄⁺, estuaries can produce a large amount of N₂O by the coupled nitrification and denitrification. In the Saigon River, this can be supported by the dominance of NH₄⁺ in DIN. Nevertheless, the N₂O_{xs} vs. AOU relationship does not allow calculating the proportion of nitrification, nitrifier denitrification or denitrification contributing to N₂O production (Nevison et al., 2003).

In rainy season in contrast, the linear relationship N₂O_{xs} vs. AOU was broken at the lowest N₂O_{xs}. The maximum N₂O_{xs} in the urban area in rainy season was 10–20 times lower than in the dry season (Figure 3.13). The oxygen depletion in the urban and downstream sectors was much higher (a difference of about 2 mg L⁻¹) than in the dry season caused by organic matter inputs from bottom sediment of the canals and the river, and edges (Figure 3.11). The slope of N₂O_{xs} vs AOU in the upstream stations was lower than for the dry season despite higher ammonium substrate, but it would also indicate nitrification in this period. In the urban sector, high TOC level with the low oxygenation (0.5–1.0 mg L⁻¹ in the urban canals,

3. Eutrophication and greenhouse gases

Figure 3.11) would promote denitrification as shown by the decrease in nitrate. Denitrification was even complete, as shown by the null values of N₂O (Figure 3.13b). The N₂O production by nitrification in the downstream sector in rainy season was weaker than in dry season (i.e. the N₂O_{xs}/AOU slope was less steep) even with similar NH₄⁺ concentrations. The lower temperature, together with a high dilution in rainy season, might account for the lower activities of nitrifying bacteria. However, the difference in N₂O concentration downstream between the two seasons was not significant.

Photosynthesis and respiration

Most of estuaries are net heterotrophic systems because bacterial degradation of organic carbon exceeds gross primary production (Daniel et al., 2013; Gupta et al., 2009; Robin et al., 2016). Nevertheless, other studies have reported that some systems with potential eutrophication can reduce CO₂ emissions when photosynthesis uptake is greater than respiration (Grasset et al., 2020). In tropical systems with high impacts from urban discharge (low DO, high TOC), the respiration of these anthropogenic organic carbon sources is mainly responsible for the CO₂ supersaturation (Gupta et al., 2009; H. T. M. Nguyen et al., 2018). Such a CO₂ supersaturation was also observed in the Saigon River. The relationship between excess CO₂ (CO₂_{xs}) and AOU can also be used to describe mechanisms responsible for CO₂ production and DO consumption in the water column (Cotovicz et al., 2021; Han et al., 2017; Zhai et al., 2005).

We observed a linear relationship between CO₂_{xs} and AOU, mainly in urban and downstream of Saigon River (Figure 3.14). The correlation of AOU and CO₂_{xs} indicated that the high CO₂ concentration derived mainly from aerobic respiration of organic matter in urban and downstream of Saigon River. The high concentration of CO₂_{xs} in upstream of Saigon River could also be due to allochthonous inputs of inorganic and organic carbon such as groundwater discharges, leading to an increase of CO₂. The urban area might have additional contributions by anaerobic bacterial metabolism, supported by very low DO concentration (Figure 3.14).

Based on the phytoplankton respiration equation (Redfield et al., 1963) of the degradation of organic carbon into CO₂, the ratio CO₂_{xs}/AOU (mol/mol, phytoplanktonic respiration quotient in aerobic) should be 0.77 (106/138) or 1.0 (106/106) in lower DO and pH conditions. In dry season, our study's ratios of CO₂_{xs}/AOU were 0.7 – 1.0 mainly in urban and downstream sections, 1.1 – 1.6 in the upstream and some parts of urban area (Figure 3.14). The respiration quotient was close to the range of theoretical Redfield respiration, indicating that aerobic respiration was the main factor producing CO₂ in most urban areas and downstream. Meanwhile, potentially lateral inputs of CO₂ or another internal process might occur in upper parts of urban and upstream sections because of

3. Eutrophication and greenhouse gases

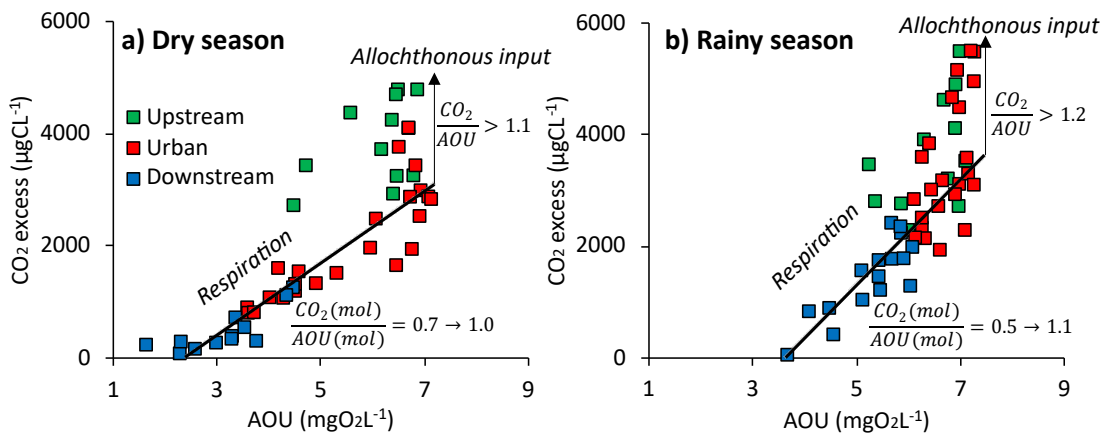


Figure 3.14: Relationship between CO₂ excess (CO₂_{xs}) and apparent oxygen utilization (AOU) in dry and rainy seasons in the Saigon River. The linear correlations of AOUCO₂_{xs} indicate respiration as a major cause for CO₂ supersaturation. The allochthonous inputs of CO₂ can be either from rivers or lateral inputs.

higher CO₂_{xs}/AOU quotient (>1.0) (R. M. Smith et al., 2017). For example, higher CO₂ concentrations upstream in the Seine Riverere due to organic carbon inputs from soils, carbonate-enriched and enriched CO₂ from groundwater discharges (Marescaux et al., 2018). These patterns were similar to the CO₂ simulation results in Red River (Northern Vietnam), where a large contribution of allochthonous inputs of CO₂ was found (H. T. M. Nguyen et al., 2018). The CO₂ concentrations in rivers can be affected by the catchment geology (Duvert et al., 2018). However, the Saigon River is dominated by igneous rocks with a low carbonate content (David et al., 2018). With a very low total alkalinity (mean 32 mgCaCO₃ L⁻¹), the CO₂ concentrations in surface water of the Saigon River would not thus be affected by buffering effect of bicarbonate concentration.

Methanogenesis and methanotrophy

While dissolved CO₂ can be produced by both aerobic and anaerobic respiration of organic matter, CH₄ is mainly produced by the methanogenesis process under anaerobic conditions and consumed by methanotrophy (Hanson & Hanson, 1996). In estuarine systems, the methanogenesis process in water column only proceeds when oxidants such as O₂, NO₃⁻ are completely depleted, the CH₄ production thus mainly occurs in the sediment (Borges & Abril, 2011). The positive trend between CH₄ excess and AOU can show how much CH₄ can be left with increasing AOU in the water column, i.e., less oxygen for methane oxidation (Figure 3.15).

Similar to AOU-CO₂_{xs} (Figure 3.14), extreme supersaturations of CH₄ in the AOU-CH₄_{xs} were distributed in the areas with the lowest DO concentration (Figure 3.15b). However, no correlation was found based on AOU-CH₄_{xs} analysis for the Saigon River. This result confirmed that high oxygen utilization (AOU) in

3. Eutrophication and greenhouse gases

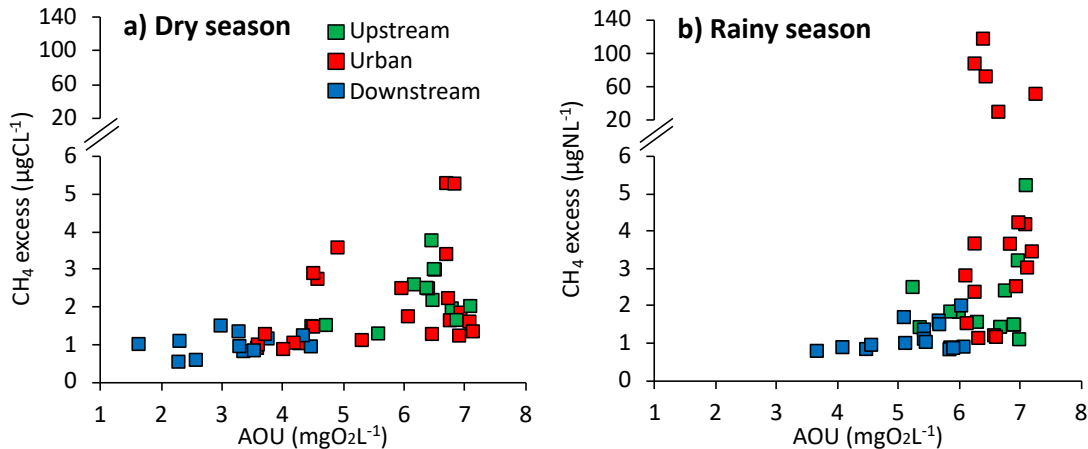


Figure 3.15: Relationship between CH_4 excess (CH_{4xs}) and apparent oxygen utilization (AOU) in dry and rainy seasons in the Saigon River. The negative correlations of AOU- CH_{4xs} indicate methane oxidation (CH_4 consumption/methanotrophy).

this urbanized estuary was not conducive to CH_4 oxidation in the water column. This finding was similar to an urbanized tropical lagoon in Brazil (Jacarepagua Lagoon) where CH_4 concentrations could reach more than $1000 \mu\text{gCL}^{-1}$ (Cotovicz et al., 2021). This study suggested that nitrifiers outcompeted the methanotroph community because of the strong nitrification process. Indeed, the analysis of AOU- N_2O_{xs} (Figure 3.13) and AOU- CO_{2xs} (Figure 3.14) shown that DO concentration in the water column was affected by oxic respiration and nitrification, leading to DO depletion in the Saigon River. Our result differs from the studies of Bui and Thi Ngoc Oanh (2018) or Sierra et al. (2020) which observed a negative correlation between AOU- CH_{4xs} , indicating a CH_4 decrease by methane oxidation in aerobic conditions. Similarly, Y. Zhang et al. (2020) found that 90% of CH_4 formed from sediment was microbially consumed in the water column under aerobic conditions. In other words, the higher DO in water column tends to increase the methanotrophy and decrease the methanogenesis rate. This was consistent with lower concentrations of CH_4 (about $1 \mu\text{gCL}^{-1}$) in downstream of Saigon River where DO concentrations are higher ($6 \text{ mgO}_2\text{L}^{-1}$ in dry season and $4 \text{ mgO}_2\text{L}^{-1}$ in rainy season, Figure 3.11).

3.3.4 Relationship of urban discharge, eutrophication and GHGs

Highly polluted water discharged in the river can promote eutrophication and biogeochemical processes responsible for GHGs production, such as mineralization of organic matter, denitrification, nitrification (Brigham et al., 2019; Cotovicz et al., 2021; Li et al., 2021). GHGs concentrations often peak at sampling sites located close to urban discharges. Marescaux et al. (2018) also found a spatial gradient

3. Eutrophication and greenhouse gases

of GHGs in the downstream Seine River (France) and estuarine system under the impact of wastewater treatment plants effluents of Paris. Similarly, the urban discharge had a clear impact on the concentration of CH₄ and CO₂ in both seasons in the Saigon River. As shown in Figure 3.11, CO₂ and CH₄ concentrations in urban and suburban (10 km upstream of HCMC) were 5 and 14 times higher than in non-urban areas, respectively, while a factor of about three times was observed for N₂O. This shows that urban rivers with high availability of organic matter and oxygen deficiency are hotspots for GHGs formation like CO₂ and CH₄. We found CH₄ concentrations in the urban stretch of the Saigon River much higher than those measured in rural areas, i.e., upstream and downstream, as already reported for other highly urbanized watersheds (X. Wang et al., 2018).

Regarding N₂O, its concentrations were related to urban domestic effluent of temperate rivers, together with CO₂ and CH₄, e.g., downstream from Paris effluents (Garnier et al., 2009, 2013; Nixon, 1995), or in the Meuse River (Borges et al., 2018). Several studies indicated that the eutrophic status might not have the same relationship with all the three GHGs (Grasset et al., 2020; Li et al., 2021). For instance, CH₄ and CO₂ concentrations were reported as often coupled during phytoplankton blooms (CH₄ increasing and CO₂ decreasing), and N₂O would be decoupled from these others GHGs (Bartosiewicz et al., 2021). Regression models have been used to explore the effects of eutrophication and other environmental factors (e.g., nutrients) to explain patterns of GHGs concentrations (Brigham et al., 2019; Galantini et al., 2021). Therefore, we applied multivariate statistical analysis (RDA and HP methods) on the environmental variables and GHGs to identify their relationship and assess the impact of urban discharge on GHGs production (Figure 3.16).

Overall, the ten parameters (physio-chemical parameters, nutrients, eutrophication indicators) accounted for about 80% of the variation of GHGs in both seasons. The two axes of RDA1 and RDA2 contributed nearly 70% to the interpretation of GHGs and about 30% of the unexplained variation (Figure 3.16). A stepwise selection was applied after running RDA to help remove non-significant explanatory variables. As a result, there were five explanatory variables, including DO, TSS, TOC, Chl-a and TRIX in the dry season. During the rainy season, the results of RDA determined the impact of DO, TSS, NH₄⁺, alkalinity and salinity on GHGs concentrations.

N₂O vs. environmental parameters

Several studies found that anthropogenic inputs (with high DIN concentration) correlated significantly with N₂O production (e.g., Murray et al. (2015); Marescaux et al. (2018); Burgos et al. (2017)). These findings suggested that most eutrophic

3. Eutrophication and greenhouse gases

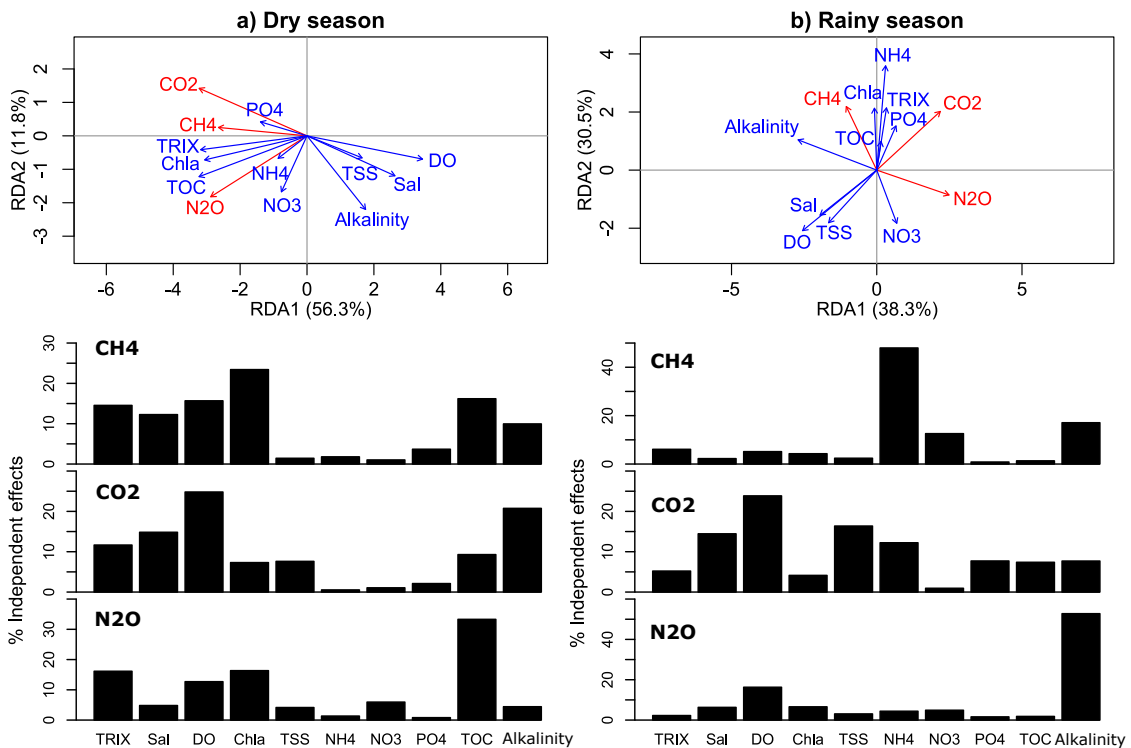


Figure 3.16: RDA and hierarchical partitioning analysis between explanatory variables (physio-chemical parameters, eutrophication) and responses (GHGs) in the Saigon River in (a) dry and (b) rainy season. The cosines of angles between vectors approximate their relationship (e.g., the approaching angles of 0° and 180° indicate positive and negative relationships). The vector with a longer length indicates a higher impact on the variation of the dataset.

and polluted estuaries would probably experience an N_2O supersaturation (Manjrekar et al., 2020). However, there was no linear correlation between N_2O and NH_4^+ , NO_3^- in the Saigon River, which received a large number of nutrients from urban discharge.

Based on the RDA results, TOC, Chl-a and eutrophication index had strong relationships with the variation of N_2O concentration in dry season in the Saigon River (Figure 3.16a). High concentrations of pollutants and heavy eutrophication help explain such high concentrations of N_2O . In rainy season, dissolved N_2O was not detected in both the urban area and downstream of Saigon River, despite the nutrient concentrations were even higher than in dry season (Figure 3.11). During the rainy season, N_2O concentrations did not correlate with nutrient concentrations. Instead, alkalinity contributed to 53% to the variation of N_2O . In dry period, the impact of urban wastewater (high TOC, low DO concentrations, eutrophication) corresponds to an increase in N_2O concentration in the receiving urban area, with alkalinity supporting ammonium oxidation, and hence N_2O production (Peng et al., 2015). The alkalinity concentration in dry season is higher than in rainy season, but in low concentration ($50 \text{ mgCaCO}_3\text{L}^{-1}$). Based on the statistical approach,

3. Eutrophication and greenhouse gases

the contribution of alkalinity was not enough to explain the significant decrease of N₂O from dry season to rainy season in urban area of Saigon River. Eutrophication was the factor having the most significant impact on N₂O in this study. TRIX or Chl-a was significantly correlated with N₂O during the dry season. From upstream (UP01) to urban area (SG05), Chl-a concentration increased steadily from 0.5 to 15 $\mu\text{g L}^{-1}$, N₂O concentration also increased from about 2 to 30 $\mu\text{g N L}^{-1}$ (Figure 3.11). This result was similar to previous studies with the confirmation of the effect on eutrophication on N₂O production in rivers and estuaries; e.g, Rivière du Nord in Canada (Galantini et al., 2021), Xiaoyue River in China (J. Wang et al., 2020), or Elbe estuary in Germany (Bräse et al., 2017).

CO₂ vs. environmental parameters

Studies dealing with the impact of urbanization on CO₂ production shown that the CO₂ concentration was higher in the rivers with higher urban coverage (Tang et al., 2021). In the Saigon River, CO₂ concentrations were supersaturated in both seasons even if its concentration significantly decreased in the downstream section of the estuary (Figure 3.11).

RDA and HP analysis results show that DO was linked to CO₂ concentration in the Saigon River (>20% independent effects) in both seasons. The DO concentrations frequently ranging from moderate to severe hypoxic conditions (0.5 mg L^{-1}), while dissolved organic carbon (DOC) was maintained at a concentration of $3.6 \pm 1.1 \text{ mg CL}^{-1}$. In other words, the Saigon River shown all the conditions (polluted and anoxic states, anaerobic/anoxic processes) for decomposing organic carbon and depleting oxygen and producing CO₂ (T. T. N. Nguyen et al., 2019). In general, CO₂ concentration in both seasons tended to decrease gradually along the estuarine gradient (Figure 3.11) due to the dilution effect. However, compared to global atmospheric CO₂ concentration, the CO₂ downstream of Saigon River was 2-4 times higher (Figure 3.11). The Can Gio mangrove at the interface of Saigon River and the coastal zone was considered as a source of CO₂ to the atmosphere, with the highest emissions near the inflowing river. David et al. (2018) concluded that the high CO₂ emissions in this sector were due to high water temperature (26 to 31°C), high POC content in TSS originating from upstream urban ar, and organic matter degradation in the mangrove.

The variation of CO₂ was also linked to independent effects of TRIX (12%) and TOC (10%) in the dry season (Figure 3.16a). Although a negative relationship between Chl-a and CO₂ was considered as uptake of CO₂), in the Saigon River, the trophic index (TRIX) or Chl-a was positively correlated with CO₂ in both seasons. This result was similar to another recent study in a subtropical lake in China (Sun et al., 2021). These results suggested that a large amount of CO₂ concentrations was due to abundant organic carbon or to the contribution

3. Eutrophication and greenhouse gases

of lateral inputs, overwhelming the CO₂ consumption by phytoplankton through photosynthesis. In rainy season, TSS, salinity, NH₄⁺ also accounted for 16%, 14%, 12% of independent effects on CO₂ variation, respectively (Figure 3.16b). Although HP analysis determined that alkalinity and salinity in the dry season accounted for 15% of independent effects on CO₂, the significant model selection by RDA indicated that they were non-significant explanatory variables in dry season. The POC content in TSS also shown a proportion many times higher in the upstream and urban area than in the downstream ones (Figure 3.11), which supported the high CO₂ concentrations in these two areas, with a gradual decrease towards the sea. However, the results of RDA, HP analysis, and the monitoring dataset still do not fully explain the high CO₂ concentration in the upstream less polluted area. The upstream area of Saigon River may be affected by CO₂ from allochthonous inputs. e.g., CO₂-rich sources in groundwater (Marescaux et al., 2018).

Overall, the positive correlation between CO₂ and the eutrophic status in the Saigon River indicated that respiration was significantly higher than photosynthesis, resulting in high CO₂ emissions. The CO₂ concentrations seemed to decrease only under the influence of dilution with coastal water along the estuarine gradient.

CH₄ vs. environmental parameters

in the Saigon River, CH₄ concentrations were much higher in urban than non-urban areas, as N₂O. Besides, an interesting finding was the significantly higher CH₄ concentrations in rainy than in dry season (Figure 3.11). Figures 2 and 3 indicate that the water quality and eutrophication were worst in the extended urban area. The POC, TOC, and Chl-a had higher concentrations in these areas, which explained the higher concentration of CH₄. Among the ten environmental variables explored, the contribution of Chl-a, TOC, DO and TRIX to CH₄ variation in dry season was 23%, 16%, 15%, 14%, respectively, while TSS and nutrients (N, P) accounted for less than 3% (Figure 3.8a). DelSontro et al. (2019) indicated that the CH₄ emissions exponentially rose with the Chl-a concentration. A study in an urbanized tropical bay (Guanabara Bay, Brazil) found a high correlation between Chl-a and CH₄ (Cotovicz et al., 2016), confirming the high impact of urbanization on eutrophication and CH₄ production in tropical regions.

The CH₄ concentration in the urban section of Saigon River in the rainy season was much higher than in the dry season (Figure 3.11). NH₄⁺ and alkalinity accounted for the largest independent effects on 48% and 17% of CH₄ variation (Figure 3.16b). CH₄ formation occurs mainly in anoxic/anaerobic conditions, when most oxidants (e.g., O₂, NO₃⁻, Mn, SO₄²⁻) are completely depleted (Likens 2010). The NO₃⁻ concentration remained in the range of 0.3 - 0.6 mgNL⁻¹ in the Saigon River in both seasons. Therefore, the emission of CH₄ in the water column was probably negligible in comparison to CH₄ production in sediment. Although Saigon

3. Eutrophication and greenhouse gases

River had high TOC concentration of about 6 mgCL^{-1} and low DO (about 1 mgO_2L^{-1}) during the dry season, the CH_4 concentration remained about 70 times lower than in the rainy season in the urban section. The lower CH_4 in the dry season might be due to methanotrophy, which consumed CH_4 . During dry season, there was an increase in salinity in the urban area, leading to the generation of more electron acceptors and a consecutive decrease in methanogenesis. Lower CH_4 concentrations in the dry period could also be attributed to high respiration rates at the roots of the floating aquatic plants (supported by CH_4 -oxidising bacteria) such as water hyacinths (Attermeyer et al., 2016; Nijman et al., 2021), while in the rainy season with stronger flushing capacity, macrophytes in the Saigon River were not as dense. The lower CH_4 concentrations in the surface water covered here by water hyacinths in dry season were comparable to the open water areas in a tropical lake in India (Attermeyer et al., 2016). This study indicated that the coverage of water hyacinths only affected the CH_4 concentration but did not strongly alter the CO_2 concentrations. Besides, Rosentreter et al. (2018) suggested that the distinct CH_4 difference between the two seasons in tropical estuaries was contributed by flushing capacity. Stronger flushing capacity can promote remobilization of bottom organic matter as well as sediment-water process, which increases CH_4 concentration. Indeed, the average discharge in rainy season is ten times higher than in the dry season in the Saigon River (T. T. N. Nguyen et al., 2019). This suggests that the flushing capacity in the rainy season is much higher than that in the dry season (A. T. Nguyen, Némery, et al., 2021).

3.4 Conclusion of Chapter 3

This research provides comprehensive information about the impact of the urban discharge on eutrophication and GHGs emissions of an urbanized tropical estuary, the Saigon River Estuary. Average concentrations of CO_2 , CH_4 , and N_2O were higher than the global GHGs concentration from about 10 to 300 times. Based on global warming potential, the total GHGs concentration in the Saigon River was nearly $15,000 \mu\text{gCO}_2\text{-eqL}^{-1}$, in which CO_2 contributes to 70-90% of total GHGs. While CO_2 concentration did not differ between the two seasons, the concentration of N_2O and CH_4 significantly differed between the dry and the rainy seasons. Based on the statistical analysis, the concentrations of three GHGs were linearly correlated with the eutrophication status of the estuary, especially in the dry season when phytoplankton was abundant. The analysis of AOU and CO_2 , N_2O excess allows identifying an important contribution of oxic respiration and nitrification and denitrification in the formation of these GHGs. GHGs fluxes in the Saigon River were comparable to other urbanized estuaries worldwide regardless of climatic conditions. This study suggests that effective control of urban wastewater

3. Eutrophication and greenhouse gases

will minimize eutrophication, which is also an effective solution to reduce the greenhouse effect from estuaries.

4

Biogeochemical functioning of an urbanized tropical estuary: Implementing the generic C-GEM (reactive transport) model

Contents

4.1	Introduction	116
4.2	Materials and methods	119
4.2.1	Study area	119
4.2.2	Data collection	120
4.2.3	Model implementation	122
4.3	Results and discussion	130
4.3.1	Model simulations	130
4.3.2	Tidal effects on pollutant clouds	133
4.3.3	Processes and flux budgets	135
4.4	Conclusion	143

Abstract

Estuaries are amongst the most productive ecosystems of the land ocean continuum, but they are also under high anthropic pressures due to coastal urbanization. Too sparse observations have hindered the understanding of complex interactions between water quality and estuarine hydrodynamics and biogeochemical transformations. Until now, estuarine modelling studies have mainly focused on temperate estuarine systems in industrialized countries. This study investigates the responses of a tropical estuary to pollution load from a megacity (Ho Chi Minh City, Southern Vietnam) by applying a one-dimensional, biogeochemical estuarine model (C-GEM). The Saigon River Estuary flows through the megacity of Ho Chi Minh

4. Biogeochemical functioning of an urbanized estuary

(HCMC) and is subject to episodic hypoxia events due to wastewater inputs from urban discharges. Good agreements are found between simulation outputs and observations for tidal propagation, salinity, total suspended sediment, and water quality variables in dry season in the Saigon River Estuary. C-GEM reproduces the increases in ammonium, total organic carbon, phytoplankton and dissolved oxygen depletion in the urban section of the Saigon River as an impact of untreated wastewaters from HCMC. The steady-state version of C-GEM also reveals the formation of a pollutant cloud (30-km stretch) resulting from the combined effects of tidal fluctuation and low flushing capacity during the dry season. Furthermore, the quantification of the reaction fluxes simulated by the model demonstrates that nitrification is the main process removing NH_4^+ from the Saigon River. For the first time in such a type of environment, our study demonstrates the effectiveness of C-GEM at unraveling the complex interplay between biogeochemical reactions and transport in a tropical estuary with a minimized data requirement. This is significant for tropical estuaries in developing countries, where intensive monitoring programs are rare and have thus been rarely the object of modeling investigations.

Keywords: biogeochemical modelling, self-purification, Saigon River Estuary, Ho Chi Minh megacity, Vietnam

Published as:

Nguyen, A. T., Némery, J., Gratiot, N., Garnier, J., Dao, T. S., Thieu, V., & Laruelle, G. G. (2021). Biogeochemical functioning of an urbanized tropical estuary: Implementing the generic C-GEM (reactive transport) model. *Science of the Total Environment*, 784, 147261.

4.1 Introduction

Estuaries are complex ecosystems under the simultaneous influences of tides and rivers, where nutrient loads are controlled by urban, industrial, and agricultural emissions. Although estuaries have selfpurification capacity supported by the tidal mixing of inland and coastal waters, excessive nutrients loads are likely to cause eutrophication (Lanoux et al., 2013; Paerl, 2006). This phenomenon threatens water resources safety, especially for megacities in developing countries, where the balance between urbanization and environmental management is commonly a difficult tradeoff. In this context, reactive transport models can provide valuable insight to better understand the complex biogeochemical dynamics of such estuaries and help predict the potential response of water quality to anthropic perturbations. Under the pressure of multiple pollution sources (e.g., domestic wastewater, industrial inputs), the main factors controlling water quality in estuaries are biological and physical processes; in particular: (1) biogeochemical processes such as nitrification, denitrification, remineralization, primary production in water columns (J. Hu &

4. Biogeochemical functioning of an urbanized estuary

Li, 2009; Vanderborght et al., 2007; Volta, Laruelle, Arndt, & Regnier, 2016) as well as adsorption-desorption processes at the water-sediment interface (Mortimer et al., 1999; Némery & Garnier, 2007; Vilmin et al., 2015); (2) dilution process between riverine and marine waters (Etcheber et al., 2011; Lajaunie-Salla et al., 2019; Lanoux et al., 2013). Understanding these processes is often facilitated by using numerical models that usually require high-frequency data series (Tappin, 2002; Wild-Allen and Rayner, 2014).

Studies on the anthropogenic impact on water quality in estuaries by biogeochemical models are mainly available in temperate estuaries of industrialized countries (Gawade et al., 2017; Regnier et al., 2013). The Carbon Generic Estuarine Model (C-GEM) is a generic one-dimensional, reaction-transport model that takes advantage of the relationship between estuarine geometry and hydrodynamics to minimize data requirements (Volta et al., 2014). Steady-state simulations of C-GEM have provided accurate descriptions of estuarine hydrodynamics and biogeochemical transformations in several temperate estuaries (G. Laruelle et al., 2017; Volta et al., 2014; Volta, Laruelle, Arndt, & Regnier, 2016). The biogeochemical reaction network of C-GEM and its parameterization were built upon the study of more than 40 temperate estuaries Volta et al. (2014); Volta, Laruelle, Arndt, and Regnier (2016). Although several studies have been carried out in tropical estuaries through monitoring and experiments (e.g. Miguel, Lucas Lavo António Jimo (2018), Vipindas et al. (2018), J. Wu et al. (2013)), estuarine biogeochemical modelling applications are still missing in many countries in tropical regions such as Southeast Asia, India, Africa, South and Central America (Regnier et al., 2013; Volta, Laruelle, Arndt, & Regnier, 2016). There is now a need to improve this temperate parameterization of C-GEM to allow for the robust simulation of tropical estuaries. This is of particular importance for water resource management in urbanized tropical estuaries such as in the Saigon River Estuary, Vietnam (T. T. N. Nguyen et al., 2019), Recife estuarine system, Brazil (Noriega et al., 2013); Cochin Estuary, India (Gupta et al., 2009; Vipindas et al., 2018); Cross River estuary system, Nigeria (Dan et al., 2019); Cisadane estuary, Indonesia (Dong et al., 2011). The most notable difference between temperate and tropical systems is the rate of biological processes. The higher temperature of tropical estuaries often increases the biological uptake, excretion of nutrients and microbial activity (e.g., nitrification and denitrification) (B. Eyre & Balls, 1999; Tappin, 2002). Another major difference between the two types of estuaries is the flow regime with a direct impact on the retention time of water bodies. In most tropical estuaries, two distinct flow rates and retention time are found during the dry and rainy seasons (Dong et al., 2011), whereas higher flow rates occur in winter in temperate estuaries. Vipindas et al. (2018) suggested that nitrification rate can increase 10-40 folds when encountering a low flushing rate of tropical estuary during pre-monsoon. Similarly, oxidation rate of organic matter would not be significantly affected by temperature,

4. Biogeochemical functioning of an urbanized estuary

but by the river discharge magnitude (Gawade et al., 2017; Y. Wu et al., 2013) . Therefore, the factors controlling the intensity of biogeochemical processes will differ between the temperate and tropical systems.

The Saigon River Estuary (Southern Vietnam) is a tropical estuary located in Southeast Asia. This estuary is considered as a natural collector for domestic wastewaters of about 9 million people living in Ho Chi Minh City (HCMC). Urban canals of HCMC and the Saigon River receive about 90% of untreated domestic wastewater from HCMC (T. T. Nguyen et al., 2020). The high polluted loads regularly lead to an excess of nutrients and intense periods of anoxia, especially during the dry season (T. T. N. Nguyen et al., 2019). There have been several studies in recent years showing the risk of eutrophication in this estuary, especially in the dry season because of low flushing capacity (Camenen et al., 2021; A. T. Nguyen, Némery, et al., 2021; T. T. N. Nguyen et al., 2019). In addition, the research results of T. T. N. Nguyen et al. (2019) showed that there was no significant difference between water quality variables in rainy season and dry season (except chlorophyll *a*). Besides that, the phytoplankton abundances were very low in rainy season, but more than 100 times higher in dry season which mainly concentrated in urban section of Saigon River (A. T. Nguyen, Dao, et al., 2021). Simultaneously, the risk of estuarine pollution is expected to increase in the coming years, under the impact of megacity's development. The population of HCMC is indeed expected to reach 23 million by 2050, the Saigon River would then receive three times more pollution than what is currently released by the city (T. T. Nguyen et al., 2020). Understanding the self-purification capacity of this tropical estuary is important for HCMC's development plans related to water resources safety.

This study aims to quantify the biogeochemical processes and tidal fluctuations controlling the water quality in a tropical estuary. We applied C-GEM to simulate the evolution of water quality over a tidal cycle representative of the dry season in the Saigon River Estuary during the 2014 – 2017 period, as a representative case study of an urban impacted tropical estuary. In the first part of the paper, the characteristics of the study area are described, including those of the estuary (Saigon River Estuary) and of the megacity (Ho Chi Minh City). The second part of the paper presents the protocol for implementing C-GEM model in this tropical estuary, in terms of description of data collection, the model constraints, the fundamental equations for building hydrodynamics, transport modules, biogeochemical reactions, and associated parameters that need to be calibrated. The last part of the paper deals with the quantification of interactions between estuaries and water quality including tidal effects and biogeochemical transformations. Intensity of biogeochemical reactions and fluxes are also calculated and compared with other studies in temperate and tropical estuaries.

4. Biogeochemical functioning of an urbanized estuary

4.2 Materials and methods

4.2.1 Study area

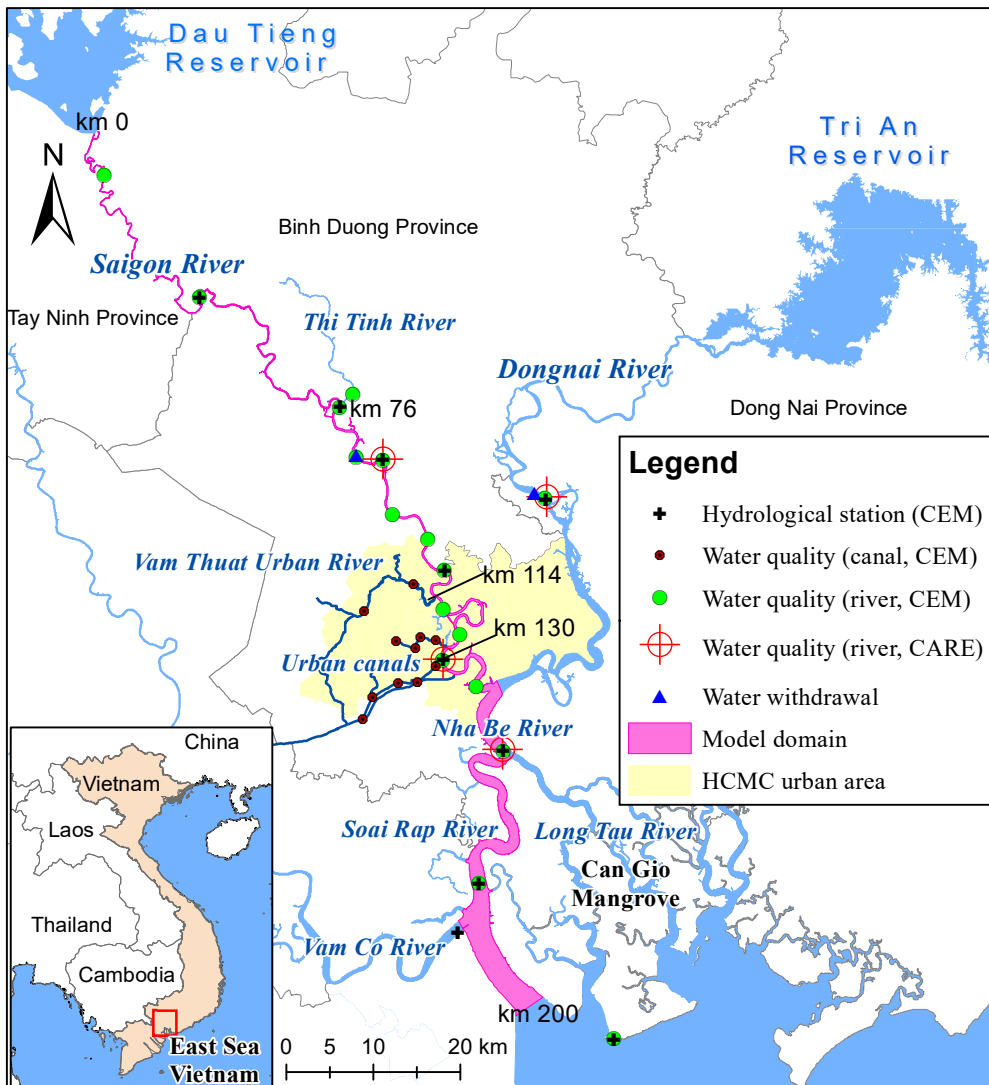


Figure 4.1: Model domain of Saigon River Estuary and monitoring stations

The Saigon River Estuary system is located in Southern Vietnam. The river flows from its source in southeastern Cambodia to the Dau Tieng Reservoir in Vietnam. Dau Tieng Reservoir (270 km^2 and $1580 \times 106 \text{ m}^3$) was designed for flood control, domestic and industrial water demands and preventing the saltwater intrusion in the Saigon River (Trieu et al., 2014). The Saigon River then flows through the natural boundaries of Tay Ninh province, Binh Duong province and Ho Chi Minh City. From Dau Tieng Reservoir to the estuary mouth, 200 km downstream, the Saigon River ($18 \pm 14 \text{ m}^3 \text{ s}^{-1}$) joins in turn several notable

4. Biogeochemical functioning of an urbanized estuary

tributaries such as the Thi Tinh River ($20 \pm 11 \text{ m}^3 \text{ s}^{-1}$) and the Dongnai River ($632 \pm 446 \text{ m}^3 \text{ s}^{-1}$), forming Nha Be River, which then splits into two river mouths (Soai Rap River and Long Tau River) flowing into the East Sea of Vietnam (Figure 4.1). In addition, the Saigon River is connected to an urban river (Vam Thuat River, $4 \text{ m}^3 \text{ s}^{-1}$) and three urban canals of HCMC (combined discharge of $5.5 \text{ m}^3 \text{ s}^{-1}$) before the confluence with Dongnai River (T. T. Nguyen et al., 2020).

The climate of this estuarine area is tropical monsoon, which has two distinct seasons (dry and rainy season), with a relatively constant temperature (about 29°C). The rainy season lasts from May to November, with an average annual rainfall of 1800 mm (T. T. N. Nguyen et al., 2019). Under the semi-diurnal tidal mixing, the saline intrusion diffuses up to 90 km upstream (Aygun et al., 2019). The tidal amplitude ranges from 1m during neap tide to about 4m during spring tide (Schwarzer et al., 2016).

Land use in the watershed of the Saigon River significantly varies from North to South. Upstream of HCMC (North of the city), agricultural activities dominate with paddy rice and rubber tree farms. The central area hosts urban settlements and industrial zones belonging to HCMC. Downstream of the estuary, the Can Gio mangrove system is recognized as a biosphere reserve by UNESCO.

The status of water quality in the Saigon River strongly varies along its path. The water quality status at the upstream and downstream ends of the estuary are considered good, based on Vietnamese regulation on surface water quality (T. T. N. Nguyen et al., 2019). The water quality status of Saigon River becomes moderate to bad condition after connecting with the Vam Thuat River (an urban river, km 114) and urban canals of HCMC (km 130, T. T. Nguyen et al. (2020)). While nitrate (NO_3^-) concentrations in canals are similar or lower than in the upstream stretch of Saigon River (Strady et al., 2017), the ammonium (NH_4^+) and total organic carbon (TOC) concentrations in those canals are many times higher than the threshold of $0.3 \text{ mg NH}_4^+ \text{ L}^{-1}$, 4 mg TOC L^{-1} provided by the Vietnamese regulation for surface water – QCVN 08:2015/BNM (T. T. Nguyen et al., 2020). However, the concentration of these pollutants at the outlet of the canals decreases several folds before entering the Saigon River supported by three factors: firstly, the high retention and removal capacity of urban rivers and canals of HCMC, secondly, the mud dredging activities and finally, the dilution effect during flood tide (T. T. Nguyen et al., 2020). In the downstream section, the water quality of Saigon River Estuary improves markedly after joining the Dongnai River.

4.2.2 Data collection

Bathymetry, freshwater inflow, water level, water quality and climate conditions were collected to implement C-CEM.

4. Biogeochemical functioning of an urbanized estuary

Mean depth and width for 83 cross-sections along the 200 km long Saigon River Estuary were extracted from bathymetry surveys performed in 2008 and 2016, provided by the Southern Institute of Water Resources Research (SIWRR, Vietnam). Climate condition data (sunshine hours and wind speed) were obtained from the statistical office of HCMC (www.pso.hochiminhcitv.gov.vn).

Variable	Location	Frequency	Period
Water level, velocity, discharge	7 stations in mainstream 3 stations in tributaries	Monthly	2014 – 2017
T°, salinity, TSS, DO, NH ₄ ⁺ , PO ₄ ³⁻ , COD, BOD ₅	13 stations in mainstream 11 stations in canals 1 station estuary mouth	Monthly Bi-weekly Monthly	2014 – 2017 2014 – 2017 2008 – 2013
T°, salinity, TSS, DO, NH ₄ ⁺ , PO ₄ ³⁻ , TN, TP, NO ₃ ⁻ , TOC, DSi, chlorophyll a	3 stations at Saigon River 1 station at Dongnai River	Bi-weekly	2016 – 2017
Sunshine hours and wind speed	At HCMC	Monthly	2014 – 2017
Estuarine width and depth	83 cross-sections	One time	2008, 2016

Table 4.1: Data collection for model implementation and validation (see Figure 2.21 for the locations of the hydrological and water quality sampling stations)

Water quality data were obtained from the Center of Environment Monitoring (CEM, Vietnam) and the Centre Asiatique de Recherche sur l'Eau (CARE, Vietnam). CEM has monitored the water quality in the Saigon River Estuary (bi-weekly) and urban canals of HCMC (monthly) since 2005. The measured variables include temperature (ToC), salinity, total suspended sediment (TSS), dissolved oxygen (DO), ammonium (NH₄⁺), phosphate (PO₄³⁻), chemical oxygen demand (COD), biochemical oxygen demand (BOD₅). The CARE laboratory has observed water quality at three locations along the Saigon River and one in the Dongnai River since July 2015 (Figure 4.1). These locations are the same as those used by the CEM monitoring program, but CARE's analyses include additional variables such as total nitrogen (TN), total phosphorus (TP), nitrate (NO₃⁻), total organic carbon (TOC), dissolved silica (DSi) and chlorophyll-a as described in T. T. N. Nguyen et al. (2019).

Hydrological data (water level, velocity, discharge) were measured monthly at 10 stations along the Saigon and Dongnai rivers by the CEM. Once a month, the hydrological monitoring stations track the evolution of water level and velocity

4. Biogeochemical functioning of an urbanized estuary

over 24 hours (2 tidal cycles) to calculate the net water discharge by removing the influence of tidal fluctuations in the Saigon River Estuary (Camenen et al., 2021).

Implementing a water quality model for the assessment of daily to seasonal fluctuations in river flow was limited by the low frequency of hydrological measurements. The simulation of water quality for conditions representative of an average dry season is therefore a reasonable choice for our study. During the dry season, the upstream flow discharge is low and quite steady (Camenen et al., 2021; T. T. Nguyen et al., 2020). In contrast, a lack of high-resolution data for precipitation, runoff and river discharge during the rainy season would have resulted in reliability issues of the modeling, especially in developing countries such as in Southeast Asia with a low monitoring effort. Besides, the high flow in the rainy season can create very short residence times and high flushing capacity, pollutants thus being mainly washed away from the estuary towards coastal waters.

Table 4.1 summarizes the data used for the implementation and validation of the model for the dry season from 2014 to 2017 in the Saigon River Estuary. The 2014 - 2017 period has the most complete data set along the Saigon River and urban canals in this study.

4.2.3 Model implementation

The generic estuarine model C-GEM was applied in the Saigon River Estuary to reproduce the nutrient dynamics over a generic tidal cycle representative of dry season conditions. The version of C-GEM used in this study was built upon the steady-state version described in Volta, Laruelle, Arndt, and Regnier (2016) with some parameter values adjusted for tropical monsoon conditions in the Saigon River Estuary. The updated values of the modified parameters (discussed below) fall within the ranges provided by Volta, Laruelle, Arndt, and Regnier (2016) based on a literature survey.

C-GEM's application domain spans 200 km of the Saigon River Estuary, from the outlet of Dau Tieng Reservoir (km 0) to the estuary mouth (km 200) (Figure 4.1). The three main modules of C-GEM (geometry module, hydrodynamics – transport module and biogeochemical module) were implemented following the set-up protocol proposed by Volta et al. (2014). The partial differential equations governing the hydrodynamics module were solved using a finite difference scheme applied along a 1D grid, with a grid size of 2000 m and an integration time step of 300 seconds, insuring the stability of the numerical scheme. A operator-splitting method was used to solve the transport and biogeochemical reactions within a single time step (Regnier et al., 1997). C-GEM required a spin-up of 180 days to get into a steady-state regime for the Saigon River Estuary. A dynamic steady state was considered reached once two consecutive tidal cycles generated similar hydrological and biogeochemical results that could then be compared with observations.

4. Biogeochemical functioning of an urbanized estuary

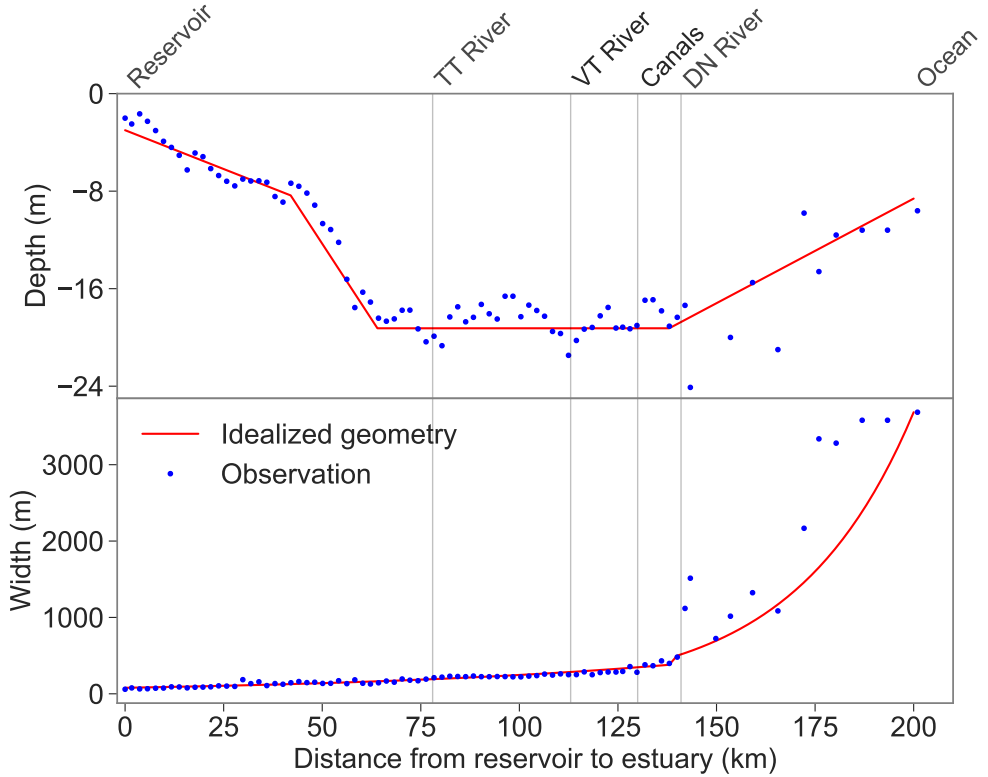


Figure 4.2: Depth and Width of Saigon River Estuary

Geometry module

Following Savenije's work on alluvial estuaries (H. H. Savenije, 2005), C-GEM uses an idealized representation of the estuarine geometry which can describe the estuarine width by an exponential equation along the estuary gradient.

$$\bar{B}(x) = B_0 \cdot \exp\left(-\frac{x}{b}\right)$$

where x is the distance from estuary mouth [m], B_0 is the width at estuary mouth [m], b is the width convergence length [m].

4. Biogeochemical functioning of an urbanized estuary

Description	Value	Unit
Width at the estuary mouth, at km 140 (Dongnai tributary) and estuarine upper limit	3690, 350, 60	m
Width convergence length at the estuary mouth, at km 140 (Dongnai tributary)	28000, 92500	m
Depth at the estuary mouth and upstream limit of model domain	9.61, 2.49	m
Tidal amplitude at estuary mouth	2.80	m
Tidal period	45720	s
Mean freshwater inflow (from reservoir) in dry season 2014-2017	17.61	m^3s^{-1}
Lateral discharge from tributaries at Thi Tinh (TT River), Dongnai (DN River) in dry season 2014-2017	6.29, 392.9	m^3s^{-1}
Lateral discharge from urban river (VT River) and three urban canals	4.3, 5.54	m^3s^{-1}
Chézy coefficient C_h (0 – 40 km), C_h (40 – 140 km), C_h (140 – 200 km)	15, 25, 60	$\text{m}^{1/2}\text{s}^{-1}$
Storage water ratio, r_s	1.0	-

Table 4.2: Physical parameters to build the estuarine geometry and hydrodynamic module in the Saigon River Estuary

C-GEM was designed to account for the interdependency between geometry and hydrodynamics in tidal alluvial estuaries. The width convergence length, which controls the system's shape, is thus a very sensitive parameter for hydrodynamics. Therefore, the value of the convergence length was carefully calibrated against observations (Figure 4.2). The impact of freshwater flow on this estuarine morphology was very different between the upstream (before Dongnai River confluence) and downstream sections (Gugliotta et al., 2020). The estuarine width ranges from 60 m from Dau Tieng Reservoir (km 0) to 350 m (km 140), and rapidly increases to 3690 m at the estuary mouth. This particular geometry justifies the use of a second convergence length to reproduce the entire width profile of the Saigon River Estuary. C-GEM geometry used a short convergence length from the estuary mouth (km 200) to the confluence of the Saigon and Dongnai rivers (km 142). From this confluence to the upstream section (km 142 – km 0), the width of the river only decreases slowly and gradually (with longer convergence length) (Figure 4.2 and Table 4.2). Such strategy was previously used with C-GEM for applications to other estuaries (G. G. Laruelle et al., 2019; Volta, Laruelle, & Regnier, 2016).

The depth of the Saigon River Estuary gradually increases from 2.5 m at the outlet of Dau Tieng reservoir to 19 m at km 60. The depth of the river is then almost constant over the next 80 km (i.e. until the confluence with the Dongnai River), it then decreases gradually to 9.6 m at the estuary mouth. The idealized geometry in the model captured well the mean estuarine depth and width which were extracted from 83 cross-sections of the bathymetry.

4. Biogeochemical functioning of an urbanized estuary

Hydrodynamics and transport module

The hydrodynamics of the 200 km long reach along Saigon River Estuary was described by the one-dimensional hydrodynamic module of C-GEM based on the continuity and cross-sectional integrated momentum equations (Nihoul & F.C., 1976; Regnier et al., 1998; Regnier & Steefel, 1999):

$$r_s \frac{\partial A}{\partial t} + \frac{\partial Q}{\partial x} = 0$$

$$\frac{\partial U}{\partial t} + U \frac{\partial U}{\partial x} = -g \frac{\partial \xi}{\partial x} - g \frac{U |U|}{C_h^2 H}$$

where \$x\$ is distance along the longitudinal axis [m], \$t\$ represents time [s], \$r_s\$ is the dimensionless storage water ratio, \$A\$ is the cross-sectional area [m^2], \$H\$ is the instantaneous water depth [m], \$Q\$ is the cross-sectional discharge [$m^3 s^{-1}$] and \$Ch\$ is the Chézy coefficient [$m^{1/2} s^{-1}$].

Modified parameters	Unit	This study	Reference range
Biological dynamics			
Maximum specific photosynthetic rate	s ⁻¹	5.58 x 10 ⁻⁵	0.107 – 18.2 x 10 ⁻⁵ (a)
Photosynthetic efficiency	m ² s (μ mol photons s) ⁻¹	4.11 x 10 ⁻⁷	1.67 – 6.94 x 10 ⁻⁷ (a)
Phytoplankton mortality rate constant	s ⁻¹	37 x 10 ⁻⁸	23 – 350 x 10 ⁻⁸ (a)
Phytoplankton growth constant	-	0.3	0.1 – 0.5 (a)
Aerobic degradation rate constant	µmolC L ⁻¹ s ⁻¹	1.44 x 10 ⁻⁴	0.8 – 9.26 x 10 ⁻⁴ (a)
Denitrification rate constant	µmolC L ⁻¹ s ⁻¹	5.00 x 10 ⁻⁴	0.26 – 522 x 10 ⁻⁴ (a)
Nitrification rate constant	µmolN L ⁻¹ s ⁻¹	4.62 x 10 ⁻⁴	0.106 – 21.7 x 10 ⁻⁴ (a)
Particle dynamics			
Critical shear stress for erosion and deposition: km 0 – km 140; km 140 – estuary mouth	Newton m ⁻²	0.25; 0.6	0.17 – 0.6 (b)
Erosion coefficient: from km 0 – km 140; km 140 – estuary mouth	kgTSS m ⁻² s ⁻¹	6.0 x 10 ⁻⁶ 1.0 x 10 ⁻⁶	1.0 – 5.0 x 10 ⁻⁶ (b)
Settling velocity	m s ⁻¹	1.0 x 10 ⁻⁴	0.1 – 10 x 10 ⁻⁴ (b, c)

(a): Volta et al., (2016) ; (b): Letrung et al., (2016) ; (c): Le et al., (2020)

Table 4.3: Determination of sediment parameters and adjustment of biological parameters for application of the C-GEM model in the Saigon River Estuary

4. Biogeochemical functioning of an urbanized estuary

Water elevation at estuary mouth and freshwater discharge at the upstream limit of the model domain were required to solve the hydrodynamics module. Parameters related to the characteristics of the tidal amplitude and period are also required to calculate the water elevation at the estuary mouth to constrain the downstream boundary. Table 4.2 summarizes the parameters used to solve these equations for the Saigon River Estuary. Chézy coefficient was the only parameter being fixed for the calibration of the hydrodynamic module, as it was not measured in the Saigon River Estuary. Chézy coefficient typically ranges from $40 - 60 \text{ m}^{1/2} \text{ s}^{-1}$ along alluvial estuaries (H. H. G. Savenije, 2001). The Chézy coefficient was calibrated based on the comparison between simulated tidal amplitude profiles and mean tidal observations at seven stations along Saigon River Estuary. Calibrated results showed that the Chézy coefficient applied Saigon Estuary ranged from 15 to $60 \text{ m}^{1/2} \text{ s}^{-1}$. The upper reaches of the Saigon River were much rougher than other alluvial estuaries. The sudden change of topography of upstream Saigon River Estuary compared to downstream probably explains this larger difference between Chézy coefficients in these two areas than the values reported by H. H. G. Savenije (2001).

After validating the hydrodynamics module, the transport module was implemented to reproduce the dynamics of dissolved variables (e.g., ammonium, dissolved oxygen) and total suspended sediment. The advection-dispersion equation for C (x, t) given by:

$$\frac{\partial C}{\partial t} + \frac{Q}{A} \frac{\partial C}{\partial x} = \left(AD \frac{\partial D}{\partial x} \right) + P$$

where C is the concentration of solutes or Total Suspended Sediments (TSS), D is the effective dispersion coefficient [$\text{m}^2 \text{ s}^{-1}$] which is automatically calculated following the geometry of the system, P is the net biogeochemical processes related to the solutes or solid $C(x,t)$.

The transport module was validated by comparing salinity simulation and observation during the dry season 2014 - 2017. Salinity was used because it is not affected by biogeochemical processes (variable $P = 0$). In addition, salinity distributions reflect the combined processes such as advection-dispersion and mixing processes along Saigon River Estuary. Salinity simulation results for the 2014-2017 dry season in the Saigon River are depicted in Figure 4.3. The salinity distribution agreement between simulation and observation has ensured the precise transport of solutes along the Saigon River over tidal cycles.

Biogeochemical module

The biogeochemical module implemented in C-GEM in this study allows assessing the concentrations of eight state variables, namely ammonium (NH_4^+), ni-

4. Biogeochemical functioning of an urbanized estuary

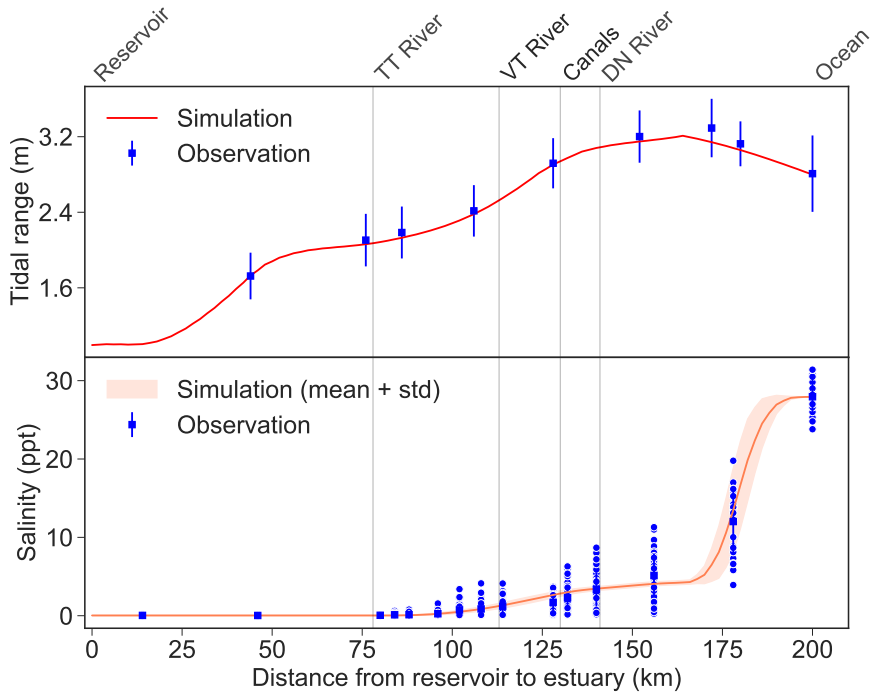


Figure 4.3: Comparison between observed (red marks) and simulated (red lines) profiles for average tidal amplitude and salinity along the Saigon River Estuary. The vertical gray lines correspond to tributaries or canals. Standard deviations (grey area) of simulation come from hourly fluctuations over tidal cycles.

trate (NO_3^-), phosphate (PO_4^{3-}), total organic carbon (TOC), Silica (DSi), dissolved oxygen (DO), phytoplankton (diatoms and non-diatoms) and TSS. Seven biogeochemical processes are simulated in C-GEM (Figure 4.4), including oxygen exchange through the air-water interface, aerobic degradation (organic carbon mineralization), nitrification, denitrification, primary production, phytoplankton mortality and TSS erosion/deposition (Volta et al., 2014; Volta, Laruelle, Arndt, & Regnier, 2016).

C-GEM uses eighteen biogeochemical parameters to calculate the intensity of biogeochemical processes. Their determination is based on a comprehensive literature review of 49 estuarine biogeochemical model applications in temperate regions (Volta, Laruelle, Arndt, & Regnier, 2016). The primary production process corresponds to the growth of phytoplankton and oxygen production through the uptake of C, N, P, and Si in the water column under soluble form depending on environmental forcings, especially light penetration. The light availability in the water column is affected by TSS, which is calculated by the model through the simulation of erosion/deposition processes. Nitrification consumes DO in the water column, which potentially eliminates a high concentration of ammonium. Denitrification contributes to anaerobic TOC consumption, PO_4^{3-} production and nitrogen elimination by converting NO_3^- into the inert N_2 gas that escapes from

4. Biogeochemical functioning of an urbanized estuary

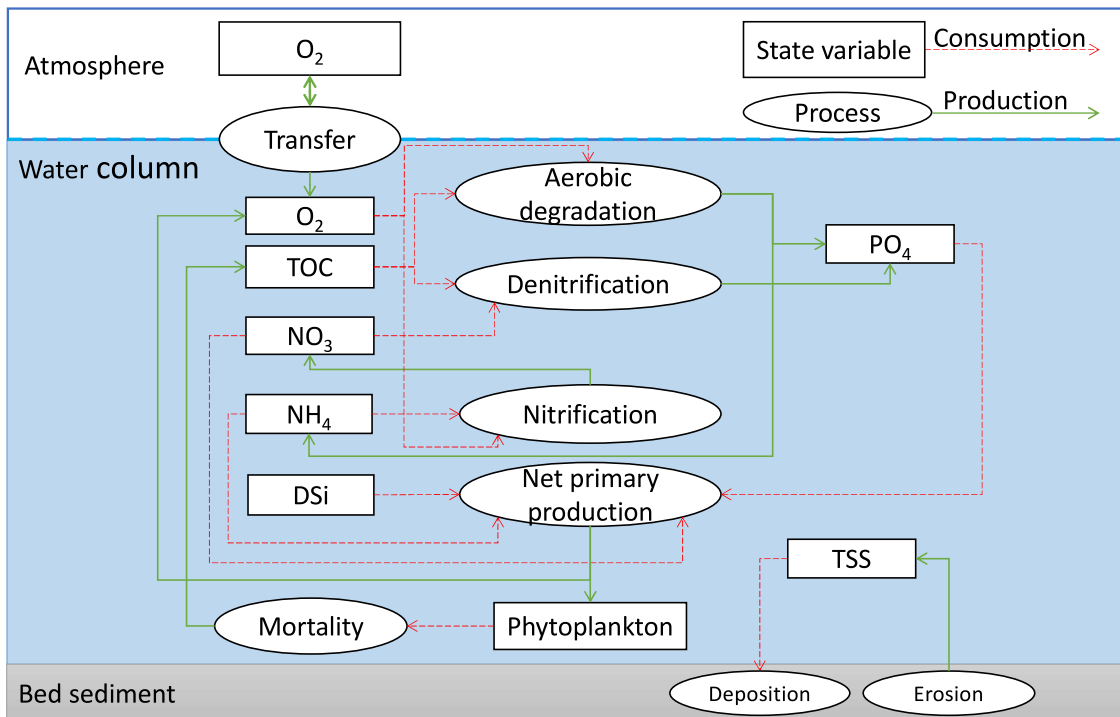


Figure 4.4: The state variables (rectangle) and processes (ellipse) in the biogeochemical module of C-GEM applied in the Saigon River Estuary. Red and green lines represent the consumption and production processes

the water column into the atmosphere. Mineralization of organic matter (aerobic degradation) consumes TOC and O_2 while producing PO_4^{3-} and NH_4^+ . Currently the application of C-GEM to shallow, pristine estuarine systems might be critical, when processes are dominated by intense element recycling within the sediments. The current lack of some N processes such as anammox does likely not significantly alter our result because these processes are relatively minor contributors to the nitrogen cycle in tropical estuaries (Dong et al., 2011). However, the NO_3^- simulation might be affected by dissimilatory nitrate reduction to ammonium process in tropical estuaries with low NO_3^- concentration (Dong et al., 2011). Phosphate release from bottom sediment might have a high impact on the phosphorus simulation at shallow estuaries (Vilmin et al., 2015). Note that the modular structure of C-GEM allows for a relatively simple implementation of new processes in its biogeochemical module and increasing the complexity of the N and P cycles could be the subject of future studies.

In our simulations, seven of the eighteen biogeochemical parameters used by C-GEM were modified to suit the tropical conditions in the Saigon River Estuary (Table 4.3). These reaction rate constants (except aerobic degradation rate constant) are mostly higher than the C-GEM applications for temperate estuaries. In particular, nitrification, denitrification rate constants are 2-12 times higher. However, these parameters were in the ranges reported by Volta, Laruelle, and Regnier (2016).

4. Biogeochemical functioning of an urbanized estuary

In addition, they are similar to findings of biogeochemical reactions in tropical estuaries reported by Miranda et al. (2008) or Vipindas et al. (2018). The eleven other biogeochemical parameters were similar, including phytoplankton maintenance rate constant ($4.11 \times 10^{-7} s^{-1}$), phytoplankton excretion constant (0.05), phytoplankton growth constant (0.29), Redfield ratio (C:Si:N:P = 106:15:16:1), Michaelis – Menten constant terms for dissolved silica (1.07), phosphate (0.2), ammonium (228.9), nitrate (26.07), organic carbon (186.25), oxygen in aerobic degradation (31.0), oxygen in nitrification (51.25), dissolved nitrogen (1.13).

The TSS concentration has a direct impact on light extinction and then on phytoplankton development. The sediment parameters (critical shear stress and erosion coefficient) were thus determined before adjusting biological ones though a calibration process only involving hydrological parameters and SPM concentration profiles.

Site	Unit	Upper	TT River	VT River	Canals	DN River	Lower*
Salinity	-	0.03	0.06	1.70	1.69	0.04	27.95
TSS	mgL^{-1}	49.0	54.9	67.7	50.8	68.8	83.5
Chl-a**	μgL^{-1}	4.02	4.02	149.71	104.28	7.61	1.62
DSi	mgL^{-1}	0.80***	2.84***	1.14	1.06	2.48	0.50
NO_3^- **	mgNL^{-1}	0.40	0.50	0.71	0.45	0.39	0.70
NH_4^+	mgNL^{-1}	0.23	0.29	3.36	2.06	0.10	0.01
PO_4^{3-}	mgPL^{-1}	0.05	0.07	0.11	0.07	0.03	0.03
DO	mgL^{-1}	5.02	4.20	1.66	2.32	4.16	5.34
TOC****	mgL^{-1}	3.58	3.85	13.66	12.41	3.86	3.21

* Lower boundary used the mean concentrations from 2008 – 2013

** Mean concentrations 2016 – 2017

*** Unpublished data from snapshot measurements 2019-2020

**** TOC was calculated based on BOD_5 . $\text{TOC} = 1.4 \times \text{BOD}_5 + 0.6$ ($R^2 = 0.67, n = 87$)

TT River is Thi Tinh River, VT River is Vam Thuat River, DN River is Dongnai River.

Table 4.4: Boundary conditions used for the steady-state simulation of water quality variables in the Saigon River Estuary 2014-2017

The boundary conditions of variables concentrations were the mean values of observations from 2014 – 2017 in dry season (Table 4.4).

Model evaluation

The model calibration and validation processes were quantitatively evaluated using statistical criteria (Table 4.5). The parameters used for the evaluation included the coefficient of determination (R^2), root mean square error (RMSE) and the bias percentage (pbias). The performance of hydrodynamics module was

4. Biogeochemical functioning of an urbanized estuary

assessed by comparing the mean values of simulated variables to observations at eight hydrological stations. The simulation of water quality variables was compared with the mean data at 14 water quality monitoring stations along the Saigon River Estuary (Figure 4.1).

Statistical indicator	Equation	Range	Optimal value
R ²	$\left[\frac{\sum_{i=1}^n (O_i - \bar{O})(S_i - \bar{S})}{\sqrt{\sum_{i=1}^n (O_i - \bar{O})^2} \sqrt{\sum_{i=1}^n (S_i - \bar{S})^2}} \right]^2$	0.0 to 1.0	1.0
RMSE	$\sqrt{\frac{1}{n} \sum_{i=1}^n (O_i - S_i)^2}$	0.0 to $+\infty$	0
pbias	$\frac{\sum_{i=1}^n O_i - S_i}{\sum_{i=1}^n O_i} \times 100$	$-\infty$ to $+\infty$	0

O: Observation; **S:** Simulation; **n:** number of samples

Table 4.5: Equations, ranges, and optimal values for assessing model performance

4.3 Results and discussion

4.3.1 Model simulations

Simulation results included hourly water depth, flow velocity, concentrations of eight water quality variables and intensity of biogeochemical processes over generic tidal cycles along the Saigon River Estuary. Table 4.6 summarizes the statistical comparison between simulated and observed variables during the dry season.

Variables	Number of samples	R ²	RMSE	Percent bias (%)
Tidal range (m)	8	0.98	0.06	0.5
Salinity	14	0.98	0.70	-16
TSS (mgL ⁻¹)	14	0.86	13.51	3
DO (mgL ⁻¹)	14	0.70	0.50	4
NH ₄ -N (mgL ⁻¹)	14	0.91	0.21	18
TOC (mgL ⁻¹)	14	0.78	0.86	-3
PO ₄ -P (mgL ⁻¹)	14	0.60	0.02	39
Phytoplankton (mgL ⁻¹)	3	0.88	0.4	178
DSi (mgL ⁻¹)	3	0.80	0.54	30
NO ₃ -N(mgL ⁻¹)	3	0.63	0.15	-18

4. Biogeochemical functioning of an urbanized estuary

Table 4.6: Model performance statistics in the Saigon River Estuary during an average dry season for the 2014-2017 period

Simulations using the hydrodynamics and transport modules were only evaluated using average tidal amplitude and salinity profiles collected during the average dry season from 2014 to 2017 (Figure 4). The model demonstrated realistic tidal amplitudes within the Saigon Estuary throughout its entire length ($R^2 > 0.9$, pbias < 3%, Table 4.6).

The statistical comparison between simulated and observed salinity showed that the model properly captures salinity profiles along the estuary with a R^2 of 0.98. The salinity distribution reveals a strong saline intrusion in the Saigon River which is consistent with previous literature (Aygun et al., 2019). Salinity gradually decreases from 28 to 0.4 at 120 km from the estuary mouth. Salinity strongly drops (from 28.0 - 5.0) within the first 30 km, then gradually decreases to almost zero at km 120 within HCMC.

Our results reveal that the model properly reproduces concentrations and spatial trends for most of the biogeochemical state variables over the generic tidal cycles in the dry season. The simulations of TSS, DO, NH_4^+ , TOC reveal a pretty good agreement with observations based on model performance statistics (Table 4.6) with $R^2 > 0.7$ and percent bias < 20%. NO_3^- and DSi also fall within the range of observations at three sampling stations along the Saigon River. Phytoplankton is rather well represented by the model despite a high pbias of 178% (Figure 4.5f). PO_4^{3-} is the only variable not properly captured by C-GEM (pbias = 39%), but the simulated profiles still remain well within the standard deviations of the observations (Figure 4.5e).

In the upstream section of the estuary (km 0 to 60-80), most variables are low and almost constant, except DO and DSi (Figure 4.5). Water quality in this area is highly dependent on water discharge from Dau Tieng Reservoir which is rated in good status according to Vietnamese regulation on surface water quality (QCVN 08: 2015/BTNMT) (T. T. N. Nguyen et al., 2019). The sudden increase in DSi concentration from km 60 to 80 originates from the higher DSi concentration of TT river tributary (Table 4.4). The simulation overestimates PO_4^{3-} concentration and underestimates TOC concentration. The underestimation of TOC may first stem from the intensity of the TOC degradation process, but also from TOC inputs to the system which may not be well considered. PO_4^{3-} overestimation can be explained by the lack of an important process in C-GEM, such as adsorption within the water column or in the sediment because the current version of the model does not have an explicit benthic module. This assumption is consistent with the study of Vilmin et al. (2015) who confirmed that the concentration of PO_4^{3-} in

4. Biogeochemical functioning of an urbanized estuary

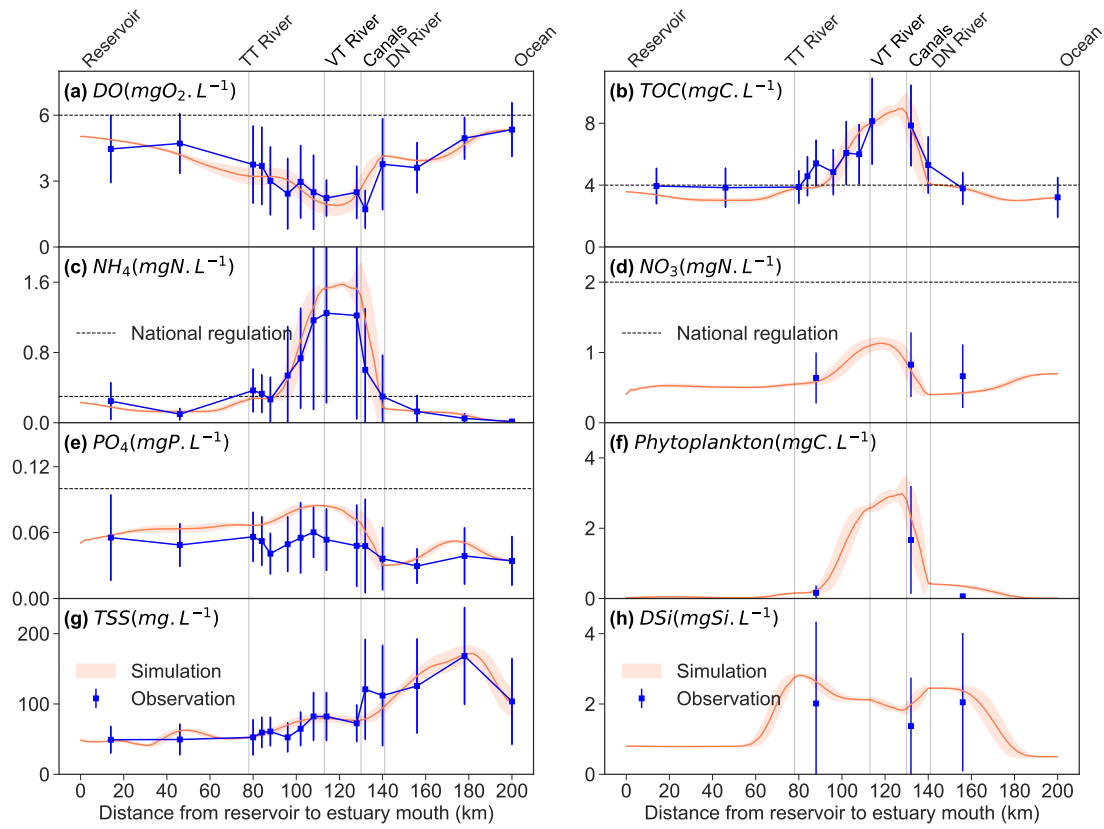


Figure 4.5: Comparison of observed and simulated results of water quality along the Saigon River Estuary over a tidal cycle. The vertical lines are tributaries or canals. Lateral input are described by vertical lines. The black dotted lines are the maximum permissible limit for domestic use, aquatic life based on Vietnamese regulation on surface water quality QCVN 08:2015/BTNMT.

estuaries is very sensitive to the adsorption of PO_4^{3-} onto the surface sediment. The concentration of PO_4^{3-} can indeed be reduced by 50% in the presence of adsorption in estuaries (Vilmin et al., 2015). Using a modelling approach, J. Hu and Li (2009) indicated that PO_4^{3-} adsorption can account for about 99% of total PO_4^{3-} removal in the Pearl River, a subtropical estuary in China. T. T. N. Nguyen et al. (2019) also reported that the Saigon River exhibits a high potential of phosphate adsorption onto the sediments ranging from 1 to 64%. However, the current water quality monitoring programs in the Saigon River (by CEM and CARE laboratory) mainly analyze PO_4^{3-} , without measuring particulate inorganic phosphorus (PIP) in routine. PO_4^{3-} and PIP are indeed two necessary indicators for building the representation of sorption processes (Billen et al., 2007; Vilmin et al., 2015). The addition of PIP measurements in future monitoring programs can thus support the improvement of C-GEM.

In the urban section (km 80 to 140), the Saigon River Estuary's water quality, which receives domestic wastewater through the connected urban canals of HCMC,

4. Biogeochemical functioning of an urbanized estuary

was clearly different from the upstream section. The concentrations of NH_4^+ and TOC in the canal were much higher than in the upstream area (T. T. Nguyen et al., 2020; Strady et al., 2017). Both simulations and observation data confirm that water quality has been significantly deteriorated in this area. The model successfully simulates DO, NH_4^+ , NO_3^- , TOC, DSi and phytoplankton concentrations in this section. Most of the variables impacted by the urban canal's inputs present concentrations higher than those simulated upstream in the Saigon River. NH_4^+ concentrations brought by the urban river (VT) and canals are ten times higher than those in the upstream sector. The NO_3^- concentrations from urban canals are not significantly different from the upstream concentration ($\sim 0.4 \text{ mg L}^{-1}$), and the contribution of the urban VT river was fixed to 0.71 mg L^{-1} (Table 4.4). The increase in NO_3^- in this urban section reaching more than 1 mg L^{-1} would be thus linked to biogeochemical processes in the water column rather than the NO_3^- anthropogenic contribution. In our simulations, PO_4^{3-} concentrations are overestimated (Figure 4.5f) which could likely be attributed to an inefficient PO_4^{3-} uptake by the phytoplankton to compensate the higher load of PO_4^{3-} brought by the urban VT river and PO_4^{3-} production from aerobic degradation and denitrification processes. The decrease of DSi and increase of phytoplankton biomass were well simulated in this section and can be attributed to diatom growth. The abrupt decrease in phytoplankton and a slight increase in DSi between km 130 and 140 (Figure 4.5f,h) corresponds to a dilution effect resulting from the mixing with the Dongnai River.

Downstream of the confluence with the Dongnai River (km 140-160 to 200), the concentrations of NH_4^+ , TOC, phytoplankton and DSi gradually decreased towards the estuary mouth (Figure 4.5). Most of the variables in this area meet the Vietnamese regulation QCVN 08: 2015/BTNMT on surface water quality for domestic use and aquatic life. The water quality in the downstream section of Saigon River Estuary largely depends on the Dongnai River confluence's water quality, its discharge being about 10 times larger than that of Saigon River ($392.9 \text{ m}^3 \text{ s}^{-1}$ against $17.6 \text{ m}^3 \text{ s}^{-1}$). Therefore, the concentrations of the simulated variables at this confluence (km 140) are almost similar to those from the Dongnai tributary, except TSS that increases from 100 to 180 mg L^{-1} from km 140 to km 180, in dry season (Figure 4.5g). This increase in TSS concentration is not caused by the Dongnai River, but instead by sediment erosion and resuspension (see section 3.3). Further, the gradually decreasing concentration of TSS from the 180 km to the estuary mouth is due to the dilution with coastal water.

4.3.2 Tidal effects on pollutant clouds

Saigon River Estuary is dominated by a semi-diurnal tidal regime from the East Vietnam Sea which changes four times a day. Sea water can penetrate inland to

4. Biogeochemical functioning of an urbanized estuary

more than 120 km during the dry season. Although tides can improve water quality through the mixing of urban and saline waters, the tidal fluctuation jointly diffuses the highly polluted sources into a pollutant cloud along the estuary.

Our simulation over 24-hours (two tidal cycles) shows that there a pollutant cloud of about 30 km remains centered around kilometer 120 regardless of the time of day with low DO ($< 2 \text{ mgL}^{-1}$) (Figure 4.6a). At 0h (in a generic day), the contaminated area is located from km 108 to km 138, while it roughly expends from kilometers 98 to 128 after six hours (Figure 4.6a). These upstream and downstream movements are controlled by the flood and ebb tides in the Saigon River Estuary. During the dry season, tidal oscillation dominates because the freshwater discharge from upstream the river is very small (few tens of $\text{m}^3 \text{ s}^{-1}$). From the outlet of the urban discharge (km 114) to the confluence with the Dongnai River (140 km), the residual discharge at the Saigon River is about $30 \text{ m}^3 \text{ s}^{-1}$ during the dry season. A rough estimate of the residual velocity for a segment of 26 km (km 114 to 140 km) using an average cross-section of 5700 m^2 (width x depth: 300m x 19m) yields a value of 0.45 km d^{-1} .

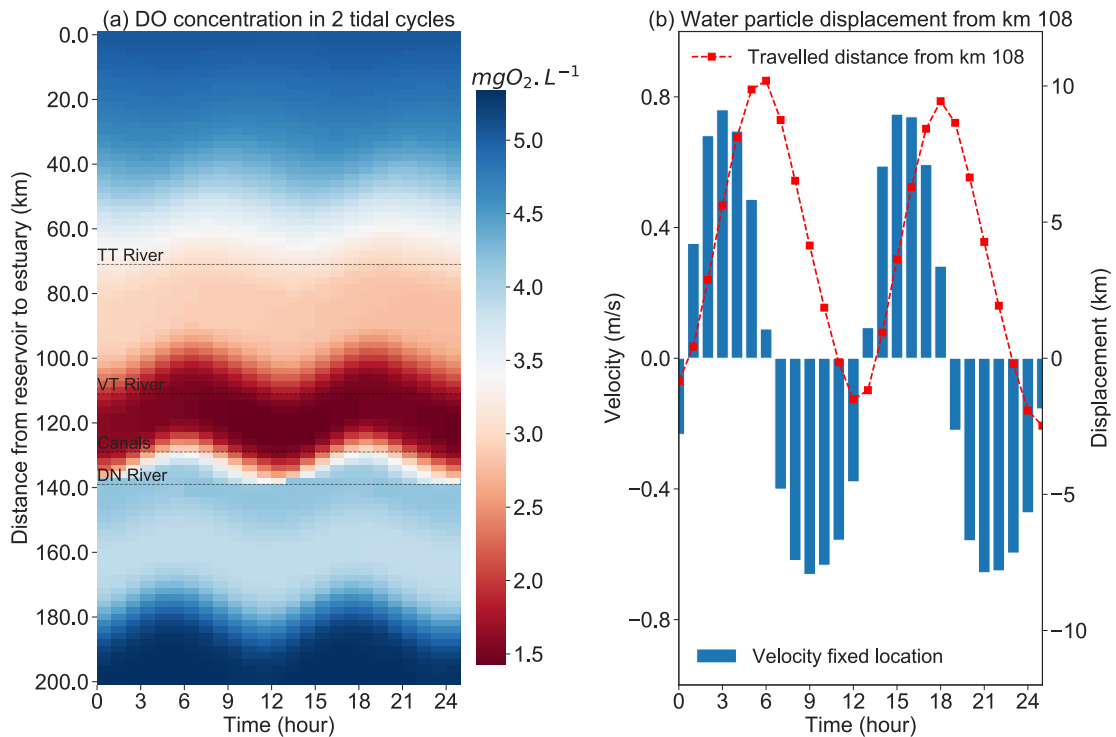


Figure 4.6: The tidal effect on the transport of the low DO concentration cloud along Saigon River Estuary. (a) DO concentration along Saigon River Estuary, (b) water particle displacement from km 108 during two tidal cycles. The displacement is calculated by multiplying velocity (m s^{-1}) and each hour (3600s). This displacement is only considered by the velocity (advection) of the water particle.

As a result of our simulations, a water particle could travel a distance of 10

4. Biogeochemical functioning of an urbanized estuary

km over six hours during flood tide (Figure 4.6b). It would then almost return to its original position after six hours of receding tide. The maximum tidal velocity at km 108 could reach 0.8 m s^{-1} during flooding tide. The residence time of the water body in this urban section was thus estimated to be around 57 days. Low discharge not only makes pollutants unable to flush out during the dry season, but it also increases the risk of eutrophication. The long residence times of water with high concentrations of nutrients facilitate algae's growth in this section before being flushed out of the estuary. As mentioned previously by T. T. N. Nguyen et al. (2019), high concentrations of chlorophyll-a as a eutrophication indicator are only evidenced in the dry season in the urban section of Saigon River Estuary. Similarly, oxygen depletion ($\text{DO} < 2 \text{ mgL}^{-1}$) was also observed in the Gironde Estuary (a west European estuary) during summer with a low river discharge and long residence time of water (from 20 to 86 days) (Lanoux et al., 2013). However, urban pollution discharges in most temperate European countries have been decreasing since the 2000's European Union directive, so that low summer water flow is nowadays less degraded (Romero et al., 2016). In tropical estuaries, despite high pollution levels during the dry season, much larger water flows during the rainy season usually lead to a strong flushing which helps the water quality in estuaries to be reset every year (B. Eyre & Balls, 1999).

4.3.3 Processes and flux budgets

Intensity of biogeochemical processes

While tidal mixing is the main control of the model's state variables concentrations in the downstream section of the estuary, the biogeochemical processes play a much larger role in regulating the biogeochemical dynamics of the system in its upstream and urban sections, especially in the pollutant cloud (Figure 4.7). Once evaluated, C-GEM allows to quantify the intensity of each process controlling the consumption or production of oxygen, nutrients, and organic carbon along the estuary, together with the physical processes such as erosion/deposition of TSS and oxygen exchange. In general, the Saigon River Estuary tends to (i) consume O_2 in the urban section and NH_4^+ , DSi, TOC in the entire estuary; (ii) produce DO in the upstream and downstream sections, TSS in both urban and downstream sections and NO_3^- , PO_4^{3-} and phytoplankton in the whole estuary.

Erosion/deposition of TSS A change in TSS in the urban section and downstream of the confluence with the Dongnai River was simulated (Figure 4.7g). The sudden shallowness in river depth combined with the increase in river width at the Dongnai River confluence would promote erosion process in this section, as previously observed by Gugliotta et al. (2020). This erosion phenomenon was also observed in the coastal Can Gio mangrove (downstream of the Saigon River)

4. Biogeochemical functioning of an urbanized estuary

which eroded rapidly within four years of observation (2014 – 2017) (H. T. Nguyen & Luong, 2019). H. T. Nguyen and Luong (2019) observed that the erosion—deposition intensity in the dry season was stronger than in the rainy season because of the stronger waves in dry season. The suspended sediment was influenced strongly by the currents in the dry season and had a strong tidal asymmetry. Therefore, the impact of hydrodynamics in the dry season were stronger than the ones in the rainy season(H. T. Nguyen & Luong, 2019).

Oxygen exchange Oxygen exchange (between surface water and atmosphere) and net primary production (NPP) are the two processes that provide oxygen to the estuary in C-GEM. The oxygen exchange at the air-water interface strongly contributes to the oxygenation of the water column in the Saigon River Estuary while most of other processes (except for NPP) consume oxygen. From upstream to downstream of the Saigon River, the oxygen exchange produces between 4.0 and $8.3 \mu\text{M O}_2 \text{ d}^{-1}$ (Figure 4.7a). This amount of oxygen introduces into the water through the air-water interface is quite similar to the amount of oxygen consumed by TOC aerobic degradation. Consumption of oxygen by nitrification process appears slightly smaller in the upstream and downstream sections, but significantly increases in the urban sector. Oxygen production by phytoplankton also increases in the urban section but remains negligible in the upstream and downstream sections compared to the other oxygen production/consumption processes.

Nitrification and denitrification Nitrification primarily leads to DO depletion and NH_4^+ consumption in the Saigon River. The nitrification process is particularly intense in the urban section (from km 98 to km 138). Nitrification could convert a maximum of $9.3 \mu\text{M N d}^{-1}$ of NH_4^+ into NO_3^- at km 130 (Figure 4.7c, d). In the urban section, NH_4^+ consumption by nitrification surpasses the NH_4^+ production by TOC degradation. This contributes to explain the decrease of NH_4^+ upstream and downstream of the Saigon River. The simulated nitrification rate in the Saigon River is similar to observations at Kochi estuary ($0 - 4 \mu\text{M N d}^{-1}$), a tropical monsoon estuary in India which receives untreated sewage from urban activities (Miranda et al., 2008). Further, in another study in the Cochin estuary (southeast Arabian Sea), Vipindas et al. (2018) observed particularly high nitrification rates in the dry season (about $10 \mu\text{M N d}^{-1}$) because of the low flushing rate of the estuary, a situation also met in the Saigon estuary.

Denitrification is a process controlling the concentration of NO_3^- by transforming NO_3^- into atmospheric gaseous N_2 (and possibly N_2O , as an intermediate product, although this step is not explicitly modelled by C-GEM) under anoxic conditions. In addition, denitrification forms PO_4^{3-} under anoxic conditions Arndt et al. (2011) which partly explains the increase of PO_4^{3-} in the urban section of the Saigon River. Besides, under anoxic condition, a possible release of bottom PO_4^{3-}

4. Biogeochemical functioning of an urbanized estuary

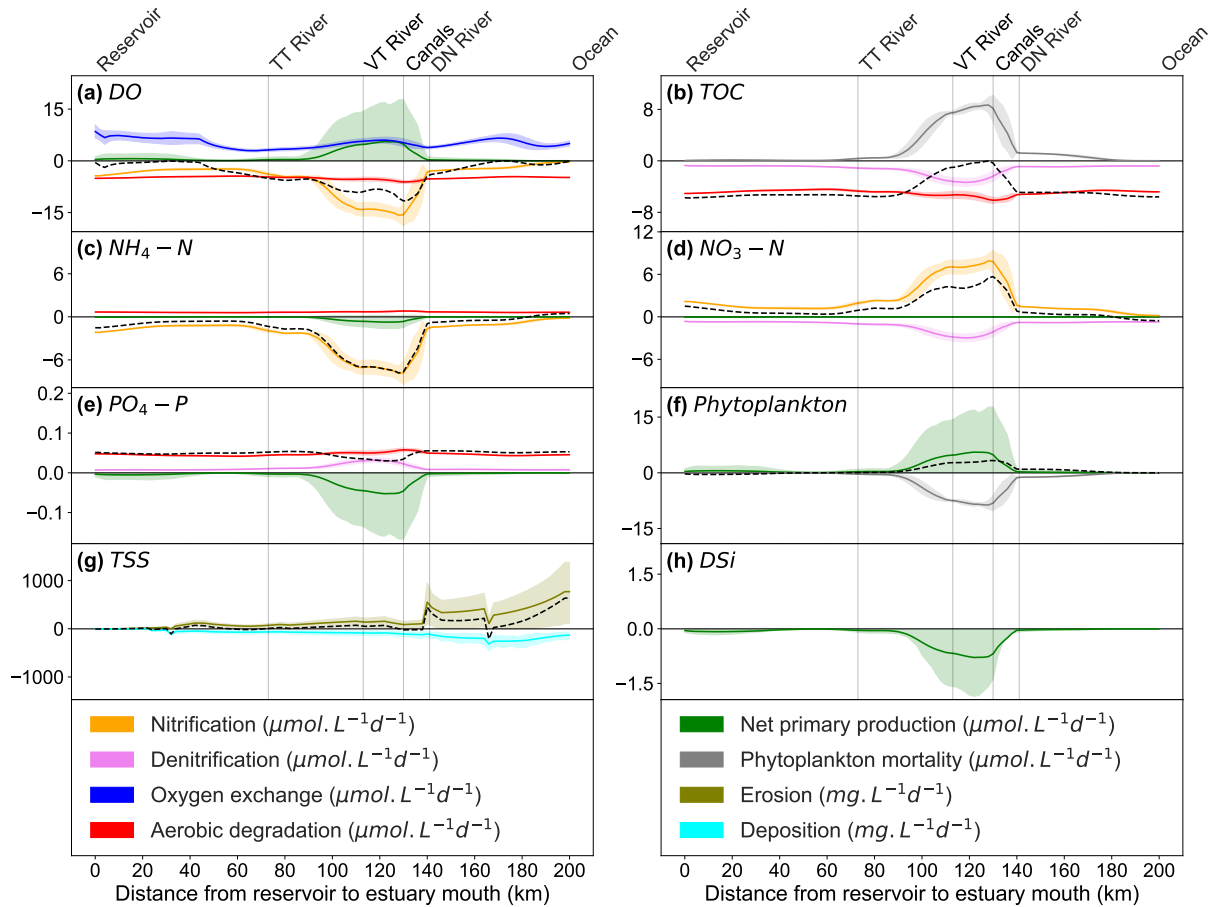


Figure 4.7: Intensity of biogeochemical processes and erosion/deposition rates affecting the concentrations of (a) DO, (b) TOC, (c) NH₄⁺, (d) NO₃⁻, (e) PO₄³⁻, (f) Phytoplankton, (g) TSS and (h) DSi. For example, Oxygen exchange, Net primary production and nitrification are affecting DO concentrations. The dashed lines are the net biogeochemical reactions.

through sediment desorption might occur (Némery & Garnier, 2007; Vilmin et al., 2015). The simulated denitrification rate in the Saigon River reached a maximum of $3.3 \mu\text{M N d}^{-1}$ in the urban section. The intensity of the removal of NO₃⁻ through denitrification is only one-third of NO₃⁻ formation through nitrification (Figure 4.7d). This rate is nonetheless higher than what was reported experimentally in some of other tropical regions such as the Barra Bonita Reservoir ($1.36\text{--}1.77 \mu\text{M N d}^{-1}$) (Abe et al., 2003). According to this study, denitrification processes in tropical conditions often occur with a high intensity because of the fast DO consumption (aerobic respiration) by heterotrophic bacteria using the high labile organic carbon. Such an environmental setting is consistent with the Saigon River's conditions in the urban section where low oxygen concentrations are frequent during the dry season ($\sim 1.0 \text{ mgL}^{-1}$).

4. Biogeochemical functioning of an urbanized estuary

Aerobic degradation of organic carbon (aerobic respiration) The simulated aerobic degradation rate in the Saigon River Estuary ranges from 5 to $6.5 \mu\text{M C d}^{-1}$. In addition, in the urban section, the intensity of aerobic degradation does not appear to be as high as other processes when receiving contaminated water from urban canals. This could be explained by the low availability of DO in this section ($\sim 1.0 \text{ mgL}^{-1}$, Figure 4.6) that makes the TOC degradation preferentially anaerobic (i.e., denitrification) as observed in Figure 4.7b. The sum of TOC consumption by the aerobic degradation and denitrification almost equals the TOC production by phytoplankton mortality ($8.5 \mu\text{M C d}^{-1}$) in urban section. Therefore, a biogeochemical balance is reached in this section which does not reduce TOC concentration. However, TOC's net biogeochemical reactions are negative in upstream and downstream. This would lead to a decrease in TOC concentrations in these two sections. However, according to the observations, the TOC concentration from reservoir to km 80 is almost constant. Other sources of TOC in the upstream section can be the cause of TOC compensation due to the aerobic degradation process. According to a well-water quality survey from 233 wells in agricultural, urban and industrial areas of HCMC, the wells with high concentration of organic carbon are only observed in agricultural areas (upstream of Saigon River) (B. T. Nguyen et al., 2020). This suggests that agricultural activities in the upstream Saigon River can release high TOC content, affecting groundwater and surface water in this area.

Compared to previous biogeochemical applications of C-GEM (Volta, Laruelle, Arndt, & Regnier, 2016), the aerobic degradation constant rate applied in our study was set at the low end of the range of possible values for this parameter (Table 4.3). Such low value strongly diverges with some studies performed in highly urbanized estuaries such as the Recife estuarine system (Brazil). Noriega et al. (2013) also argued that the respiration process was the dominant process in a highly urbanized estuary which was the cause of the constant low oxygen concentration. Unlike the Recife estuarine system, the low oxygen concentrations in the Saigon River would be due to the nitrification of NH_4^+ brought by urban canals, as shown by increasing NO_3^- concentration (from about 0.5 to 1.1 mgL^{-1}) in the urban section. The TOC degradation might strongly occur in the canal system with a long residence time before discharging to the Saigon River. We assumed that the less labile organic carbon was mainly stay in mainstream of Saigon River while the labile organic carbon was already degraded in the inner canal system. Based on C-GEM application in typical temperate estuaries (Volta, Laruelle, Arndt, & Regnier, 2016), the aerobic degradation rate could reach $20 \mu\text{M C d}^{-1}$, which was about two times higher than in our study. Although aerobic degradation was reported to be the main factor leading to oxygen depletion in many studies carried out in other systems, nitrification was the main factor in this tropical estuary.

4. Biogeochemical functioning of an urbanized estuary

Phytoplankton primary production (NPP) NPP uses nutrients and produces O₂. In the Saigon River, NPP only plays a minor role in eliminating nutrient pollution but still contributes to the oxygen regeneration in the system. In the urban section, oxygen seems to be a scarce element because of its consumption through nitrification and aerobic degradation. However, the intensity of oxygen production through NPP is similar to the oxygen exchange in the urban area (Figure 4.7a), but is negligible upstream and downstream due to low phytoplankton levels. While NH₄⁺ is consumed by nitrification and NPP, PO₄³⁻ can only be consumed through primary production in C-GEM. Besides, the production of PO₄³⁻ by aerobic degradation and denitrification is higher than the PO₄³⁻ uptake associated with primary production in the Saigon River's urban section, a positive net biogeochemical reaction that led to an increase in PO₄³⁻ in this section (Figure 4.7e).

NPP is the only process in C-GEM that consumes silica. Silica is a naturally occurring element essential for the development of diatoms which account for about 90% of the total phytoplankton observed in the Saigon River in the dry season (A. T. Nguyen, Dao, et al., 2021). According to the Redfield stoichiometric ratio in the Saigon River, DSi was always in excess over nitrogen and phosphorus for diatom's development (T. T. N. Nguyen et al., 2019) and its availability is thus never a limiting factor to diatom's growth currently. DSi concentrations however, are relatively low in the upstream section (Figure 4.5h, km 0 to km 60), but they are 2-3 times higher in the urban section (km 80 to km 160), where diatom frustule dissolution might occur in this highly productive section, accentuated by e.g., resuspension by navigation, feeding in return diatom uptake, feeding in return diatom uptake. In addition, the increase in DSi could come from high concentration of DSi of tributaries (see Table 4.4) and groundwater (not taken as an input by C-GEM). Indeed, according to Oehler et al. (2019), DSi concentration in the water column can be particularly elevated during the ebb tide by the contribution of DSi in groundwater which is greater than in surface water. Further, results of interaction analysis between groundwater and river showed that Saigon River indeed received water from groundwater at upstream and contributed to groundwater at downstream (Van & Koontanakulvong, 2018). In the following downstream section, the concentration of DSi then decreases because of dilution with the sea and the Dongnai River (Figure 4.5h) . There might be a risk of DSi depletion and the formation of harmful non-diatom phytoplankton if the pollutant cloud (from km 98 to km 138, Figure 4.6a) further spreads towards the upstream section. The decrease in freshwater inflow and the increase in tidal amplitude could indeed move the pollutant cloud upstream (Park and Song, 2018). However, the freshwater discharge from Dau Tieng Lake (upstream of Saigon River Estuary) is usually maintained at a stable level during the dry season (Trieu et al., 2014).

4. Biogeochemical functioning of an urbanized estuary

Comparison with temperate estuaries The results of our simulations in the Saigon River Estuary highlight some differences between a tropical estuary and other temperate estuaries. C-GEM application for three idealized temperate estuaries (marine estuary, riverine estuary, mixed estuary) showed that NH_4^+ consumption rates ranged from 0.2 to 0.3 $\mu\text{M N d}^{-1}$ (Volta, Laruelle, Arndt, & Regnier, 2016) which is about 30 times smaller than what was simulated in the Saigon Estuary. This is likely the consequence of higher NH_4^+ concentrations and higher temperatures that facilitate the nitrification process in the Saigon River. Indeed, the average temperature of this tropical estuary falls within the optimal temperature range for the growth of nitrifying bacteria (25–35°C) (B. Eyre & Balls, 1999). Besides, the biogeochemical models for typical temperate estuaries showed that denitrification rates reached a maximum of about 1.5 $\mu\text{M N d}^{-1}$ (Volta, Laruelle, Arndt, & Regnier, 2016), which is two times lower than in the Saigon River. In tropical regions, denitrification is usually much more intense than in areas with relatively lower temperatures, such as temperate regions (Abe et al., 2003).

Biogeochemical reaction fluxes

This section assesses the self-purification capacity of this tropical estuary by calculating mainstream fluxes and reaction fluxes of O_2 , TOC, and NH_4^+ in urban and downstream sections of Saigon River Estuary (Figure 4.8).

In the Saigon River, about 90% of the nutrients from untreated wastewaters are retained in sludge within the canal network of HCMC and partly lost (denitrified into N_2) (T. T. Nguyen et al., 2020). These polluted sludges are occasionally removed through canal dredging programs. However, at the output of canals, about 10% of the wastewater still has a very high concentration in nutrients and organic matter, well beyond the thresholds recommended by the Vietnamese regulation on surface water quality QCVN 08:2015/BTNMT.

In the urban section of the Saigon River Estuary, the average fluxes of DO, TOC, and NH_4^+ were 8.1 $\text{tonO}_2 \text{d}^{-1}$, 15.5 tonC d^{-1} and 2.2 tonN d^{-1} , respectively. Biogeochemical reaction fluxes remove 12% of DO, 1% of TOC and 18% of NH_4^+ within the urban section. These results show that the Saigon River Estuary is more effective at transforming/removing nutrients than organic carbon. Nitrification plays a key role in the self-purification of the Saigon River Estuary (Figure 4.8c). Phytoplankton's contribution to the removal of nutrients is negligible, but NPP contributes to the oxygenation of water in the urban section. Nitrification consumes about 2 $\text{tonO}_2 \text{d}^{-1}$, while NPP provides about 0.75 $\text{tonO}_2 \text{d}^{-1}$. The high abundance of phytoplankton facilitates an increase of TOC through the phytoplankton mortality process. The phytoplankton mortality flux in the urban section reaches 0.30 tonC d^{-1} , while the aerobic degradation only removed 0.27 tonCd^{-1} (Figure 4.8b). This makes the Saigon River Estuary an inefficient TOC filter, which is a

4. Biogeochemical functioning of an urbanized estuary

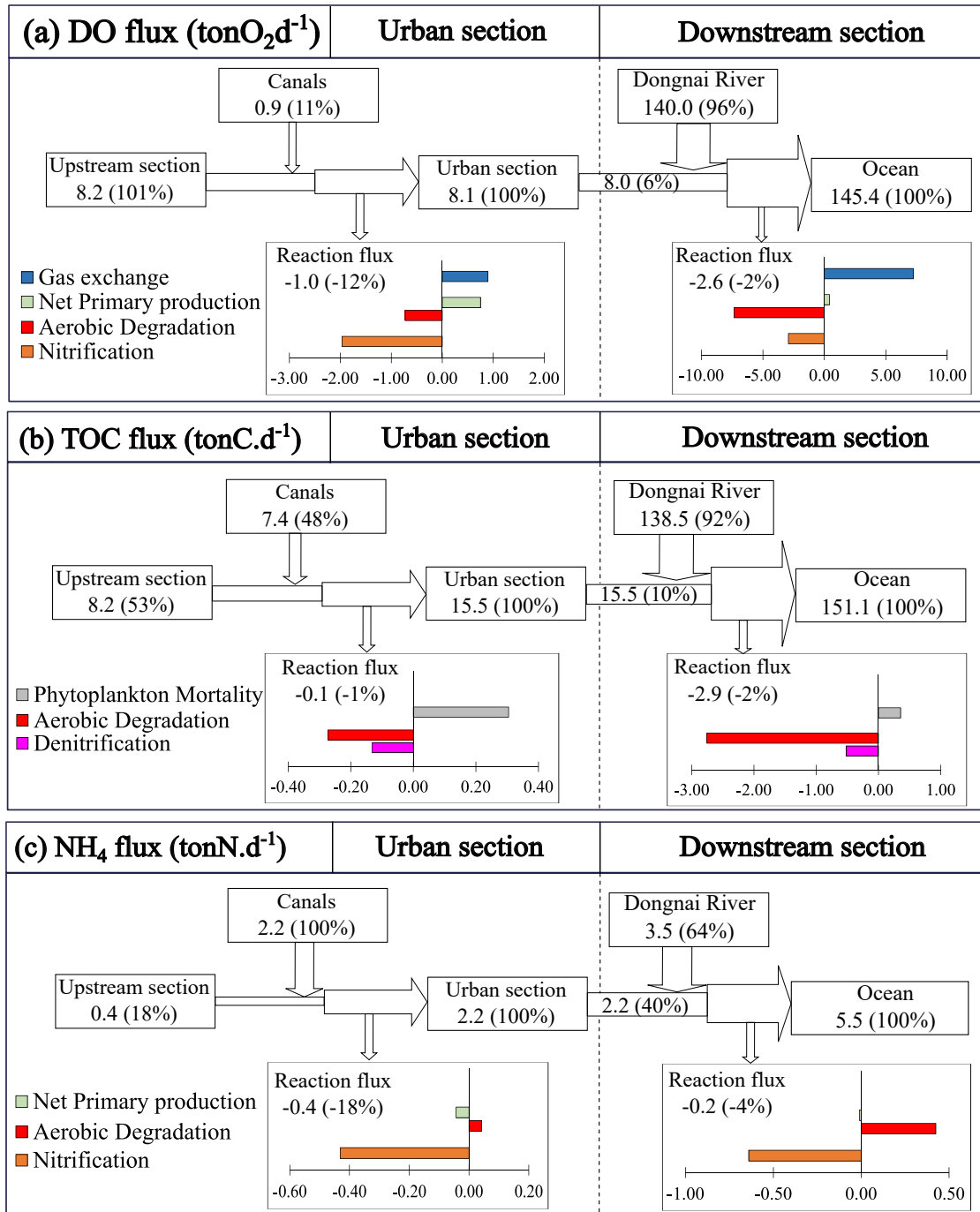


Figure 4.8: Fluxes and reaction fluxes of (a) DO, (b) TOC, (c) NH_4^+ in urban and downstream sections of Saigon River Estuary in dry season 2014–2017. Process rates are in tons

strong difference with the behavior of several temperate systems (G. Laruelle et al., 2017; G. G. Laruelle et al., 2019; Volta, Laruelle, & Regnier, 2016) calculated using C-GEM.

In the downstream section, the flux calculation mainly depends on the Dongnai

4. Biogeochemical functioning of an urbanized estuary

River's fluxes, with a much higher discharge than in the Saigon River. The reaction fluxes are negligible and only reduce the downstream fluxes by 2 - 4%. As discussed earlier, the concentrations of water quality variables in the downstream section of the Saigon River are almost similar to those in the Dongnai River with a good water quality status. Therefore, the biogeochemical reactions in this section are weaker than in the urban section. The most notable difference between these sections is the dominant biogeochemical processes. While nitrification has a strong impact on DO in the urban section, this process is much weaker in the downstream section. Oxygen supply through gas exchange ($7.25 \text{ tonO}_2 \text{ d}^{-1}$) plays a key role in improving DO in this section (Figure 4.8a), compensating for the consumption taking place upstream. Besides, TOC degradation is also larger than the TOC produced by phytoplankton mortality. However, the overall net biogeochemical flux is not significant compared to the TOC flux downstream of the Saigon River (Figure 4.8b).

Compared to other studies, the self-purification capacity of the Saigon River based on biogeochemical processes is relatively small. For example, the Scheldt Estuary (Belgium, Netherlands) in the 1990s received high concentrations of lateral inputs and could consume 73% NH_4^+ , 78% TOC and almost all O_2 (Vanderborgh et al., 2007). Another modelling study conducted in the Pearl River Estuary, a sub-tropical estuary in China, one of the most densely populated and economically developed regions of the country, showed that the biogeochemical processes could eliminate 50% BOD and 37% of NH_4^+ in the estuary (J. Hu & Li, 2009). The lower reduction capacity in the Saigon River Estuary can be explained by the high retention or removal of pollutants in the inner canal system of HCMC. While the Pearl River Estuary or Scheldt Estuary can remove high amounts of both organic carbon and NH_4^+ , in the Saigon River Estuary, NH_4^+ was mostly left for removal. The high concentration of TOC created by phytoplankton mortality process, mostly biodegradable, would effectively fuel aerobic degradation process within water column and TOC removal. This would mean that urban TOC discharged in the mainstream would be refractory, the biodegradable fraction of TOC being directly consumed in the canals. As a result, the urban canal and river (VT) network within the city plays a role of pretreatment, mineralizing first TOC and lowering oxygen, before the urban effluents reach the river itself where ammonia could find enough oxygen for nitrification.

Overall, our simulations suggest that the urban section of Saigon River mainly plays a role in retaining/eliminating macropollutants, which can be explained by the low flushing and long residence time, especially during the dry season. In the downstream section, the large discharge from the Dongnai River increases the capacity of the system to flush out pollutants into the coastal waters. In this downstream area, biogeochemical reactions then only play a minor role (2-4%) compared to hydro-physical controls.

4.4 Conclusion

Water quality in tropical estuaries is often under great pressure from urban and industrial wastewater sources, especially in developing countries. The lack of extensive monitoring programs in such regions makes difficulties in developing or applying water quality models for water management in these estuaries. In this study, the application of a generic reaction-transport model (C-GEM) allows to describe the dynamics of biogeochemical reactions and tidal effects on the water quality in a tropical estuary (the Saigon River Estuary, Vietnam). The simulation results capture the movement of a pollutant cloud in this estuary which confirms the impact of megapole wastewater on water quality. During the dry season, this cloud (30km stretch) moves up and down within a radius of 10km within the urban section of Saigon River Estuary, under the combined influences of the tidal effect and low discharge. In addition, a long residence time and high nutrient concentrations facilitate the development of phytoplankton which rapidly grows in such conditions. C-GEM allows quantifying the intensity of the different biogeochemical processes controlling nutrient dynamics in the system. Nitrification plays an important role in the Saigon River Estuary, removing about 18% of NH_4^+ flux in the urban section. The contribution of phytoplankton growth to the consumption of nutrients was negligible, but significant to the improvement of DO in a water column. Unlike many studies in other estuaries, the Saigon River Estuary only removed TOC originating from phytoplankton. Untreated ammonia-rich effluents were not diluted in the dry season, which indeed favored nitrification. This study indicated that the optimal temperature and abundant nutrients created favorable conditions for the growth of nitrifying bacteria in tropical estuaries. This study highlighted some fundamental differences between sanitation conditions in high- and low-income countries, the latter showing higher vulnerability as furthermore located in tropical zones.

Acknowledgements

This study was conducted at the International Joint Laboratory Le CARE and funded by the NUTRIM project EC2CO Bioheffect Structurante Initiative (2017-2018). We acknowledge the Center of Monitoring Of the Department of Natural Resource and Environment for the water quality data. Goulven G. Laruelle is a research associate of the F.R.S-FNRS at the Université Libre de Bruxelles.

5

Modeling the seasonal nutrient dynamics and phytoplankton development in the Saigon River tropical estuary

Contents

5.1 Introduction	145
5.1.1 Risk of phytoplankton blooms at urbanized tropical estuaries	145
5.1.2 The complex interaction between phytoplankton and controlling factors	146
5.1.3 Estuarine biogeochemical modeling in emerging countries	147
5.1.4 Objectives	149
5.2 Materials and methods	149
5.2.1 Study area	149
5.2.2 Saigon River Estuary	149
5.2.3 Ho Chi Minh Megacity	150
5.2.4 Data collection	151
5.2.5 Model implementation	153
5.3 Results and discussion	160
5.3.1 Evaluation of model performance	160
5.3.2 Spatio-temporal evolution of nutrients and phytoplankton biomass	166
5.3.3 Seasonal evolution of primary production and nutrients cycling	169
5.3.4 Driving factors of phytoplankton evolution	171
5.4 Conclusion	173
5.5 Conclusion of Chapter 5	174

Eutrophication in urbanized tropical estuaries of emerging countries is increasing. The understanding of eutrophication dynamics in the Saigon River Estuary

5. Modeling the seasonal nutrient dynamics

has not been achieved because of the sparse observations and consequent lack of biogeochemical modeling application. The distinct differences in phytoplankton densities and eutrophication risk between dry and rainy seasons were implicitly interpreted through multivariate data analysis (Chapter 3). The C-GEM model (steady-state version) described the strong nitrification, denitrification processes, and phytoplankton development during the dry season (Chapter 4). In this chapter, the transient version of the C-GEM model is extended to describe the seasonal evolution of nutrients and phytoplankton under megacity's influence in the Saigon River Estuary from 2017 - 2018. The model was validated for hydrodynamics and water quality variations of longitudinal profiles in two seasons. C-GEM captured the evolution trend of organic carbon and phytoplankton over these two years. The temporal variation is still not achieved for some variables such as phosphate and ammonium upstream and downstream of the Saigon River. The simulated biogeochemical processes and hydrological effects have elucidated the mechanism of phytoplankton succession. The high nutrient availability in the urban section and low upstream and downstream explains for the spatial phytoplankton differences. The distinct seasonal residence time explains the high and low phytoplankton densities in the dry and rainy seasons, respectively. The advantages and disadvantages of C-GEM application for estuaries in developing countries are then discussed to evaluate the effectiveness and significance of the model in supporting tools for water quality management and reducing the risk of eutrophication in urbanized tropical estuaries (Chapter 6). This chapter follows the format for further submission in a scientific journal.

5.1 Introduction

5.1.1 Risk of phytoplankton blooms at urbanized tropical estuaries

Seasonal variation of phytoplankton has been observed in tropical estuaries, with phytoplankton densities usually very high in the dry season and low in the rainy season (Damar et al., 2019; Duong, Nguyen, et al., 2019; A. T. Nguyen, Dao, et al., 2021). Climate change makes the hydrological difference between the two seasons more obvious in tropical estuaries (B. Eyre & Balls, 1999; Tappin, 2002). Besides, the rapid urbanization and ineffective water management practices lead to the risk of water pollution in rivers, estuaries and coastal areas. Indeed, the megacities are mainly located in the coastal areas supported by the abundant provision of ecosystems, maritime services (Hoornweg & Pope, 2017; Vitousek et al., 1997). The estuaries are also known as the natural treatment plant for urban, agricultural and industrial wastewaters (Billen et al., 2011; Howarth et al., 2011). Thus, increasing the risk of eutrophication in the dry season in emerging countries is unavoidable.

5. Modeling the seasonal nutrient dynamics

In contrast to megacities in developed countries, population growth and domestic wastewater volume have increased rapidly in recent years in developing countries, but wastewater treatment systems have not kept pace with urbanization (Lee et al., 2016). Eutrophication in urbanized estuaries is increasingly reported. For example, urban wastewater of the megacity of Ho Chi Minh City (Vietnam) pollutes the Saigon River Estuary (A. T. Nguyen, Némery, et al., 2021; T. T. N. Nguyen et al., 2019). Widespread strong hypoxia in near-bottom waters was detected in over half of the Gulf of Thailand during the dry season in 2015 (Buranapratheprat et al., 2021). In Jakarta Bay (Indonesia), urban wastewater increases eutrophication which has affected the aquatic environment, and the trend of eutrophication is increasing over the 13-year survey 2001–2013 (Damar et al., 2019). Other tropical countries such as Guanabara Bay (Brazil) and Ivory Coast (Africa) also observed an increase in the risk of eutrophication under the pressure of urbanization (de Carvalho Aguiar et al., 2011; Dröge & Kroeze, 2007). Currently, 75% of 20 megacities (more than 10M inhabitants) worldwide are located in coastal areas (Bange et al., 2017). It is estimated that in 2050, 122 cities with more than 5M inhabitants will be mostly in coastal areas (Hoornweg & Pope, 2017). This estimation warns that the impact of megacities on coastal ecosystems will continue to increase in the coming decades.

5.1.2 The complex interaction between phytoplankton and controlling factors

Understanding the response mechanism of estuaries to wastewater emissions on phytoplankton dynamics is difficult because of the complex processes of estuaries and their interplay (Gypens et al., 2013; Lancelot & Muylaert, 2011). Tidal estuaries have a large capacity to receive and dilute wastewater with tides and seawater (Billen et al., 2011). The drivers to the seasonal variation of phytoplankton characterization (abundance, type of species) at estuaries are affected by nutrient limitations, solar radiation, the residence time of the water body (Arndt et al., 2011; Billen et al., 1994; Dijkstra et al., 2019; Lancelot & Muylaert, 2011). Temperature and tidal effects also cause phytoplankton fluctuations in estuarine systems (Bianchi, 2007). Several studies suggest that residence time is the key factor that directly affects the density of phytoplankton (Lancelot & Muylaert, 2011). For estuaries with long residence time and weak flushing capacity, phytoplankton has enough time to grow before being flushed out of the system. In contrast, in estuaries with short residence and strong flushing capacity, phytoplankton is often pushed out of the system before rapidly growing even with high nutrient concentration. Indeed, the phytoplankton densities only increase when net specific growth rates exceed the residence time of the water (Miguel, Lucas Lavo António Jimo, 2018). In tropical estuaries, the causes leading to differences in eutrophication in estuaries often stem

5. Modeling the seasonal nutrient dynamics

from fluctuations in hydrology and weather conditions (Buranapratheprat et al., 2021; Damar et al., 2019). Lancelot and Muylaert (2011) indicated that subtropical and tropical estuaries often observed a significant difference in phytoplankton densities between dry and rainy seasons due to the intense seasonal monsoons and the occurrence of droughts. However, some studies reported that residence times did not greatly affect phytoplankton densities and species, but rather light penetration intensity influenced by suspended sediments and nutrient availability (Hoang et al., 2018). In upstream of the estuaries, light availability is generally better than downstream because of shallow water and active sediment resuspension in the mouth of estuaries. Nutrient limitation is also crucial in the studies of phytoplankton development (Arndt et al., 2011; Costa et al., 2009; L. M. Smith et al., 2006). Rivers and estuaries controlled by dam discharge often reduce silica formation, changing the nutrients ratio (Likens, 2010).

The preference for the statistical interpretation of the controlling factors is often reported in tropical estuaries. Some results are contradictory even under the same climatic conditions. For instance, at two contrast interpretations for the seasonal phytoplankton difference at Red River Delta (Vietnam) by Hoang et al. (2018) and Duong, Hoang, et al. (2019). The difference interpretation can be due to the nature of the wastewater source with different C, N, P, Si ratios, or the difference of external forcings such as tidal fluctuations, upstream flow control such as by dams. The C:N:P:Si ratio changes can lead to a huge difference in phytoplankton development. For instance, North Atlantic spring bloom in 1989 showed that dissolved silicate (DSi) was rapidly depleted to a minimum before nitrate was depleted. This coincided with a shift in dominant phytoplankton from diatoms to small flagellates (Sieracki et al., 1993). The deficiency of Si is mainly due to the consumption during diatom bloom. The addition of phytoplankton from natural processes such as weathering is much slower than DSi consumption or dissolution of diatom shells (Arndt & Regnier, 2007; Garnier et al., 2010). In estuaries, the evolution of phytoplankton species is more complex than in freshwater environments such as rivers and lakes because of the transition between freshwater and saltwater (B. D. Eyre, 2000). It seems to be that diatoms are regulated/interfered by salinity rather than dilution. Freshwater species cannot grow in saline conditions; in contrast, marine diatoms cannot develop in low brackish/freshwater conditions.

5.1.3 Estuarine biogeochemical modeling in emerging countries

The modeling application can support the understanding on phytoplankton variation (species and density, biovolume/biomass), along with the dynamics of nutrients

5. Modeling the seasonal nutrient dynamics

(C, N, P, Si), hydrological conditions (e.g., discharge, flow velocity, tides, precipitation), climate (e.g., temperature, light, wind). Theoretically, phytoplankton formation and conversion mechanisms are generally similar across environments such as tropical, temperate regions (Le Moal et al., 2019). However, the growth rate and nutrient consumption of phytoplankton are often different in different climates. In the survey of about 40 biogeochemical model applications, the kinetics rates applied to different models often have large fluctuations (Volta, Laruelle, Arndt, & Regnier, 2016). Even within an estuary, the coefficients applied have varied depending on the model. The model selection and calibration process are thus critical to ensure the effective application and minimize the misjudgement of management solutions. In emerging countries, extensive monitoring programs are rarely implemented. Choosing a suitable model is currently difficult because the over-simplified models do not explain the complex processes in the estuaries.

For example, in Gulf of Mexico, Turner et al. (2014) argued the importance of zooplankton in describing nutrients and phytoplankton dynamics in modeling application. In addition, benthic-pelagic processes can significantly contribute to phytoplankton bloom dynamics in the water column (Arndt & Regnier, 2007). The application of water quality models to urbanized estuaries of emerging countries is increasingly required to ensure the sustainable development of the region. Saigon River Estuary is a tropical estuary in Southern Vietnam heavily influenced by domestic wastewater from megacities. Similar to other tropical estuaries of developing countries, the application of water quality modeling in assessing eutrophication in this estuary is still limited. In well-mixed estuaries, without the significant contribution of benthic processes, the 1D models allow to reduce the data but still ensure the interpretation of biogeochemical processes in the water column such as Carbon-Generic Estuarine Model (C-GEM). C-GEM is an optimized model to minimize data requirements by taking advantage of the relationship between estuarine geometry and hydrodynamics while ensuring that important biogeochemical processes in the water column and hydrodynamics of estuaries (Volta et al., 2014; Volta, Laruelle, Arndt, & Regnier, 2016). C-GEM has been applied in several temperate estuaries in Western Europe (G. G. Laruelle et al., 2019; Volta et al., 2014; Volta, Laruelle, Arndt, & Regnier, 2016), North America (G. G. Laruelle et al., 2019), and recently in a tropical estuary (Saigon River Estuary, Vietnam, A. T. Nguyen, Némery, et al. (2021)). Based on the results of C-GEM simulation for the dry season in the Saigon River Estuary, the water quality in this estuary is affected by domestic wastewater from Ho Chi Minh Megacity. However, the steady-state version of C-GEM did not characterize the significant differences in phytoplankton between the rainy and dry seasons. Similarly, the eutrophication risk of tropical estuaries also varies depending on hydrological conditions. The survey results in 2016-2017 on the density of phytoplankton at Saigon River Estuary showed a clear difference between the dry and rainy seasons, with more than 100 times higher density in dry

5. Modeling the seasonal nutrient dynamics

season (A. T. Nguyen, Dao, et al., 2021). In 2019-2020, four longitudinal profiles were carried out along the Saigon River Estuary (two times in the rainy season, two times in the dry season). There was a clear difference in the phytoplankton biomass between the two seasons and between the monitoring areas. Therefore, to understand the temporal fluctuations of phytoplankton biomass, the application of the steady-state version of C-GEM is no longer appropriate. The application of the transient version of C-GEM allows the description of these processes on a daily, seasonal and annual resolution with input data requirements consistent with existing data in the Saigon River Estuary.

5.1.4 Objectives

This study investigates spatio-temporal patterns of nutrients, phytoplankton biomass (chlorophyll-a), organic carbon, nutrients, suspended sediment in the Saigon River Estuary by applying the C-GEM. The objectives are (i) to reproduce the variation of water quality and phytoplankton from 2017 to 2018, (ii) to quantify nutrient cycles and phytoplankton development under hydrological influences and urban wastewater discharge, and (iii) to identify the drivers of increased eutrophication in this urbanized tropical estuary.

5.2 Materials and methods

A detailed description of the study area is presented in Chapter 2 with information about Saigon River Estuary and Ho Chi Minh Megacity. This section only briefly summarizes the research area and presents the difference between applying transient version versus steady-version of the C-GEM model for Saigon River Estuary.

5.2.1 Study area

5.2.2 Saigon River Estuary

Saigon River Estuary is located in the south of Vietnam, with a catchment area of 4500 km^2 . From Dau Tieng Reservoir to the estuary mouth, the Saigon River has a length of about 200km. The Saigon River has an average discharge of $50 m^3 s^{-1}$ ($30m^3 s^{-1}$ in dry season and more than $100 m^3 s^{-1}$ in rainy season). It confluences with Thi Tinh River (10 and $30m^3 s^{-1}$ in dry and rainy season) and Dongnai River (600 and $1200m^3 s^{-1}$ in dry and rainy season) at km 40 and km 130, respectively. At km 110 and 126, the Saigon River receives wastewater from Vam Thuat River – urban river ($4m^3 s^{-1}$) and urban canals ($5m^3 s^{-1}$). The urban rivers and canals discharge are calculated based on the total amount of domestic wastewater accounted for the province population (approximately 150L/day/inhabitant). The

5. Modeling the seasonal nutrient dynamics

Saigon River Estuary has a funnel shape, with a width of about 5000 m at the estuary mouth and about 300 m at the urban section (from km 80 to km 160) and 50 m at the upstream. Saigon River Estuary is deepest in the urban section with a maximum depth of 20m. At upstream and downstream, there are depths of 5 - 10 m. This estuary is influenced by the semi-diurnal asymmetric tidal regime of the East Sea of Vietnam, with a tidal period of 12.42h and a tidal range of 3m. Salinity at the estuary mouth ranges from 20 to 30 ppt, and can spread about 100km inland in the dry season and about 40km (km 160) in the rainy season. The residence time at the urban section of Saigon River Estuary in the dry and rainy seasons is about 80-120 days and 20-40 days, respectively calculated based on volume/freshwater inflow (Salman, 2021).

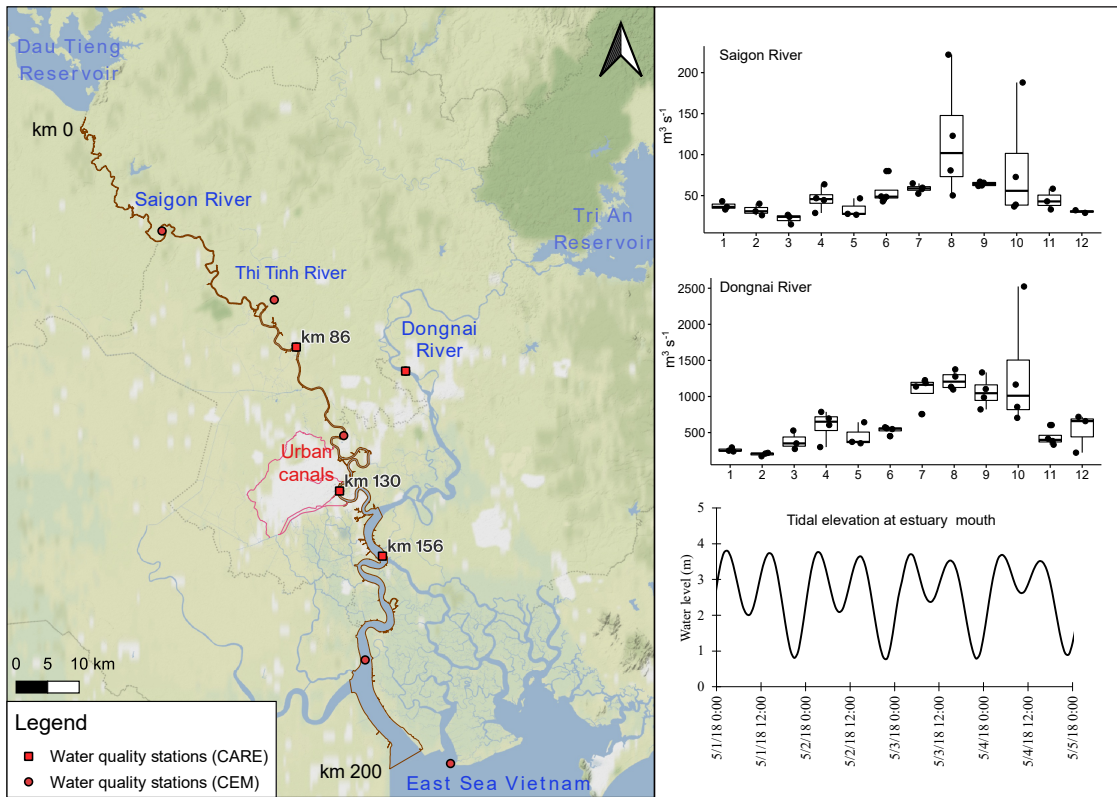


Figure 5.1: The model domain of C-GEM, water quality stations in the Saigon River Estuary. Monthly discharge of Saigon River (at km 130) and Dongnai River are average data from 2014 – 2017. CARE and CEM are two monitoring and research centers, described in section 2.2

5.2.3 Ho Chi Minh Megacity

Most of the length of the Saigon River lies within the territory of Ho Chi Minh City (HCMC). HCMC is the largest economic center of Vietnam, contributing 22% of GDP (in 2020) and having the highest population density in the country

5. Modeling the seasonal nutrient dynamics

(4292 inhabitants km^{-2} , 9% national population in 2020). Measures to improve environmental quality in Ho Chi Minh City are not at the same rate as the population growth of HCMC. In 2008, HCMC built the first wastewater treatment plant to meet 10% of the wastewater of about 6.8 million people. By 2018, Ho Chi Minh City had three WWTPs, but only treated about 18% of wastewater from about 8.7 million people. Currently, one WWTP is under construction, while other WWTPs are still in the fundraising stage. More than 80% of urban domestic wastewater from Ho Chi Minh City is discharged directly into the canal system of HCMC, and finally to the Saigon River Estuary. The outlet of these canals belongs to km 120 - 130 of the Saigon River, about 80 km from the estuary mouth. Urban canals have very high concentrations of nutrients, much further beyond the regulated threshold of recommendation of surface water quality in Vietnam (QCVN 08:2008/BTNMT), and higher than concentrations in upstream of the Saigon River Estuary (Figure 5.2). The phenomenon of mass fish deaths has appeared regularly in urban canals from 2014 – 2021. For example, from April to July 2014 (14 tons of dead fish, [Saigon News, 2014](#)), 19/5/2015 (25 tons of dead fish, [Thanhnien News, 2015](#)), 18/5/2016 (70 tons of dead fish, source: [Vietnamnet News, 2016](#)), 4-7/4/2017 ([Vietnamnet News, 2017](#)), 3/5/2018 ([Saigon Online, 2018](#)). From 2019 to 2020, there was no mass fish death, but April 4, 2021, there was a fish death like in previous years ([Tuoitre News, 2021](#)). The phenomenon of mass fish deaths in urban canals of HCMC has the common feature that all occur in the dry season, around April-May. However, there is no mass fish death in the Saigon River, where urban canals' wastewater is received, although the Saigon River is often in hypoxia condition and high nutrient concentrations.

5.2.4 Data collection

Data used for the transient version of C-GEM includes hydrological, water quality, weather condition data. The data are mainly extracted from Vietnamese Center of Environmental Monitoring (CEM) and Center Asiatique de Recherche sur l'Eau (CARE). In general, the input data for the model is bi-weekly or monthly monitoring; only tidal elevation and solar radiation are hourly data.

Hydrological data

Hydrological data is collected from CEM's monthly measurements. C-GEM model only requires average discharge at the upstream boundary and generic tidal variation at the downstream boundary. The steady-state version of C-GEM, using a generic tidal variation, which is calculated based on the tidal period and tidal range at the estuary mouth. The steady-state C-GEM can only access the dynamics of processes within a tidal cycle. The changes in tidal forcings can affect the contaminant's spread to the upstream area, where domestic water

5. Modeling the seasonal nutrient dynamics

production of HCMC is located. Therefore, the use of hourly tidal elevation would allow a more accurate depiction of tidal variation. The hourly tidal elevation at the estuary mouth is extracted from the global tide gauge data of UHSLC (<https://uhslc.soest.hawaii.edu/datainfo/>, accessed 10/02/2021). CEM monitoring program only provides water level, velocity, and discharge for 48 hours (i.e. 4 tides cycles) of each month. The average discharge in upstream and tributaries are the average of monthly measurement from 2014 to 2017. For model validation, the simulated tidal range are compared to the daily observed tidal range at three stations provided Vietnamese Center of Water Management and Climate Change (WACC) with 1.5 years (1/2017 to 6/2018) of available data.

Water quality data

CEM water quality data included concentrations of BOD_5 , PO_4^{3-} , NH_4^+ , DO, and TSS. CARE data were used in addition (Chl-a, TOC, DSi and NO_3^-). C-GEM allows for diatoms and non-diatom simulations. The results of the phytoplankton densities survey 2016-2017 showed that diatom accounted for 90% of total phytoplankton density (A. T. Nguyen, Némery, et al., 2021). In addition, Chl-a was significantly correlated with total phytoplankton density, Chl-a was thus used instead of biomass of diatoms (90% Chl-a) and non-diatom (10% Chl-a). Currently, CARE only observes at four stations (Figure 5.1), so the data for boundary conditions are supplemented from the longitudinal profile along the Saigon River during the dry and rainy seasons 2019-2020. The survey results showed that the concentrations of TSS, NH_4^+ , NO_3^- , PO_4^{3-} , Chl-a, TOC, DSi in the upstream boundary were not significantly different from the monitoring station at km 76. Therefore, the data of Chl-a, DSi and NO_3^- at the upper boundary (km 0) and the lower boundary (km 200) is applied according to the average data of the four surveys. We assumed that the complex evolution of the variable concentrations in the estuary mainly originates from the interactions of biogeochemical processes and hydrology and external forcings (temperature, solar radiation, wind) rather than from changes in inflow water and saltwater.

Weather condition

Climatic conditions data applied to the C-GEM model include solar radiation, wind speed at 10m, and water temperature. The solar radiation was extracted from the data of a weather station of CARE located in HCMC, about 10 km from Saigon River Estuary and applied to the entire estuary. The monthly wind speed is collected from the HCMC Statistical Office data and applied to the whole estuary. Water temperature was used from CARE's bi-weekly monitoring survey.

5. Modeling the seasonal nutrient dynamics

5.2.5 Model implementation

The set-up procedure for the transient version C-GEM model in this study is similar to those reported by A. T. Nguyen, Némery, et al. (2021) for the steady-state version, including building idealized geometry and hydrodynamics for Saigon River Estuary. The notable difference in this version is the addition of the P adsorption/desorption process to the biogeochemical module and the use of monthly input data. Calibration to determine the parameters for geometry (convergent length), hydrodynamics (Chézy), sediments (critical shear stress and erosion/deposition coefficient) was performed as in steady-state version. For biogeochemical parameters, three parameters, including aerobic degradation rate, phytoplankton mortality rate, were modified according to the range recommended by (Volta, Laruelle, Arndt, & Regnier, 2016). Calibration data includes bi-weekly data at three stations PC, BD, BK for the period 11/2017 - 05/2018, a period in which there was no marked change in the concentration of Chl-a. The choice of this calibration period is to minimize the error in overfitting the model because the model's input data is still mostly monthly (e.g., discharge, external loadings from tributaries, canals).

Biogeochemical module

The variables and biogeochemical processes applied in the C-GEM model for Saigon River Estuary are shown in Figure 5.2. The processes and their interpretations are shown in Table 5.1. Compared with the steady-state version (A. T. Nguyen, Némery, et al., 2021), the maximum mortality rate in this version increases from 2%/day to 9%/day. This change stems from solar radiation during 2017-2018, about three times higher than the calculated average values in the steady-state version, based on 9 hours of sunshine duration per day at 60% cloud coverage.

The P sorption process was supplemented because P was identified as a limiting factor for eutrophication at the Saigon River Estuary (T. T. Nguyen et al., 2020). Deficiency of this process is likely to lead to overestimated PO_4^{3-} concentration and phytoplankton biomass concentration and ultimately to Si depletion leading to a loss of predominance of diatom, which was not found at Saigon River Estuary. The P sorption process includes the adsorption/desorption PO_4^{3-} onto/from surface suspended sediment, which depends on the concentrations of TSS, PO_4^{3-} , particulate inorganic phosphate (PIP). The simulated PO_4^{3-} is calculated by on sorption equation based on Langmuir equilibrium. This process requires two equilibrium parameters maximal P sorption capacity (Pac) and half-saturation constant (Kps). These equilibrium parameters can be determined by sorption experiments. These parameters are calibrated based on the P sorption experiments of T. T. Nguyen et al. (2019) for Saigon River Estuary in 2017. PIP concentration data are only available in the experiment of T. T. N. Nguyen et al. (2019), but not in the routine monitoring program of CARE and CEM. Therefore, the average concentration of

5. Modeling the seasonal nutrient dynamics

PIP is declared for the upper and lower boundary. The variations of simulated PIP in estuaries depend only on the adsorption/desorption processes process, not contributed by PIP from tributaries and canals.

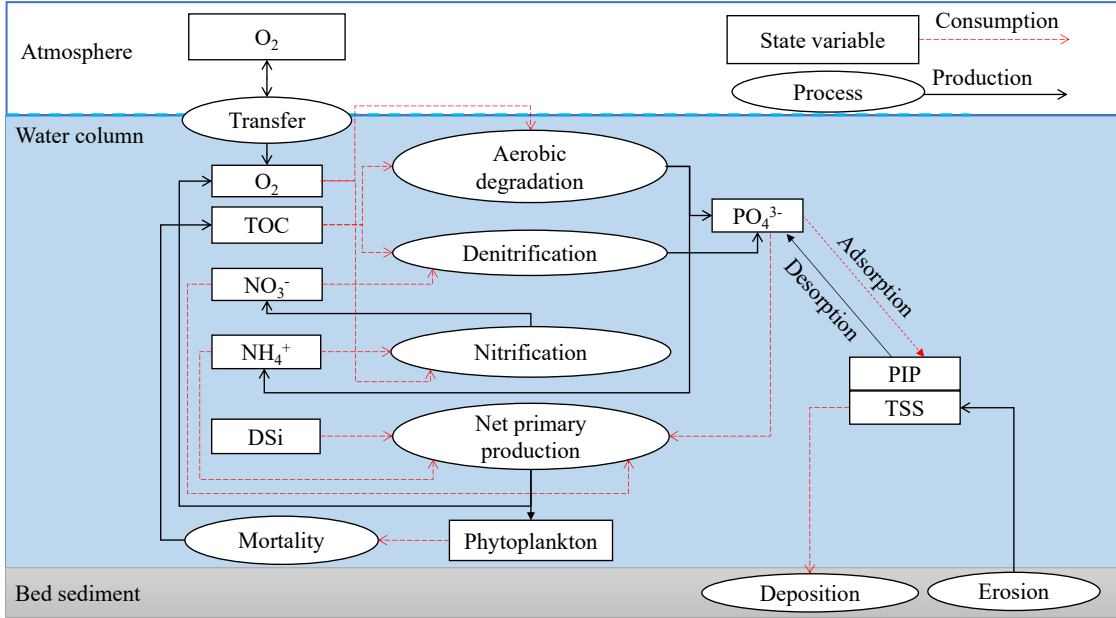


Figure 5.2: Biogeochemical processes in C-GEM applied for Saigon River Estuary.

Although the P exchange between the particulate phase (PIP) to the liquid phase (PO₄³⁻) and vice versa is very slow (from one week to one year) and never achieve equilibrium (Némery et al., 2005), the P sorption process in C-GEM reaches equilibrium at each time step to reduce model complexity. The potential PIP is calculated based on Langmuir equilibrium isotherm. The PO₄³⁻ at each time step is calculated in the below equation (based on Vilmin et al. (2015)).

$$\frac{PIP}{TSS} = P_{ac} \times \frac{PO4}{PO4 + K_{ps}}$$

$$[PO4](t + dt) = [PO4](t) - ([PIP]_{potential} - [PO4](t)) \times \frac{dt}{dt + K_{dt}}$$

if $PIP_{potential} > PIP$: adsorption, otherwise desorption

Process	Biochemical reaction	Formulation	Description
Gross primary production (GPP)	$106\text{CO}_2 + 16\text{HNO}_3 + \text{H}_3\text{PO}_4 + 122\text{H}_2\text{O} + (\text{sunlight}) \rightarrow (\text{CH}_2\text{O})_{106}(\text{NH}_3)_{16}\text{H}_3\text{PO}_4 + 138\text{O}_2$ <p>Nutrient limitation for phytoplankton growth</p> $\text{nlim} = \frac{\text{NO}_3 + \text{NH}_4}{\text{NO}_3 + \text{NH}_4 + K_N} \times \frac{\text{PO}_4}{\text{PO}_4 + K_{\text{PO}_4}}$ $\times \frac{DSi}{DSi + K_{\text{Si}}}$	$\text{GPP} = P_{\max}^B(T) \times \text{nlim} \times \text{phytoplankton}$ $\times \int_H^0 1 - \exp\left(-\frac{\alpha}{P_{\max}^B(T)} \times I(0) \times \exp(-K_D \cdot H)\right) dz$ <p>P_{\max}^B: photosynthesis rate</p> <p>nlim: Nutrient limitation for phytoplankton growth</p>	<p>GPP refers to the total rate of organic carbon production by phytoplankton based on the rate of photosynthesis</p> <p>$I(0)$: solar radiation</p> <p>K_D: Light extinction coefficient</p> <p>H: water depth</p>
Net primary production (NPP)	<p>NPP is the rate of phytoplankton produces biomass which already subtract the respiration of primary producers, including:</p> <p>k_{excr} phytoplankton excretion</p> <p>k_{maint} phytoplanktonic maintenance</p> $\text{NH}_4^+ + 2\text{O}_2 \rightarrow \text{NO}_3^- + \text{H}_2\text{O} + 2\text{H}^+$	$\text{NPP} = \frac{\text{GPP}}{H} \times (1 - k_{\text{excr}}) \times (1 - k_{\text{growth}}) - k_{\text{maint}}(T) \times \text{phytoplankton}$ <p>k_{growth} growth constants of phytoplankton</p>	<p>NPP is GPP minus the autotrophs' respiration rate (i.e., only by the primary producers).</p>
Nitrification		$N = k_{\text{nit}}(T) \times \frac{\text{NH}_4}{\text{NH}_4 + K_{\text{NH}_4}} \times \frac{\text{O}_2}{\text{O}_2 + K_{\text{O}_2, \text{nit}}}$ <p>$k_{\text{nit}}(T)$ maximum rate constant</p>	<p>Under aerobic conditions, ammonia is oxidized to nitrite and nitrate via nitrification</p> <p>K_{NH_4} half-saturation constants</p>
Denitrification	$94.4\text{HNO}_3 + (\text{CH}_2\text{O})_{106}(\text{NH}_3)_{16}(\text{H}_3\text{PO}_4) \rightarrow 106\text{CO}_2 + 55.2\text{N}_2 + \text{H}_3\text{PO}_4 + 177.2\text{H}_2\text{O}$	$D = k_{\text{denit}}(T) \times \frac{\text{TOC}}{\text{TOC} + K_{\text{TOC}}} \times \frac{\text{NO}_3}{\text{NO}_3 + K_{\text{NO}_3}}$ $\times \frac{K_{\text{in}, \text{O}_2}}{\text{O}_2 + K_{\text{in}, \text{O}_2}}$	<p>Under anaerobic conditions, nitrate is reduced to gas forms as N_2, N_2O while organic P is degraded to inorganic PO_4^{3-}</p>
Aerobic degradation (respiration)	$138\text{O}_2 + (\text{CH}_2\text{O})_{106}(\text{NH}_3)_{16}(\text{H}_3\text{PO}_4) \rightarrow 106\text{CO}_2 + 16\text{HNO}_3 + \text{H}_3\text{PO}_4 + 122\text{H}_2\text{O}$	$R = k_{\text{ox}}(T) \cdot \frac{\text{TOC}}{\text{TOC} + K_{\text{TOC}}} \cdot \frac{\text{O}_2}{\text{O}_2 + K_{\text{O}_2, \text{ox}}}$	<p>Degradation of organic carbon in the aerobic condition that converts into inorganic matters</p>
<p>Phytoplankton = NPP - Phytoplankton mortality</p> <p>DSi = NPP of Diatom = NPP x Redfield ratio for silica (15/106)</p> <p>NH_4^+ = Aerobic degradation – Nitrification – NPP_{NH_4}</p> <p>NO_3^- = Nitrification - Denitrification - NPP_{NO_3}</p> <p>TOC = Phytoplankton mortality – Aerobic degradation – Denitrification</p> <p>O_2 = Oxygen air exchange + NPP – Aerobic degradation – Nitrification</p> <p>PO_4^{3-} = Aerobic degradation + Denitrification – NPP_{PO_4} – PO_4 adsorption</p>			

Table 5.1: Biochemical reactions and formulations of the processes applied in C-GEM for Saigon River

5. Modeling the seasonal nutrient dynamics

Although there have been changes in kinetic reaction rates compared to the original version of C-GEM to improve suitability for application at Saigon River Estuary, deficiencies of some other processes may affect simulation results. On one hand, benthic-pelagic processes need to be added to accommodate shallow depths upstream. On the other hand, the addition of zooplankton will improve the accuracy of phytoplankton dynamics. However, these processes are not available in this study because of missing data for calibration. The calibration of phytoplankton mortality rate includes the impact of bacteria and zooplankton grazing. Besides, the omission of benthic processes is accepted based on the longitudinal depth profiles in 2019, 2020. The concentrations of DO, Chl-a, pH are not significantly different between surface water and riverbed, indicating a well-mixed estuary (Figure 5.3). Only TSS increased strongly in the riverbed, but more than 50% TSS concentration did not change significantly with depth except the last 30 km downstream (Figure 5.3), a well-known turbidity maxima estuarine process. Besides, the biogeochemical module in C-GEM only presents the Si consumption by diatoms but not for the dissolution of diatom shells. In addition, the assessment of the retention capacity of the estuary by C-GEM currently mainly depends on the biogeochemical processes in the water column and tidal effects because the current model does not include the burial process.

Model performance criteria

Simulation efficiency is evaluated through three parameters R^2 , RMSE and percent bias (pbias). The spatial simulation results will be compared with the average concentrations in the dry and rainy seasons along the Saigon River 2017-2018. Temporal simulated results are compared with water quality bi-weekly data of CARE and a monthly tidal range of CEM at three monitoring stations at km 86, 130 and 156.

The formulas for model performance evaluation are presented in Table 5.2. Phytoplankton (sum of diatom and non-diatom) is converted to Chl-a concentrations with an equivalent conversion factor (1 μg chl-a is equal to 40 μgC). The input data of phytoplankton biomass for C-GEM was also converted from Chl-a concentration.

5. Modeling the seasonal nutrient dynamics

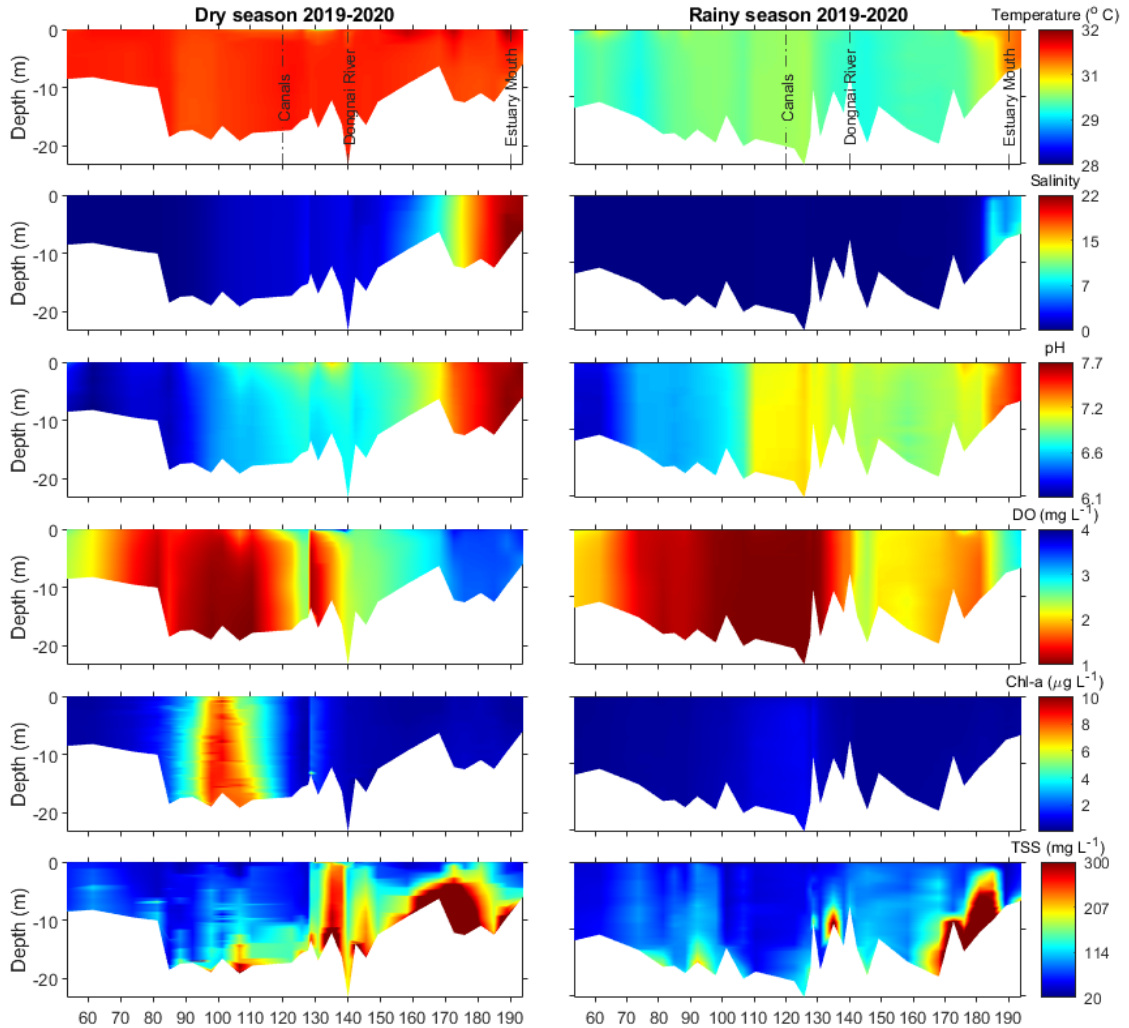


Figure 5.3: Longitudinal depth profiles along Saigon River Estuary in 2019 - 2020.

Statistical indicator	Equation	Range	Optimal value
R ²	$\left[\frac{\sum_{i=1}^n (\mathbf{O}_i - \bar{\mathbf{O}})(\mathbf{S}_i - \bar{\mathbf{S}})}{\sqrt{\sum_{i=1}^n (\mathbf{O}_i - \bar{\mathbf{O}})^2} \sqrt{\sum_{i=1}^n (\mathbf{S}_i - \bar{\mathbf{S}})^2}} \right]^2$	0.0 to 1.0	1.0
RMSE	$\sqrt{\frac{1}{n} \sum_{i=1}^n (\mathbf{O}_i - \mathbf{S}_i)^2}$	0.0 to $+\infty$	0
pbias	$\frac{\sum_{i=1}^n \mathbf{O}_i - \mathbf{S}_i}{\sum_{i=1}^n \mathbf{O}_i} \times 100$	$-\infty$ to $+\infty$	0%

O: Observation; **S:** Simulation; **n:** number of samples

5. Modeling the seasonal nutrient dynamics

Table 5.2: Evaluation criteria for model performance

5.3 Results and discussion

5.3.1 Evaluation of model performance

The model performance evaluation is presented in Figure 5.4, 5.5, 5.6, and summarized in Table 5.3. The application of a steady-state version of C-GEM in the dry season at Saigon River Estuary has been highly appreciated for its effectiveness in describing spatial fluctuations, describing well the influence of megacity (A. T. Nguyen, Némery, et al., 2021). In this study, the C-GEM also performs well the spatial trend of water quality along Saigon River Estuary for both dry and rainy seasons. The simulation results are extended to evaluate the effectiveness of temporal variation of water quality at three typical areas of Saigon River Estuary (Table 5.3, Figure 5.6).

The current version of C-GEM generally allows a good description of the tidal range and the salinity intrusion in both seasons with R^2 about 0.6 - 0.9, bias 11 - 16%. The water quality simulation is not as good as hydrodynamics. The model only achieves good results for some variables in some periods and some locations. Specifically, for the efficiency of describing the temporal trends (R^2), DSi, Chl-a, TOC have good simulation results in the urban section with R^2 of 0.4 - 0.8. The simulation of DO concentration trend is only acceptable upstream with $R^2=0.5$. The simulation of NO_3^- reaches R^2 of 0.4 – 0.5 in the rainy season in the upstream and urban sections. C-GEM does not well describe NH_4^+ , PO_4^{3-} , TSS with only R^2 of about 0.1 – 0.3. Although the simulated results are not appreciated for some parameters, the percentage error such as NO_3^- is still less than 20% during the rainy season. Likewise, the error in the DO simulation is just around 5% in downstream.

5. Modeling the seasonal nutrient dynamics

Period	Station	Parameters	NH4	NO3	PO4	DSi	Chl-a	TOC	DO	TSS
Entire year	Upstream	R ²	0.10	0.09	0.06	0.17	0.02	0.02	0.56	0.01
		RMSE	0.16	0.33	0.08	0.45	4.54	3.22	1.75	13.98
		pbias (%)	-58	-46	287	86	>1000	-62	58	-28
	Urban	R ²	0.01	0.08	0.03	0.70	0.60	0.58	0.06	0.00
		RMSE	0.89	0.94	0.10	0.73	19.47	4.26	1.18	43.43
		pbias (%)	144	78	212	76	54	46	45	-7
	Downstream	R ²	0.03	0.08	0.16	0.00	0.26	0.06	0.01	0.01
		RMSE	0.20	0.33	0.15	0.98	2.49	1.57	0.83	32.95
		pbias (%)	235	1	391	90	309	7	-1	-28
Dry season	Upstream	R ²	0.24	0.08	0.03	0.32	0.01	0.03	0.06	0.45
		RMSE	0.17	0.30	0.09	0.44	6.38	3.74	2.40	6.77
		pbias (%)	-64	-27	295	85	3	-66	118	-12
	Urban	R ²	0.19	0.00	0.02	0.82	0.44	0.78	0.13	0.37
		RMSE	1.18	1.23	0.07	0.61	26.95	5.39	1.45	59.82
		pbias (%)	264	160	147	70	20	69	77	-41
	Downstream	R ²	0.23	0.36	0.20	0.00	0.48	0.16	0.16	0.95
		RMSE	0.15	0.33	0.18	0.57	2.58	2.03	1.10	45.04
		pbias (%)	201	19	516	29	340	-11	3	-58
Rainy season	Upstream	R ²	0.09	0.36	0.00	0.03	0.35	0.16	0.54	0.29
		RMSE	0.15	0.36	0.08	0.46	0.66	2.60	0.58	18.58
		pbias (%)	-52	-64	278	86	>1000	-57	-1	-44
	Urban	R ²	0.10	0.51	0.04	0.91	0.04	0.40	0.01	0.33
		RMSE	0.47	0.49	0.12	0.83	5.65	2.69	0.85	13.93
		pbias (%)	24	-5	276	82	88	23	13	26
	Downstream	R ²	0.06	0.07	0.10	0.26	0.03	0.24	0.42	0.34
		RMSE	0.24	0.32	0.10	1.27	2.40	0.89	0.39	11.93
		pbias (%)	270	-18	266	152	278	24	-5	1

Model performance was calculated based on a comparison of daily simulated concentrations and observed data from CARE bi-weekly monitoring at three stations km 86 (upstream), km 130 (urban) and km 156 (downstream), from January 2017 – December 2018.

Table 5.3: The performance of the simulated temporal variation by C-GEM in the Saigon River in dry, rainy seasons

The following two subsections discuss the dynamics of the hydrological regime and water quality of the Saigon River, respectively. The advantages and disadvantages of applying C-GEM model in terms of existing data of Saigon River Estuary are also discussed.

5. Modeling the seasonal nutrient dynamics

Hydrodynamics and transport

The simulated tidal fluctuations in the Saigon River by C-GEM are well evaluated. However, the accuracy in describing hydrodynamics processes gradually decreases from the estuary to the upstream. At km 130, the model efficiency has R^2 , RMSE, error of 0.9, 0.2 m, 11%, respectively, while at the upstream area of km 86, the efficiency is reduced to 0.6, 0.33m, 16% (Figure 5.4). C-GEM underestimated the tidal range mainly from May to November, during the rainy season at Saigon River Estuary. A shortening of the tidal range from reality can cause errors in assessing pollutant mobility over tidal cycles. Salinity can spread about 70 km from the sea mouth to the mainland in the rainy season, while the simulation results only describe 50 km of saline intrusion. In the dry season, the resulting salinity intrusion is only about 70 km inland, while the monitoring data shows this number can be up to 100 km. This error originates from the great influence of Dongnai River, at km 130 (70 km from the sea mouth) with a freshwater flow of about $300m^3 s^{-1}$ (more than ten times that of Saigon River) which greatly increases the flushing capacity from km 130 to estuary mouth. In addition, the simulated depth and cross-sectional area are used to calculate the volume of three sections along the Saigon River to estimate the retention time in these areas. Residence time varies from about 20 days in the rainy season to 120 days in the dry season (Figure 5.4).

Applying C-GEM with hourly data at estuary mouth and monthly freshwater inflow has enabled a good description of the trend and intensity of tidal oscillations at Saigon River Estuary. Compared with high-resolution flow data (10 minutes) from Camenen et al. (2021), monthly monitoring data does not capture the high variations of daily discharge in the Saigon River. The difference can be explained by Dau Tieng Reservoir's activities upstream, markedly controlling the freshwater discharge in the Saigon River (Camenen et al., 2021). However, the flooding of the Dau Tieng Reservoir mostly occurs in the rainy season with a highly flushing capacity. The use of hourly tidal variation from global gauge data in C-GEM still ensures the assessment of tidal intensity changes to the propagation and diffusion of substances along the estuary. It should be noted that although the model was able to describe contaminant propagation, the lack of daily discharge data at the upstream boundary and tributaries could cause large concentration differences in the dilution equation. Arndt et al. (2009) suggested that the transient behaviours of variables in estuaries are often derived from fluctuating riverine boundary conditions. The failure to describe the peaks in the concentrations of the observed substances is inevitable if using the data of average conditions. Therefore, daily discharges for the upstream and all tributaries are recommended to describe the short-term variations at the estuaries.

5. Modeling the seasonal nutrient dynamics

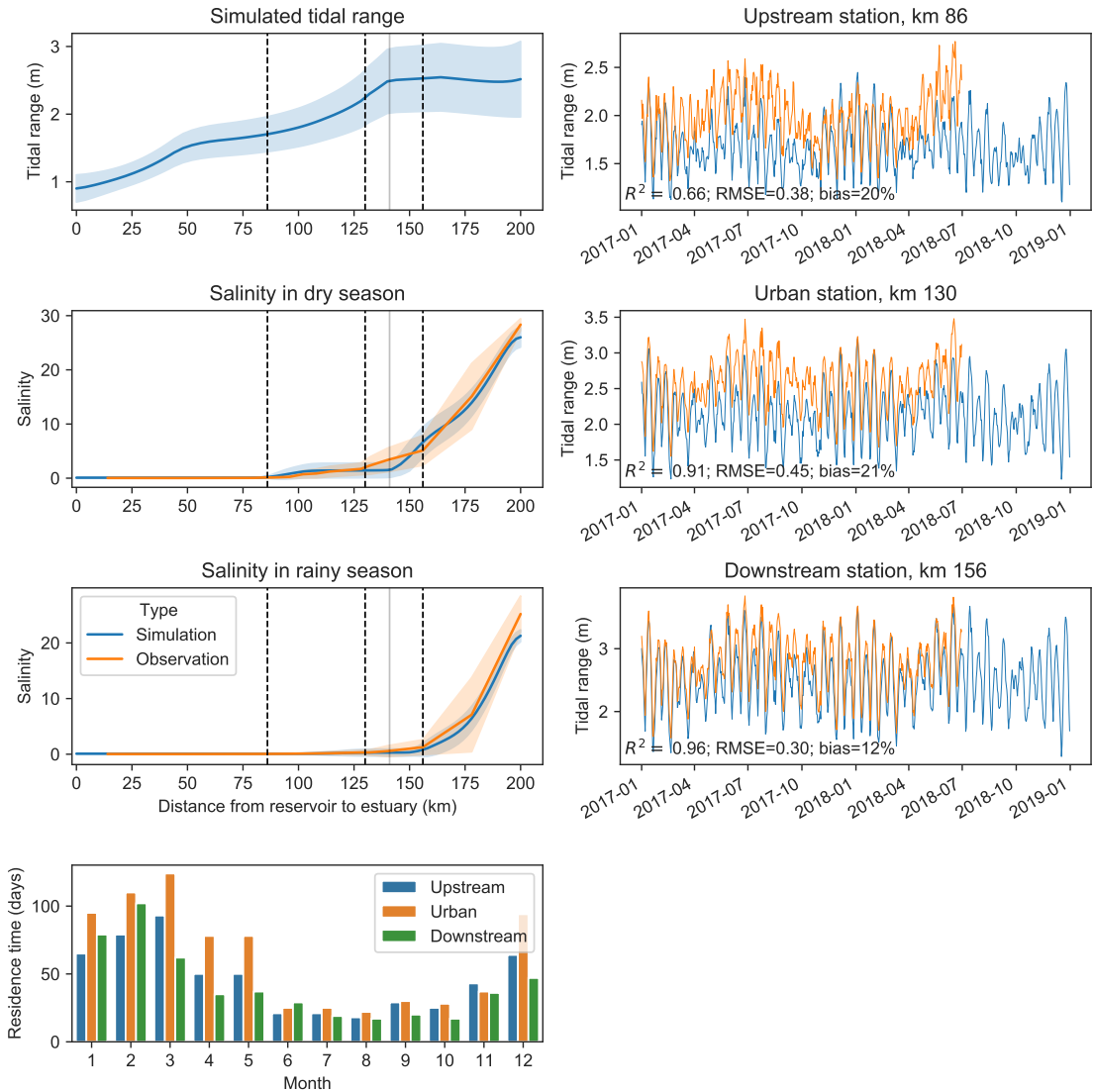


Figure 5.4: The observed and simulated tidal range, salinity in the Saigon River from 2017 to 2018. Three dotted lines in the left panels are locations of three stations at km 86, 130 and 156. The grey line indicates Dongnai River. The tidal range observation data are calculated based on hourly water level data from the Vietnamese Center of Water Management and Climate Change (WACC). The residence time is calculated by dividing the simulated volume by the flow of each section.

Nutrients and phytoplankton dynamics

The transient version of C-GEM describes well the water quality trends along the Saigon River under the impact of urban wastewater of HCMC for both dry and rainy seasons (Figure 5.5). Similar to observed data, NH_4^+ , TOC, Chl-a, DO have significant differences between the three sections, upstream (km 0 – 86), urban (km 86 – 130) and downstream (km 130 – 200) of Saigon River estuary. C-GEM has well described NH_4^+ , NO_3^- , DSi, Chl-a in both seasons with R^2 from 0.7 – 0.9. Note that spatial variations of Chl-a, DSi, NO_3^- are only compared with the

5. Modeling the seasonal nutrient dynamics

observed data of three monitoring stations, while the remaining parameters are compared with 6-7 stations. Although only a few stations represent three areas along the Saigon River, the trend of water quality change under the impact of urban discharge has been clarified.

In the dry season, the observed concentrations of TOC and NH_4^+ both increased, leading to a decrease in DO to anoxic conditions ($< 1 \text{ mg O}_2 L^{-1}$). However, the simulation results of C-GEM for DO concentrations are from 2 to 5 mg L^{-1} , and R^2 only reaches 0.35, the lowest R^2 compared to the remaining variables. The overestimated DO stems from a rapid increase in phytoplankton density from near zero to more than $60 \mu\text{g Chl-a L}^{-1}$ in the urban section of Saigon River. The phytoplankton bloom increases the DO concentration in the water by photosynthesis, roughly equal to the oxygen consumption by nitrification and organic carbon respiration in the simulation. The simulated phytoplankton in the dry season is almost always in high density because the simulated nutrient source (N, P) is not exhausted. The high nutrients availability allowed the growth of phytoplankton not to be limited by the required nutrients, especially PO_4^{3-} . Based on the C:N:P:Si ratio analysis by T. T. N. Nguyen et al. (2019), PO_4^{3-} is the limiting factor for phytoplankton development in the Saigon River Estuary. Indeed, there were several times the the PO_4^{3-} was lower than 0.01 mg PL^{-1} during the dry season. Phytoplankton biomass in the urban section in the dry season can reach more than $130 \mu\text{g Chl-a L}^{-1}$ in the dry season, while many periods are still below the detection threshold. This shows that the intensity of biogeochemical processes and phytoplankton bloom is very strong in the Saigon River. Strong fluctuations of phytoplankton over a short period (days to weeks) are also detected according to studies conducted in other estuaries such as Scheldt Estuary in 2006. Phytoplankton biomass at this estuary reached $150 \mu\text{g Chl-a L}^{-1}$ in summer and can decrease to almost undetected levels in winter (Gypens et al., 2013). The study at Scheldt Estuary detected phytoplankton depletion under low temperature and DSi depletion. in the Saigon River Estuary, solar radiation is almost unchanged throughout the year and is not limited in DSi concentration. Meanwhile, the C-GEM model applied at Saigon River Estuary has not yet detected these extreme values neither in the observations. The two main causes of overestimation are the lack of other important biogeochemical processes (e.g., benthic processes, zooplankton grazing, burial processes), and the use of average monthly data as input values. Based on simulation results at a subtropical estuary of Vietnam, Day River, which also receives highly untreated domestic wastewater, the burial process played an important role in reducing nutrient concentrations in the water column (Trinh et al., 2012). Specifically, domestic wastewater with high P concentration at Day River is discharged into this river, but up to 38% of phosphorus is retained in bed sediment (Trinh et al., 2012). Therefore, beside the consumption of PO_4^{3-} by phytoplankton uptake and P adsorption, the P burial process is important. Downstream, the sudden decrease

5. Modeling the seasonal nutrient dynamics

in concentration from km 130 is due to the dilution of the Dongnai River. A gradual decrease in concentrations is observed at the estuary due to dilution with seawater (e.g., Chl-a, NH_4^+ , NO_3^- , DSi). The improvement of the downstream oxygen concentration is also contributed by the aeration of the water column.

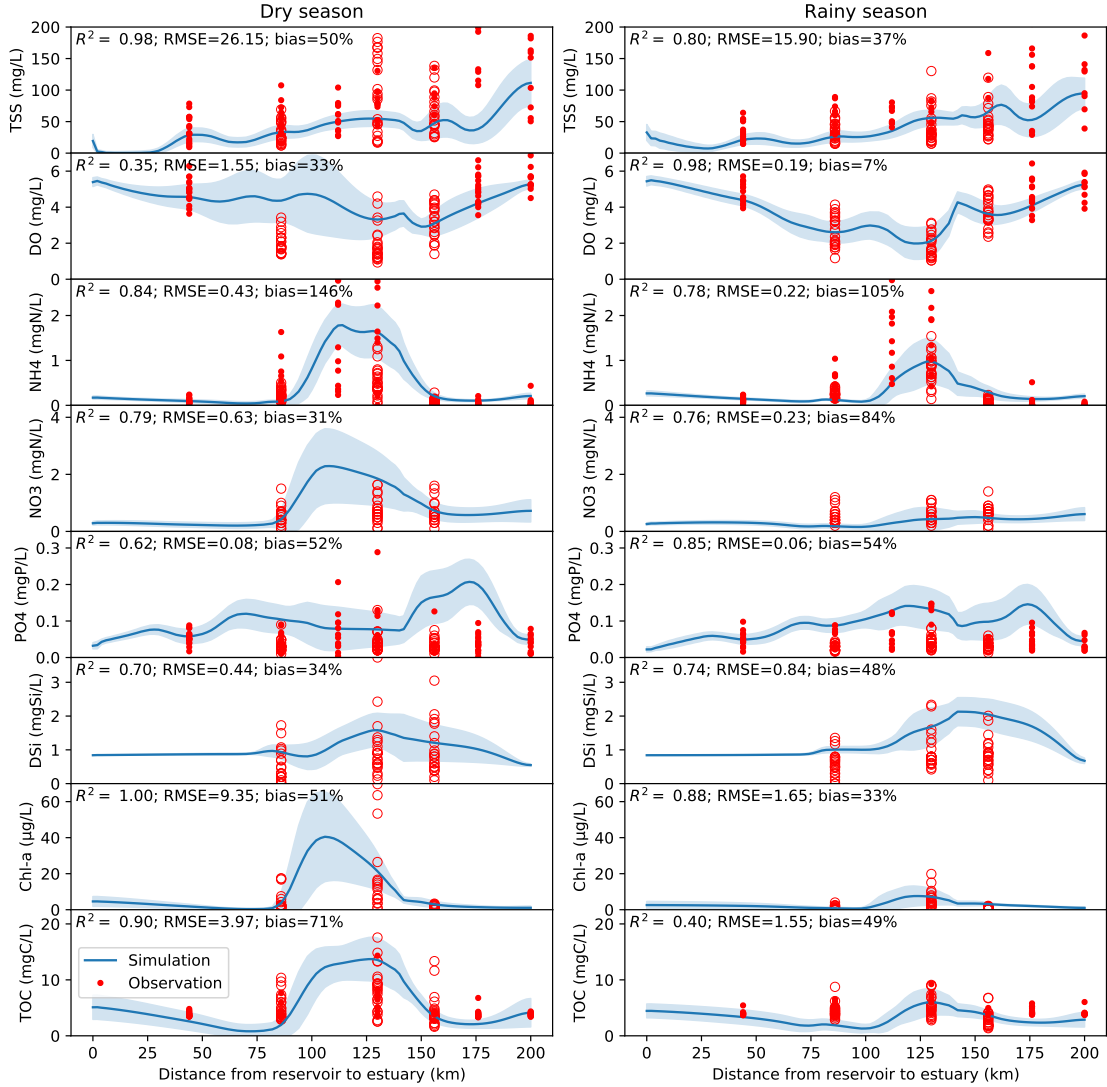


Figure 5.5: Comparison of simulated and observed water quality along Saigon River. The model performance is calculated based on average values in the dry and rainy season 2017–2018.

The R^2 of spatial simulations is mostly from 0.7 to 0.9, except for TOC with R^2 of 0.4. In rainy season, concentrations of TOC, NO_3^- , Chl-a, were not significantly different between the upstream, downstream and urban sections of the Saigon River (Figure 5.5). The concentrations of NH_4^+ and DO change significantly when the Saigon River received the domestic wastewater of Ho Chi Minh City. In contrast to ineffective simulated DO in the dry season, the simulation efficiency in the rainy season reached $R^2 = 0.98$ with an error of 7%. The NH_4^+ simulation results also

5. Modeling the seasonal nutrient dynamics

have an R^2 of about 0.80 but have an error of 105%. This large error is detected in km 116, where the observed NH_4^+ concentration was exceptionally high. The high NH_4^+ concentration cloud at approximately 30 km long in the dry season is similar to the dry season. However, as a result of saline intrusion in the rainy season, the dispersion is not as strong as in the dry season. This explains the ineffective spreading of high NH_4^+ from km 116 to km 130, as observed. The underestimation is unlikely from an error in the pollutant diffusivity simulation but perhaps from other biogeochemical processes or another external NH_4^+ source which is still unanswered.

NO_3^- , DSi, PO_4^{3-} , TSS do not have the spatial trends as Chl-a, NH_4^+ when receiving wastewater from urban canals. The C-GEM model has well described this anomaly through the role of processes such as denitrification ($\text{NO}_3^- \rightarrow \text{N}_2\text{O}$, N_2) and PO_4^{3-} adsorption. The concentration of PO_4^{3-} in the urban section is not significantly different from other sections. The addition of P sorption processes avoids the overestimated PO_4^{3-} as compared with the results of A. T. Nguyen, Némery, et al. (2021). According to Minaudo et al. (2018), PO_4^{3-} adsorption/desorption is an important process in understanding the dynamics of phytoplankton and nutrients. While PO_4^{3-} adsorption in urban section plays a role in reducing PO_4^{3-} concentration, the downstream PO_4^{3-} simulation results are not good. Downstream, there is an increase in PO_4^{3-} mainly from P desorption due to an increase in TSS deposition. However, this process may not be suitable because observed TSS downstream tends to increase gradually. The sediment erosion and increase of PO_4^{3-} adsorption is thus reasonable. According to the experiment of T. T. N. Nguyen et al. (2019), at high salinity, P desorption will greatly increase in the Saigon River. This coincides with the desorption phenomenon simulated downstream. However, PO_4^{3-} downstream always has a lower concentration than PO_4^{3-} in the urban section in T. T. Nguyen et al. (2020) and in this study. Dongnai River with low PO_4^{3-} concentration strongly impacts PO_4^{3-} dilution, which can lead to a gradual decrease in PO_4^{3-} concentration.

5.3.2 Spatio-temporal evolution of nutrients and phytoplankton biomass

Temporal variation of water quality was analyzed in three sections representing upstream, urban and downstream of Saigon River Estuary. These sections correspond to the three monitoring stations of CARE at km 86 (freshwater, less affected by urban wastewater and tides), km 130 (receiving urban wastewater), km 156 (after the confluence with Dongnai River). Figure 5.6 depicts spatio-temporal variations of TSS, DO, nutrients (NH_4^+ , NO_3^- , PO_4^{3-} , DSi), organic carbon and phytoplankton biomass (Chl-a) over two years.

5. Modeling the seasonal nutrient dynamics

Simulated NH_4^+ , NO_3^- , Chl-a, and PO_4^{3-} have seasonal trends with higher concentrations in the dry season. The most distinct difference of water quality parameters between dry and rainy seasons is phytoplankton biomass, but mainly in the urban section of Saigon River Estuary. In addition, simulation and observation data show that the intensity and timing of phytoplankton peaks are also different between the dry seasons of 2017 and 2018. C-GEM well capture the phytoplankton mass development in two periods in 2017-2018, specifically from late November to late May in dry season. The peak of simulated phytoplankton concentration is only $40 \mu\text{g Chl-a L}^{-1}$ at km 130, approximately two times lower than the maximum value observed in 2017. As discussed in hydrodynamics evaluation, the use of average inflow may interfere with the short-term variations of phytoplankton. However, the model still provides a good description of the seasonal trends of phytoplankton. The phytoplankton mortality rate can explain the phytoplankton underestimation. This process has implicitly considered the process of phytoplankton reduction by bacteria and zooplankton grazing. Statistical results from tropical estuaries in India, show that zooplankton is the main factor controlling phytoplankton density in low flow conditions in dry season (Bharathi & Sarma, 2019). Fluctuations in the inflow of freshwater may cause fluctuations in zooplankton and phytoplankton in the Saigon River.

Monitoring data and simulation both show that there is no seasonal trend of TSS, DO, PO_4^{3-} . The simulated transient variations of TSS have the same signal as the tidal fluctuations. This result is similar to simulation results of higher resolution models at Vietnamese Mekong Delta (Le Tu et al., 2019; Marchesiello et al., 2019) or in other temperate estuaries such as Scheldt Estuary (Arndt et al., 2009, 2011). Besides, tidal elevation has no seasonal trend but only changes according to the semi-diurnal regime (i.e., two high tides and two low tides per day). Therefore, TSS also has a similar tendency and creates transient variations of PO_4^{3-} adsorption onto TSS. Using the simple sediment erosion/deposition module allowed a good description of the fluctuation range and concentration of TSS in the Saigon River. However, the model is not effective in describing the changing trend of TSS in the urban area (km 130). Indeed, Vanderborght et al. (2007) argued that extending the reaction-transport model (e.g., C-GEM) to describe sediment dynamics accurately will increase the model complexity and is often out of reach of a simplified model to minimize the input data. However, in this study, the established P adsorption/desorption process reached equilibrium at each time step. The small fluctuation of TSS thus led to a significant change in the concentration of simulated PO_4^{3-} . As a result, the simulated PO_4^{3-} concentration downstream increased three times from 0.1 to 0.3 mg PL^{-1} during sedimentation (Figure 5.6). Simulated PO_4^{3-} in the urban section regularly increases due to P desorption from sediment, especially in the rainy season and the dry season (from July to January

5. Modeling the seasonal nutrient dynamics

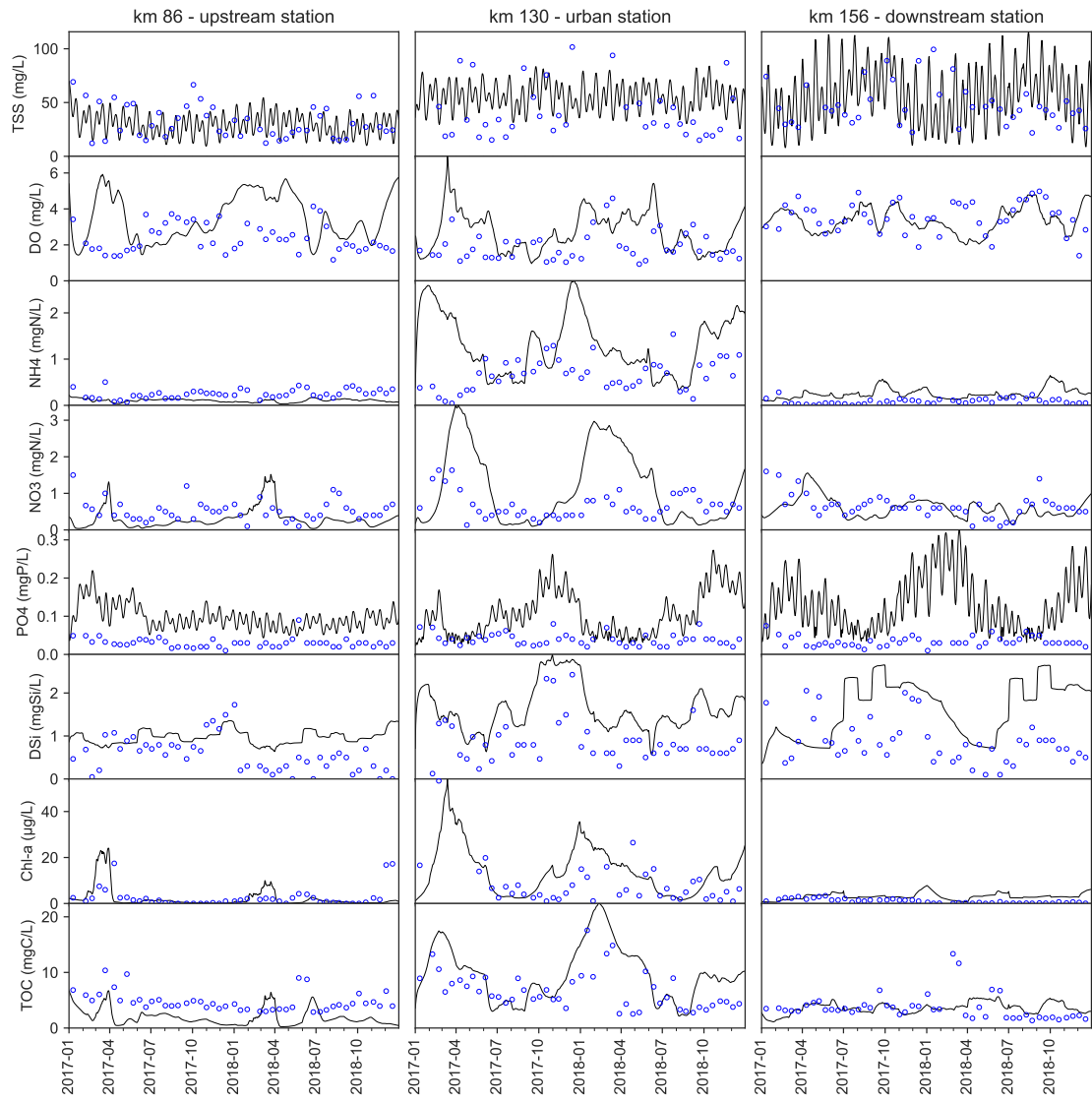


Figure 5.6: The daily evolution of suspended sediment, dissolved oxygen, nutrients, organic carbon and phytoplankton biomass in three stations along Saigon River Estuary from 2017 to 2018. Blue points are observed data of bi-weekly monitoring.

next year). In the upstream, the P sorption process has almost no significant influence because of the small concentration of TSS in this area.

While the C-GEM model accurately depicts pollution levels in the urban section and downstream, the C-GEM simulation results underestimated the NH_4^+ , TOC concentration upstream. Low simulated TOC concentrations are associated with low phytoplankton densities upstream and lead to lower phytoplankton mortality. According to the observation, concentrations of TOC and Chl-a have a linear correlation in the upstream and urban sections, suggesting that phytoplankton contribute significantly to organic carbon concentration in these areas (A. T. Nguyen, Dao, et al., 2021). This statement is described by C-GEM at the phytoplankton

5. Modeling the seasonal nutrient dynamics

peak events in April 2017 and April 2018 at the upstream station (Figure 5.6). The concentrations of TOC at these two periods both increased markedly. However, the simulated TOC concentrations were lower than observed in the remaining periods because of the lack of external organic carbon sources. B. T. Nguyen et al. (2020) determined that the upstream area of Saigon River Estuary increases organic carbon in groundwater due to the strong agricultural activities. The exchange between freshwater and groundwater upstream of Saigon River Estuary has not yet been implemented in the C-GEM model. Likewise, simulated NH_4^+ concentrations were underestimated. However, this result does not affect the low nutrient status assessment in the Saigon River Estuary's upstream.

5.3.3 Seasonal evolution of primary production and nutrients cycling

Figure 5.7 depicts the evolution of the major biogeochemical processes involved in phytoplankton abundance and nutrients cycling. In addition to the description of biogeochemical processes, external forcings are described, including nutrients limitation, light utilization efficiency, oxygen air exchange. The nutrients limitation is calculated based on NH_4^+ , NO_3^- , PO_4^{3-} and DSi in the case of diatom simulation. The results in this study present nutrients limitations applied for all four parameters. Light utilization efficiency is calculated based on the photosynthetic rate of phytoplankton, light extinction coefficient (depending on background light attenuation and TSS) and water depth. Oxygen air exchange is calculated based on flow velocity, wind speed, water depth and current oxygen concentration.

The description of the evolution of nutrient limitation provides important information in describing the nutrient availability for phytoplankton growth and disappearance, especially for transient variations in estuaries and coastal areas (Arndt et al., 2011). To assess the risk of eutrophication, the nutrient limitation for phytoplankton growth is the keystone (Costa et al., 2009; L. M. Smith et al., 2006). Simulation results of C-GEM show that the nutrient limitation only exists about 30 km to 75 km during the rainy season. In the remaining periods, the availability of nutrients for phytoplankton growth ranges from 40% to over 80%. Especially in the urban section, from km 85 to 150, the nutrient availability for the primary production process is always high, reaching nearly 100% regularly in both the dry and rainy seasons. in the Saigon River, the simulation results show that high nutrient concentrations are readily available for phytoplankton bloom in the urban section of Saigon River regardless of the season. Simulation of Net Primary Production (NPP), i.e., biomass growth of phytoplankton after primary producers' respiration has been removed, is similar to nutrient availability. This result is similar to that observed at other tropical estuaries, e.g., Sul River Estuary (Brazil), where it was consistently found that the nutrient limitation did not vary

5. Modeling the seasonal nutrient dynamics

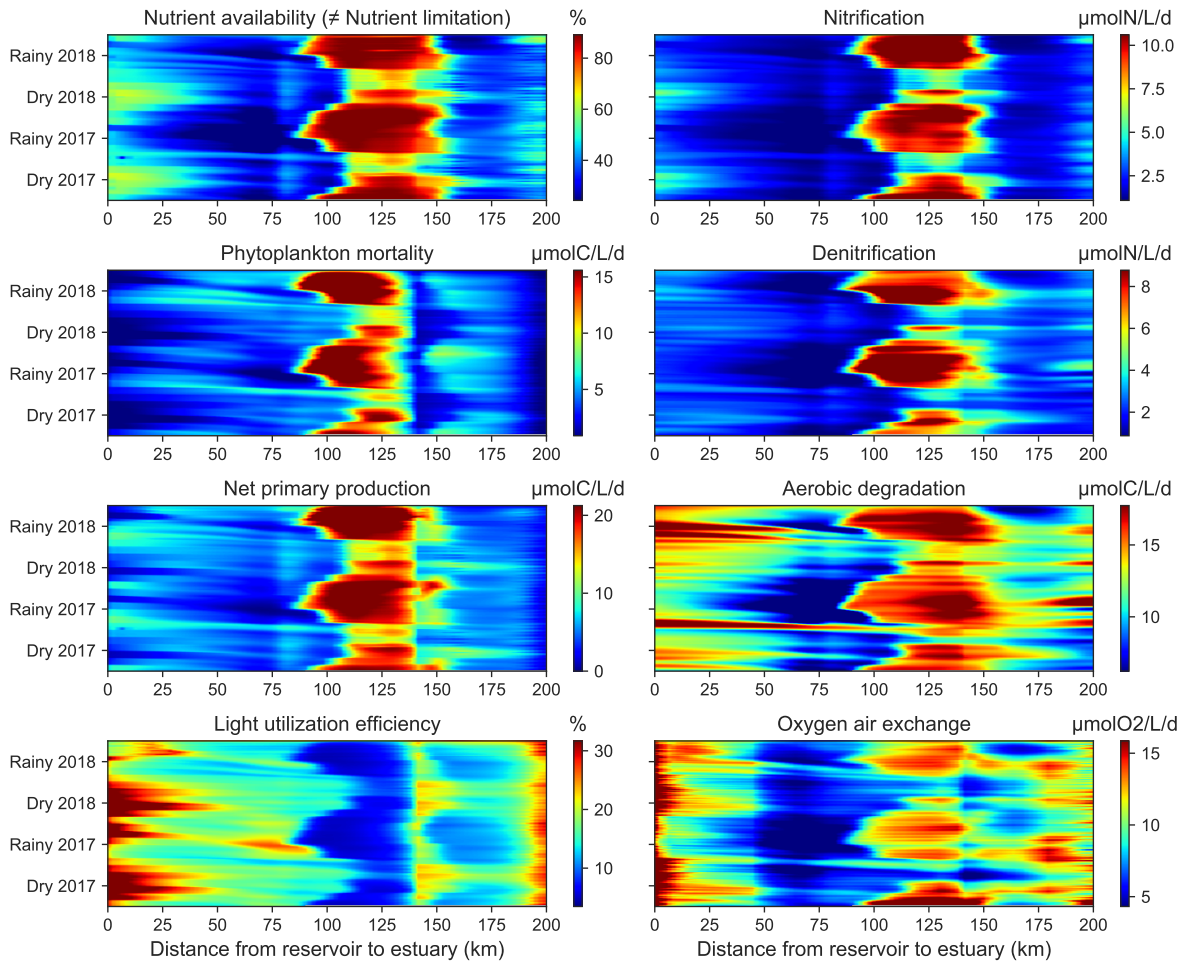


Figure 5.7: Spatio-temporal evolution of nutrient limitation and the main biogeochemical processes in dry and rainy seasons 2017-2018 along Saigon River Estuary.

significantly between seasons despite low or high flushing conditions (Costa et al., 2009). However, phytoplankton density in the rainy season is much lower than in the dry season (Costa et al., 2009). In the Saigon River, according to observations and simulations, phytoplankton bloom also only occurs in the dry season (Figure 5.5). This result contrasts the survey in the Red River Delta (subtropical estuary, Northern Vietnam). The density of phytoplankton and zooplankton in the dry season is equal to or lower than in the rainy season (Hoang et al., 2018). Hoang et al. (2018) observed that the nutrient availability is higher in the rainy season than in the dry season because of the run-off. Besides, temporal variability of phytoplankton biomass in temperate estuaries directly links to seasonal variations in light availability (Domingues et al., 2005; Lancelot & Muylaert, 2011). The light limitation is thus frequently referred to as controlling phytoplankton growth. The light utilization efficiency calculation in the urban section is the lowest compared to other sections regardless of the season. The depth of this area (about 20m) is the

5. Modeling the seasonal nutrient dynamics

main reason for phytoplankton's inefficient use of light. This finding suggests that although both upstream and downstream have higher light utilization efficiency than urban sections thanks to the shallower of the estuary (about 10m), the NPP in these two areas is still many times lower than urban sections because of nutrient limitation.

The right panels of Figure 5.7 depict the process involving oxygen concentration in the water, including nitrification, denitrification, organic carbon aerobic degradation and oxygen air exchange. C-GEM also describes strong reaction rates of these processes for the urban section of Saigon River. These processes help to explain the decrease in DO concentration under the influence of high nutrient concentrations from urban canals. Oxygen air exchange is the physical process that is most markedly different from the biogeochemical processes described at Saigon River Estuary. The transfer of oxygen from the atmosphere into the water column is particularly high in the Saigon River. From km 50 to 90, there is no significant contribution of this process compared to other areas. This is mainly due to the decrease in current velocity while the water level of this area is still relatively deep compared to about 5m in the upstream area.

5.3.4 Driving factors of phytoplankton evolution

According to a synthesis by Lancelot and Muylaert (2011), under adequate nutrient conditions in estuaries, salinity gradient, light availability, and water residence time are factors controlling phytoplankton dynamics. This statement is consistent with urbanized tropical estuaries suffering the domestic wastewater of megacities such as in the Saigon River but existing the short-term variations of phytoplankton (days to weeks) and distinct phytoplankton density between dry and rainy seasons (Figure 5.5).

The implementation of model sensitivity analysis allows understanding the mechanisms controlling the dynamics of simulated phytoplankton in the estuary (Gypens et al., 2013; Volta et al., 2014). This approach can evaluate the interaction of biogeochemical processes and hydrological conditions on phytoplankton growth. Gypens et al. (2013) proposed to assess the tidal effects on phytoplankton by setting all biological activities to zero. However, in the Saigon River Estuary, phytoplankton density downstream was very low, and there was not much impact of marine phytoplankton on the change of phytoplankton density in the urban section (A. T. Nguyen, Dao, et al., 2021). In addition, based on the nutrient limitation simulation results, the origin of phytoplankton bloom in the urban section of Saigon River is due to abundant nutrients in this area, while the upstream and downstream areas have relatively low nutrient concentrations. Therefore, we propose determining the independent effects of potential factors (e.g., biogeochemical processes, hydrodynamics, weather conditions) on phytoplankton biomass through

5. Modeling the seasonal nutrient dynamics

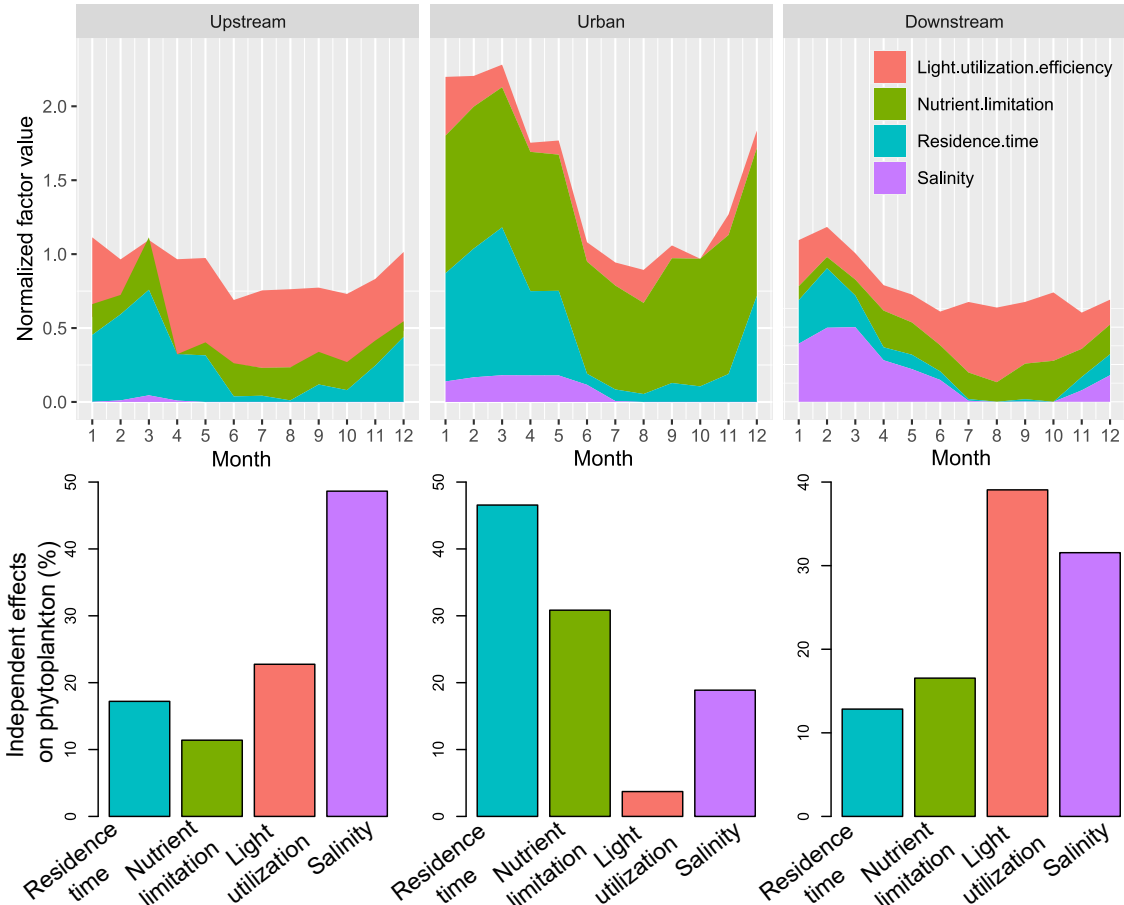


Figure 5.8: Schematic representation of the contribution of driving factors to phytoplankton bloom in the Saigon River Estuary in the dry and rainy season. The top panels are calculated based on the normalized factors in upstream, urban and downstream in 12 months. The independent effects on phytoplankton in lower panels are calculated based on the hierarchical partitioning method, calculated for each section.

the hierarchical partitioning (HP) method. The HP method effectively separated the independent effects of each environmental parameter which could not be done by regression methods (Nally, 1996). Different from the purely statistical studies in determining the driving factors to phytoplankton in tropical estuaries (e.g., A. T. Nguyen, Dao, et al. (2021) and Hoang et al. (2018)), this study uses explicit factors such as nutrient limitation, light availability, residence time, salinity from simulation to calculate their independent effects on phytoplankton development.

Figure 5.8 depicts the independent effects of four representative parameters of nutrient availability, hydrological, climatic and environmental conditions affecting phytoplankton biomass. In addition, all these parameters are normalized to compare the cooperative effects of these factors. Note that the effects of these factors on phytoplankton do not follow a linear trend but are as complex as formulas presented in Table 5.1. This approach aims to explain the significant differences in phytoplankton between the rainy and dry seasons. The sum of normalized factors in

5. Modeling the seasonal nutrient dynamics

the dry season from December to May of the following year was highest, which is reasonable for the observed and simulated phytoplankton in this period. Specifically, nutrient limitation and residence time have the greatest impact on phytoplankton. The nutrient limitation does not significantly differ between the two seasons, while residence time had a marked difference. At upstream and downstream, salinity and light utilization factors are dominant and differ to urban section. This is consistent with the shallow water with more light diffusion upstream. The upstream salinity contribution probably describes the sensitivity of freshwater phytoplankton to saltwater. However, this area is rarely subject to a high rate of saline intrusion.

In the urban section, the results of hierarchical partitioning analysis also show that residence time is the key factor that has the greatest impact on the fluctuation of phytoplankton. This result is similar to the output of a simple box model applied in the Gulf of Thailand, where widespread strong hypoxia and phytoplankton bloom over half of the gulf was observed during the dry season with a residence time of about 40 days. In the rainy season, the residence time was only about three days and strongly flushed pollutants into the sea and improved oxygen levels (Buranapratheprat et al., 2021). in the Saigon River Estuary, the residence time is about 20 days in the rainy season and 120 days in the dry season (Figure 5.4), creating higher phytoplankton densities. This result contradicts the observation in a subtropical estuary, Red River Delta (Vietnam), as discussed previously (Hoang et al., 2018). This estuary also receives high nutrient concentrations from domestic wastewater of about 8 million inhabitants (only 20% are treated) in Hanoi City. The nutrient limitation is the cause of this difference. While nutrient availability tends to remain stable during the entire year in the Saigon River (T. T. N. Nguyen et al., 2019), it increases in the Red River (Hoang et al., 2018). Therefore, the residence time has become a key factor for the development of phytoplankton at Saigon River Estuary.

5.4 Conclusion

The application of C-GEM in characterizing changes in nutrient and phytoplankton concentrations has allowed understanding the mechanisms leading to fluctuations in water quality at Saigon River Estuary. Compared with the steady-state C-GEM version, which only described the spatial variation in the dry season, this study reproduces the distinct phytoplankton biomass between the two seasons, which is questionable for many tropical estuaries. The addition of the PO_4^{3-} sorption module has reduced the overestimation of PO_4^{3-} simulation, but the complexity of the sediment dynamics in downstream causes several unexpected behaviours. The model extensively described biogeochemical processes to determine their role in responding to the megacity's domestic wastewater. Nitrification, denitrification, organic carbon degradation, and primary production occurred strongly in the urban

5. Modeling the seasonal nutrient dynamics

section of Saigon River Estuary. Simulation results for two years showed that nutrient availability in the urban section was abundant for phytoplankton growth in both seasons. By applying multivariate data analysis for simulated results, the significant contribution of residence time to the difference in phytoplankton density is exposed. This study confirms the potential of C-GEM in using a minimal amount of input data while providing essential information for eutrophication management. Applying this model in tropical estuaries in emerging countries will be particularly useful in supporting the assessment of the effectiveness of reducing nutrient pollution through the construction of wastewater treatment plants such as in Ho Chi Minh City.

5.5 Conclusion of Chapter 5

Questions about biogeochemical functioning and hydrological impact on nutrients and phytoplankton dynamics at an urbanized tropical estuary are answered in Chapters 4 and 5. The current version of C-GEM application in the Saigon River is now suitable for assessing the several scenarios of HCMC in the future. The next chapter will present the results of water quality simulation according to the development of this megacity. The risk of future eutrophication is thus discussed to recommend additional solutions to meet the region's sustainable development.

6

Eutrophication assessment in an urbanized estuary based on past, present and future nutrient loadings: A modeling approach

Contents

6.1	Introduction	176
6.1.1	Risk of eutrophication in coastal megacities	176
6.1.2	Ho Chi Minh Megacity, Vietnam	177
6.1.3	Tools for eutrophication management	178
6.2	Materials and methods	179
6.2.1	Study area	179
6.2.2	Urban canals and WWTPs	181
6.2.3	Nutrient loadings from urban canals	181
6.2.4	Description of scenarios	184
6.2.5	Model validation	186
6.3	Results and discussion	188
6.3.1	Responses of the tropical estuary to nutrient loadings	188
6.3.2	Role of WWTPs in eutrophication management	192
6.4	Conclusion	193
6.5	Conclusion of Chapter 6	194

In the context of densification of urban centers and climate change, coastal megacities in emerging countries have to face new issues about water management. With more than 9 million inhabitants, Ho Chi Minh City (HCMC), the economic capital of Vietnam, is in full demographic and economic expansion. The city does not have water treatment networks that meet urgent needs. Indeed, in 2020, less than 15% of the population is connected to a sewerage network and treatment plant. The

6. Eutrophication assessment

deterioration of the water quality of the Saigon River crossing the city is dramatic. Therefore, Ho Chi Minh City authorities plan to build new sanitation networks and ten new wastewater treatment plants (WWTPs) over the next fifteen years, drawing inspiration from industrialized countries' centralized water management models. However, the relevance of this extremely expensive choice arises and is not necessarily adapted to the particular conditions of this megacity in tropical monsoon zone and under the influence of tidal cycles. Assessing the assimilative pollutant capacity of the Saigon River and the requirement of wastewater treatment capacity is extremely complex at tidal estuaries. The significant difference in eutrophication risk between the dry and rainy seasons was observed in the Saigon River Estuary under the variation condition of hydrology, climate, and urban discharge (Chapter 4, 6). Using the estuarine biogeochemical model (C-GEM), this study aims at assessing the water quality and eutrophication of the Saigon River in response to four scenarios of HCMC development from the past to the future (the 2000s to 2050). The scenarios are implemented based on population growth, new water management infrastructures in HCMC and projected climatic conditions (temperature, hydrology) in the next decades. The results of four scenarios show that the construction of new WWTPs is supported. However, the rapid population growth in HCMC may overcome the WWTPs' capacity, which returns the water quality in the Saigon River to bad condition.

Chapter 6 uses the information presented in the conference proceedings:

Nguyen, Truong An, et al. "Evaluating the response of water quality to pollutant loading in the Saigon River system (Vietnam): modelling scenarios by C-GEM, an estuarine biogeochemical model." Water, Megacities and Global Change. 2020.

6.1 Introduction

6.1.1 Risk of eutrophication in coastal megacities

Accounting for more than 10% of the world's population, megacities have been attracting people and increasing population densities themselves. Around 70% of the megacities are distributed along estuaries and coastal areas known to provide numerous ecosystem services for the development of the surrounding region (GRID-Arendal and UNEP, 2016; von Glasow et al., 2013). Estuaries are also considered a high self-purification system, with the ability of transformation or pollutant removal (Wilk et al., 2018). However, the rapid population growth coupled with the lack of investment in water environmental protection in the megacities of the developing countries threatens the safety of water resources (Choudhury & Pal, 2010). In the 21st century, water pollution from megacities is well known in Southeast Asia countries (Choudhury & Pal, 2010; Tran Ngoc et al., 2016). According to Hoonrweg & Pope, 2014, the rate of population growth and the formation of

6. Eutrophication assessment

megacities by 2050 will be dominated by countries in Asia in tropical regions. Comparing the nutrients export between 2000 and 2050 projection shows that the total amount of nitrogen exported by rivers to the sea in South Asia will be many times higher than in other regions such as Europe, North America, Africa, Australia (Lee et al., 2016). The rapid development of agriculture, industry, and urbanization of emerging countries will significantly increase the nutrients loading into the estuaries and, ultimately, the ocean. This indicates that the pressures of population growth and urbanization for tropical estuaries in emerging countries will intensify in the future. Facing the threat of water safety, these megacities have been implementing environmental rehabilitation projects, particularly the construction of municipal wastewater treatment plants (WWTPs) (Sajor & Thu, 2009; Tran Ngoc et al., 2016).

6.1.2 Ho Chi Minh Megacity, Vietnam

Located in Vietnam's most rapid urbanization area, Saigon River Estuary (Southern Vietnam) has been affected by urban wastewater from Ho Chi Minh City (HCMC) for many years. Canals in HCMC and the Saigon River received about 90% of untreated domestic wastewater in 2016 (T. T. Nguyen et al., 2020). The high polluted loads regularly lead to an excess of nutrients and an intense period of anoxia in the Saigon River, especially during the dry season in the Saigon River (T. T. N. Nguyen et al., 2019). Water pollution also threatens water production for the region. Over 90% of the water supply used in HCMC is taken from two raw water collection stations on the Saigon River and Dongnai River (Tran Ngoc et al., 2016). Under the impact of tides from the East Sea of Vietnam, some water production stations have to shut down several times because of saline intrusion and polluted water from the inner city of HCMC in the Saigon River (Le et al., 2012). The risk of estuarine pollution in the Saigon River is expected to increase in the coming years, under the impact of megacity's development. Following the actual trend, the population of HCMC is expected to reach 23 million by 2050, and the Saigon River will then receive three times more pollution (T. T. Nguyen et al., 2020). In response to the current and future major sources of urban wastewater, the HCMC is implementing an ambitious environmental sanitation project for the urban canals and Saigon River, i.e., more than ten WWTPs to treat about 80% of domestic wastewater in HCMC by 2025. However, because of the huge cost of the project (about 2 billion USD), most of WWTPs are still in stage of calling for capital investments. In this context of rapid changes in pollutant loadings to the Saigon River Estuary (i.e., new WWTPs, increased population), the use of models capable of describing the biogeochemical functioning of aquatic ecosystems and simulating the potential impact of improved urban water treatment is crucial.

6. Eutrophication assessment

6.1.3 Tools for eutrophication management

Managing estuaries involves managing human activities, which involve complex socio-economic-political issues (Atkins et al., 2011). As a result, the management of estuaries and coasts has a long track record of a few successes and many failures. According to Wolanski and Elliott (2014), the essence the anthropogenic problems come from three sources: (1) materials that are put into the estuaries, (2) materials taken out from the estuaries, and (3) wider problems such as climate change. The failure to control “materials that are put into the estuaries” clearly lacks a balance between wastewater volume and wastewater treatment capacity. In addition, there is the effect of a lack of control of products with a high risk of eutrophication. The failure to quantify the “materials taken out from the estuaries” is due to the lack of intensive monitoring and biogeochemical model application that allows the calculation of retention capacity and transformation of nutrients.

In tropical estuaries, phytoplankton blooms and eutrophication risk often experience short-term variation (hours to days) and long-term variation (months to seasons) depending on hydrology, climate, and the duration of anthropogenic nutrient loading (Livingston, 2000). To understand the level of eutrophication and the water quality of urbanized estuaries, it is necessary to consider the aspect of nutrient loadings (i.e., control of waste sources) and consider other aspects such as season, climate and tidal effects. Chapter 5 exposed the importance of nutrient limitation and residence time of water body to phytoplankton growth in a tropical estuary. The accurate assessment of several nutrient loadings scenarios on water quality is thus required an estuarine biogeochemical model to describe transient variations, seasonal effects of estuaries.

Applying biogeochemical models in developing scenarios in urbanized tropical estuaries is not as widespread as in developed countries. Some lessons on applying the model in assessing pollution scenarios in urbanized tropical estuaries are as prominent as in Bay of Santa Catarina in Brazil (Cabral & Fonseca, 2019), Shenzhen Bay in China (Zhou et al., 2020). Shenzhen Bay is an urbanized estuary heavily influenced by anthropogenic activities, which have influenced eutrophication since the 1990s. Therefore, the government has developed and applied several scenarios to alleviate water degradation and improve coastal ecosystems. The survey results and nutrient limitation simulation show that eutrophication in Shenzhen Bay was limited by phosphorus; the government thus decided to improve the effectiveness of WWTP to reduce phosphorus first to alleviate the serious aquatic situation immediately. The results show that since 2005 the trophic status at this bay has improved, and then the several practices to reduce the nitrogen concentration and keep Shenzhen Bay water quality in good condition as currently (Zhou et al., 2020). At the Bay of Santa Catarina, based on over 30 years of monitoring results and a simple model of eutrophication evaluation, this urbanized estuary

6. Eutrophication assessment

is susceptible to eutrophication due to domestic wastewater. Modeling results show that trophic status ranges from moderate to eutrophic in this bay. The main cause of the eutrophication of this area was the low rate of domestic wastewater treatment (27%) and the treatment technology of WWTPs, which only removes 20-50% of nitrogen while nitrogen is the limiting factor for eutrophication in this system. The results of this study suggest that improving WWTPs technology and expanding capacity will be an effective solution in eutrophication management (Cabral et al., 2020). Overall, these two examples show that upgrading WWTPs is inevitable to ensure the water security of urbanized estuaries. In addition, identification of the controlling factors that affect eutrophication through estuarine modeling is necessary.

The Carbon Generic Estuarine Model (C-GEM) is a generic one-dimensional, reaction-transport model which takes advantage of the relationship between estuarine geometry and hydrodynamics to minimize data requirements (Volta et al., 2014). C-GEM has provided accurate descriptions of estuarine hydrodynamics and biogeochemical transformations in several estuaries, especially in temperate regions (G. G. Laruelle et al., 2009; G. Laruelle et al., 2017; Volta, Laruelle, & Regnier, 2016; Volta et al., 2014). The model allows the assessment of the estuary response to the simultaneous effects of point sources (e.g., domestic, industrial wastewater) and the effects of the estuary tidal regime (Volta et al., 2014). This modeling approach is particularly relevant to the urban estuary of developing countries where there is a limited extensive monitoring program. This study aims to evaluate the water quality in the Saigon River Estuary under the impact of urban wastewater from HCMC's development by C-GEM application. The research results allow us to evaluate the efficiency of the construction of WWTPs according to the direction of HCMC's development.

6.2 Materials and methods

6.2.1 Study area

The Saigon River catchment with 4717 km^2 is located in Southern Vietnam. The whole Saigon River has a length of 280 km within Vietnam. The river originates in Cambodia and is firstly controlled at Dau Tieng Reservoir (270 km^2 and $1580 \times 106 \text{ m}^3$), designed for ood and saline intrusion control, irrigation, domestic, agricultural and industrial demands (Ngoc, Hiramatsu and Harada, 2014). From Dau Tieng Reservoir to the estuarine mouth (200 km), the Saigon River (net discharge $18 \pm 14 \text{ m}^3 \text{ s}^{-1}$) in turn joins notable tributaries such as the Thi Tinh River (TT River, $20 \pm 11 \text{ m}^3 \text{ s}^{-1}$) and the Dongnai River ($632 \pm 446 \text{ m}^3 \text{ s}^{-1}$), forming Nha Be River, it then splits into two distributaries (Soai Rap River and Long Tau River) flowing into East Sea of Vietnam (Figure 6.1). In addition, the Saigon River is also

6. Eutrophication assessment

connected to an urban river (Vam Thuat River, $4 \text{ m}^3 \text{ s}^{-1}$) and three urban canals (total net discharge, $5.5 \text{ m}^3 \text{ s}^{-1}$) of HCMC before the confluence with Dongnai River (T. T. Nguyen et al., 2020). The typical climate of this region is tropical monsoon which has two distinct seasons (dry and rainy seasons), with a relatively constant temperature (about 28°C). The rainy season lasts from June to November, with an average annual rainfall of 1800 mm, of which 80% fall in the rainy season (Nguyen et al., 2019). The status of water quality in the Saigon Estuary River is spatially different. Upstream and downstream of the estuary, water quality status is considered good. The quality status of the water became moderate to bad right after connecting with the Vam Thuat River (an urban river) and urban canals of HCMC (T. T. N. Nguyen et al., 2019).

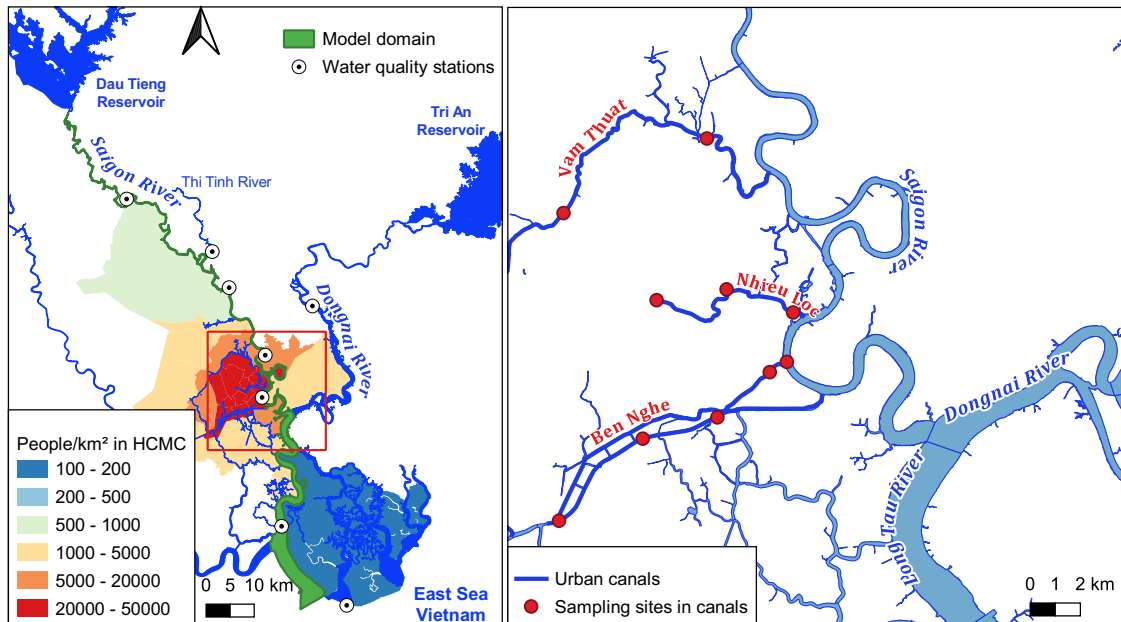


Figure 6.1: Map of Saigon River Estuary, monitoring stations and HCMC population density in 2019.

Ho Chi Minh City's development is intrinsically linked with the Saigon River. This megacity's economy has developed considerably over the last decades, and HCMC was the third most dynamic city in the world in 2020, followed by Hyderabad and Bengaluru, India (City Momentum Index, 2020). In 2015, the Department of Natural Resources and Environment reported that land use in HCMC is dominated by agricultural activities in the north (41% of HCMC's area), an urban settlement in the center (23%) and mangrove forest to the south (26%). The population growth rate in Ho Chi Minh City is about 3.48% per year (Ho Chi Minh City Statistical Yearbook, 2017), leading to the city has the highest population density in Vietnam. However, the development of water treatment systems is not in line with that population growth. In the early 2000s, HCMC discharged about $532000 \text{ m}^3 \text{ d}^{-1}$ domestic wastewater of about 6 million inhabitants (80130 liters

6. Eutrophication assessment

per capita per day) and $51300\ m^3 d^{-1}$ industrial wastewater of 18 industrial parks mainly untreated (Le *et al.*, 2012).

Consequently, most water quality variables exceeded Vietnamese surface water quality standards (QCVN 08:2015/BTNMT). In addition, the influence of tides causes saline intrusion and pollutant transport from an urban area to the upstream area. This caused a temporary shutdown of drinking water treatment plants in the dry season in 2004 and 2005 (Le *et al.*, 2012).

6.2.2 Urban canals and WWTPs

Figure 6.1 depicts the canal systems in HCMC with the main canals of Tham Luong Canal- Vam Thuat River, Nhieu Loc - Thi Nghe canal, Ben Nghe canal. These canals systems were built in the late 19th century during the French colonial period. Until now, domestic water and rainwater have been collected and transported together by the sewer system and by urban canals and creeks (Tran Ngoc *et al.*, 2016).

Before 2006, all domestic wastewater was discharged directly into canals and the Saigon River. The current WWTPs system in Ho Chi Minh City still does not meet the total domestic wastewater volume of about nine million people (about $2.5\ \text{million} m^3 d^{-1}$, in 2020). Therefore, most domestic wastewater is discharged into the canal system of HCMC, with 12% treated wastewater in 2021 (Figure 6.2). Since 2010, the Vietnamese government has called for the construction of 12 WWTPs to treat about $3\ \text{million} m^3 d^{-1}$ by 2025 (Vietnam Prime Ministerial Decision Jan. 2010, n24/Q-TTg). However, there are currently only three WWTPs in operation; one WWTP is under construction, while other WWTPs are still in the fundraising stage. The total estimated cost is over 2 billion USD for the remaining WWTPs. Therefore, we estimate that in 2025 HCMC can treat about $780,000\ m^3 d^{-1}$, equivalent to 27% of the total wastewater volume of about 2.8 million people. By 2050, WWTPs in HCMC may treat $3,000,000\ m^3 d^{-1}$, equivalent to 54% of the wastewater of about 16 million people (Figure 6.2).

6.2.3 Nutrient loadings from urban canals

Chapter 5 described that phytoplankton blooms could only exist in the urban section (about 50 km of the 200 km length of the river) of the Saigon River. Nutrient limitations upstream and downstream have limited the growth of phytoplankton, and the water quality of these two areas is assessed as good. Therefore, the scenarios for the Saigon River water quality mainly focus on the urban section affected by domestic wastewater of HCMC. More specifically, the quality of wastewater from urban canals is a decisive influence on the water quality of the Saigon River. Correctly determining the quality of the input data applied in the model will ensure the simulation results' meaning.

6. Eutrophication assessment

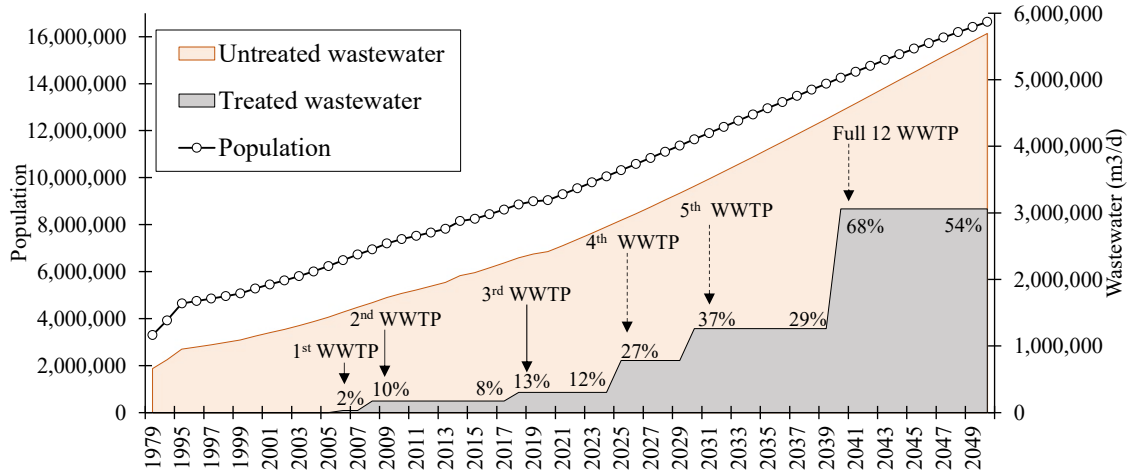


Figure 6.2: Population in HCMC from 1979 to 2020, predicted to 2050, and WWTP capacity. Population data from 1979 to 2019 is from GSO Vietnam; prediction population is based on UN World Urbanization Prospects with a growth rate of 2.7% in 2020 and 1.3% in 2050. Total domestic wastewater discharge is calculated based on water consumption per capita

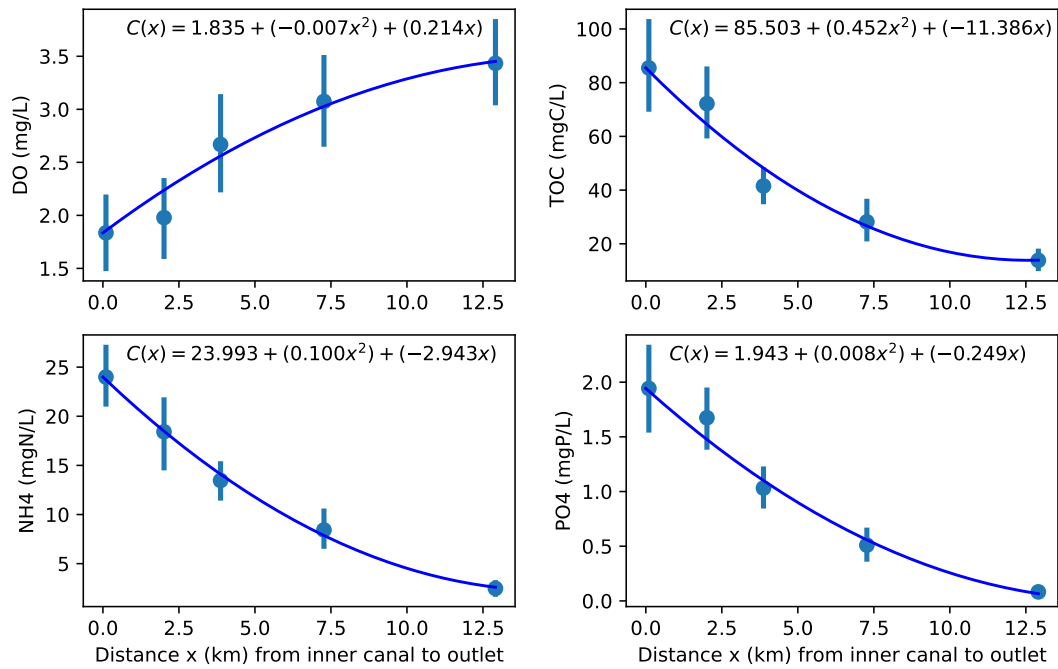


Figure 6.3: The nutrients concentration along canal axis based on parabola best-fit equation. The concentration is a function of distance, with the initial concentration at pollutant sources is. The blue points with standard deviation are observed data of 5 sampling sites in Ben Nghe canal in 2014-2017.

The data used in this study are mainly from the Vietnam Center of Environmental Monitoring (CEM, Vietnam) and Center Asiatique de Recherche sur l'Eau (CARE). The monitoring program of these two centers has been detailed in

6. Eutrophication assessment

previous chapters. In this section, CEM monitoring program is repeated to explain the calculation method to supplement data used for simulations in the past period without sufficient monitoring data.

The monitoring program by CEM, Vietnam, started in the 2000s and was almost completed in 2012 with the addition of many monitoring sites along the river and at the canal systems of HCMC. The data of the 2000s only allowed to assess the water quality at a few monitoring points along the Saigon River while the water quality of the canals was not monitored in routine. Since 2014, the canal monitoring has been improved with more complete sampling sites with monthly measurements. Therefore, it is difficult to quantify the impact of urban discharge with very sparse data in the 2000s. However, 2014-2017 allows one to estimate the retention capacity of the nutrient pollutants in the canals. The use of nutrient retention capacity at canals can be applied to calculate nutrients of past and future scenarios. Figure 6.3 shows the gradual decrease in average concentrations of NH_4^+ , PO_4^{3-} from the inner city to the outlet of the canals where the Saigon River is received. This study considers retention capacity in urban canals to transform, remove pollutants in the water column, and retain pollutants in the sediment (burial process). Besides, the dilution capacity of the Saigon River and during flooding tides, nutrient concentrations in the canals gradually decrease over the distance. Therefore, in the absence of data, nutrient concentrations were calculated according to nutrient emission per capita, and the parabola best-fit equation was applied to estimate the concentration of nutrients entering the Saigon River. According to the synthesis of Nguyen et al., 2020, the nutrient emission per capita human in HCMC is about $11 \text{ gN/capita } d^{-1}$ and $2.4 \text{ gP/capita } d^{-1}$ with water use of $150L \text{ } d^{-1}/\text{capita}$. This estimate allows estimating the concentration of TN and TP in domestic wastewater in HCMC. However, C-GEM model needs to declare the concentrations of NH_4^+ and PO_4^{3-} at the outlet of urban canals. Based on the Japan International Cooperation Agency (JICA) report in 2020 on the quality of inlet and outlet wastewater of WWTPs in HCMC, the NH_4^+/TN and $\text{PO}_4^{3-}/\text{TP}$ ratios are estimated. Finally, nutrient concentrations at the urban outlet were calculated using the parabola best-fit equation as a function of canal distance (Figure 6.3). These parabola best-fit equations were set up based on the non-linear least squares to fit the estimated and observed data. To simplify the determination of the nutrient retention capacity of canals, we hypothesized that the parabola equations already include processes such as transformation, removal and burial of nutrients according to the distance from the pollutant source. Since 2008, the sludges in urban canals have been regularly dredged to remove pollutants and improve water quality. Therefore, the parabola best-fit equations are suitable for the condition after 2008. Before 2008, nutrient retention capacity is estimated to be about 50% smaller.

6. Eutrophication assessment

6.2.4 Description of scenarios

The calibrated and validated C-GEM model was used to evaluate the responses of the Saigon River Estuary under the impact of changes in nutrient loadings from the 2000s to 2050 according to HCMC's development plan and projections of climate change in 2050. The four scenarios in turn were tested by the C-GEM model are presented in Table 6.1.

These scenarios were based on plans to develop WWTPs in HCMC and forecasts of temperature and sea level rise in the Saigon River (MONRE et al., 2016). The number of WWTPs and their capacity were after the decision n24/QD-TTg approved by the Prime Minister of Vietnam on January 6th, 2010. Under this plan, a total of 12 WWTPs will ensure efficient domestic wastewater treatment for 12 basins in HCMC. Four scenarios (2005, 2015, 2025, 2050) allow predicting the effect of WWTPs on water quality in the Saigon Estuary under the impact of increased waste loads (population growth in HCMC). Therefore, the model parameters in all three scenarios remain the same except for the wastewater source from urban discharge and climate parameters for the year 2050.

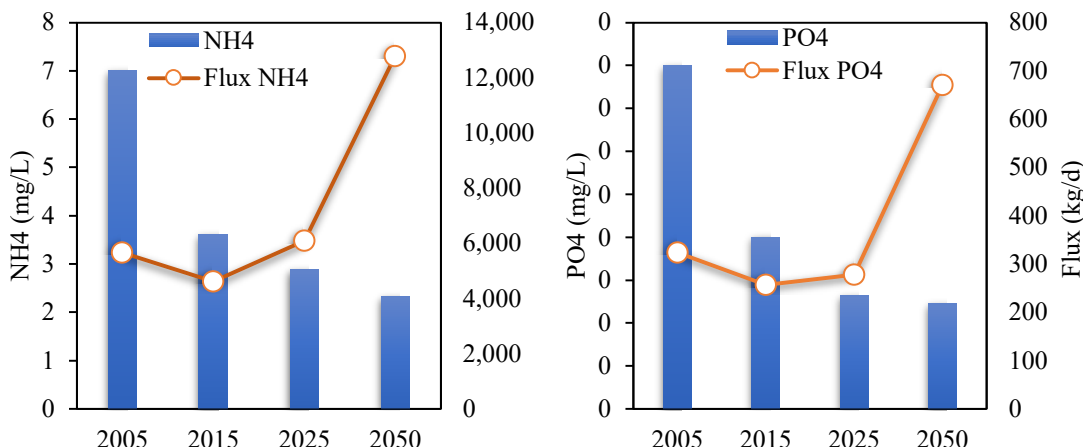


Figure 6.4: The NH_4^+ , PO_4^{3-} concentrations and fluxes at the outlet of canals. The nutrient concentrations are calculated based on the nutrient emission per capita and then applied the parabola best-fit equation to get the concentration at the outlet of the canals.

Scenario 1: Without WWTPs in 2005.

This period represents the 2000s when HCMC did not have WWTPs. All domestic wastewater was discharged directly into the canal system in this period. The simulation during this period allows us to assess the pollution level of the Saigon River in extreme conditions. The nutrient concentration in canals was higher than the recommended concentration threshold for surface water quality (QCVN 08: 2015/BTNMT, National technical regulation on surface water quality). $\{\text{NH}_4^+\}$ and PO_4^{3-} in 2005 were $7.0 \text{ mgNH}_4^+ L^{-1}$ and $0.4 \text{ mgPO}_4^{3-} L^{-1}$, respectively. Based on QCVN 08: 2015/BTNMT, the nutrient concentrations were

6. Eutrophication assessment

many times higher than the recommended concentrations for domestic usage of 0.3 mg L⁻¹ NH₄⁺ and 0.2 mg L⁻¹ PO₄³⁻, respectively. The input PO₄³⁻ concentration was about 4.0 mg L⁻¹. However, most of the PO₄³⁻ was retained in the canal before being discharged into the Saigon River. Meanwhile, NH₄⁺ did not have a high retention efficiency in the canal as PO₄³⁻, leading to a much higher NH₄⁺ concentration.

Scenario 2: With two WWTPs in 2015.

This scenario represents the present condition of Saigon River Estuary, with the complete data to validate the model. C-GEM uses the average data of the dry and rainy season from 2014 to 2017 to calibrate some parameters in biogeochemical module and evaluate the effectiveness of the model. This period also marks HCMC's efforts when two WWTPs effectively treat about 10% of urban wastewater.

Scenario 3: With four WWTPs in 2025 and an increase in the population.

This scenario aims to evaluate the effectiveness of the two new WWTPs according to the current WWTP construction ability. The HCMC government aimed to achieve 12 WWTPs by 2025 to treat 80% of domestic wastewater. However, we believe that only four WWTPs can be achieved in this period because the remaining WWTPs are still in the fundraising stage. In addition, during this period, a temperature increase of 0.5°C is also applied to represent the effects of global warming on sea temperature in southern Vietnam (Vietnam Ministry of Natural Resources and Environment – MONRE, 2016).

Scenario 4: With twelve WWTPs in 2050, increasing population and climate change.

By 2050, the population of the HCMC is forecasted to increase almost three times compared to the population in the 2000s. The remaining WWTPs have been in the capital raising phase, including the socialization of investment from 2018. The proportion of domestic wastewater connected to 12 WWTPs can be 54% in 2050. C-GEM model has also adjusted parameters related to the impact of climate change. Tidal amplitude can be determined to increase by about 20 mm by 2050 (Bindoff et al., 2016) . In addition, MONRE et al., 2016 suggested that the surface temperature of the seawater of Southern Vietnam can be increased to 1.5°C by 2050 (MONRE, 2016). An increase in temperature can contribute to the increased activity of biogeochemical processes in the estuary.

6. Eutrophication assessment

Scenarios	2005	2015	2025	2050
Population ^a (inhabitant)	6,200,000	8,400,000	10,300,000	16,600,000
Number of WWTPs ^b	0	2	4	12
WWTPs treatment capacity ($m^3 d^{-1}$) ^b	0	171 000	1,253,000	2,813,000
Population connected to WWTPs (%) ^c	0%	10%	27%	54%
NH_4^+ flux from canals to river ($kg Nd^{-1}$) ^d	5,670	4,611	6,100	12,780
PO_4^{3-} flux from canals to river ($kg Pd^{-1}$) ^d	324	256	278	671
TOC flux from canals to river ($kg Cd^{-1}$) ^d	24,300	15,114	20,410	43,830
Temperature ($^{\circ}C$) ^e	28	28	28+0.5 ^e	28+1.5 ^e
Tidal range (m) ^f	2.80	2.80	2.80	2.80 + 0.2 ^f
Freshwater inflow in dry and rainy season ($m^3 s^{-1}$) ^g	28 & 120	28 & 120	28 & 120	28 & 120

^a Based on calculation of UN World Urbanization Prospects for population growth rate in HCMC which are 2.7% in 2020 and decrease to 1.3% in 2050.

^b Planning of the building of new WWTPs from (Tran Ngoc *et al.*, 2016).

^c Percentage of the population connected to WWTPs is equal to WWTPs volume capacity divided by the total water consumption (200 liters/capita/day).

^d Total flux of treated wastewater and untreated wastewater. The treated flux was calculated based on removal efficiency, 40–50% of TN, TP and 85% of TOC in the conventional active sludge treatment process from Metcalf and Eddy/AECOM, 2014 for the WWTP outlet. The untreated flux was calculated based on the nutrient emission per capita from Nguyen *et al.*, 2020.

^e Increase in sea surface temperature of 1.5°C by 2050 under RCP8.5 scenario, adapted for HCMC (MONRE *et al.*, 2016).

^f Increase of tidal amplitudes by 2050 (Bindoff *et al.*, 2019).

^g The upstream boundary condition discharge Dau Tieng Reservoir is maintained for all three scenarios. The increase in water demand in HCMC in the future will be addressed by increasing additional water sources mainly from Dongnai River (net discharge 613 $m^3 s^{-1}$) (Tran Ngoc *et al.*, 2016).

Table 6.1: Four scenarios for C-GEM application in Saigon River Estuary

6.2.5 Model validation

C-GEM is a one-dimensional, reactive transport model. This model was developed to minimize the data required while ensuring the accurate description of estuarine hydrodynamics, salt transport and biogeochemistry (Volta *et al.*, 2014). Three main modules of C-GEM (geometry, hydrodynamics, and transport - reaction modules) were implemented following the set-up protocol proposed by Volta *et al.* (2014). The hydrodynamic module was solved by using a finite difference scheme applied along a one-dimensional grid, with a grid size of 2000 m and an integration time step of 300 seconds. Transport-biogeochemical reaction module was solved by the operator-splitting method within a single time step (Regnier *et al.*, 1997). The application of C-GEM in the Saigon River Estuary required a spin-up of 180 days

6. Eutrophication assessment

to reach a steady-state condition. The C-GEM version in this study was adapted from the transient version of Volta, Laruelle, Arndt, and Regnier (2016) to simulate the water quality along 200 km of Saigon River Estuary.

This study applies a transient version of C-GEM (Chapter 5) to describe the spatial variation between dry and rainy seasons. The description of the model is detailed in Chapter 2 – Methods and Materials.

The current version of C-GEM in this study can simulate the concentrations of eight state variables, namely ammonium (NH_4^+), nitrate (NO_3^-), phosphate (PO_4^{3-}), total organic carbon (TOC), Silica (DSi), dissolved oxygen (DO), phytoplankton (diatoms and non-diatoms) and Total Suspended Solid (TSS). Seven biogeochemical processes are considered in C-GEM, including oxygen exchange, aerobic degradation (organic carbon mineralization), nitrification, denitrification, primary production, phytoplankton mortality and TSS erosion/deposition. The rate constants of these processes were adjusted in the limit of their values from experimental or literature determination based on 49 estuarine biogeochemical model applications (Volta, Laruelle, Arndt, & Regnier, 2016).

Water quality data to calibrate biogeochemical parameters were obtained from bi-weekly monitoring data of Center of Environment Monitoring (CEM, Vietnam) and Center Asiatique de Recherche sur l'Eau (CARE, Vietnam) from 2014 - 2017. The sampling and analytical methods were described by Nguyen et al. (2020). Most of the observed data were BOD5 but not the TOC. However, there were three stations (at km 88, 130 and 156) where we measured BOD5 and TOC. Therefore, TOC used in the model was the converted BOD5 concentrations using a relationship equation.

The water quality simulation results were compared with monitoring data of 13 stations along Saigon River Estuary in the dry and rainy seasons 2016 - 2017 (Figure 6.5). Although the current C-GEM model allows for the simulation of eight environmental variables, only four (DO, TOC, NH_4^+ , PO_4^{3-}) are discussed in this study because they are of particular interest for the municipal WWTPs construction plan in HCMC. In addition, the two monitoring programs of CARE and CEM provided the complete data sets of these variables for the calibration and validation process in C-GEM. Statistical analysis for model performance shows that the simulation results and observation data of 13 monitoring stations have a coefficient correlation (R^2) from 0.6 to 0.9; the percentage bias is less than 20% for most of the variables (except PO_4^{3-}). PO_4^{3-} simulation has a percent bias of 37% (0.02 mgPL^{-1}), which is just equivalent to the experimental error of PO_4^{3-} (0.01 mgPL^{-1} , standard colorimetric methods). These simulation results show that C-GEM model has a good ability to simulate water quality at Saigon River. In addition, C-GEM allows determining the intensity of biogeochemical processes such as nitrification, organic carbon aerobic degradation affecting the concentration of these environmental parameters. Nitrification is the process with

6. Eutrophication assessment

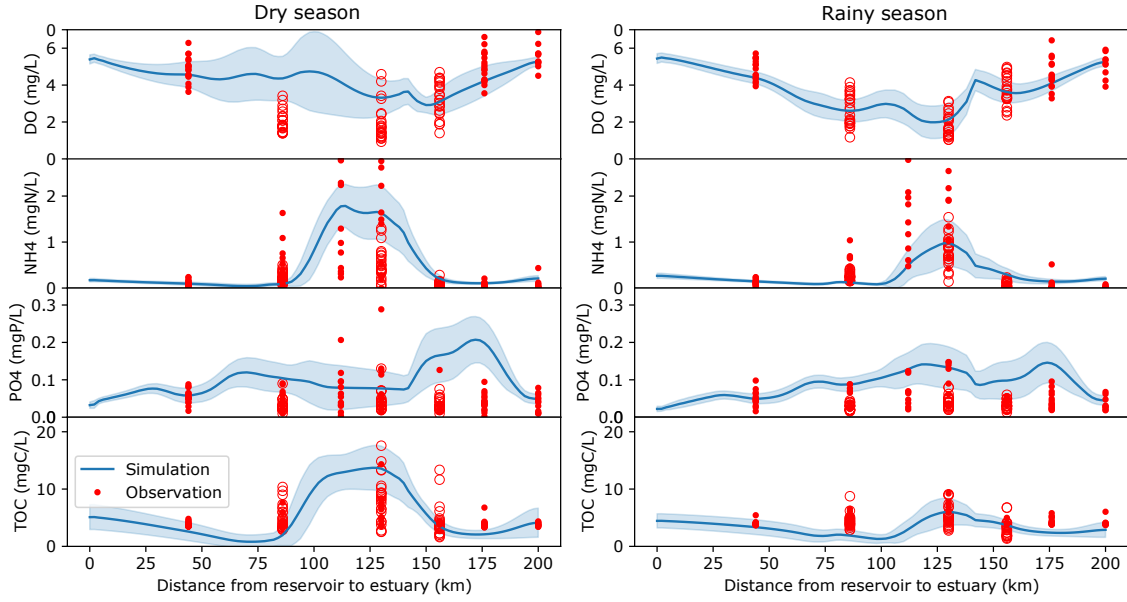


Figure 6.5: Comparison of observed and simulated water quality variables along Saigon River Estuary.

the largest consumption of dissolved oxygen in the Saigon River when it receives a high concentration of NH_4^+ from urban canal discharge (results are not shown in this study).

6.3 Results and discussion

6.3.1 Responses of the tropical estuary to nutrient loadings

Figure 6.6 depicts the simulation results of water quality at the Estuary Saigon River under the four scenarios driven by the construction of WWTPs in HCMC. In general, the simulations show significant efficiency in the construction of WWTPs, especially for NH_4^+ and TOC. According to QCVN 08:2015/BTNMT, river water quality in Vietnam can be classified into four groups according to different concentration ranges. The river water quality is assessed as “very good” (grade A1) suitable for domestic use, aquatic life. “Good” (grade A2) can be used for domestic use but requires appropriate water treatment. “Moderate” (grade B1) and “Bad” (grade B2) are respectively used for irrigation and transport purposes.

In upstream, from km 0 to km 80, simulation results are almost unchanged for all environmental parameters, which is explained by the lack of input changes in this area (see vertical lines in Figure 6.6 for the location of external inputs). However, there is a significant decrease of the phytoplankton concentration in upstream which may be almost zero. This difference comes from the increase in temperature in the two scenarios, 2025 and 2050. Phytoplankton mortality in

6. Eutrophication assessment

the C-GEM model is a function of temperature. While nutrient limitation prevails upstream (Chapter 5), an increase in temperature leads to phytoplankton depletion due to increased phytoplankton mortality.

In the urban section, from km 80 to km 150, this area is adversely affected by domestic wastewater from HCMC. All scenarios have clear differences in the concentrations of environmental variables in this area, especially DO, NH_4^+ , Chl-a. Indeed, as forecasted by MONRE, the construction of two more WWTPs will significantly improve water quality in the Saigon River. In addition, the improvement in DO concentration enhances the nitrification efficiency, which further helps to increase the NH_4^+ consumption. Unfortunately, NH_4^+ concentrations in the two future scenarios will not improve as much as TOC. This can be explained by the WWTPs treatment efficiency of TN of only about 40-50%, while the TOC can be removed at 85% (Metcalf and Eddy/AECOM, 2014). Therefore, to improve the quality of DO and NH_4^+ , there is a need to improve the efficiency of WWTPs in nutrient treatment, especially for nitrification NH_4^+ abatement. Under the 2050 scenario, all environmental variables in the Saigon River would show signs of deterioration. The concentrations of DO could be almost equivalent to the observations in 2015. DO would decrease from 2.4 to 1.4 mgDO.L^{-1} between 2025 and 2050. Although the connection rate with WWTPs reached 61% during this period, nutrients from 16 million inhabitants would cause significant DO consumption by nitrification and aerobic degradation. For the year 2050, three of four considered variables would return to a bad state compared to 2025, although their concentrations would be improved compared to the present. Meanwhile, PO_4^{3-} concentrations would always remain within the allowed concentration threshold of QCVN 08:2015/BTNMT regardless of the scenarios.

6. Eutrophication assessment

06I

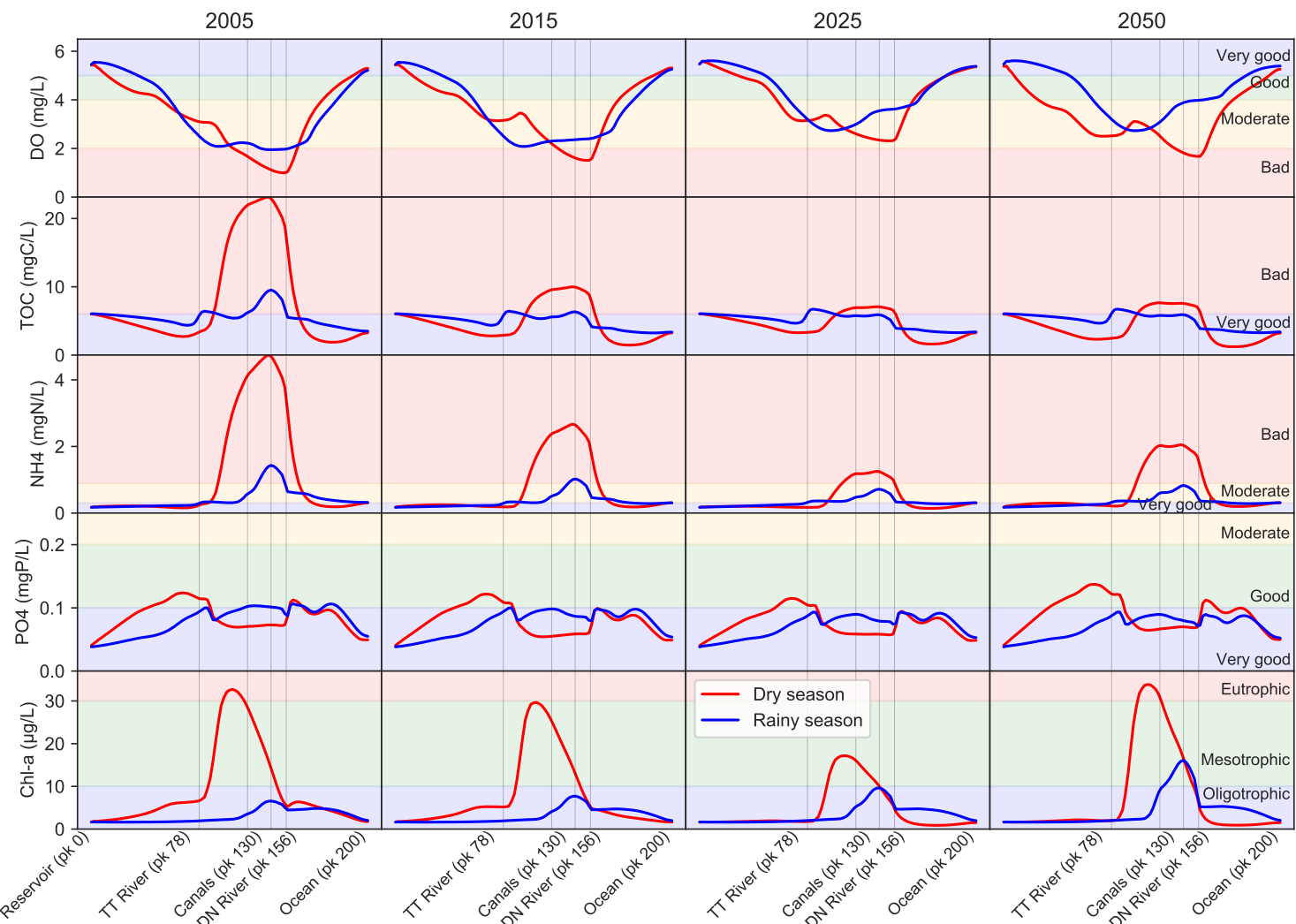


Figure 6.6: Simulated results of water quality variable along Saigon River Estuary in three scenarios. According to Vietnamese regulation on surface water quality, the background colors (red, orange, green, blue) are the concentration ranges for water quality assessment (QCVN 08:2015/_BTNMT. The trophic status is classified according to the recommendation of Dodds and Welch (2000).

6. Eutrophication assessment

In downstream, the water quality is mainly affected by seawater and tidal variation. The 2050 scenario assesses the impact of an increase in the tidal range of 20 cm. Although all four scenarios were declared with the same boundary conditions, all four scenarios showed no difference in downstream concentrations. The impact of a small tidal variation on water quality is thus weak. Therefore, there is no effect on the urban section and upstream areas by increasing 20 cm of tidal range. In addition, in the two future scenarios, there is an impact of temperature on phytoplankton biomass. According to the monitoring results of Nguyen et al., (2019), the concentration of Chl-a downstream is always low in the rainy season. Simulation results for two years, 2017-2018, also reached the same conclusion (Chapter 5). However, an increase in temperature of 1.5oC probably made phytoplankton growth superior to short residence time during the rainy season. The concentration of Chl-a in both the urban section and downstream of Saigon River may increase (Figure 6.6).

The 2005 scenario clearly shows the role of estuary in reducing pollutant concentrations because, during this period, 100% of wastewater was discharged into canals and rivers without treatment. As reported in C-GEM model, CH4 concentration in the canal was $7 \text{ mgNH}_4^+ L^{-1}$. It was reduced by 30% to about $5 \text{ mgNH}_4^+ L^{-1}$ at Saigon River in the dry season and about 80% in the rainy season. According to Nguyen et al., 2021, nitrification is the most important role in reducing nutrient contamination in the Saigon River. At Pearl River Estuary, a sub-tropical estuary in China, 37% of NH_4^+ of external loadings from urban discharge was also removed by the biogeochemical processes at this estuary (J. Hu & Li, 2009).

The response of Saigon River Estuary to different nutrient loadings is seen according to Chl-a concentration. In C-GEM model, concentrations of TOC, NH_4^+ and PO_4^{3-} are all declared and force their concentrations in the urban section (at km 110 and km 130), while the concentration of Chl-a is not bound. Therefore, the change in Chl-a concentration in the Saigon River water column reflects the estuary's obvious response to different nutrient loadings from urban discharge. The change in Chl-a concentration is most surprising in the urban section in 2050 when the trophic status may return to the eutrophic state such as the 2000s (no WWTPs) and 2015 (with 2 WWTPs). Trophic status during the rainy season has also changed from oligotrophic to mesotrophic status. This situation has never been seen in the observation in the rainy seasons from 2015 to 2020. Besides, PO_4^{3-} is a parameter that always reaches "very good" or "good" status in any scenario. The main cause of this phenomenon is that PO_4^{3-} has a high capacity to adsorb onto sediment right from urban canals.

6. Eutrophication assessment

6.3.2 Role of WWTPs in eutrophication management

Successful lessons in the management or recovery of estuaries have been observed in many developed countries, such as in European rivers (Garnier et al., 2018). Until now, the main solution is the reduction of pollutant concentrations entering estuaries (Wolanski & Elliott, 2014). For instance, the results of a 40-year survey at the Seine river and estuary (France) have shown the evolution and effectiveness of freshwater quality policies (Romero et al., 2016). Two decades ago, the Seine estuary used to have summer anoxic episodes, but the extension of WWTPs and agricultural policies has kept the estuary almost always in good condition since 2010. Besides the construction of WWTPs, policies such as the ban of phosphates in household detergents have also reduced PO_4^{3-} concentrations significantly since the 1990s (Romero et al., 2016). There are few successes in mitigating eutrophication in urbanized tropical estuaries (e.g., Shenzhen Bay in China, Zhou et al., 2020) by increasing the capacity of WWTPs.

While the assessment of nutrient concentrations in the 2005 scenario showed estuary responses to high nutrient concentrations of urban discharge, the comparison of concentrations in the Saigon River in 2015, 2025 and 2050 scenarios with 2005 shows the role of WWTPs in pollution control. NH_4^+ concentrations in urban section in the scenarios 2005, 2015, 2025 and 2050 are 5 mg L^{-1} , 2.5 mg L^{-1} , 1.5 mg L^{-1} and 2 mg L^{-1} , respectively (Figure 6.6). The NH_4^+ loadings from canals in the four scenarios are 5670, 4611, 6100 and $12780 \text{ kgNH}_4^+ d^{-1}$ (Figure 6.4). The reduction in NH_4^+ loading from 2005 to 2015 demonstrates the role of WWTPs and the improvement of canal retention through sludge dredging. Therefore, in the first three scenarios with the support of WWTPs, nutrient loadings from the canals into the Saigon River are not significantly different. Simulated concentrations of TOC and NH_4^+ in the 2015 and 2025 scenarios are markedly lower than in 2005. The concentrations of NH_4^+ and TOC in 2025 can be reduced respectively by 52% and 37% compared to 2015. Thanks to the increase of the total treatment capacity of WWTPs in HCMC (from 10% to 27%), TOC concentrations can be judged as good or very good in 2025. Likewise, DO under the 2025 scenario changes from a bad to a moderate quality in both seasons.

Reducing the inputs from wastewater in the inner city is the main factor in reducing NH_4^+ concentrations in the river. However, in the 2050 scenario, with the population increase from 6 million in 2005 compared to 16 million in 2050, the total nutrient loading increases significantly even concentration of NH_4^+ from the canal in 2050 is lower than in previous years. As a result, NH_4^+ concentrations have increased again, suggesting that 12 WWTPs in 2050 still do not allow for NH_4^+ reduction. The increase in NH_4^+ concentration has resulted in DO depletion in the water column because the Saigon River is an intense system with nitrification. Therefore, the efficient collection and treatment of a large amount of wastewater

6. Eutrophication assessment

from about 16 million people in 2050 is a major challenge for HCMC. In addition, NH_4^+ treatment efficiency is not as high as TOC.

In terms of eutrophication control, WWTPs do not play a key role as there is no significant decrease of Chl-a in the Saigon River in all scenarios. The control of eutrophication requires determining limiting factors for phytoplankton development. For instance, the Loire River, Seine River had Chl-a regularly exceeding $120 \mu\text{g L}^{-1}$ during the 1980s. Chl-a levels were controlled when limiting nutrient loading was controlled, PO_4^{3-} in the case of the Seine and Loire River with concentrations of about $0.05 \text{ mgPO}_4^{3-} \text{ L}^{-1}$ (Garnier et al., 2018). According to T. T. N. Nguyen et al. (2019), PO_4^{3-} is also limiting for phytoplankton growth in the Saigon River. Although the concentration of PO_4^{3-} has decreased many times from inner urban canals before entering the Saigon River, its concentration are still about $0.4 \text{ mgPO}_4^{3-} \text{ L}^{-1}$ (in the 2000s), $0.2 \text{ mgPO}_4^{3-} \text{ L}^{-1}$ (in 2010s), $0.15 \text{ mgPO}_4^{3-} \text{ L}^{-1}$ (in 2050). The oxygen concentration has improved compared to the 2000s, and PO_4^{3-} is within the recommended concentration according to QCVN 08:2015/BTNMT. The risk of eutrophication by 2050 may occur if PO_4^{3-} concentrations are not controlled. While the increase in temperature and the growing intensity of phytoplankton cannot be controlled, the reduction of pollutant sources of PO_4^{3-} is crucial. Therefore, the role of WWTPs or alternative solutions in mitigating eutrophication under the 2050 scenario is extremely important.

6.4 Conclusion

The application of the C-GEM model at the Saigon Estuary well reproduces the water quality parameters such as DO, NH_4^+ , PO_4^{3-} and TOC. After calibration and validation based on the Saigon River observed data in the dry seasons 2014 - 2017, C-GEM allows evaluating the changes of water quality in the Saigon River under various conditions of pollution input in dry and rainy season in 2005, 2015, 2025, and 2050. Model results for two future scenarios show a marked effect in improving river water quality by WWTPs construction, especially under scenario 2025. This result shows that the construction of WWTPs is essential for the sustainable development of HCMC. However, population growth from about 6 million inhabitants in 2005 to 16 million in 2050 can make the water quality return to bad condition, as in 2005 and 2015. Although the construction of new WWTPs could treat around 60% of the population in Ho Chi Minh City, the water quality in the Saigon River would not meet the water quality standards on surface water quality QCVN 08:2015/BTNMT for NH_4^+ . Under the 2050 scenario with climate change factors, the increase in temperature stimulates the growth of phytoplankton, the ineffectiveness of removing PO_4^{3-} as a limiting factor may lead to the return of eutrophic status in the Saigon River. To solve this problem,

6. Eutrophication assessment

improvement of nutrient processing technology in WWTPs and implementing alternative urban wastewater management (Nature-based Solutions) are probably the effective solution for eliminating oxygen shortages or nutrient pollution (e.g., NH_4^+) phytoplankton bloom in the urban section of the Saigon River.

6.5 Conclusion of Chapter 6

The efforts in applying the C-GEM model and calibration, validation in the dry season (Chapter 4) and expanding the seasonal assessment (Chapter 5) have ensured the applicability of C-GEM in the evaluation of scenarios at Saigon River Estuary. This chapter has assessed the urgent need to reduce pressure from pollution sources of Ho Chi Minh megacity on water quality and eutrophication in the Saigon River. With the help of an estuarine biogeochemical model (C-GEM), factors for improving water quality and minimizing eutrophication were identified. The extended application of the model will provide important information in ensuring the sustainable development of urbanized tropical estuaries.

Conclusion and perspectives

Conclusion

Nutrient pollution, eutrophication and greenhouse gases (GHGs) emissions in urbanized tropical estuaries are hot topics in the rapidly growing trend of emerging countries. This thesis is one of the first efforts covering all these related issues, from monitoring to statistical analysis and modeling eutrophication processes in Saigon River Estuary, an urbanized tropical estuary in Southern Vietnam affected by Ho Chi Minh Megacity (HCMC).

The monitoring program with complete parameters such as nutrients, greenhouse gases and phytoplankton from 2016-2020 observed spatial and temporal fluctuations in water quality and eutrophication in Saigon River Estuary. The application of multivariate statistics has allowed the identification of controlling factors for phytoplankton growth and the interaction of GHGs with eutrophication. This work also highlighted the important role of biogeochemical processes in water column, including nitrification and denitrification responding to high NH_4^+ concentrations from urban discharge. Saigon River Estuary has GHGs emissions similar to those observed in other urbanized estuaries with much higher GHGs concentrations in the urban section of the estuary. The impact of nutrient limitation on phytoplankton development at Saigon River is similar to many tropical estuaries where PO_4^{3-} is a limiting factor for phytoplankton development.

The calibrated and validated C-GEM was first applied in the dry season at Saigon River Estuary to capture spatial variations of nutrients and phytoplankton under the influence of megacity. C-GEM allowed measuring the intensity of biogeochemical processes involved in the metabolism and removal of nutrients from urban canals and tributaries. In the context of scarce hydrological and water quality data at Saigon River, the biogeochemical functioning of this tropical estuary was discovered by C-GEM. In addition, the tidal range and tidal period data applied in the C-GEM allowed the estimation of the movement of a 50 km pollutant cloud (high TOC, NH_4^+ , and low DO concentrations). This pollutant cloud can move within a radius of about 10 km according to tidal fluctuations. Future climate change impacts may have the risk of spreading this polluted area upstream of the Saigon River, where one strategic water production plant is located.

Seasonal simulation of nutrients and phytoplankton by the transient version of C-GEM explained huge differences in phytoplankton biomass between dry and rainy seasons in this tropical estuary. Efforts to apply seasonal simulation helped

Conclusion and perspectives

fill in most of the knowledge gaps that the current monitoring program and steady-state models have not addressed. Simulation results determined that nutrient limitation was the driving factor for spatial variation of phytoplankton between urban section and other sections of Saigon River. At the same time, the residence time of water body was responsible for the difference between phytoplankton in dry and rainy seasons. The distinct characteristics of hydrological conditions between the two seasons in tropical estuaries have led to the different states in the risk of eutrophication. Therefore, management solutions need to consider both nutrient availability and seasonal aspects to ensure the region's sustainable development.

Based on the development of HCMC, scenarios of nutrient loadings under the construction of wastewater treatment plants (WWTPs), population growth and climate change were examined. Past, present and future scenarios all show that the dry season is at risk of eutrophication. Oxygen depletion in the urban section of Saigon River persisted in both seasons because of high concentrations of NH_4^+ from urban canals. Although the construction of WWTPs is a very expensive solution for developing countries, the future water quality of HCMC megacity is not guaranteed. In order to improve water quality (dissolved oxygen condition in urban section), it is necessary to upgrade NH_4^+ treatment technology. It is necessary to control the concentration of PO_4^{3-} for eutrophication management in the Saigon River. The temperature rise scenario in 2050 warned of the risk of turning the Saigon River back to the eutrophication state of the 2000s when there was no WWTP.

Limitation

Although this study has been carried out to the fullest extent from sampling, analysis to modeling application to address some of the remaining questions in urbanized tropical estuaries, we believe that three main limitations remain in this study, including:

- The calibration parameters of the biogeochemical module are still not stable for the steady-state and transient version of C-GEM for Saigon River. The C-GEM application in tropical estuaries needs more improvement for calibrated parameters because the generic parameters in the biogeochemical module were developed mainly for temperate estuaries.
- The description of sediment dynamics is still limited, affecting other processes such as PO_4^{3-} sorption, light utilization efficiency and finally, phytoplankton development. Since PO_4^{3-} is a limiting factor of eutrophication in the Saigon River, errors in PO_4^{3-} simulations can lead to inappropriate interpretations.

Conclusion and perspectives

- Monitoring and modeling programs focus mainly on the mainstream of Saigon River. The dynamics of a major tributary (Dongnai River) downstream with a discharge 10 times higher than Saigon River were omitted. There is only one monitoring station at Dongnai River, and this river is rated as having good water quality thanks to a large freshwater discharge. However, according to the development plan of HCMC megacity, the population will gradually concentrate around Dongnai River, not just in Saigon River (as described in future scenarios in Chapter 6). Pollution of the Dongnai River and changes in its hydrological regime can lead to completely different concentrations of nutrients and phytoplankton downstream of Saigon River.

Future research directions

Urbanization and pollution emissions of coastal megacities in emerging countries are inevitable. In the last decades, eutrophication of many developed countries has been controlled based on long-term monitoring and biogeochemical modeling results. The first successful application of the C-GEM model at Saigon River Estuary shows the prospect of applying this model to other urbanized tropical estuaries, for example, in Southeast Asia. With the advantage of minimizing data requirement while ensuring accurate characterization of hydrodynamics and most biogeochemical processes, it would be a particularly meaningful tool in these developing countries.

The application and expansion of C-GEM in other tropical estuaries will establish a parameter set of the biogeochemical module for the tropics. The unification of parameters and processes allows improving the computational efficiency of C-GEM for the regional scale such as Southeast Asia. In addition, C-GEM is also capable of estimating CO_2 emissions from estuaries. This can compensate for uncertainties in estimating GHGs from estuaries in Asia in global models.

Besides applying C-GEM to other tropical estuaries, improvements in the monitoring program and other components to the C-GEM model are needed. As discussed in chapters 4 and 5, the addition of other processes to C-GEM is entirely achievable. The addition of benthic processes and the classification of major phytoplankton groups will allow the application of C-GEM to be extended to other estuarine types with strong benthic processes (e.g., shallow estuaries) and at risk of phytoplankton shift. C-GEM can take advantage of available models such as freshwater RIVE (Garnier et al., 2002), QUAL-NET (Minaudo et al., 2018), marine MIRO (Lancelot et al., 2007) to complement these important processes.

Bibliography

- Abe, D. S., Matsumura-Tundisi, T., Rocha, O., & Tundisi, J. G. (2003). Denitrification and bacterial community structure in the cascade of six reservoirs on a tropical river in brazil. *Hydrobiologia*, 504, 67–76.
- Abril, G., Commarieu, M.-V., Sottolichio, A., Bretel, P., & Guérin, F. (2009). Turbidity limits gas exchange in a large macrotidal estuary. *Estuarine, Coastal and Shelf Science*, 83(3), 342–348.
- Abril, G., Guérin, F., Richard, S., Delmas, R., Galy-Lacaux, C., Gosse, P., Tremblay, A., Varfalvy, L., Dos Santos, M. A., & Matvienko, B. (2005). Carbon dioxide and methane emissions and the carbon budget of a 10-year old tropical reservoir (petit saut, french guiana). *Global Biogeochemical Cycles*, 19(4), n/a–n/a.
- Aissa-Grouz, N., Garnier, J., & Billen, G. (2018). Long trend reduction of phosphorus wastewater loading in the seine: Determination of phosphorus speciation and sorption for modeling algal growth. *Environmental Science and Pollution Research*, 25(24), 23515–23528. <http://dx.doi.org/10.1007/s11356-016-7555-7>
- Arndt, S., & Regnier, P. (2007). A model for the benthic-pelagic coupling of silica in estuarine ecosystems: Sensitivity analysis and system scale simulation. *Biogeosciences*, 4(3), 331–352.
- Arndt, S., Lacroix, G., Gypens, N., Regnier, P., & Lancelot, C. (2011). Nutrient dynamics and phytoplankton development along an estuary-coastal zone continuum: A model study. *J. Mar. Syst.*, 84(3-4), 49–66. <http://dx.doi.org/10.1016/j.jmarsys.2010.08.005>
- Arndt, S., Regnier, P., & Vanderborght, J.-P. (2009). Seasonally-resolved nutrient export fluxes and filtering capacities in a macrotidal estuary. *J. Mar. Syst.*, 78(1), 42–58. <http://dx.doi.org/10.1016/j.jmarsys.2009.02.008>
- Atkins, J. P., Burdon, D., Elliott, M., & Gregory, A. J. (2011). Management of the marine environment: Integrating ecosystem services and societal benefits with the dpsir framework in a systems approach. *Marine Pollution Bulletin*, 62(2), 215–226.
- Attermeyer, K., Flury, S., Jayakumar, R., Fiener, P., Steger, K., Arya, V., Wilken, F., van Geldern, R., & Premke, K. (2016). Invasive floating macrophytes reduce greenhouse gas emissions from a small tropical lake. *Scientific reports*, 6, 20424.
- Aygun, O., Jonoski, A., & Popescu, I. (2019). Salinity control on saigon river downstream of dautieng reservoir within multi-objective simulation-optimisation framework for reservoir operation. *Lect. Notes Comput. Sci. (including Subser. Lect. Notes Artif. Intell. Lect. Notes Bioinformatics)*, 11539 LNCS. http://dx.doi.org/10.1007/978-3-030-22747-0_26
- Baek, S. H., Lee, M., Park, B. S., & Lim, Y. K. (2020). Variation in phytoplankton community due to an autumn typhoon and winter water turbulence in southern korean coastal waters. *Sustainability*, 12(7), 2781.
- Bange, H. W., Bathmann, U., Behrens, J., Dahlke, F., Ebinghaus, R., Ekau, W., Emeis, K.C., Ferse, S., Gerecke, D., & Hornidge, A.K. and Tennerjahn, T. (2017). *World ocean review: Coasts – a vital habitat under pressure*.

Bibliography

- Bange, H. W. (2006). Nitrous oxide and methane in european coastal waters. *Estuarine, Coastal and Shelf Science*, 70(3), 361–374.
- Bange, H. W. (2008). Gaseous nitrogen compounds (no, n₂o, n₂, nh₃) in the ocean, 51–94.
- Bartosiewicz, M., Maranger, R., Przytulska, A., & Laurion, I. (2021). Effects of phytoplankton blooms on fluxes and emissions of greenhouse gases in a eutrophic lake. *Water Research*, 196, 116985.
- Bauer, J. E., Cai, W.-J., Raymond, P. A., Bianchi, T. S., Hopkinson, C. S., & Regnier, P. A. G. (2013). The changing carbon cycle of the coastal ocean. *Nature*, 504(7478), 61–70.
- Beaulieu, J. J., DelSontro, T., & Downing, J. A. (2019). Eutrophication will increase methane emissions from lakes and impoundments during the 21st century. *Nature communications*, 10(1), 1375.
- Benassi, R. F., de Jesus, T. A., Coelho, L. H. G., Hanisch, W. S., Domingues, M. R., Taniwaki, R. H., Peduto, T. A. G., Da Costa, D. O., Pompêo, M. L. M., & Mitsch, W. J. (2021). Eutrophication effects on ch₄ and co₂ fluxes in a highly urbanized tropical reservoir (southeast, brazil). *Environmental science and pollution research international*.
- Bharathi, M. D., & Sarma, V. (2019). Impact of monsoon-induced discharge on phytoplankton community structure in the tropical indian estuaries. *Regional Studies in Marine Science*, 31, 100795.
- Bianchi, T. S. (2007). *Biogeochemistry of estuaries*. Oxford University Press.
- Billen, G., Garnier, J., Némery, J., Sebilo, M., Sferratore, A., Barles, S., Benoit, P., & Benoît, M. (2007). A long-term view of nutrient transfers through the seine river continuum. *Sci. Total Environ.*, 375(1-3), 80–97.
- Billen, G., Garnier, J., & Hanset, P. (1994). Modelling phytoplankton development in whole drainage networks: The riverstrahler model applied to the seine river system. *Hydrobiologia*, 289(1-3), 119–137.
- Billen, G., Silvestre, M., Grizzetti, B., Leip, A., Garnier, J., Voss, M., Howarth, R., Bouraoui, F., Lepistö, A., Kortelainen, P., Johnes, P., Curtis, C., Humborg, C., Smedberg, E., Kaste, Ø., Ganeshram, R., Beusen, A., & Lancelot, C. (2011). Nitrogen flows from european regional watersheds to coastal marine waters, 271–297.
- Bindoff, N. L., Cheung, W. W., Kairo, J. G., & Arístegui, J., Guinder, V. A., Hallberg, R., ... & Williamson, P. (2016). Changing ocean, marine ecosystems, and dependent communities. *IPCC special report on the ocean and cryosphere in a changing climate*.
- Blauw, A. N., Los, H. F., Bokhorst, M., & Erfemeijer, P. L. (2009). Gem: A generic ecological model for estuaries and coastal waters. *Hydrobiologia*, 618(1), 175–198.
- Bledsoe, E. L., Phlips, E. J., Jett, C. E., & Donnelly, K. A. (2004). The relationships among phytoplankton biomass, nutrient loading and hydrodynamics in an inner-shelf estuary. *Ophelia*, 58(1), 29–47.
- Bogorad, L. (1966). The biosynthesis of chlorophylls. In *The chlorophylls* (pp. 481–510). Elsevier.
- Borcard, D., Gillet, F., & Legendre, P. (2018). *Numerical ecology with r*. Springer International Publishing.

Bibliography

- Borges, A. V., & Abril, G. (2011). Carbon dioxide and methane dynamics in estuaries. In *Treatise on estuarine and coastal science* (pp. 119–161). Elsevier.
- Borges, A. V., Darchambeau, F., Lambert, T., Bouillon, S., Morana, C., Brouyère, S., Hakoun, V., Jurado, A., Tseng, H.-C., Descy, J.-P., & Roland, F. A. E. (2018). Effects of agricultural land use on fluvial carbon dioxide, methane and nitrous oxide concentrations in a large european river, the meuse (belgium). *The Science of the total environment*, 610-611, 342–355.
- Bräse, L., Bange, H. W., Lendt, R., Sanders, T., & Dähnke, K. (2017). High resolution measurements of nitrous oxide (n₂o) in the elbe estuary. *Front. Mar. Sci.*, 4(MAY), 1–11.
- Brigham, B. A., Bird, J. A., Juhl, A. R., Zappa, C. J., Montero, A. D., & O'Mullan, G. D. (2019). Anthropogenic inputs from a coastal megacity are linked to greenhouse gas concentrations in the surrounding estuary. *Limnology and Oceanography*, 64(6), 2497–2511.
- Brion, N., Billen, G., Guézennec, L., Ficht, A., Guezennec, L., & Ficht, A. (2000). Distribution of nitrifying activity in the seine river (france) from paris to the estuary. *Estuaries*, 23(5), 669.
- Bui & Thi Ngoc Oanh. (2018). *Dissolved methane distribution in seawater and its controlling factors in the polar regions* [Doctoral dissertation].
- Buranapratheprat, A., Morimoto, A., Phromkot, P., Mino, Y., Gunbua, V., & Jintasaeranee, P. (2021). Eutrophication and hypoxia in the upper gulf of thailand. *Journal of Oceanography*.
- Burgos, M., Sierra, A., Ortega, T., & Forja, J. M. (2015). Anthropogenic effects on greenhouse gas (ch4 and n₂o) emissions in the guadalete river estuary (sw spain). *Sci. Total Environ.*, 503-504, 179–189.
<http://dx.doi.org/10.1016/j.scitotenv.2014.06.038>
- Burgos, M., Ortega, T., & Forja, J. M. (2017). Temporal and spatial variation of n₂o production from estuarine and marine shallow systems of cadiz bay (sw, spain). *The Science of the total environment*, 607-608, 141–151.
- Buttigieg, P. L., & Ramette, A. (2014). A guide to statistical analysis in microbial ecology: A community-focused, living review of multivariate data analyses. *FEMS microbiology ecology*, 90(3), 543–550.
- Cabral, A., Bonetti, C. H. C., Garbossa, L. H. P., Pereira-Filho, J., Besen, K., & Fonseca, A. L. (2020). Water masses seasonality and meteorological patterns drive the biogeochemical processes of a subtropical and urbanized watershed-bay-shelf continuum. *The Science of the total environment*, 749, 141553.
- Cabral, A., & Fonseca, A. (2019). Coupled effects of anthropogenic nutrient sources and meteo-oceanographic events in the trophic state of a subtropical estuarine system. *Estuarine, Coastal and Shelf Science*, 225, 106228.
- Camenen, B., Gratiot, N., Cohard, J.-A. A., Gard, F., Tran, V. Q., Nguyen, A.-T. T., Dramais, G., van Emmerik, T., & Némery, J. (2021). Monitoring discharge in a tidal river using water level observations: Application to the saigon river, vietnam. *Sci. Total Environ.*, 761(40), 143195.
<http://dx.doi.org/10.1016/j.scitotenv.2020.143195>
- Caivacanti, L. F., Cutrim, M. V. J., Lourenço, C. B., Sá, Ana Karoline D.S. S, Oliveira, A. L. L., & de Azevedo-Cutrim, Andrea C.G. G. (2020). Patterns of phytoplankton structure in response to environmental gradients in a macrotidal

Bibliography

- estuary of the equatorial margin (atlantic coast, brazil). *Estuar. Coast. Shelf Sci.*, 245(March 2019), 106969.
- Choudhury, A. K., & Pal, R. (2010). Phytoplankton and nutrient dynamics of shallow coastal stations at bay of bengal, eastern indian coast. *Aquatic Ecology*, 44(1), 55–71.
- Cloern, J. E. (2001). Our evolving conceptual model of the coastal eutrophication problem. *Marine Ecology Progress Series*, 210, 223–253.
- Coelho, S., Gamito, S., & Pérez-Ruzafa, A. (2007). Trophic state of foz de almargem coastal lagoon (algarve, south portugal) based on the water quality and the phytoplankton community. *Estuarine, Coastal and Shelf Science*, 71(1-2), 218–231.
- Costa, L. S., Huszar, V. L. M., & Ovalle, A. R. (2009). Phytoplankton functional groups in a tropical estuary: Hydrological control and nutrient limitation. *Estuaries and Coasts*, 32(3), 508–521.
- Cotovicz, L. C., Knoppers, B. A., Brandini, N., Poirier, D., Costa Santos, S. J., & Abril, G. (2016). Spatio-temporal variability of methane (ch4) concentrations and diffusive fluxes from a tropical coastal embayment surrounded by a large urban area (guanabara bay, rio de janeiro, brazil). *Limnology and Oceanography*, 61(S1), S238–S252.
- Cotovicz, L. C., Ribeiro, R. P., Régis, C. R., Bernardes, M., Sobrinho, R., Vidal, L. O., Tremmel, D., Knoppers, B. A., & Abril, G. (2021). Greenhouse gas emissions (co2 and ch4) and inorganic carbon behavior in an urban highly polluted tropical coastal lagoon (se, brazil). *Environmental science and pollution research international*.
- Damar, A., Hesse, K.-J., Colijn, F., & Vitner, Y. (2019). The eutrophication states of the indonesian sea large marine ecosystem: Jakarta bay, 2001–2013. *Deep Sea Research Part II: Topical Studies in Oceanography*, 163, 72–86.
- Dan, S. F., Liu, S. M., Udoh, E. C., & Ding, S. (2019). Nutrient biogeochemistry in the cross river estuary system and adjacent gulf of guinea, south east nigeria (west africa). *Cont. Shelf Res.*, 179(March), 1–17.
- Daniel, I., DeGrandpre, M., & Farias, L. (2013). Greenhouse gas emissions from the tubul-raqui estuary (central chile 36°s). *Estuar. Coast. Shelf Sci.*, 134(3), 31–44. <http://dx.doi.org/10.1016/j.ecss.2013.09.019>
- Dao, T.-S., & Bui, T.-N.-P. (2016). Phytoplankton from vam co river in southern vietnam. *Environmental Management and Sustainable Development*, 5(1), 113. <http://dx.doi.org/10.5296/emsd.v5i1.8775>
- David, F., Meziane, T., Tran-Thi, N.-T., Truong Van, V., Thanh-Nho, N., Taillardat, P., & Marchand, C. (2018). Carbon biogeochemistry and co2 emissions in a human impacted and mangrove dominated tropical estuary (can gio, vietnam). *Biogeochemistry*, 138(3), 261–275.
- Davidson, T. A., Audet, J., Svenning, J.-C., Lauridsen, T. L., Søndergaard, M., Landkildehus, F., Larsen, S. E., & Jeppesen, E. (2015). Eutrophication effects on greenhouse gas fluxes from shallow-lake mesocosms override those of climate warming. *Global Change Biology*, 21(12), 4449–4463.
- de Bie, M. J., Middelburg, J. J., Starink, M., & Laanbroek, H. J. (2002). Factors controlling nitrous oxide at the microbial community and estuarine scale. *Marine Ecology Progress Series*, 240, 1–9.

Bibliography

- de Carvalho Aguiar, V. M., Neto, J. A. B., & Rangel, C. M. (2011). Eutrophication and hypoxia in four streams discharging in guanabara bay, rj, brazil, a case study. *Marine Pollution Bulletin*, 62(8), 1915–1919.
- de Domitrovic, Y. Z. (2002). Structure and variation of the paraguay river phytoplankton in two periods of its hydrological cycle. *Hydrobiologia*, 472(1), 177–196.
- de Jonge, V. N., Elliott, M., & Brauer, V. S. (2006). Marine monitoring: Its shortcomings and mismatch with the eu water framework directive's objectives. *Marine Pollution Bulletin*, 53(1-4), 5–19.
- de Souza Machado, Anderson Abel, Spencer, K., Kloas, W., Toffolon, M., & Zarfl, C. (2016). Metal fate and effects in estuaries: A review and conceptual model for better understanding of toxicity. *Sci. Total Environ.*, 541, 268–281.
- Delhez, É. J. M., de Brye, B., de Brauwere, A., & Deleersnijder, É. (2014). Residence time vs influence time. *J. Mar. Syst.*, 132, 185–195.
- DelSontro, T., Beaulieu, J. J., & Downing, J. A. (2019). Greenhouse gas emissions from lakes and impoundments: Upscaling in the face of global change. *Limnology and oceanography letters*, 3(3), 64–75.
- Dijkstra, Y. M., Chant, R. J., & Reinfelder, J. R. (2019). Factors controlling seasonal phytoplankton dynamics in the delaware river estuary: An idealized model study. *Estuaries and Coasts*, 42(7), 1839–1857.
- Dinauer, A., & Mucci, A. (2017). Spatial variability in surface-water pco₂ and gas exchange in the world's largest semi-enclosed estuarine system: St. lawrence estuary (canada). *Biogeosciences*, 14(13), 3221–3237.
- Domingues, R. B., Barbosa, A., & Galvão, H. (2005). Nutrients, light and phytoplankton succession in a temperate estuary (the guadiana, south-western iberia). *Estuarine, Coastal and Shelf Science*, 64(2-3), 249–260.
- Dong, L. F., Sobey, M. N., Smith, C. J., Rusmana, I., Phillips, W., Stott, A., Osborn, A. M., & Nedwell, D. B. (2011). Dissimilatory reduction of nitrate to ammonium, not denitrification or anammox, dominates benthic nitrate reduction in tropical estuaries. *Limnol. Oceanogr.*, 56(1), 279–291.
- Dröge, R., & Kroeze, C. (2007). Critical load exceedance for nitrogen in the ebrié lagoon (ivory coast): A first assessment. *Environmental Sciences*, 4(1), 5–19.
- Duong, T. T., Hoang, T. T. H., Nguyen, T. K., Le, T. P. Q., Le, N. D., Dang, D. K., Lu, X. X. I., Bui, M. H., Trinh, Q. H., van Dinh, T. H., Pham, T. D., & Rochelle-Newall, E. (2019). Factors structuring phytoplankton community in a large tropical river: Case study in the red river (vietnam). *Limnologica*, 76(March), 82–93.
- Duong, T. T., Nguyen, H. Y., Le, T. P. Q., Nguyen, T. K., Tran, T. T. H., Le, N. D., Dang, D. K., Vu, T. N., Panizzo, V., & McGowan, S. (2019). Transitions in diatom assemblages and pigments through dry and wet season conditions in the red river, hanoi (vietnam). *Plant Ecology and Evolution*, 152(2), 163–177.
- Durand, P., Breuer, L., Johnes, P. J., Billen, G., Butturini, A., Pinay, G., van Grinsven, H., Garnier, J., Rivett, M., Reay, D. S., Curtis, C., Siemens, J., Maberly, S., Kaste, Ø., Humborg, C., Loeb, R., de Klein, J., Hejzlar, J., Skoulidakis, N., ... Wright, R. (2011). Nitrogen processes in aquatic ecosystems, 126–146.

Bibliography

- Duvert, C., Butman, D. E., Marx, A., Ribolzi, O., & Hutley, L. B. (2018). Co2 evasion along streams driven by groundwater inputs and geomorphic controls. *Nature Geoscience*, 11(11), 813–818.
- Espey, W. H., & GH Ward. (1972). Review paper: Estuarine water quality models." *Water Research*, Vol 6(No 10).
- Etcheber, H., Schmidt, S., Sottolichio, A., Maneux, E., Chabaux, G., Escalier, J. M., Wennekes, H., Derriennic, H., Schmeltz, M., Quéméner, L., Repecaud, M., Woerther, P., & Castaing, P. (2011). Monitoring water quality in estuarine environments: Lessons from the magest monitoring program in the gironde fluvial-estuarine system. *Hydrol. Earth Syst. Sci.*, 15(3), 831–840.
- Eyre, B., & Balls, P. (1999). A comparative study of nutrient behavior along the gradient of tropical and temperate estuaries. *Estuaries*, 22(2), 313–326.
- Eyre, B. D. (2000). Regional evaluation of nutrient transformation and phytoplankton growth in nine river-dominated sub-tropical east australian estuaries. *Mar. Ecol. Prog. Ser.*, 205, 61–83.
- Fernandez, J. M., Townsend-Small, A., Zastepa, A., Watson, S. B., & Brandes, J. A. (2020). Methane and nitrous oxide measured throughout lake erie over all seasons indicate highest emissions from the eutrophic western basin. *Journal of Great Lakes Research*, 46(6), 1604–1614.
- Ferreira, J. G., Wolff, W. J., Simas, T. C., & Bricker, S. B. (2005). Does biodiversity of estuarine phytoplankton depend on hydrology? *Ecological Modelling*, 187(4), 513–523.
- Fossati, M., & Piedra-Cueva, I. (2013). A 3d hydrodynamic numerical model of the río de la plata and montevideo's coastal zone. *Appl. Math. Model.*, 37(3), 1310–1332. <http://dx.doi.org/10.1016/j.apm.2012.04.010>
- Galantini, L., Lapierre, J.-F., & Maranger, R. (2021). How are greenhouse gases coupled across seasons in a large temperate river with differential land use? *Ecosystems*.
- Garnier, J., Billen, G., Hannon, E., Fonbonne, S., Videnina, Y., & Soulie, M. (2002). Modelling the transfer and retention of nutrients in the drainage network of the danube river. *Estuar. Coast. Shelf Sci.*, 54(3), 285–308.
- Garnier, J., Billen, G., & Cébron, A. (2007). Modelling nitrogen transformations in the lower seine river and estuary (france): Impact of wastewater release on oxygenation and n2o emission. *Hydrobiologia*, 588(1), 291–302.
- Garnier, J., Billen, G., Némery, J., & Sebilo, M. (2010). Transformations of nutrients (n, p, si) in the turbidity maximum zone of the seine estuary and export to the sea. *Estuar. Coast. Shelf Sci.*, 90(3), 129–141. <http://dx.doi.org/10.1016/j.ecss.2010.07.012>
- Garnier, J., Billen, G., Vilain, G., Martinez, A., Silvestre, M., Mounier, E., & Toche, F. (2009). Nitrous oxide (n2o) in the seine river and basin: Observations and budgets. *Agriculture, Ecosystems & Environment*, 133(3-4), 223–233.
- Garnier, J., Ramarson, A., Billen, G., Théry, S., Thiéry, D., Thieu, V., Minaudo, C., & Moatar, F. (2018). Nutrient inputs and hydrology together determine biogeochemical status of the loire river (france): Current situation and possible future scenarios. *Science of the Total Environment*, 637-638, 609–624.
- Garnier, J., Vilain, G., Silvestre, M., Billen, G., Jehanno, S., Poirier, D., Martinez, A., Decuq, C., Cellier, P., & Abril, G. (2013). Budget of methane emissions from soils, livestock and the river network at the regional scale of the seine basin (france). *Biogeochemistry*, 116(1-3), 199–214.

Bibliography

- Gawade, L., Sarma, V. V., Rao, Y. V., & Hemalatha, K. P. (2017). Variation of bacterial metabolic rates and organic matter in the monsoon-affected tropical estuary (godavari, india). *Geomicrobiology Journal*, 34(7), 628–640.
- Grasset, C., Sobek, S., Scharnweber, K., Moras, S., Villwock, H., Andersson, S., Hiller, C., Nydahl, A. C., Chaguaceda, F., Colom, W., & Tranvik, L. J. (2020). The co₂ -equivalent balance of freshwater ecosystems is non-linearly related to productivity. *Global Change Biology*, 26(10), 5705–5715.
- GRID-Arendal and UNEP. (2016). World ocean assessment overview. *GRID-Arendal*.
- Guédron, S., Tolu, J., Delaere, C., Sabatier, P., Barre, J., Heredia, C., Brisset, E., Campillo, S., Bindler, R., Fritz, S. C., Baker, P. A., & Amouroux, D. (2021). Reconstructing two millennia of copper and silver metallurgy in the lake titicaca region (bolivia/peru) using trace metals and lead isotopic composition. *Anthropocene*, 34, 100288.
- Gugliotta, M., Saito, Y., Ta, T. K. O., van Nguyen, L., Uehara, K., Tamura, T., Nakashima, R., & Lieu, K. P. (2020). Sediment distribution along the fluvial to marine transition zone of the dong nai river system, southern vietnam. *Mar. Geol.*, 429(August), 106314.
- Gupta, G. V. M., Thottathil, S. D., Balachandran, K. K., Madhu, N. V., Madeswaran, P., & Nair, S. (2009). Co₂ supersaturation and net heterotrophy in a tropical estuary (cochin, india): Influence of anthropogenic effect: Carbon dynamics in tropical estuary. *Ecosystems*, 12(7), 1145–1157.
- Gypens, N., Delhez, E., Vanhoutte-Brunier, A., Burton, S., Thieu, V., Passy, P., Liu, Y., Callens, J., Rousseau, V., & Lancelot, C. (2013). Modelling phytoplankton succession and nutrient transfer along the scheldt estuary (belgium, the netherlands). *J. Mar. Syst.*, 128, 89–105.
<http://dx.doi.org/10.1016/j.jmarsys.2012.10.006>
- Han, P., Li, Y., Yang, X., Xue, L., & Zhang, L. (2017). Effects of aerobic respiration and nitrification on dissolved inorganic nitrogen and carbon dioxide in human-perturbed eastern jiaozhou bay, china. *Marine Pollution Bulletin*, 124(1), 449–458.
- Hanson, R. S., & Hanson, T. E. (1996). Methanotrophic bacteria. *Microbiological reviews*, 60(2), 439–471.
- Hartnett, M., Wilson, J. G., & Nash, S. (2011). Irish estuaries: Water quality status and monitoring implications under the water framework directive. *Marine Policy*, 35(6), 810–818.
- Hoang, H. T. T., Duong, T. T., Nguyen, K. T., Le, Q. T. P., Luu, M. T. N., Trinh, D. A., Le, A. H., Ho, C. T., Dang, K. D., Némery, J., Orange, D., & Klein, J. (2018). Impact of anthropogenic activities on water quality and plankton communities in the day river (red river delta, vietnam). *Environ. Monit. Assess.*, 190(2).
- Hofmann, A. F., Soetaert, K., & Middelburg, J. J. (2008). Present nitrogen and carbon dynamics in the scheldt estuary using a novel 1-d model. *Biogeosciences*, 5(4), 981–1006.
- Hoornweg, D., & Pope, K. (2017). Population predictions for the world's largest cities in the 21st century. *Environment and Urbanization*, 29(1), 195–216.
- Howarth, R., Chan, F., Conley, D. J., Garnier, J., Doney, S. C., Marino, R., & Billen, G. (2011). Coupled biogeochemical cycles: Eutrophication and hypoxia

Bibliography

- in temperate estuaries and coastal marine ecosystems. *Front. Ecol. Environ.*, 9(1), 18–26.
- Hu, B., Wang, D., Zhou, J., Meng, W., Li, C., Sun, Z., Guo, X., & Wang, Z. (2018). Greenhouse gases emission from the sewage draining rivers. *The Science of the total environment*, 612, 1454–1462.
- Hu, J., & Li, S. (2009). Modeling the mass fluxes and transformations of nutrients in the pearl river delta, china. *Journal of Marine Systems*, 78(1), 146–167. <http://dx.doi.org/10.1016/j.jmarsys.2009.05.001>
- Huertas, I. E., de La Paz, M., Perez, F. F., Navarro, G., & Flecha, S. (2019). Methane emissions from the salt marshes of doñana wetlands: Spatio-temporal variability and controlling factors. *Frontiers in Ecology and Evolution*, 7, 2234.
- Hugo Fischer. (1979). *Mixing in inland and coastal waters*. Elsevier.
- Huttunen, J. T., Alm, J., Liikanen, A., Juutinen, S., Larmola, T., Hammar, T., Silvola, J., & Martikainen, P. J. (2003). Fluxes of methane, carbon dioxide and nitrous oxide in boreal lakes and potential anthropogenic effects on the aquatic greenhouse gas emissions. *Chemosphere*, 52(3), 609–621.
- Jay, D. A. (2009). Evolution of tidal amplitudes in the eastern pacific ocean. *Geophys. Res. Lett.*, 36(4), 1–5.
- Ji, Z.-G. (2017). *Hydrodynamics and water quality*. John Wiley & Sons, Inc.
- Jiang, L., Gerkema, T., Kromkamp, J. C., van der Wal, D., La Carrasco De Cruz, P. M., & Soetaert, K. (2020). Drivers of the spatial phytoplankton gradient in estuarine–coastal systems: Generic implications of a case study in a dutch tidal bay. *Biogeosciences*, 17(16), 4135–4152.
- Kaul, L. W., & Froelich, P. N. (1984). Modeling estuarine nutrient geochemistry in a simple system. *Geochimica et Cosmochimica Acta*, 48(7), 1417–1433.
- Komárek, J., & Anagnostidis, K. (1988). Modern approach to the classification system of cyanophytes. 3 - oscillatoriales. *Algological Studies/Archiv für Hydrobiologie, Supplement Volumes*, 50-53, 327–472. http://www.schweizerbart.de//papers/archiv_algolstud/detail/50-53/65276/Modern_approach_to_the_classification_system_of_cyanophytes_3_Oscillatoriales
- Komárek, J., & Anagnostidis, K. (1999). *Bd. 19/1: Cyanoprokaryota: Teil 1: Chroococcales*. Jena [etc.]: Fischer.
- Komárek, J., & Anagnostidis, K. (2005). *Bd. 19/2: Cyanoprokaryota: Teil 2: Oscillatoriales*. Elsevier, München.
- Krammer, K. (1991). Süßwasserflora von mitteleuropa. bacillariophyceae. 3. teil: Centrales, fragilariaeae, eunotiaceae. *Süßwasserflora von Mitteleuropa*.
- Kyeong Park, Albert Y. Kuo, Jian Shen, & John M. Hamrick. *A three-dimensional hydrodynamic-eutrophication model (hem-3d) : Description of water quality and sediment process submodels*. 1995.
- Lajaunie-Salla, K., Sottolichio, A., Schmidt, S., Litrico, X., & Binet, G. (2019). Comparing the efficiency of hypoxia mitigation strategies in an urban, turbid tidal river via a coupled hydro-sedimentary-biogeochemical model. *Nat. Hazards Earth Syst. Sci.*, 19(11), 2551–2564.
- Lancelot, C., & Muylaert, K. (2011). Trends in estuarine phytoplankton ecology. In *Treatise on estuarine and coastal science* (pp. 5–15). Elsevier.

Bibliography

- Lanoux, A., Etcheber, H., Schmidt, S., Sottolichio, A., Chabaud, G., Richard, M., & Abril, G. (2013). Factors contributing to hypoxia in a highly turbid, macrotidal estuary (the gironde, france). *Environ. Sci. Process. Impacts*, *15*(3), 585–595.
- Laruelle, G. G., Roubeix, V., Sferratore, A., Brodherr, B., Ciuffa, D., Conley, D. J., Dürr, H. H., Garnier, J., Lancelot, C., LeThiPhuong, Q., Meunier, J. D., Meybeck, M., Michalopoulos, P., Moriceau, B., Ni Longphuirt, S., Loucaides, S., Papush, L., Presti, M., Ragueneau, O., ... van Cappellen, P. (2009). Anthropogenic perturbations of the silicon cycle at the global scale: Key role of the land-ocean transition. *Global Biogeochem. Cycles*, *23*(4), 1–17.
- Laruelle, G., Goossens, N., Arndt, S., Cai, W. J., & Regnier, P. (2017). Air-water co₂ evasion from us east coast estuaries. *Biogeosciences*, *14*(9), 2441–2468.
- Laruelle, G. G., Marescaux, A., Le Gendre, R., Garnier, J., Rabouille, C., & Thieu, V. (2019). Carbon dynamics along the seine river network: Insight from a coupled estuarine/river modeling approach. *Front. Mar. Sci.*, *6*(APR), 1–16.
- Le, T. P. Q., Gilles, B., Garnier, J., Sylvain, T., Denis, R., Anh, N. X., & van Minh, C. (2010). Nutrient (n, p, si) transfers in the subtropical red river system (china and vietnam): Modelling and budget of nutrient sources and sinks. *Journal of Asian Earth Sciences*, *37*(3), 259–274.
<http://dx.doi.org/10.1016/j.jseaes.2009.08.010>
- Lê, S., Josse, J., & Husson, F. (2008). Factominer: Anrpackage for multivariate analysis. *Journal of Statistical Software*, *25*(1). <http://dx.doi.org/10.18637/jss.v025.i01>
- Le Moal, M., Gascuel-Odoux, C., Ménesguen, A., Souchon, Y., Étrillard, C., Levain, A., Moatar, F., Pannard, A., Souchu, P., Lefebvre, A., & Pinay, G. (2019). Eutrophication: A new wine in an old bottle? *Science of the Total Environment*, *651*, 1–11.
- Le Tu, X., Thanh, V. Q., Reynolds, J., Van, S. P., Anh, D. T., Dang, T. D., & Roelvink, D. (2019). Sediment transport and morphodynamical modeling on the estuaries and coastal zone of the vietnamese mekong delta. *Continental Shelf Research*, *186*, 64–76.
- Lee, R. Y., Seitzinger, S., & Mayorga, E. (2016). Land-based nutrient loading to lmes: A global watershed perspective on magnitudes and sources. *Environmental Development*, *17*, 220–229.
- Li, Y., Shang, J., Zhang, C., Zhang, W., Niu, L., Wang, L., & Zhang, H. (2021). The role of freshwater eutrophication in greenhouse gas emissions: A review. *The Science of the total environment*, *768*, 144582.
- Likens, G. E. (2010). *Biogeochemistry of inland waters: A derivative of encyclopedia of inland waters*. Elsevier/Academic Press.
- Liu, X., Lu, Q., Zhou, Y., Li, K., Xu, Y., Lv, Q., Qin, J., Ouyang, S., & Wu, X. (2020). Community characteristics of phytoplankton and management implications in poyang lake basin. *Limnology*, *21*(2), 207–218.
- Livingston, R. J. (2000). *Eutrophication processes in coastal systems: Origin and succession of plankton blooms and effects on secondary production in gulf coast estuaries / robert j. livingston* (Vol. no. 43). CRC Press.
- López-Sandoval, D. C., Delgado-Huertas, A., Carrillo-de-Albornoz, P., Duarte, C. M., & Agustí, S. (2019). Use of cavity ring-down spectrometry to quantify ¹³c-primary productivity in oligotrophic waters. *Limnology and Oceanography: Methods*, *17*(2), 137–144.

Bibliography

- Manjrekar, S., Uskaikar, H., & Morajkar, S. (2020). Seasonal production of nitrous oxide in a tropical estuary, off western india. *Regional Studies in Marine Science*, 39, 101418.
- Marchesiello, P., Nguyen, N. M., Gratiot, N., Loisel, H., Anthony, E. J., Dinh, C. S., Nguyen, T., Almar, R., & Kestenare, E. (2019). Erosion of the coastal mekong delta: Assessing natural against man induced processes. *Continental Shelf Research*, 181, 72–89.
- Marescaux, A., Thieu, V., & Garnier, J. (2018). Carbon dioxide, methane and nitrous oxide emissions from the human-impacted seine watershed in france. *The Science of the total environment*, 643, 247–259.
- Martin, J. L., McCutcheon, S. C., & Schottman, R. W. (1998). *Hydrodynamics and transport for water quality modeling*. CRC Press.
- McKee, L. J., Eyre, B. D., & Hossain, S. (2000). Transport and retention of nitrogen and phosphorus in the sub-tropical richmond river estuary, australia - a budget approach. *Biogeochemistry*, 50(3), 241–278.
- Mhlanga, L., Day, J., Cronberg, G., Chimbari, M., Siziba, N., & Annadotter, H. (2006). Cyanobacteria and cyanotoxins in the source water from lake chivero, harare, zimbabwe, and the presence of cyanotoxins in drinking water. *African Journal of Aquatic Science*, 31(2), 165–173. <http://dx.doi.org/10.2989/16085910609503888>
- Miguel, Lucas Lavo António Jimo. (2018). Study on seasonal hydrology and biogeochemical variability in a tropical estuarine system, central mozambique coast, africa. *Marine Pollution Bulletin*, 131 (December 2017), 674–692.
- Minaudo, C., Curie, F., Jullian, Y., Gassama, N., & Moatar, F. (2018). Qual-net, a high temporal-resolution eutrophication model for large hydrographic networks. *Biogeosciences*, 15(7), 2251–2269.
- Miranda, J., Balachandran, K. K., Ramesh, R., & Wafar, M. (2008). Nitrification in kochi backwaters. *Estuar. Coast. Shelf Sci.*, 78(2), 291–300.
- Mojica, K. D. A., van de Poll, W. H., Kehoe, M., Huisman, J., Timmermans, K. R., Buma, A. G. J., van der Woerd, H. J., Hahn-Woernle, L., Dijkstra, H. A., & Brussaard, C. P. D. (2015). Phytoplankton community structure in relation to vertical stratification along a north-south gradient in the northeast atlantic ocean. *Limnology and Oceanography*, 60(5), 1498–1521.
- MONRE. (2016). Climate change and sea level rise scenarios. *Science*, 294(5547), 1379–1388.
- Mortimer, R. J. G., Krom, M. D., Watson, P. G., Frickers, P. E., Davey, J. T., & Clifton, R. J. (1999). Sediment-water exchange of nutrients in the intertidal zone of the humber estuary, uk. *Mar. Pollut. Bull.*, 37(3-7), 261–279.
- Müller, D., Bange, H. W., Warneke, T., Rixen, T., Müller, M., Mujahid, A., & Notholt, J. (2016). Nitrous oxide and methane in two tropical estuaries in a peat-dominated region of northwestern borneo. *Biogeosciences*, 13(8), 2415–2428.
- Murray, R. H., Erler, D. V., & Eyre, B. D. (2015). Nitrous oxide fluxes in estuarine environments: Response to global change. *Global Change Biology*, 21(9), 3219–3245.
- Nally, R. M. (1996). Hierarchical partitioning as an interpretative tool in multivariate inference. *Austral Ecology*, 21(2), 224–228.
- Némery, J., & Garnier, J. (2007). Typical features of particulate phosphorus in the seine estuary (france). *Hydrobiologia*, 588(1), 271–290.

Bibliography

- Némery, J., Garnier, J., & Morel, C. (2005). Phosphorus budget in the marne watershed (france): Urban vs. diffuse sources, dissolved vs. particulate forms. *Biogeochemistry*, 72(1), 35–66.
- Nevison, C., Butler, J. H., & Elkins, J. W. (2003). Global distribution of n₂o and the Δn₂o-aou yield in the subsurface ocean. *Global Biogeochemical Cycles*, 17(4), n/a–n/a.
- Nguyen, A. T., Némery, J., Gratiot, N., Garnier, J., Dao, T. S., Thieu, V., & Laruelle, G. G. (2021). Biogeochemical functioning of an urbanized tropical estuary: Implementing the generic c-gem (reactive transport) model. *Science of the Total Environment*, 147261.
- Nguyen, A. T., Dao, T.-S., Strady, E., Nguyen, T. T. N., Aimé, J., Gratiot, N., & Némery, J. (2021). Phytoplankton characterization in a tropical tidal river impacted by a megacity: The case of the saigon river (southern vietnam). *Environmental science and pollution research international*.
- Nguyen, B. T., Nguyen, T. M. T., & Bach, Q.-V. (2020). Assessment of groundwater quality based on principal component analysis and pollution source-based examination: A case study in ho chi minh city, vietnam. *Environmental monitoring and assessment*, 192(6), 395.
- Nguyen, H.-Q., Ha, N.-T., & Pham, T.-L. (2020). Inland harmful cyanobacterial bloom prediction in the eutrophic tri an reservoir using satellite band ratio and machine learning approaches. *Environmental Science and Pollution Research*, 27(9), 9135–9151. <http://dx.doi.org/10.1007/s11356-019-07519-3>
- Nguyen, H. D., Hong Quan, N., Quang, N. X., Hieu, N. D., & Le Thang, V. (2019). Spatio-temporal pattern of water quality in the saigon-dong nai river system due to waste water pollution sources. *Int. J. River Basin Manag.*, 5124.
- Nguyen, H. T., & Luong, H. P. (2019). Erosion and deposition processes from field experiments of hydrodynamics in the coastal mangrove area of can gio, vietnam. *Oceanologia*, 61(2), 252–264.
- Nguyen, H. T. M., Billen, G., Garnier, J., Le, T. P. Q., Pham, Q. L., Huon, S., & Rochelle-Newall, E. (2018). Organic carbon transfers in the subtropical red river system (viet nam): Insights on co₂ sources and sinks. *Biogeochemistry*, 138(3), 277–295.
- Nguyen, T. T. N., Némery, J., Gratiot, N., Strady, E., Tran, V. Q., Nguyen, A. T., Aimé, J., & Payne, A. (2019). Nutrient dynamics and eutrophication assessment in the tropical river system of saigon - dongnai (southern vietnam). *The Science of the total environment*, 653, 370–383.
- Nguyen, T. T., Némery, J., Gratiot, N., Garnier, J., Strady, E., Nguyen, D. P., Tran, V. Q., Nguyen, A. T., Cao, S. T., & Huynh, T. P. (2020). Nutrient budgets in the saigon-dongnai river basin: Past to future inputs from the developing ho chi minh megacity (vietnam). *River Research and Applications*, 36(6), 974–990.
- Nguyen, T. T., Némery, J., Gratiot, N., Garnier, J., Strady, E., Tran, V. Q., Nguyen, A. T., Nguyen, T. N., Golliet, C., & Aimé, J. (2019). Phosphorus adsorption/desorption processes in the tropical saigon river estuary (southern vietnam) impacted by a megacity. *Estuar. Coast. Shelf Sci.*, 227(March), 106321.
- Nguyen Van Tien. (2021). Some solutions to ho chi minh city's urbanization in the future. Retrieved October 21, 2021, from

Bibliography

- <https://tapchicongthuong.vn/bai-viet/ham-y-mot-so-giai-phap-phat-trien-do-thi-thanh-pho-ho-chi-minh-trong-tuong-lai-82561.htm?print=print>
- Nihoul, J. C. J., & F.C., R. (1976). Modeles d'un estuaire partiellement stratifie. *O(1)*.
- Nijman, T. P. A., Davidson, T. A., Weideveld, S. T. J., Audet, J., Esposito, C., Levi, E. E., Ho, A., Lamers, L. P. M., Jeppesen, E., & Veraart, A. J. (2021). Warming and eutrophication interactively drive changes in the methane-oxidizing community of shallow lakes. *ISME Communications*, *1*(1).
- Nixon, S. W. (1995). Coastal marine eutrophication: A definition, social causes, and future concerns. *Ophelia*, *41*(1), 199–219.
- Noriega, C. E. D., Araujo, M., & Lefèvre, N. (2013). Spatial and temporal variability of the co₂ fluxes in a tropical, highly urbanized estuary. *Estuaries and Coasts*, *36*(5), 1054–1072.
- Oehler, T., Tamborski, J., Rahman, S., Moosdorf, N., Ahrens, J., Mori, C., Neuholz, R., Schnetger, B., & Beck, M. (2019). Dsi as a tracer for submarine groundwater discharge. *Frontiers in Marine Science*, *6*.
- O’Kane, J. P., & Regnier, P. (2003). A mathematically transparent low-pass filter for tidal estuaries. *Estuar. Coast. Shelf Sci.*, *57*(4), 593–603.
- Oksanen, J., Blanchet, F. G., Friendly, M., Kindt, R., Legendre, P., McGlinn, D., Minchin, P. R., O’Hara, R. B., Simpson, G. L., & Solymos, P. (2019). Vegan: Community ecology package. r package version 2.5–6. 2019.
- Paerl, H. W. (2006). Assessing and managing nutrient-enhanced eutrophication in estuarine and coastal waters: Interactive effects of human and climatic perturbations. *Ecol. Eng.*, *26*(1), 40–54.
- Paerl, H. W., & Huisman, J. (2009). Climate change: A catalyst for global expansion of harmful cyanobacterial blooms. *Environmental Microbiology Reports*, *1*(1), 27–37. <http://dx.doi.org/10.1111/j.1758-2229.2008.00004.x>
- Paerl, H. W., Valdes, L. M., Peierls, B. L., Adolf, J. E., & Harding, L. W., JR. (2006). Anthropogenic and climatic influences on the eutrophication of large estuarine ecosystems. *Limnology and Oceanography*, *51*(1part2), 448–462.
- Park, I., & Song, C. G. (2018). Analysis of two-dimensional flow and pollutant transport induced by tidal currents in the han river. *Journal of Hydroinformatics*, *20*(3), 551–563.
- Park, K., Jung, H. S., Kim, H. S., & Ahn, S. M. (2005). Three-dimensional hydrodynamic-eutrophication model (hem-3d): Application to kwang-yang bay, korea. *Mar. Environ. Res.*, *60*(2), 171–193.
- Peng, L., Ni, B.-J., Ye, L., & Yuan, Z. (2015). N₂O production by ammonia oxidizing bacteria in an enriched nitrifying sludge linearly depends on inorganic carbon concentration. *Water Research*, *74*, 58–66.
- Pierella Karlusich, J. J., Ibarbalz, F. M., & Bowler, C. (2020). Phytoplankton in the tara ocean. *Annual review of marine science*, *12*, 233–265.
- Pinto, R., Weigelhofer, G., Brito, A. G., & Hein, T. (2021). Effects of dry-wet cycles on nitrous oxide emissions in freshwater sediments: A synthesis. *PeerJ*, *9*, e10767.
- Rajkumar, A., Barnes, J., Ramesh, R., Purvaja, R., & Upstill-Goddard, R. C. (2008). Methane and nitrous oxide fluxes in the polluted adyar river and estuary, se india. *Marine Pollution Bulletin*, *56*(12), 2043–2051.
- Redfield, A. C., B. H. Ketchum, & F. A. Richards. (1963). The influence of organisms on the composition of seawater. *The sea*, *2*(2), 26–77.

Bibliography

- Regnier, P., Mouchet, A., Wollast, R., & Ronday, F. (1998). A discussion of methods for estimating residual fluxes in strong tidal estuaries. *Cont. Shelf Res.*, 18(13), 1543–1571.
- Regnier, P., Wollast, R., & Steefel, C. I. (1997). Long-term fluxes of reactive species in macrotidal estuaries: Estimates from a fully transient, multicomponent reaction-transport model. *Mar. Chem.*, 58(1-2), 127–145.
- Regnier, P., Arndt, S., Goossens, N., Volta, C., Laruelle, G. G., Lauerwald, R., & Hartmann, J. (2013). Modelling estuarine biogeochemical dynamics: From the local to the global scale. *Aquat. Geochemistry*, 19(5-6), 591–626.
- Regnier, P., & Steefel, C. I. (1999). A high resolution estimate of the inorganic nitrogen flux from the scheldt estuary to the coastal north sea during a nitrogen-limited algal bloom, spring 1995. *Geochim. Cosmochim. Acta*, 63(9), 1359–1374.
- Reithmaier, G. M. S., Ho, D. T., Johnston, S. G., & Maher, D. T. (2020). Mangroves as a source of greenhouse gases to the atmosphere and alkalinity and dissolved carbon to the coastal ocean: A case study from the everglades national park, florida. *Journal of Geophysical Research: Biogeosciences*, 125(12).
- Reynolds, C. S. (2006). *The ecology of phytoplankton*. Cambridge University Press.
<http://dx.doi.org/10.1017/cbo9780511542145>
- Robin, R. S., Kanuri, V. V., Muduli, P. R., Ganguly, D., Patra, S., Hariharan, G., & Subramanian, B. R. (2016). Co₂ saturation and trophic shift induced by microbial metabolic processes in a river-dominated ocean margin (tropical shallow lagoon, chilika, india). *Geomicrobiology Journal*, 33(6), 513–529.
- Robson, B. J., & Hamilton, D. P. (2004). Three-dimensional modelling of a microcystis bloom event in the swan river estuary, western australia. *Ecol. Modell.*, 174(1-2), 203–222.
- Romero, E., Garnier, J., Billen, G., Ramarson, A., Riou, P., & Le Gendre, R. (2019). Modeling the biogeochemical functioning of the seine estuary and its coastal zone: Export, retention, and transformations. *Limnol. Oceanogr.*, 64(3), 895–912.
- Romero, E., Le Gendre, R., Garnier, J., Billen, G., Fisson, C., Silvestre, M., & Riou, P. (2016). Long-term water quality in the lower seine: Lessons learned over 4 decades of monitoring. *Environ. Sci. Policy*, 58, 141–154.
<http://dx.doi.org/10.1016/j.envsci.2016.01.016>
- Rosentreter, J. A., Maher, D. T., Erler, D. V., Murray, R., & Eyre, B. D. (2018). Factors controlling seasonal co₂ and ch₄ emissions in three tropical mangrove-dominated estuaries in australia. *Estuarine, Coastal and Shelf Science*, 215, 69–82.
- Sajor, E. E., & Thu, N. M. (2009). Institutional and development issues in integrated water resource management of saigon river. *J. Environ. Dev.*, 18(3), 268–290.
- Santoro, A. E., Buchwald, C., Knapp, A. N., Berelson, W. M., Capone, D. G., & Casciotti, K. L. (2021). Nitrification and nitrous oxide production in the offshore waters of the eastern tropical south pacific. *Global Biogeochemical Cycles*, 35(2).
- Saunois, M., Stavert, A. R., Poulter, B., Bousquet, P., Canadell, J. G., Jackson, R. B., Raymond, P. A., Dlugokencky, E. J., Houweling, S., Patra, P. K., Ciais, P., Arora, V. K., Bastviken, D., Bergamaschi, P., Blake, D. R., Brailsford, G., Bruhwiler, L., Carlson, K. M., Carroll, M., ... Zhuang, Q. (2020). The global methane budget 2000–2017. *Earth System Science Data*, 12(3), 1561–1623.

Bibliography

- Savenije, H. H. G. (2012). Salinity and tides in alluvial estuaries; second completely revised edition. *Open Access*, 163.
- Savenije, H. H. G. (2001). A simple analytical expression to describe tidal damping or amplification. *J. Hydrol.*, 243(3-4), 205–215.
- Savenije, H. H. (2005). Salinity and tides in alluvial estuaries. *Salinity and Tides in Alluvial Estuaries*.
- Sawant, S. S., Prabhudessai, L., & Venkat, K. (2007). Eutrophication status of marine environment of mumbai and jawaharlal nehru ports. *Environmental monitoring and assessment*, 127(1-3), 283–291.
- Schindler, D. W., Hecky, R. E., Findlay, D. L., Stainton, M. P., Parker, B. R., Paterson, M. J., Beaty, K. G., Lyng, M., & Kasian, S. E. M. (2008). Eutrophication of lakes cannot be controlled by reducing nitrogen input: Results of a 37-year whole-ecosystem experiment. *Proceedings of the National Academy of Sciences of the United States of America*, 105(32), 11254–11258.
- Schwarzer, K., Thanh, N. C., & Ricklefs, K. (2016). Sediment re-deposition in the mangrove environment of can gio, saigon river estuary (vietnam). *J. Coast. Res.*, 1(75), 138–142.
- Sepulveda-Jauregui, A., Hoyos-Santillan, J., Martinez-Cruz, K., Walter Anthony, K. M., Casper, P., Belmonte-Izquierdo, Y., & Thalasso, F. (2018). Eutrophication exacerbates the impact of climate warming on lake methane emission. *The Science of the total environment*, 636, 411–419.
- Shanahan, P., Henze, M., Koncsos, L., Rauch, W., Reichert, P., Somlyódy, L., Vanrolleghem, P., & Somlyody, L. (1998). River water quality modelling: II. problems of the art. *Water Sci. Technol.*, 38(11), 245–252.
- Sieracki, M. E., Verity, P. G., & Stoecker, D. K. (1993). Plankton community response to sequential silicate and nitrate depletion during the 1989 north atlantic spring bloom. *Deep. Res. Part II Top. Stud. Ocean.*, 40(1-2), 213–225.
- Sierra, A., Jiménez-López, D., Ortega, T., Fernández-Puga, M. C., Delgado-Huertas, A., & Forja, J. (2020). Methane dynamics in the coastal – continental shelf transition zone of the gulf of cadiz. *Estuarine, Coastal and Shelf Science*, 236, 106653.
- Silvennoinen, H., Liikanen, A., Rintala, J., & Martikainen, P. J. (2008). Greenhouse gas fluxes from the eutrophic temmesjoki river and its estuary in the liminganlahti bay (the baltic sea). *Biogeochemistry*, 90(2), 193–208.
- Skerratt, J., Wild-Allen, K., Rizwi, F., Whitehead, J., & Coughanowr, C. (2013). Use of a high resolution 3d fully coupled hydrodynamic, sediment and biogeochemical model to understand estuarine nutrient dynamics under various water quality scenarios. *Ocean Coast. Manag.*, 83, 52–66.
<http://dx.doi.org/10.1016/j.ocecoaman.2013.05.005>
- Smayda, T. J., & Sournia, A. (1978). Phytoplankton manual. *Phytoplankton to biomass*. Paris: UNESCO, 273–279.
- Smith, D. R., King, K. W., & Williams, M. R. (2015). What is causing the harmful algal blooms in lake erie? *Journal of Soil and Water Conservation*, 70(2), 27A–29A.
- Smith, L. M., Engle, V. D., & Summers, J. K. (2006). Assessing water clarity as a component of water quality in gulf of mexico estuaries. *Environmental monitoring and assessment*, 115(1-3), 291–305.

Bibliography

- Smith, R. M., Kaushal, S. S., Beaulieu, J. J., Pennino, M. J., & Welty, C. (2017). Influence of infrastructure on water quality and greenhouse gas dynamics in urban streams. *Biogeosciences (Online)*, 14(11).
- Soetaert, K., & Herman, P. M. J. (1995). Carbon flows in the westerschelde estuary (the netherlands) evaluated by means of an ecosystem model (moses). *Hydrobiologia*, 311(1-3), 247–266.
- Srichandan, S., Baliarsingh, S. K., Prakash, S., Lotlicher, A. A., Parida, C., & Sahu, K. C. (2019). Seasonal dynamics of phytoplankton in response to environmental variables in contrasting coastal ecosystems. *Environmental science and pollution research international*, 26(12), 12025–12041.
- Strady, E., Dang, V. B. H., Némery, J., Guédron, S., Dinh, Q. T., Denis, H., & Nguyen, P. D. (2017). Baseline seasonal investigation of nutrients and trace metals in surface waters and sediments along the saigon river basin impacted by the megacity of ho chi minh (vietnam). *Environ. Sci. Pollut. Res.*, 24(4), 3226–3243. <http://dx.doi.org/10.1007/s11356-016-7660-7>
- Sun, H., Lu, X., Yu, R., Yang, J., Liu, X., Cao, Z., Zhang, Z., Li, M., & Geng, Y. (2021). Eutrophication decreased co₂ but increased ch₄ emissions from lake: A case study of a shallow lake ulansuhai. *Water Research*, 201, 117363.
- Tang, W., Jun Xu, Y., & Li, S. (2021). Rapid urbanization effects on partial pressure and emission of co₂ in three rivers with different urban intensities. *Ecological Indicators*, 125, 107515.
- Tappin, A. D. (2002). An examination of the fluxes of nitrogen and phosphorus in temperate and tropical estuaries: Current estimates and uncertainties. *Estuar. Coast. Shelf Sci.*, 55(6), 885–901.
- Teodoru, C. R., Nyoni, F. C., Borges, A. V., Darchambeau, F., Nyambe, I., & Bouillon, S. (2015). Dynamics of greenhouse gases (co₂, ch₄, n₂o) along the zambezi river and major tributaries, and their importance in the riverine carbon budget. *Biogeosciences*, 12(8), 2431–2453.
- Tran Ngoc, T. D., Perset, M., Strady, E., Phan, T., Vachaud, G., Quertamp, F., & Gratiot, N. (Eds.). (2016). *Ho chi minh city growing with water-related challenges*.
- Trancoso, A. R., Saraiva, S., Fernandes, L., Pina, P., Leitão, P., & Neves, R. (2005). Modelling macroalgae using a 3d hydrodynamic-ecological model in a shallow, temperate estuary. *Ecol. Modell.*, 187(2-3), 232–246.
- Trieu, N. A., Hiramatsu, K., & Harada, M. (2014). Optimizing the rule curves of multi-use reservoir operation using a genetic algorithm with a penalty strategy. *Paddy Water Environ.*, 12(1), 125–137.
- Trinh, A. D., Meysman, F., Rochelle-Newall, E., & Bonnet, M. P. (2012). Quantification of sediment-water interactions in a polluted tropical river through biogeochemical modeling. *Global Biogeochem. Cycles*, 26(3), 1–15.
- Turner, E. L., Bruesewitz, D. A., Mooney, R. F., Montagna, P. A., McClelland, J. W., Sadovski, A., & Buskey, E. J. (2014). Comparing performance of five nutrient phytoplankton zooplankton (npz) models in coastal lagoons. *Ecological Modelling*, 277, 13–26.
- Van, T. P., & Koontanakulvong, S. (2018). Groundwater and river interaction parameter estimation in saigon river, vietnam. *Engineering Journal*, 22(1), 257–267.

Bibliography

- van Chu, T., Torréton, J. P., Mari, X., Nguyen, H. M. T., Pham, K. T., Pham, T. T., Bouvier, T., Bettarel, Y., Pringault, O., Bouvier, C., & Rochelle-Newall, E. (2014). Nutrient ratios and the complex structure of phytoplankton communities in a highly turbid estuary of southeast asia. *Environ. Monit. Assess.*, 186(12), 8555–8572.
- Vanderborght, J. P., Folmer, I. M., Aguilera, D. R., Uhrenholdt, T., & Regnier, P. (2007). Reactive-transport modelling of c, n, and o₂ in a river-estuarine-coastal zone system: Application to the scheldt estuary. *Mar. Chem.*, 106(1-2 SPEC. ISS), 92–110.
- Varol, M., & Sen, B. (2018). Abiotic factors controlling the seasonal and spatial patterns of phytoplankton community in the tigris river, turkey. *River Research and Applications*, 34(1), 13–23.
- Viero, D. P., & Defina, A. (2016). Water age, exposure time, and local flushing time in semi-enclosed, tidal basins with negligible freshwater inflow. *Journal of Marine Systems*, 156, 16–29.
- Vilmin, L., Aissa-Grouz, N., Garnier, J., Billen, G., Mouchel, J. M., Poulin, M., & Flipo, N. (2015). Impact of hydro-sedimentary processes on the dynamics of soluble reactive phosphorus in the seine river. *Biogeochemistry*, 122(2-3), 229–251.
- Vipindas, P. V., Anas, A., Jayalakshmy, K. V., Lallu, K. R., Benny, P. Y., & Shanta, N. (2018). Impact of seasonal changes in nutrient loading on distribution and activity of nitrifiers in a tropical estuary. *Cont. Shelf Res.*, 154(January), 37–45.
- Vitousek, P. M., Mooney, H. A., Lubchenco, J., & Melillo, J. M. (1997). Human domination of earth's ecosystems. *Urban Ecology: An International Perspective on the Interaction Between Humans and Nature*, 277(July), 3–13.
- Vollenweider, R. A., Giovanardi, F., Montanari, G., & Rinaldi, A. (1998). Characterization of the trophic conditions of marine coastal waters with special reference to the nw adriatic sea: Proposal for a trophic scale, turbidity and generalized water quality index. *Environmetrics*, 9(3), 329–357.
- Volta, C., Arndt, S., Savenije, H. H. G., Laruelle, G. G., & Regnier, P. (2014). C-gem (v 1.0): A new, cost-efficient biogeochemical model for estuaries and its application to a funnel-shaped system. *Geosci. Model Dev.*, 7(4), 1271–1295.
- Volta, C., Laruelle, G. G., & Regnier, P. (2016). Regional carbon and co₂ budgets of north sea tidal estuaries. *Estuar. Coast. Shelf Sci.*, 176, 76–90.
<http://dx.doi.org/10.1016/j.eess.2016.04.007>
- Volta, C., Laruelle, G. G., Arndt, S., & Regnier, P. (2016). Linking biogeochemistry to hydro-geometrical variability in tidal estuaries: A generic modeling approach. *Hydrol. Earth Syst. Sci.*, 20(3), 991–1030.
- von Glasow, R., Jickells, T. D., Baklanov, A., Carmichael, G. R., Church, T. M., Gallardo, L., Hughes, C., Kanakidou, M., Liss, P. S., Mee, L., Raine, R., Ramachandran, P., Ramesh, R., Sundseth, K., Tsunogai, U., Uematsu, M., & Zhu, T. (2013). Megacities and large urban agglomerations in the coastal zone: Interactions between atmosphere, land, and marine ecosystems. *Ambio*, 42(1), 13–28.
- Walsh, C., & Ralph, M. (2020). The hier. part package. ver. 1.0-6. hierarchical partitioning. documentation for r: A language and environment for statistical computing.

Bibliography

- Wang, J., Yuan, S., Tang, L., Pan, X., Pu, X., Li, R., & Shen, C. (2020). Contribution of heavy metal in driving microbial distribution in a eutrophic river. *Sci. Total Environ.*, 712, 136295. <http://dx.doi.org/10.1016/j.scitotenv.2019.136295>
- Wang, X., He, Y., Chen, H., Yuan, X., Peng, C., Yue, J., Zhang, Q., & Zhou, L. (2018). Ch₄ concentrations and fluxes in a subtropical metropolitan river network: Watershed urbanization impacts and environmental controls. *The Science of the total environment*, 622-623, 1079–1089.
- Wanninkhof, R. (1992). Relationship between wind speed and gas exchange over the ocean. *Journal of Geophysical Research*, 97(C5), 7373.
- Wetzel, R. G. (2001). *Limnology: Lake and river ecosystems*. gulf professional publishing.
- Whitall, D., Bricker, S., Ferreira, J., Nobre, A. M., Simas, T., & Silva, M. (2007). Assessment of eutrophication in estuaries: Pressure-state-response and nitrogen source apportionment. *Environmental management*, 40(4), 678–690.
- Wilk, P., Orlinska-Wozniak, P., & Gebala, J. (2018). The river absorption capacity determination as a tool to evaluate state of surface water. *Hydrol. Earth Syst. Sci.*, 22(2), 1033–1050.
- Wolanski, E., & Elliott, M. (2014). *Estuarine ecohydrology* (Second edition). Elsevier Science. <http://search.ebscohost.com/login.aspx?direct=true&scope=site&db=nlebk&AN=1055438>
- Wrage, N., Velthof, G., van Beusichem, M., & Oenema, O. (2001). Role of nitrifier denitrification in the production of nitrous oxide. *Soil Biology and Biochemistry*, 33(12-13), 1723–1732.
- Wu, J., Chen, N., Hong, H., Lu, T., Wang, L., & Chen, Z. (2013). Direct measurement of dissolved N₂ and denitrification along a subtropical river-estuary gradient, China. *Marine Pollution Bulletin*, 66(1-2), 125–134.
- Wu, Y., Bao, H. Y., Unger, D., Herbeck, L. S., Zhu, Z. Y., Zhang, J., & Jennerjahn, T. C. (2013). Biogeochemical behavior of organic carbon in a small tropical river and estuary, hainan, China. *Cont. Shelf Res.*, 57, 32–43.
- Wurtsbaugh, W. A., Paerl, H. W., & Dodds, W. K. (2019). Nutrients, eutrophication and harmful algal blooms along the freshwater to marine continuum. *WIREs Water*, 6(5).
- Yu, D., Chen, N., Krom, M. D., Lin, J., Cheng, P., Yu, F., Guo, W., Hong, H., & Gao, X. (2019). Understanding how estuarine hydrology controls ammonium and other inorganic nitrogen concentrations and fluxes through the subtropical jiulong river estuary, s.e. China under baseflow and flood-affected conditions. *Biogeochemistry*, 142(3), 443–466.
- Zhai, W., Dai, M., Cai, W.-J., Wang, Y., & Wang, Z. (2005). High partial pressure of CO₂ and its maintaining mechanism in a subtropical estuary: The pearl river estuary, China. *Marine Chemistry*, 93(1), 21–32.
- Zhang, G. L., Zhang, J., Liu, S. M., Ren, J. L., & Zhao, Y. C. (2010). Nitrous oxide in the changjiang (yangtze river) estuary and its adjacent marine area: Riverine input, sediment release and atmospheric fluxes. *Biogeosciences*, 7(11), 3505–3516.
- Zhang, L., Liao, Q., Gao, R., Luo, R., Liu, C., Zhong, J., & Wang, Z. (2021). Spatial variations in diffusive methane fluxes and the role of eutrophication in a subtropical shallow lake. *The Science of the total environment*, 759, 143495.

Bibliography

- Zhang, W., Li, H., Xiao, Q., & Li, X. (2021). Urban rivers are hotspots of riverine greenhouse gas (n₂o, ch₄, co₂) emissions in the mixed-landscape chaohu lake basin. *Water Research*, 189, 116624.
- Zhang, Y., Chen, B., & Zhai, W.-d. (2020). Exploring sources and biogeochemical dynamics of dissolved methane in the central bohai sea in summer. *Frontiers in Marine Science*, 7.
- Zhou, Y., Wang, L., Zhou, Y., & Mao, X.-Z. (2020). Eutrophication control strategies for highly anthropogenic influenced coastal waters. *The Science of the total environment*, 705, 135760.
- Zhu, X., Burger, M., Doane, T. A., & Horwath, W. R. (2013). Ammonia oxidation pathways and nitrifier denitrification are significant sources of n₂o and no under low oxygen availability. *Proceedings of the National Academy of Sciences of the United States of America*, 110(16), 6328–6333.